ZooKeys 687: 1–9 (2017)
doi: 10.3897/zookeys.687.13046
http://zookeys.pensoft.net

RESEARCH ARTICLE

A peer-reviewed open-access journal
ZooKeys
Launched to accelerate biodiversity research

A new species of *Ophryotrocha* (Annelida, Eunicida, Dorvilleidae) from hydrothermal vents on the Southwest Indian Ridge

Dong-sheng Zhang[1], Ya-dong Zhou[1], Chun-sheng Wang[1,2], Greg W. Rouse[3]

1 *Laboratory of Marine Ecosystem and Biogeochemistry, Second Institute of Oceanography, State Oceanic Administration, Hangzhou, 310012, China* **2** *State Key Laboratory of Satellite Ocean Environment Dynamics, Second Institute of Oceanography, State Oceanic Administration, Hangzhou, 310012, China* **3** *Scripps Institution of Oceanography, UCSD, La Jolla, CA 92093-0202, USA*

Corresponding author: *Chun-sheng Wang* (wang-sio@163.com; wangsio@sio.org.cn)

Academic editor: *Chris Glasby* | Received 6 April 2017 | Accepted 6 July 2017 | Published 1 August 2017

http://zoobank.org/67BA6F7E-FA66-412B-8B31-F05B29061895

Citation: Zhang D-s, Zhou Y-d, Wang C-s, Rouse GW (2017) A new species of *Ophryotrocha* (Annelida, Eunicida, Dorvilleidae) from hydrothermal vents on the Southwest Indian Ridge. ZooKeys 687: 1–9. https://doi.org/10.3897/zookeys.687.13046

Abstract

Dorvilleids were collected from hydrothermal vents on the Southwest Indian Ridge by manned submersible *Jiaolong*. These represent a new species of *Ophryotrocha* that is here described as *Ophryotrocha jiaolongi* **sp. n.** This is the first dorvilleid described from vents on the Southwest Indian Ridge. It most closely resembles another vent species, *Ophryotrocha akessoni* Blake, 1985 from the Galapagos Rift, but can be distinguished by its antennae, palps, jaw structure. The new species has particularly distinctive mandibles, which allow it to be easily identified.

Keywords

Polychaeta, new species, systematics, hydrothermal vents, Indian Ocean

Introduction

Ophryotrocha Claparède & Mecznikow, 1869 is a diverse dorvilleid genus with more than 70 species described to date. These are distributed world-wide in diversified habitats from shallow water to deep-sea. A number of species in this genus are opportunistic or stress tolerant, can reach high abundance in reducing environments, such as hydrothermal vents and cold seeps, as well as whale and wood fall ecosystems (Desbruyères et al. 2006, Levin et al. 2003, Wiklund et al. 2009, Wiklund et al. 2012, Taboada et al. 2013, Salvo et al. 2014, Ravara et al. 2015). To date five *Ophryotrocha* species: *O. akessoni* Blake, 1985, *O. fabriae* Paxton & Morineaux, 2009, *O. globopalpata* Blake & Hilbig, 1990, *O. platykephale* Blake, 1985, and *O. wubaolingi* Miura, 1997 have been reported from hydrothermal vents (Blake 1985, Blake and Hilbig 1990, Miura 1997, Paxton and Morineaux 2009). These have been recovered in association with other animals such as siboglinid worms, mussels, clams, or in microbial mats (Desbruyères et al. 2006, Paxton and Morineaux 2009).

Ophryotrocha has previously been reported from vent fields on the Central Indian Ridge (Van Dover et al. 2001, Watanabe and Beedessee 2015) and the Southwest Indian Ridge (Copley et al. 2015). However, they have not been described. In this paper, dorvilleid worms from vents field on the Southwest Indian Ridge were studied and named as the sixth *Ophryotrocha* species from the hydrothermal vents.

Material and methods

Sample collection and morphological analyses

In January 2015, the China Ocean Mineral Resource R&D Association (COMRA) cruise DY35 was carried out by the research vessel *Xiangyanghong 9*, visiting the Southwest Indian Ocean. Sampling from the vents field was undertaken by the manned submersible *Jiaolong*. Specimens collected from two sites of the Longqi vent field, were sieved through a 250 μm mesh sieve, sorted, and preserved in 95% ethanol on board. The holotype and most paratypes are deposited in the repository of the Second Institute of Oceanography (RSIO), Hangzhou, China; additional paratypes are deposited in the Scripps Institution of Oceanography Benthic Invertebrate Collection (SIO-BIC), La Jolla California, USA.

Specimens were examined and photographed using a Zeiss V20 stereomicroscope with AxioCam ICc5 camera and a Leica DM5000 compound microscope. Jaws and chaetae were analyzed by scanning electron microscope (SEM). Jaws from both holotype and paratype were obtained after digesting anterior decapitated ends with a proteinase K solution at room temperature. Once the tissue was digested, the jaw elements were cleaned with distilled water and transferred to a glass cover slip. All elements for SEM were mounted on stubs and sputter coated with platinum-palladium and imaged using a Hitachi TM1000 scanning electron microscope.

DNA extraction was done with DNeasy blood and tissue kit (Qiagen, CA, USA) following the protocol supplied by the manufacturer. About 680 bp of CO1, 500 bp of 16S and 350 bp of H3 were amplified using primers LCO1490 and CO-E (Folmer et al. 1994, Bely and Wray, 2004) for CO1, 16SarL and 16SbrH (Palumbi 1996) for 16S and H3F and H3R (Colgan et al. 2000) for H3. PCR mixtures contained ddH_2O, 1µl each primer (10 µM), 2 µl template DNA, 0.5 U of Taq polymerase (TAKARA, China), 2.5 µl of buffer solution (supplied by the polymerase manufacturer) and 0.5 µl of 2.5 mM dNTPs solution in a mixture of total 25µl. The temperature profile was as follows: 96°C/240s - (94°C/30s - 50°C/30s - 72°C/60s) * 35cycles - 72°C/420s. PCR products were purified with QIAquick PCR purification kit (Qiagen, CA, USA) following the protocol supplied by the manufacturer. Sequencing was performed by Sangon Biotech (Shanghai, China) on an ABI 3730XL DNA analyser (Applied Biosystems). Alignments of the three genes (CO1, 16S, H3) were performed using the program MAFFT (Katoh and Standley 2013) with all DNA data of dorvilleids available from Genbank. A maximum likelihood (ML) analysis was conducted by RAxML (Stamatakis 2014) using combined data of the three genes.

Systematics

Dorvilleidae Chamberlin, 1919
***Ophryotrocha* Claparède & Mecznikow, 1869**

***Ophryotrocha jiaolongi* sp. n.**
http://zoobank.org/60CF9A6D-DBB9-4048-9C1C-501E94C580E0
Figs 1–4

Holotype. (RSIO35301) Southwest Indian Ridge, Longqi vent field, HOV *Jiaolong* Dive 94, 49.6495°E; 37.7835°S, 2760m depth, 11 January 2015: ~ 10 mm long, 58 chaetigers; Paratypes: 21 specimens (RSIO35302) from same location as holotype; 7 specimens (RSIO35303) from Southwest Indian Ridge, Longqi vent field, 49.6501°E; 37.7836°S, 2737m depth; 8 specimens (SIO-BIC A6729) same locality as holotype.

Description. In life, body translucent (Fig. 1a), becoming opaque white after preservation (Fig. 2a, b). Body shape elongated, slightly dorsoventrally compressed, length up to 10 mm for more than 50 chaetigers, width 1.1 mm, uniform throughout the body, slightly tapering posteriorly (Fig. 2a, b). Prostomium wider than long, anterior margin rounded, posterior medial area slightly raised. Paired antennae short, digitiform, inserted dorsally, reaching to the anteriorly rounded edge of the prostomium (Fig. 2c, Fig. 4a). Paired palps digitiform, similar length as antennae, inserted ventrallaterally on prostomium (Fig. 2d). Eyes not visible. Peristomium with two rings subequal in length to following segments, the first ring with two notches ventrally on both sides of the jaw (Fig. 2d). Complete ciliary bands are observed on peristomium segments and chaetigers. Pygidium with terminal anus, two digitiform pygidial cirri

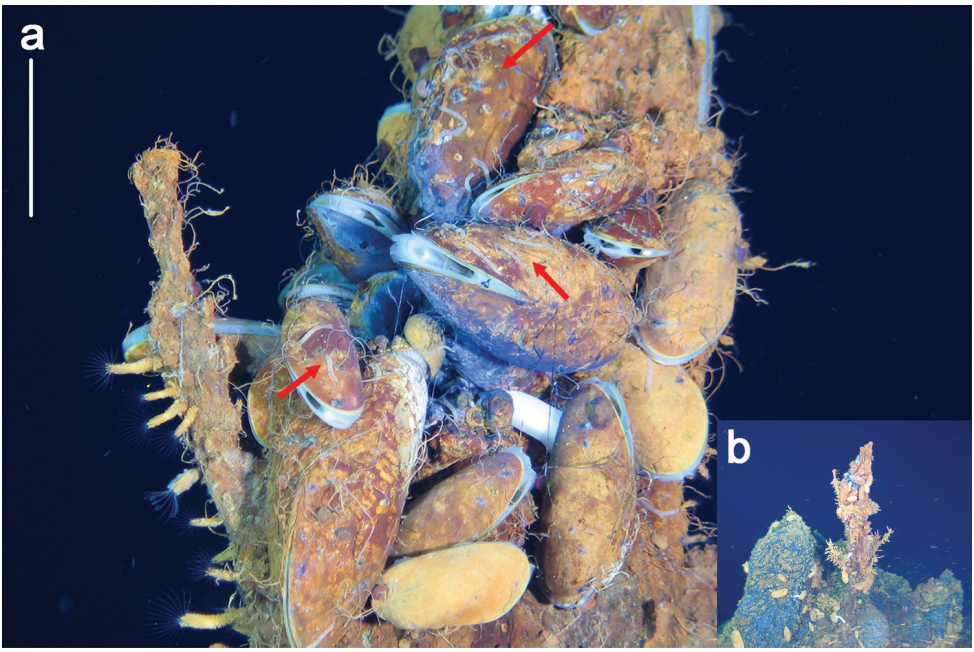

Figure 1. a *Ophyrotrocha jiaolongi* sp. n. (red arrows) specimens in vivo at the hydrothermal vent with mussels **b** same hydrothermal vent structure where *Ophryotrocha* specimens collected. Bars: 5 cm (**a**).

inserted laterally, similar in length with the parapodia on the last chaetigers, a small median papilla ventrally placed (Fig. 2a, b, Fig. 4b).

Mandibles rod-like, each cutting plate composed of two sub-triangular plates, dorsal plate larger than ventral plate, fused together from anterior and middle sides, distal edge smooth, with single blunt peak, no serration or teeth observed (Fig. 3a). Maxillae P-type (Fig. 3b, Fig. 4c), forceps comb-like with more than 30 teeth slightly decreasing in size distally (Fig. 3b), seven pairs of free denticles (D), posteriormost pair (D1) oval shaped, longer than wide, smaller than forceps, D2-D7 shovel shape, wide sub-equal with long, except D3 clearly longer than wide (Fig. 3b, d). D2-D3 with a slightly larger main fang and similar long sharp teeth (Fig. 3b, d), D4–D5 with alternating long and short teeth (Fig. 3c), D6–D7 with serrated margin similar as D4–D5 or with smooth margin (Fig. 3e). K-type maxillae not found.

Parapodia uniramous, slightly broadening distally with long sub-conical dorsal cirri and short nub-like ventral cirri (Fig. 4d). Supra-acicular chaetae simple, distally serrated, tapering abruptly into a fang, bearing several tiny spines on both sides distally (Fig. 3f), maximum 8 chaetae per fascicle. Sub-acicular chaetae compound, blades with distally curved main fang and double row of spines, heterogomph shaft with several spines distally (Fig. 3g), maximum 11 chaetae per fascicle. Some parapodiau appear to have sub-acicular retractable lobes with 1–3 simple chaetae (Fig. 3h).

Etymology. *Ophryotrocha jiaolongi* sp. n. is named after the Chinese manned submersible *Jiaolong*, in recognition of its successful expedition to the hydrothermal vents of the Southwest Indian Ridge.

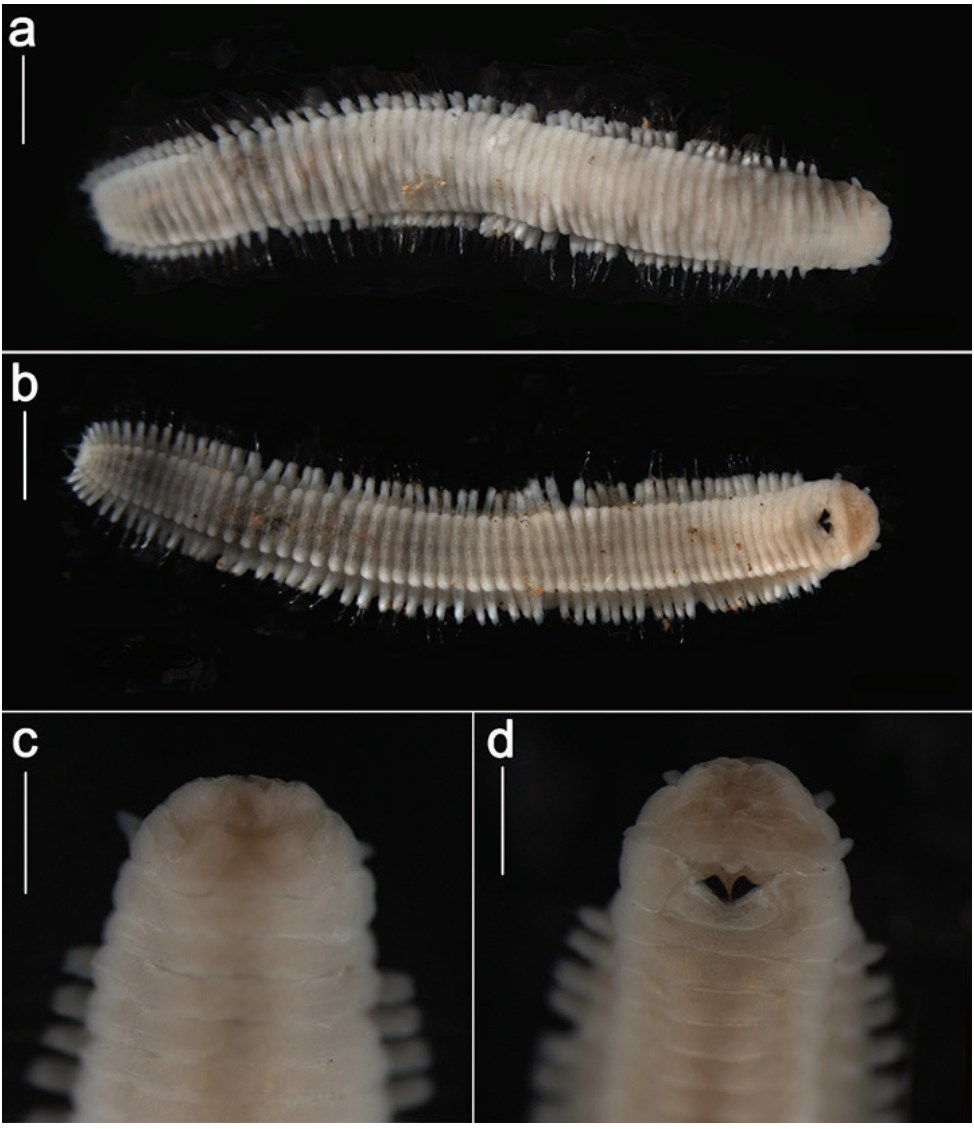

Figure 2. *Ophyrotrocha jiaolongi* sp. n., holotype. **a** dorsal view of whole body **b** ventral view of whole body **c** dorsal view of anterior region **d** ventral view of anterior region. Bars: 1 mm (**a, b**), 0.5 mm (**c, d**).

Remarks. The complex pharyngeal jaw apparatus, which is morphologically well characterized by the presence of ventral mandibles and dorsal maxillae, is an important diagnostic feature in Dorvilleidae (Rouse and Pleijel 2001). Mandibles of most *Ophryotrocha* species have been reported with a distally serrated edge or smooth anterior margin with anterior mandibular peaks. *Ophryotrocha jiaolongi* sp. n. has distinctive mandibles, with folded sub-triangular cutting plates, a distally smooth edge and a single anterior blunt peak, which easily distinguish it from other *Ophryotrocha* species. Among

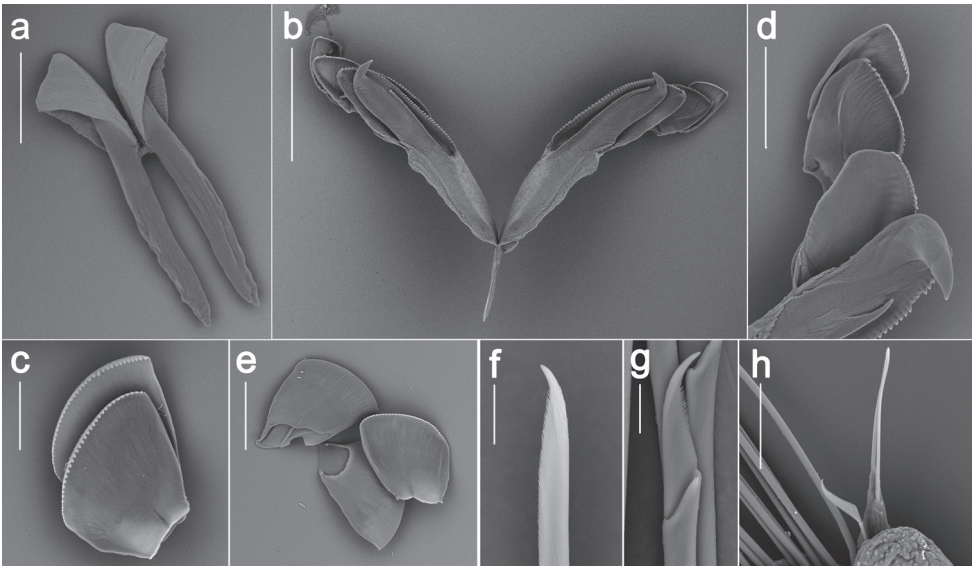

Figure 3. *Ophyrotrocha jiaolongi* sp. n. SEM images. (**a–c, f–h** holotype **d–e** paratype) **a** mandible, ventral view **b** forceps with free denticles 1-3 (D1-D3), dorsal view **c** free denticles 4-5 (D4-D5) **d** forcep with free denticles 1-3 (D1-D3) **e** free denticles 5-7 (D5-D7) **f** supra-acicular simple chaeta **g** sub-acicular compound chaeta **f** simple chaetae on sub-acicular lobe. Bars: 200 μm (**a, b**), 50 μm (**c, h**), 100 μm (**d, e**), 10 μm (**f, g**).

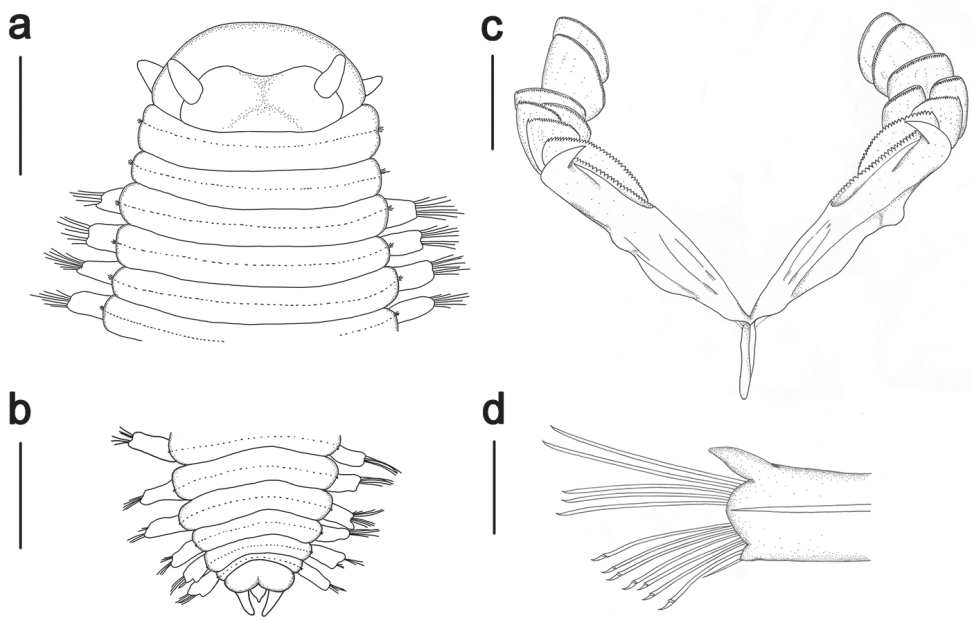

Figure 4. *Ophyrotrocha jiaolongi* sp. n. **a** prostomial, dorsal view **b** pydigium, dorsal view **c** maxillae with 7 pairs of free denticles **d** parapodia, anterior view. Bars: 500 μm (**a, b**), 200 μm (**c, d**).

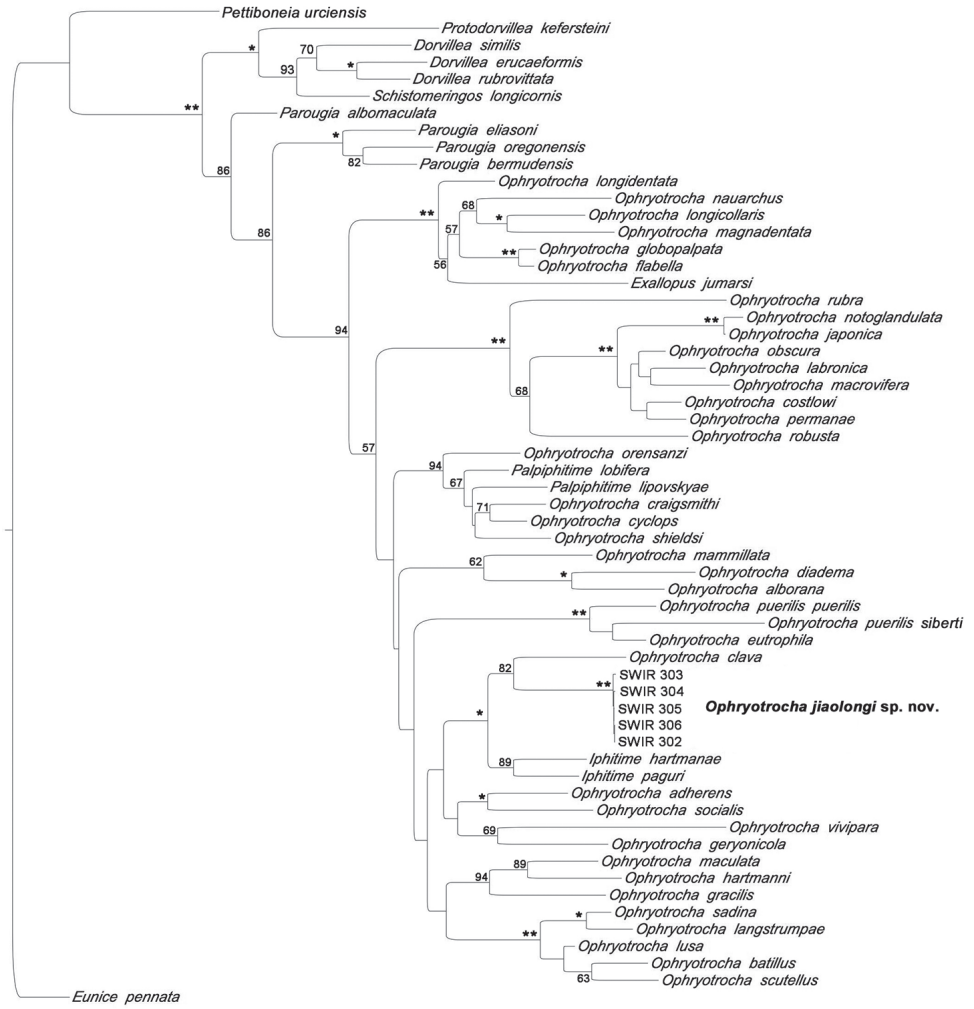

Figure 5. Maximum likelihood tree of the combined analysis from three genes (CO1, 16S, H3). Bootstrap support values (only higher than 50 were shown) were generated with a rapid bootstrapping algorithm for 1000 replicates. Double asterisk indicates support value of 100, single asterisk indicates support value of 95 or above.

Ophryotrocha species, *O. jiaolongi* sp. n. most closely resembles *O. akessoni* Blake, 1985, in the general morphology of the prostomium, peristomium, ciliary bands, parapodia and chaetae, as well as in mandibular and maxillary structure. *Ophryotrocha jiaolongi* sp. n. differs from *O. akessoni* in having shorter antennae and palps and slight differences in jaw structure. The maxillae appear to be P-type in both species, although Blake referred to that of *O. akessoni* as tending towards K-type in the adult. *Ophryotrocha jiaolongi* has alternating large and small teeth on D4-D5, while *O. akessoni* has alternating large and small teeth on the forceps and D1.

DNA. Sequences of *Ophryotrocha jiaolongi* sp. n. are deposited at NCBI Genbank with accession numbers CO1 KY906961–KY906965, 16S MF398963–MF398967, and H3 MF398968–MF398972. Preliminary phylogenetic analysis of the DNA data suggests that *O. jiaolongi* sp. n. is closely related to *O. clava* from whale bones. However, only one sequence of vent species (*O. globopalpata*) is currently available, which is located in a different clade from the new species. Further DNA data is being acquired from other vent *Ophryotrocha* species, which will help us to get a better understanding of the relationship among vents *Ophryotrocha* species in the near future (Zhang et al. in prep.).

Acknowledgements

We are grateful to all the scientists and crew on the R/V *Xiangyanghong 9* and the submersible *Jiaolong* team, for help in the collection of the deep-sea specimens. This study was supported by the National Program on Key Basic Research Project of China (No. 2015CB755902), the National Natural Science Foundation of China (NSFC) (41606156) and foundation of China Ocean Mineral Resources R & D Association (No. DYHC125-35).

References

Bely AE, Wray GA (2004) Molecular phylogeny of naidid worms (Anelida: Clitellata) based on cytochrome oxidase I. Molecular Phylogenetics and Evolution 30: 50–63. https://doi.org/10.1016/S1055-7903(03)00180-5

Blake JA (1985) Polychaeta from the vicinity of deep-sea geothermal vents in the Eastern Pacific. I. Euphrosinidae, Phyllodocidae, Hesionidae, Nereididae, Glyceridae, Dorvilleidae, Orbiniidae, and Maldanidae. Bulletin of the Biological Society of Washington 6: 67–101.

Blake JA, Hilbig B (1990) Polychaeta from the vicinity of deep-sea hydrothermal vents in the Eastern Pacific. II. New species and records from the Juan de Fuca and Explorer Ridge systems. Pacific Science 44: 219–253.

Colgan DJ, Ponder WF, Eggler PE (2000) Gastropod evolutionary rates and phylogenetic relationships assessed using partial 28S rDNA and histone H3 sequences. Zoologica Scripta 29: 29–63. https://doi.org/10.1046/j.1463-6409.2000.00021.x

Copley JT, Marsh L, Glover AG, Hühnerbach V, Nye VE, Reid WDK, Sweeting CJ, Wigham BD, Wiklund H (2016) Ecology and biogeography of megafauna and macrofauna at the first known deep-sea hydrothermal vents on the ultraslow-speading Southwest Indian Ridge. Scientific Reports 6: 39158. https://doi.org/10.1038/srep39158

Desbruyères D, Segonzac M, Bright M (2006) Handbook of deep-sea hydrothermal vent fauna, 2nd edition. Biologiezentrum der Oberösterreichischen Landesmuseen, Linz, Austria, 1–544.

Folmer O, Black M, Hoeh W, Lutz R, Vrijenhoek R (1994) DNA primers for amplification of mitochondrial cytochrome *c* oxidase subunit I from diverse metazoan invertebrate. Molecular Marine Biology and Biotechnology 3: 294–299.

Katoh L, Standley DM (2013) MAFFT multiple sequence alignment software version 7: improvements in performance and usability. Molecular Biology and Evolution 30: 772–780. https://doi.org/10.1093/molbev/mst010

Levin LA, Ziebis W, Mendoza GF, Growney VA, Tryon MD, Brown KM, Mahn C, Gieskes JM, Rathburn AE (2003) Spatial heterogeneity of macrofauna at northern California methane seeps: influence of sulfide concentration and fluid flow. Marine Ecology Progress Series 265: 123–139. https://doi.org/10.3354/meps265123

Miura T (1997) Two new species of the Genus *Ophryotrocha* (Polychaeta, Iphitimiidae) from Kagoshima Bay. Bulletin of Marine Science 60: 300–305.

Paxton H, Morineaux M (2009) Three species of Dorvilleidae (Annelida: Polychaeta) associated with Atlantic deep-sea reducing habitats, with the description of *Ophryotrocha fabriae*, new species. Proceedings of the Biological Society of Washington 122: 14–25. https://doi.org/10.2988/08-22.1

Palumbi SR (1996) Nucleic acid II: the polymerase chain reaction. In: Hillis DM, Moritz G, Mable BK (Eds) Molecular Systematics. Sinauer Associates, Sunderland, MA, 205–247.

Ravara A, Marcal AR, Wiklund H, Hilário A (2015) First account on the diversity of *Ophryotrocha* (Annelida, Dorvilleidae) from a mammal-fall in the deep-Atlantic Ocean with the description of three new species. Systematics and Biodiversity 13: 555–570.

Rouse GW, Pleijel F (2001) *Polychaetes*. Oxford University Press, London, 1–354.

Salvo F, Wiklund H, Dufour SC, Hamoutene D, Pohle G, Worsaae K (2014) A new annelid species from whalebones in Greeland and aquaculture sites in Newfoundland: *Ophryotrocha cyclops*, sp. n. (Eunicida: Dorvilleidae). Zootaxa 3887: 555–568. https://doi.org/10.11646/Zootaxa.3887.5.3

Stamatakis A (2014) RaxML version 8: a tool for phylogenetic analysis and post-analysis of large phylogenies. Bioinformatics 30: 1312–1313. https://doi.org/10.1093/bioinformatics/btu033

Taboada S, Wiklund H, Glover AG, Dahlgren TG, Cristobo J, Avila C (2013) Two new Antarctic *Ophryotrocha* (Annelida: Dorvilleidae) described from shallow-water whale bones. Polar Biology 36: 1031–1045. https://doi.org/10.1007/s00300-013-1326-4

Van Dover CL, Humphris SE, Fornari D, Cavanaugh CM, Collier R, Goffredi SK, Hashimoto J, Lilley MD, Reysenbach AL, Shank TM, Von Damm KL, Banta A, Gallant RM, Gotz D, Green D, Hall J, Harmer TL, Hurtado LA, Johnson P, McKiness ZP, Meredith C, Olson E, Pan IL, Turnipseed M, Won Y, Young CR, Vrijenhoek RC (2001) Biogeography and ecological setting of Indian Ocean hydrothermal vents. Science 294: 818–823. https://doi.org/10.1126/science.1064574

Watanabe H, Beedessee G (2015) Vent Fauna on the Central Indian Ridge. In: Ishibashi J, Okino K, Sunamura M (Eds) Subseafloor Biosphere Linked to Hydrothermal Systems: TAIGA Concept. Springer, Japan, Tokyo, 205–212. https://doi.org/10.1007/978-4-431-54865-2_16

Wiklund H, Glover AG, Dahlgren TG (2009) Three new species of *Ophryotrocha* (Annelida: Dorvilleidae) from a whale-fall in the North-East Atlantic. Zootaxa 2228: 43–56.

Wiklund H, Altamira IV, Glover AG, Smith CR, Baco AR, Dahlgren TG (2012) Systematics and biodiversity of *Ophryotrocha* (Annelida, Dorvilleidae) with descriptions of six new species from deep-sea whale-fall and wood-fall habitats in the north-east Pacific. Systematics and Biodiversity 10: 243–259. https://doi.org/10.1080/14772000.2012.693970

ZooKeys 687: 11–43 (2017)
doi: 10.3897/zookeys.687.13884
http://zookeys.pensoft.net

RESEARCH ARTICLE

A peer-reviewed open-access journal
ZooKeys
Launched to accelerate biodiversity research

A new cave centipede from Croatia, *Eupolybothrus liburnicus* sp. n., with notes on the subgenus *Schizopolybothrus* Verhoeff, 1934 (Chilopoda, Lithobiomorpha, Lithobiidae)

Nesrine Akkari[1], Ana Komerički[2], Alexander M. Weigand[2,3], Gregory D. Edgecombe[4], Pavel Stoev[5]

1 *Naturhistorisches Museum Wien, Burgring 7, 1010 Wien, Austria* **2** *Croatian Biospeleological Society, Zagreb, Croatia* **3** *University of Duisburg-Essen, Essen, Germany* **4** *Department of Earth Sciences, The Natural History Museum, Cromwell Road, London SW7 5BD, UK* **5** *National Museum of Natural History and Pensoft Publishers, Sofia, Bulgaria*

Corresponding author: *Nesrine Akkari* (nesrine.akkari@nhm-wien.ac.at)

Academic editor: *M. Zapparoli* | Received 26 May 2017 | Accepted 1 July 2017 | Published 1 August 2017

http://zoobank.org/94C0F9A5-3758-4AFE-93AE-87ED5EDF744D

Citation: Akkari N, Komerički A, Weigand AM, Edgecombe GD, Stoev P (2017) A new cave centipede from Croatia, *Eupolybothrus liburnicus* sp. n., with notes on the subgenus *Schizopolybothrus* Verhoeff, 1934 (Chilopoda, Lithobiomorpha, Lithobiidae). ZooKeys 687: 11–43. https://doi.org/10.3897/zookeys.687.13844

Abstract

A new species of *Eupolybothrus* Verhoeff, 1907 discovered in caves of Velebit Mountain in Croatia is described. *E. liburnicus* **sp. n.** exhibits a few morphological differences from its most similar congeners, all of which are attributed to the subgenus *Schizopolybothrus* Verhoeff, 1934, and two approaches to species delimitation using the COI barcode region identify it as distinct from the closely allied *E. cavernicolus* Stoev & Komerički, 2013.

E. spiniger (Latzel, 1888) is redescribed and a lectotype is designated for it as well as *E. caesar* (Verhoeff, 1899) to stabilize their respective taxonomic status. The subspecies *E. acherontis wardaranus* Verhoeff, 1937, previously suspected to be a synonym of *E. caesar* (Verhoeff, 1899), is redescribed and its taxonomy revised after the study of type material whereas the identity of *E. acherontis* (Verhoeff, 1900) described from a female from southwest Trebinje (Bosnia and Herzegovina) remains unknown. Type material of *E. stygis* (Folkmanova, 1940) is confirmed to be lost and future designation of neotypes from topotypic specimens is necessary to stabilize its taxonomy. The importance of setal arrangement on the intermediate and 14th tergites and the sexual modifications on the male 15th prefemur for species identification is discussed in the light of present findings, and a review of the species of *E.* (*Schizopolybothrus*) that display these traits is also provided.

Keywords
Biospeleology, COI barcoding, *Eupolybothrus*, new species, SEM, Velebit Mountain

Introduction

The genus *Eupolybothrus* Verhoeff, 1907 comprises *ca*. 40 valid and doubtful species and subspecies. All species are described from Eastern European and circum-Mediterranean countries, including the largest Mediterranean islands, Corsica, Crete, Cyprus, Sardinia and Sicily (Zapparoli 2002, Stoev et al. 2010, 2013).

Seven subgenera were defined for the genus *Eupolybothrus*, based on a combination of morphological characters but these groupings remain questionable and perhaps do not reflect phylogenetic relationships (see Stoev et al. 2010, 2013). However, they traditionally helped to facilitate species identification with conventional taxonomic methods. Verhoeff (1934) designated the subgenus *Schizopolybothrus* and assigned *Lithobius caesar* Verhoeff, 1899 as its type species. This subgenus was later re-defined by Jeekel (1967) and extended to include all species with posterior projections on tergites 9, 11 and 13, having spines 15VCa and 15VCm and a simple apical claw on the ultimate legs (Eason 1983). Jeekel (1967) also divided the subgenus into three species groups, based on male gonopods and modifications of the 15th leg but this subdivision was recently rejected by Stoev et al. (2013), who considered groups II and III as invalid due to an erroneous placement of several species. In group III, *E. zeus* (Verhoeff, 1901) and *E. sissi* (Kanellis, 1959) were for instance synonymized with *E.* (*Mesobothrus*) *transsylvanicus* (Latzel, 1882) by Zapparoli (2002) and *E. excellens* (Silvestri, 1894) was wrongly placed together with *E. tabularum* (Verhoeff, 1937) in group II, based only on female characters.

Currently, the subgenus *Schizopolybothrus* comprises nine species and subspecies, *viz*. *Eupolybothrus acherontis* (Verhoeff, 1900), *E. acherontis wardaranus* (Verhoeff, 1937), *E. caesar* (Verhoeff, 1899), *E. cavernicolus* Komerički & Stoev, 2013, *E. excellens* (Silvestri, 1894), *E. leostygis* (Verhoeff, 1899), *E. spiniger* (Latzel, 1888), *E. stygis* (Folkmanova, 1940), and *E. tabularum* (Verhoeff, 1937). Some of these are still poorly known and of uncertain taxonomic status. For example, *E. spiniger*, *E. stygis*, *E. acherontis* and *E. acherontis wardaranus* were known only from their original descriptions (see also Stoev 2001a, b, Stoev et al. 2010). While *E. leostygis* was recently re-described (Eason 1983, Stoev et al. 2013), all attempts to find new material of *E. stygis* have failed and the types are now confirmed to be destroyed (Tuf, personal communication). Here, we 1) describe a new species, *E. liburnicus* sp. n., recently collected in caves of Velebit Mountain in Croatia; 2) compare all species of *Schizopolybothrus* focusing on morphological characters that involve modifications of the male prefemur 15 and the intermediate tergite, and supplementing these with the cytochrome *c* oxidase subunit I (COI) gene for species delimitation; 3) examine and re-describe the type material of *E. spiniger* and *E. acherontis wardaranus* housed in Naturhistorisches Museum Wien and the Zoologische Staatssammlung München (ZSM) respectively; 4) designate a lectotype for both *E. spiniger* and *E. caesar*. *E. acherontis*,

described by Verhoeff (1900) from a single female specimen and housed in the Senckenberg Naturmuseum Frankfurt am Main, was not accessible to study.

An integrative approach with a combination of morphological and molecular methods is certainly required to better understand the evolutionary history of this group and delineate the number of valid taxa, towards which the present work is a step.

The present work is part of an ongoing revision of the subfamily Ethopolyinae (Stoev et al. 2010, Porco et al. 2011, Komerički et al. 2012, Stoev et al. 2013).

Materials and methods

Morphology

All specimens were collected by hand and preserved in 70% or 96% ethanol. The holotype was photographed in situ using a Canon 400D camera with a 65 mm macro objective. Microphotographs were obtained with a Nikon DS-F2.5 camera mounted on a Nikon SMZ25 stereomicroscope using NIS-Elements Microscope Imaging Software with an Extended Depth of Focus (EDF) patch. For scanning electron microscopy, parts of some specimens were cleaned with ultrasound, transferred to 96% ethanol then to acetone, air-dried, mounted on aluminum stubs, coated with Platinum/Palladium and studied in a JEOL JSM-6335F scanning electron microscope. All images were edited in Adobe Photoshop CS6 and assembled in Adobe InDesign CS6. Type material is shared between the Croatian Biospeleological Society – Croatian Natural History Museum (CBSS), The Natural History Museum Denmark – University of Copenhagen (ZMUC), Naturhistorisches Museum Wien (NHMW), and the National Museum of Natural History, Sofia (NMNHS).

Morphological terminology follows Bonato et al. (2010).

Molecular species delimitation

The standard DNA barcoding locus, the Folmer-fragment of the cytochrome *c* oxidase subunit I (COI) gene was sequenced to delimit *E. liburnicus* sp. n. from other *Eupolybothrus* species. Mid-body legs of four specimens conserved in 70% and 96% ethanol were sent to the Canadian Centre for DNA Barcoding, Guelph, where standard protocols for DNA isolation, PCR and sequencing were performed. The analysed specimens are stored in The Barcode of Life Data System (BOLD) (Ratnasingham and Hebert 2007) project '*Eupolybothrus* in Croatia' (EUCR). Genetic data for the molecular comparison of *Eupolybothrus* species were retrieved from Stoev et al. (2013). All COI-sequences were aligned using the MAFFT-plugin of Geneious 5.4.7 (Kearse et al. 2012) under the G-INS-i option proposed for less than 200 sequences with global homology. Primer sequences at the 5' and 3' ends of the alignment were manually trimmed. Molecular species delimitation was performed using two approaches.

Firstly, we used the Automatic Barcode Gap Discovery (ABGD) method of Puillandre et al. (2012). ABGD semi-automatically screens for the presence of a barcoding gap separating within-species (intraspecific) and between-species (interspecific) genetic diversity. We tested several prior combinations of relative gap width (X; ranging from 0.05 – 1.5), minimal intraspecific distance (Pmin; starting at 0.001) and maximal intraspecific distance (Pmax; 0.02 – 0.20). Pmin and Pmax refer to the parameter space where a barcoding gap can be expected, whereas X defines the width of the gap. The Kimura-2-parameter (K2P) model was used for calculating genetic distances in ABGD (Ts/Tv = 2.0).

Secondly, we applied the inverse statistical parsimony (SP) method proposed by Hart and Sunday (2007) for the molecular delimitation of species based on haplotype networks using the program TCS 1.21 (Clement et al. 2000). A connection probability of 95% was set. Conversely, this means that species, i.e. the number of unconnected haplotype networks, are delimitated by 95% statistical confidence. MEGA 6.06 (Tamura et al. 2013) was used for 1) the construction of a Neighbor-Joining (NJ) topology with the K2P substitution model under the pairwise deletion option and for the final visualization of the molecular delimitation results and 2) the calculation of inter- and interspecific K2P-genetic distances for the delineated species.

Material studied

In addition to recently collected material of a new species listed under its types below, the following material of previously named species was examined:

Eupolybothrus (*Schizopolybothrus*) *acherontis* ssp. *wardaranus* (Verhoeff, 1937): 1 ♂ Reg. Nr. A 200500641; 1 ♀ juv., slide preparation, Reg. Nr. A20030873, "Mazedonien: Skoplje" (ZSM). *Eupolybothrus* (*Schizopolybothrus*) *caesar* (Verhoeff, 1899): 1 ♂, "Greece, Korfu, K. W. Verhoeff leg.", NHMW 1452, lectotype, designated here. *Eupolybothrus* (*Schizopolybothrus*) *cavernicolus* Komerički & Stoev, 2013: Ad. ♂ Croatia, Knin, NP Krka, cave Miljacka II, 09.II.2013, M. Lukić leg., CBSS – CHP 536, holotype; 1 ♂ Croatia, Knin, NP Krka, cave Miljacka II, 21.X.2012, A. Komerički leg., CBSS – CHP 552 (specimen poorly preserved, damaged), 1 ♂ Croatia, Knin, NP Krka, cave Miljacka II, 10.IX.2015, A. Komerički leg., CBSS – CHP 570. *Eupolybothrus* (*Schizopolybothrus*) *leostygis* (Verhoeff, 1899): Ad. ♂ Croatia, Dubrovnik, Gromača, cave Špilja za Gromačkom vlakom, 29.IV.2004, R. Ozimec & H. Bilandžija leg., CBSS – CHP 406, BOLD ID: EUCR062; ♂ Croatia, Dubrovnik, Gromača, cave Špilja za Gromačkom vlakom, 27.IV.2010, M. Lukić & A. Komerički leg., CBSS – CHP 502, BOLD ID: EUCR017; ♂ Croatia, Dubrovnik, Gromača, cave Špilja za Gromačkom vlakom, 27.IV.2010, M. Lukić & A. Komerički leg., CBSS – CHP 503, BOLD ID: EUCR018. *Eupolybothrus* (*Schizopolybothrus*) *leostygis patens* (Attems, 1935): 2 ♂♂, Greece, "Epirus, Nisista (bei einer Quelle)", 01.V.1933, Beier M. leg., NHMW 1453, NHMW 8331, syntypes. *Eupolybothrus* (*Schizopolybothrus*) *spiniger* (Latzel, 1888): Ad. ♂, "Bosnien, 1887 J. Karlinski leg.", NHMW 1463, don. Latzel Nachlass 1919, lectotype designated here; 1 subad. ♂, Bosnien, 1887 J. Karlinski leg., NHMW 8830, don. Latzel Nachlass 1919, paralectotype.

Results

Order Lithobiomorpha Pocock, 1895
Family Lithobiidae Newport, 1844
Subfamily Ethopolyinae Chamberlin, 1915
Genus *Eupolybothrus* Verhoeff, 1907

***Eupolybothrus liburnicus* sp. n.**
http://zoobank.org/56310DD5-FB8E-483F-BF93-CE6AF9679CF1
Figs 1–6, 11H, 12A, C

Material. Holotype. Ad. ♂, Croatia, Obrovac, Gornji Čabrići, cave Plitka peć, under rock, 09.II.2013, A. Komerički leg., CBSS – CHP 545.

Paratypes. Croatia, Southern Velebit: 2 ♀, Obrovac, Gornji Čabrići, cave Plitka peć, 23.VI.2012, T. Vujnović, A. Komerički & R. Baković leg., CBSS – CHP 538; 6 juv., Obrovac, Gornji Čabrići, cave Plitka peć, 23.VI.2012, A. Komerički leg., CBSS – CHP 541; 2 ♂♂ subadult, Obrovac, Gornji Čabrići, cave Plitka peć, 20.III.2013, K. Miculinić & A. Komerički leg., CBSS – CHP543); 1 ♀, Obrovac, Gornji Čabrići, cave Plitka peć, 23.V.2013, P. Rade & T. Čuković leg., NHMW8409; 1♂, 1 ♀, Obrovac, Gornji Čabrići, cave Plitka peć, 23.V.2012, P. Rade leg., NMNHS CHILOPODA-2016-0003; 1 ♀, Seline, cave Markova špilja, under rock, 01.V.2010, J. Bedek leg., CBSS – CHP 407, BOLD ID: EUCR 048; 1 ♀, Obrovac, Krnjeza canyon, cave Bundalova pećina, 11.VII.2009, R. Baković leg., CBSS – CHP 448; BOLD ID: EUCR 052; 1 ♀, Obrovac, Gornji Čabrići, cave Plitka péc, 29.IX.2009, M. Hodžić leg., CBSS – CHP 457, BOLD ID: EUCR 067; 1 ♂, subadult, Obrovac, Gornji Čabrići, cave Skorupuša, 29.IX.2010, A. Ćukušić leg., CBSS – CHP 458, BOLD ID: EUCR068; 2 ♀♀, 1 juv. Obrovac, Gornji Čabrići, cave Skorupuša, 23.VI.2012, A. Komerički leg., CBSS – CHP539; 7 juv. Obrovac, Gornji Čabrići, cave Skorupuša, 23.VI.2012, A. Komerički leg., CBSS – CHP 540; 1 ♂, 1 juv. Obrovac, Gornji Čabrići, cave Rašeljkovac, 23.VI.2012, A. Komerički leg., CBSS – CHP 544; 1 ♀, Obrovac, Gornji Čabrići, cave Rašeljkovac, 20.III.2013, A. Komerički leg., ZMUC 00040236 ; 1 ♂, Obrovac, Gornji Čabrići, cave Rašeljkovac, 23.IV.2013, K. Miculinić leg., ZMUC 00040237; Mid-body segments and detached legs, Obrovac, Gornji Čabrići, cave Rašeljkovac, 23.V.2013, K. Miculinić leg., CHP: 551, NMNHS CHILOPODA-2016-0001; head and anterior segments, Obrovac, Gornji Čabrići, cave Rašeljkovac, 20.III.2013, A. Komerički leg., CHP: 547, NMNHS CHILOPODA-2016-0002.

Diagnosis. A species morphologically similar to *E. cavernicolus*, genetically differing from it by 11% interspecific distance based on COI, and morphologically differing by the slightly convex posterior margin of T14, presence of 15CxVp and 15PDp spines, and by the leg 15 to body length ratio of *ca.* 64% in the adult male.

Description. Males. Based on holotype CHP545 (light photographs) and paratype ZMUC 00040237 (SEM).

Body length: (from anterior margin of cephalic plate to posterior margin of telson) approx. 30 mm.

Colour: tawny-brown to yellowish, ventral part and legs paler (Fig. 1A).

Head: cephalic plate slightly broader than long (3.6 × 3.1 mm, respectively) and wider than T1 (Fig. 1B); surface smooth, with numerous scattered setae. Cephalic median sulcus contributing to biconvex anterior margin, marginal ridge with a median thickening; posterior margin straight to slightly concave; transverse suture situated at about 1/3rd of anterior edge; posterior limbs of transverse suture visible, connecting basal antennal article with anterior part of the ocellar area.

Ocelli: 1+14 blackish irregular ocelli in 3-4 rows; outermost first seriate ocellus largest; ocelli of the middle two rows medium-sized, those of inferior row smallest (Fig. 1C).

Tömösváry's organ: moderately large (as large as a medium ocellus), oval and situated on a sub-triangular sclerotisation below the inferiormost row of seriate ocelli.

Clypeus: showing a cluster of 25 setae situated on the apex and near the lateral margins (Fig. 2A).

Antennae: *ca*. 19.8 mm long, ultimate and penultimate articles of same length (Fig. 2B); left antenna composed of 61 articles, right antenna 57 articles; slightly surpassing posterior margin of T7 (right) or T9 (left) when folded backwards, basal two articles enlarged and less setose; the posterior 30 articles visibly longer than broad. Antenna to body length *ca*. 66%.

Forcipular segment (Figs 2C, 3A): coxosternite subpentagonal (Fig. 2C), shoulders almost absent (steep), lateral margins straight; anterior margin set off as a rim by furrow; coxosternal teeth 8+7, median diastema small, V-shaped, steep and narrow, short porodont arising from a pit below the dental rim, situated lateral to the lateralmost tooth; base of porodont as thin as adjacent tooth (Fig. 3A, ***po***); coxosternite sparsely setose anteriorly; setae moderately large, irregularly dispersed (Fig. 3A). Forcipular trochanteroprefemur, femur and tibia and proximal part of forcipular tarsungulum with several setae. Distal part of forcipular tarsungulum about 3 times longer than proximal part, *ca*. 2 mm long (Fig. 2C).

Tergites: T1 wider than long, subtrapeziform, wider anteriorly, posterior margin straight or slightly emarginated, marginal ridge with a small median thickening; TT3 and 5 more elongated than T1, posterior margin slightly emarginated medially, posterior angles rounded; posterior angles of T4 rounded; posterior margin of T8 slightly emarginated medially, angles rounded; TT6 and 7 with posterior angles abruptly rounded (Fig. 3B); TT9, 11, 13 with well-developed posterior triangular projections (Fig. 3B, C); posterior margin of TT10 and 12 distinctly emarginated, that of T14 slightly convex, all strongly setose on posterior margin; intermediate tergite hexagonal, with a membranous area reaching up the 2/3rd of its length (Fig. 11H) and posterior margin straight, lateral edges thickened and covered with setae (Fig. 4A); middle part of posterior third of tergite densely covered with setae (Fig. 5F); laterally, on both sides of the central setose area are two bare subtrapezoidal spots (Fig. 4A). All tergites smooth, setae present only along their lateral margins.

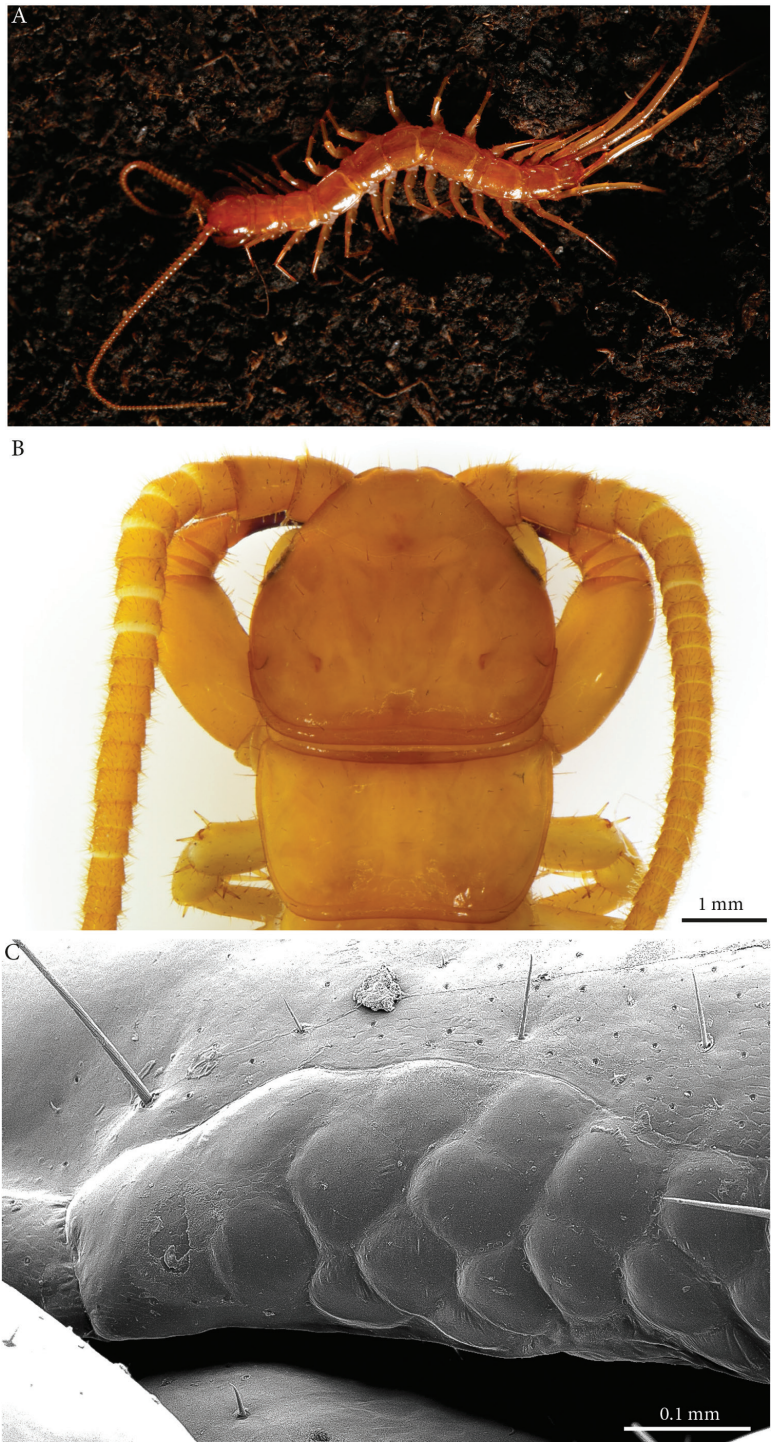

Figure 1. *Eupolybothrus liburnicus* sp. n. habitus, cephalic plate+T1 and ocelli. **A** Habitus, holotype **B** Cephalic plate and T1, holotype, dorsal view **C** Ocelli, paratype ZMUC 00040237.

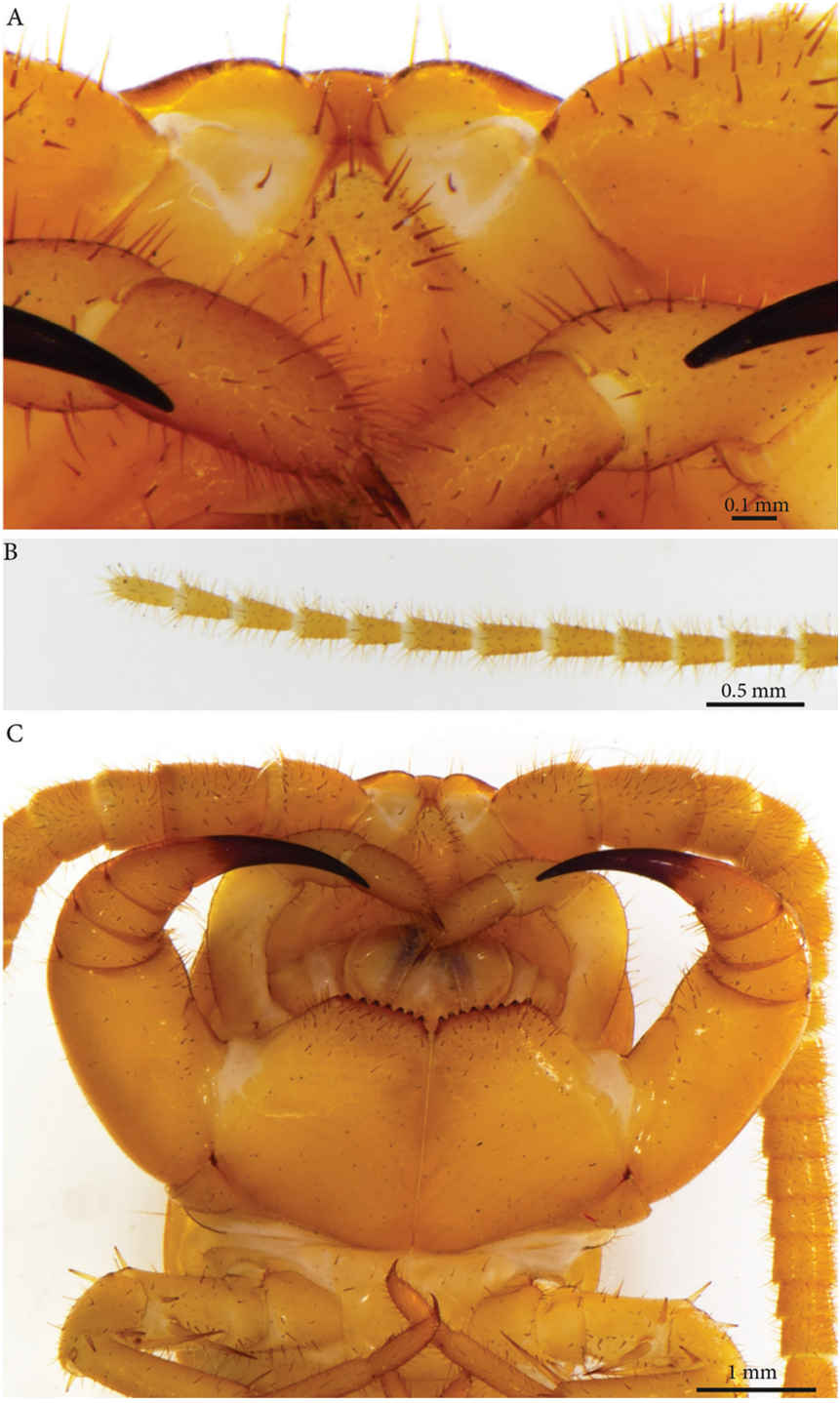

Figure 2. *Eupolybothrus liburnicus* sp. n., holotype head. **A** Clypeus, ventral view **B** Tip of antenna **C** Forcipules, ventral view.

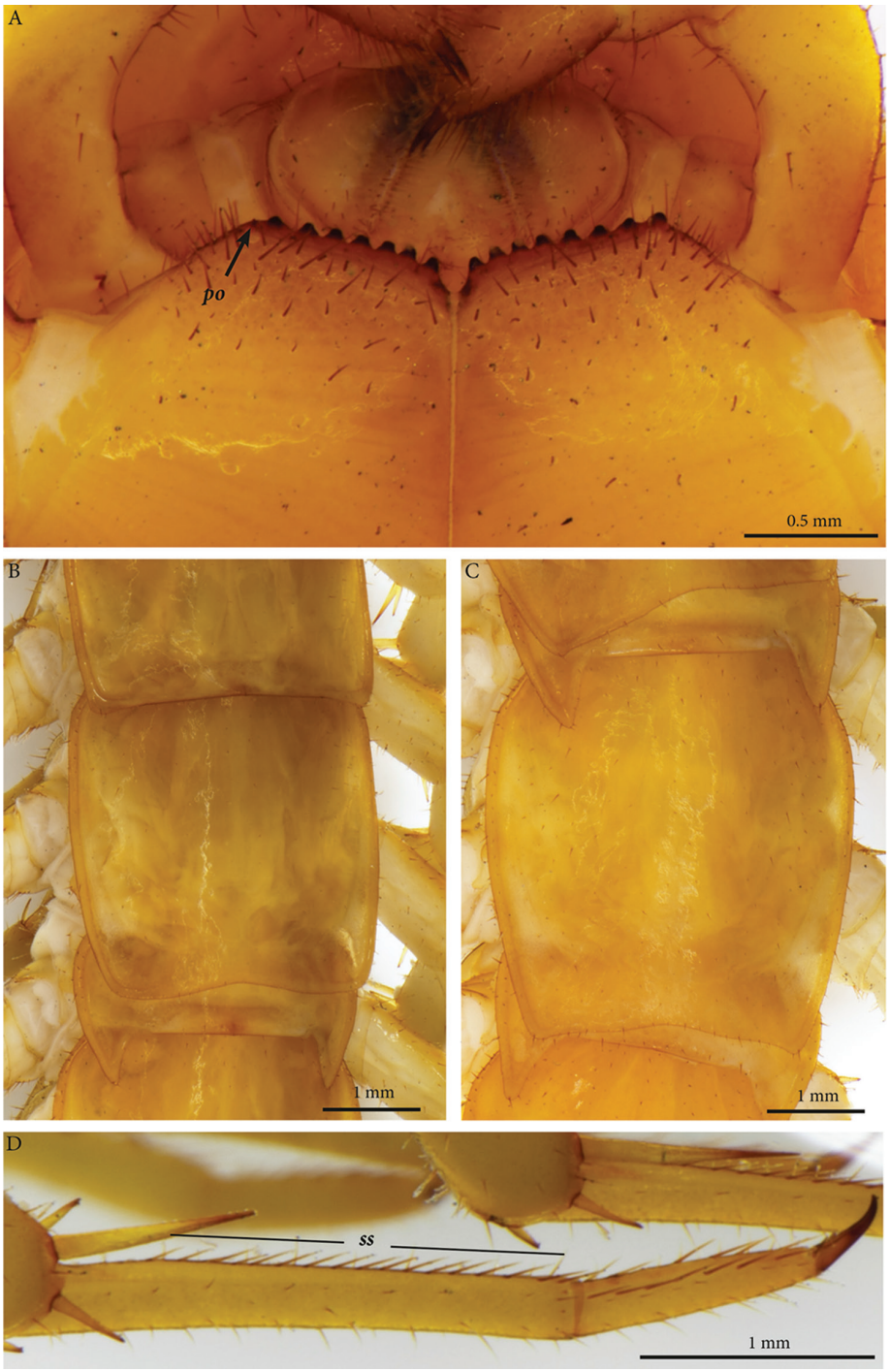

Figure 3. *Eupolybothrus liburnicus* sp. n., holotype, coxosternum, tegites and leg. **A** Close-up of coxosternum, ventral view **B** TT7-9, dorsal view **C** TT11-13, dorsal view **D** Tarsi 1, 2 and pretarsus of midbody leg. Abbreviations: ***po***: porodont, ***ss***: seriate setae.

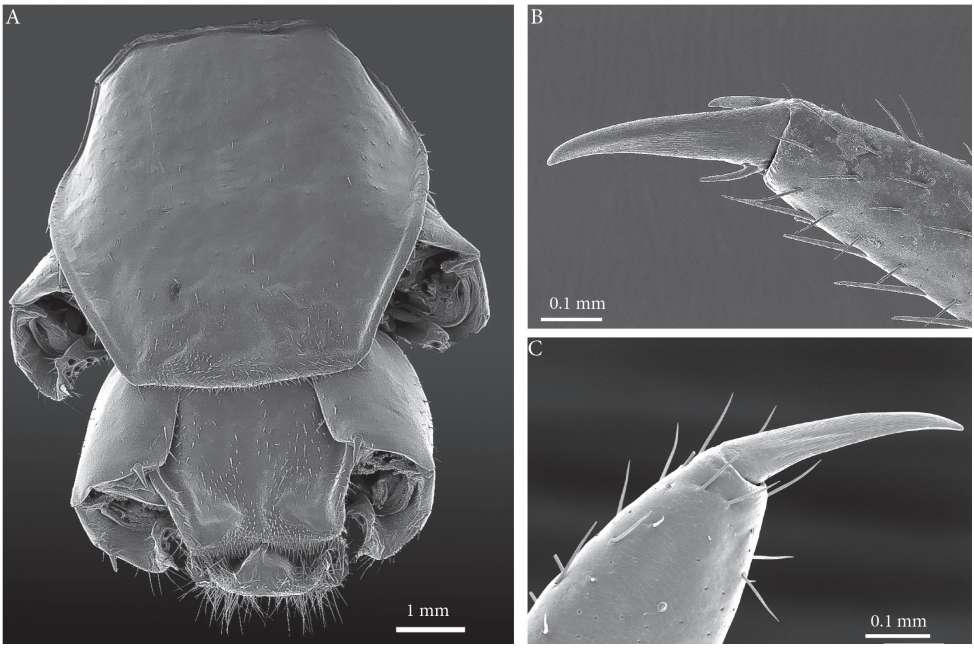

Figure 4. *Eupolybothrus liburnicus* sp. n., male paratype ZMUC 00040237, last tergites and pretarsi of leg 10 and 15. **A** T14 and intermediate tergite, dorsal view **B** Pretarsus of leg 10, dorsolateral view **C** Pretarsus of leg 15, lateral view.

Legs: leg 15 *ca*. 64% body length; leg 14 approx. 25% longer than legs 1-12, leg 13 only slightly longer than legs 1-12; pretarsus of legs 1–14 with stouter posterior accessory claw (approx. as long as fundus) and a slightly thinner anterior accessory claw (= spine, sensu Bonato et al. 2010) (Figs 4B, C); pectinal (seriate) setae missing on tarsus1 and 2 of leg 15, present in one short row on tarsus 2 of leg 14, in one row on tarsus 1 and two rows on tarsus 2 of legs 1-13, (Fig. 3D, ***ss***); pretarsus of leg 15 without accessory spines (Fig. 4C). Length of podomeres of leg 15: coxa 1 mm, prefemur 2.7 mm, femur 3.0 mm, tibia 5.3 mm, tarsus 1 4.8 mm, tarsus 2 2.3 mm, pretarsus 0.2 mm. Prefemur of leg 15 with a large proximal knob (Fig. 5A, ***pk***) protruding mediad and bearing a cluster of long setae dorsally (Figs 5B, 11H), in dorsal view the knob as broad as the prefemur, mesally continuing in a ridge reaching 2/3rd of the prefemur length and gently narrowing distad (Fig. 5A, ***pr***). Posterior edge of prefemur with a well-defined circular protuberance densely covered with short, thin setae, situated between *p* and *m* spines dorso-medially (Fig. 5A, ***cp***); rest of prefemur covered with sparse setae. Dorsal spine *p* on prefemur with furcate tip, also noticed on other podomeres and legs (Fig. 5C). Legs 1-14 without particular modifications.

Coxal pores: generally round, arranged in 6-7 irregular rows, pores of inner rows largest, size decreasing outwards; pores separated from each other by a distance more than or equal to their diameter; number of pores on leg-pair (measured on right leg) 12: 51, 13: 61, 14: 15: 44 (Fig. 5D).

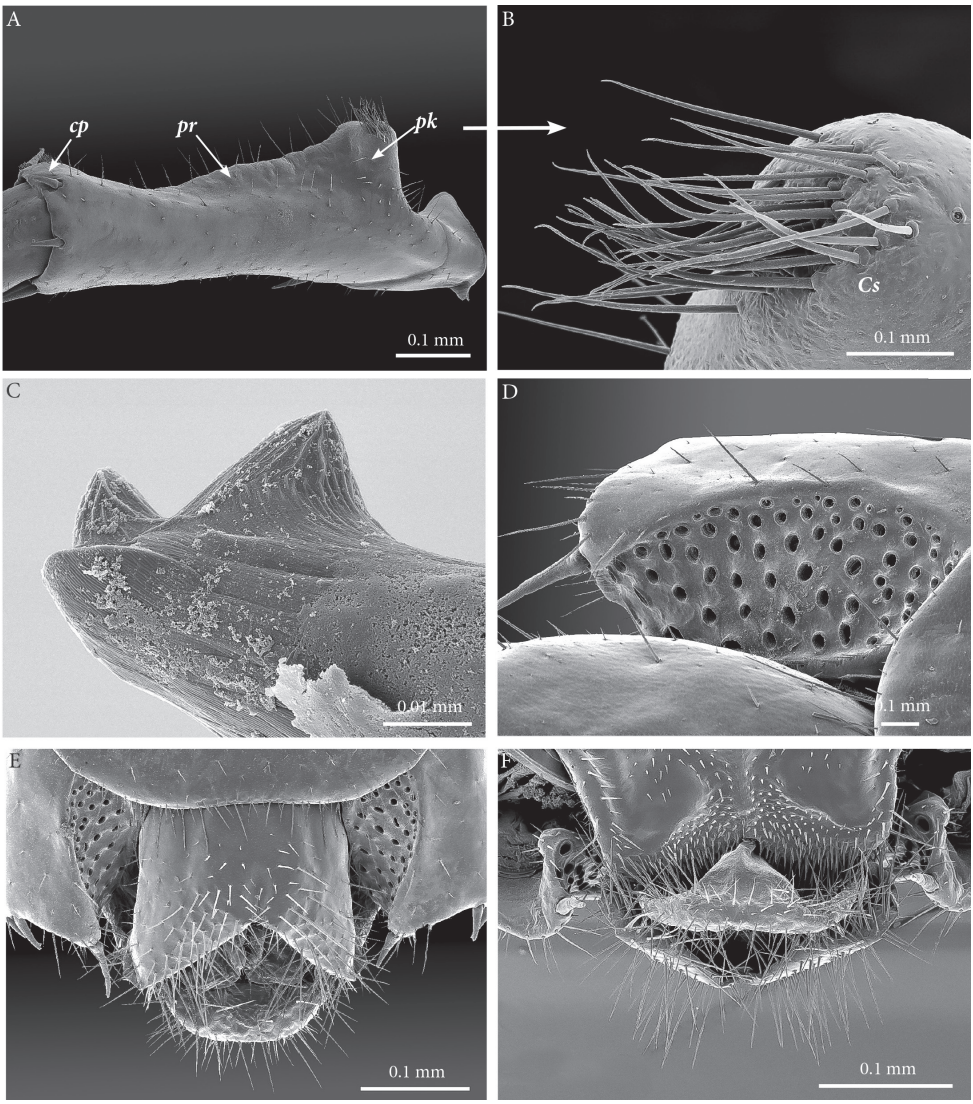

Figure 5. *Eupolybothrus liburnicus* sp. n., male paratype ZMUC 00040237, leg 15 and genital segment. **A** Prefemur 15, posteriodorsal view **B** Close-up of the setae cluster on male prefemur 15 **C** Close-up of the prefemoral spine **D** Coxal pore field, ventral view **E** Genital segment, ventral view **F** Genital segment, dorso-apical view. Abbreviations: ***cp***: circular protuberance, ***pk***: prefemoral knob, ***pr***: prefemoral ridge, ***sc***: cluster of setae.

Sternites: smooth, subtrapeziform, with few sparse setae, mainly at lateral margins; posterior margins straight.

Genitalia: posterior margin of male first genital sternite concave, posterior margin densely covered with long setae, the rest of sternite sparsely covered with shorter ones (Fig. 5E); gonopod small, concealed above sternite.

Plectrotaxy: as in Table 1.

Table 1. *Eupolybothrus liburnicus* sp. n. plectrotaxy. C – Coxa, Tr – trochanter, P – prefemur, F – femur, T – tibia, a, m, p spines in respectively, anterior, medial and posterior position.

++	Ventral					Dorsal				
	C	**Tr**	**P**	**F**	**T**	**C**	**Tr**	**P**	**F**	**T**
1			amp	amp	amp			amp	a-p	a-p
2			amp	amp	amp			amp	a-p	a-p
3			amp	amp	amp			amp	a-p	a-p
4			amp	amp	amp			amp	a-p	a-p
5			amp	amp	amp			amp	a-p	a-p
6			amp	amp	amp			amp	a-p	a-p
7			amp	amp	amp			amp	a-p	a-p
8			amp	amp	amp	a		amp	a-p	a-p
9			amp	amp	amp	a		amp	a-p	a-p
10			amp	amp	amp	a		amp	a-p	a-p
11			amp	amp	amp	a		amp	a-p	a-p
12		m	amp	amp	amp	a		amp	a-p	a-p
13		m	amp	amp	amp	a		amp	a-p	a-p
14	am	m	amp	am	a	a		amp	p	a-p
15	amp	m	amp	amp	a	a		amp	p	p

Description of the female, based on paratype NHMW 8409 (Fig. 6A, B).

Body length: *ca*. 43 mm; leg 15 *ca*. 22.8 mm or 52.9% body length.

Colour: uniformly tawny-brown to yellowish.

Head: cephalic plate broader than long (4 × 3.7 mm, respectively).

Ocelli: 18 blackish subequal ocelli in 6–7 rows.

Tömösváry's organ: moderately large (as large as or slightly larger than a medium ocellus), oval, situated slightly above the cephalic edge below the inferiormost row of ocelli.

Clypeus: with a cluster of *ca*. 25 trichoid setae situated on the apex and lateral margins.

Antennae: approx. 18.5 mm long, composed of 73 articles.

Forcipular segment: coxosternite subpentagonal, shoulders almost absent, lateral margins straight; anterior margin set off as a rim by furrow; coxosternal teeth 9+8.

Tergites: T1 wider than long, subtrapeziform, wider anteriorly, posterior margin straight or slightly emarginated, marginal ridge with a small median thickening; TT3 and 5 more elongated than T1, posterior margin slightly emarginated medially, posterior angles rounded; posterior angles of T4 rounded; posterior margin of T8 slightly emarginated medially, angles rounded; TT6 and 7 with posterior angles abruptly rounded; TT9, 11, 13 with well-developed posterior triangular projections; posterior margin of TT10 and 12 slightly emarginated, that of T14 transverse, all with scarce setae on posterior margin; intermediate tergite hexagonal, posterior margin slightly concave, lateral edges setose, its surface with scattered setae in a few rows located on the lateral margins and the posterior half (Fig. 6A). The rest of the tergites smooth, setae present only on lateral margins.

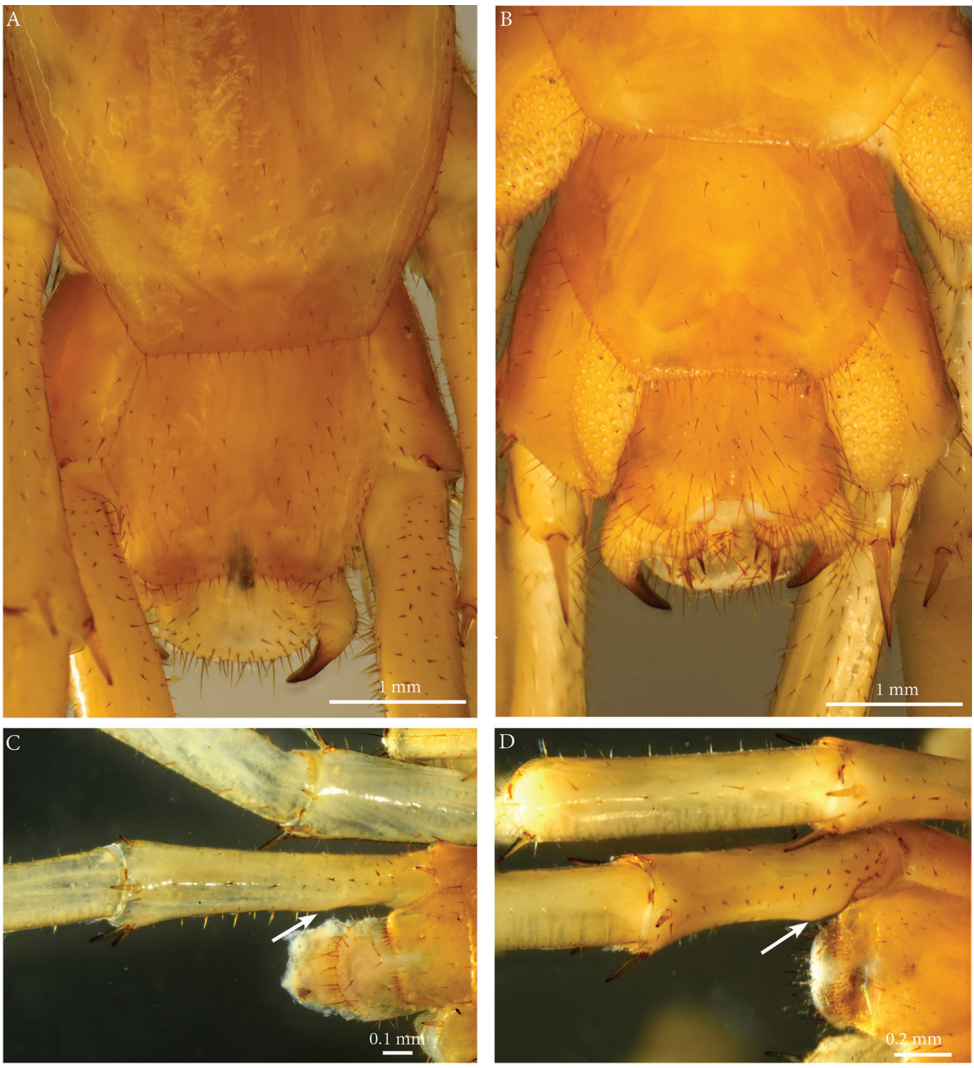

Figure 6. *Eupolybothrus liburnicus* sp. n., A, B, female paratype NHMW 8409. **A** Intermediate and terminal tergite, dorsal view **B** Female terminal sternite and gonopods **C, D** Iimmature males **C** CHP544 **D** CHP543. Arrows point to incipient proximal knob.

Legs: leg 15 longest *ca.* 22.8 mm, 53% of body length; leg 14 *ca.* 17 mm, leg 13 *ca.* 10.6 mm only slightly longer than legs 1–12, midbody leg (*ca.* 10 mm); pretarsus of legs 1–14 with a more expanded fundus, larger posterior accessory claw (approx. 1/3rd of fundus) and a slightly thinner and shorter anterior accessory claw; pectinal (seriate) setae lacking on tarsi 1 and 2 of leg 15, present in one short row on tarsus 2 of leg 14, and in one row on tarsus 1 and two rows on tarsus 2 of legs 1-13; pretarsus of leg 15 without accessory spines. Leg 15 slender and elongate, without particular modifications.

Coxal pores: generally round, forming 6-7 irregular rows, pores of inner rows largest, size decreasing outwards; pores separated from each other by a distance more than or equal to their own diameter (Fig. 6B).

Sternites: smooth, subtrapeziform, with few sparse setae, mainly at lateral margins; posterior margins straight.

Female gonopods: densely setose, with 2+2 long, slim and pointed spurs slightly bent and a single blunt claw; outer spur 1.5 longer than the inner one, approx. 5 times longer than broad at base (Fig. 6B).

Etymology. *Liburnicus* denotes „of Liburnia", a district in the coastal region of the northeastern Adriatic; adjective.

Variation. The proximal knob on the male prefemur is substantially smaller in immature males than in mature specimens. For example, CHP544 (body length 11.6 mm) has the prefemoral knob represented by only a low swelling that lacks setae (Fig. 6C), and the medial ridge extending from that swelling is low but distinct; the posterior circular, setose protuberance of adults is indistinct at this size. The posterior part of T14 bears relatively sparse setae, but the tergite of the intermediate segment has a field of dense setae on each side of the midline, and leg 15 is 61% of body length (versus 64% in the holotype). In a male of body length 8.8 mm (CHP543), the prefemur has only a faint bulge in the position of the proximal knob (Fig. 6D), but the tergite of the intermediate segment has a fringe of dense setae on each side of the desclerotized median strip. The female gonopods display spurs with a consistent number (2+2) and sharp, slender shape, with the outer spur on the order of 1.5 times the length of the inner spur. Forcipular teeth are most numerous in the largest specimens, with 6+6 or 7+7 teeth the usual number in specimens less than 25 mm long; some small specimens (e.g., CHP457, body length 10.4 mm) have only 5+5 teeth.

Habitat. *E. liburnicus* sp. n. is here recorded from five caves of the Velebit Mountain, Croatia. Four of these (Plitka peć, Skorupuša, Rašljekovac and Bundalova pećina) are situated in the area where the southern slopes of the Crnopac Massif meet the Krupa River canyon while one of them, Markova špilja, is a small anchialine cave situated a few hundred meters from the Adriatic coast near the village of Seline.

The type locality is Plitka peć (Fig. 7), a cave near the village Gornji Čabrići, Obrovac, Zadar County, Croatia. It was formed in Paleogene and Neogene limestone breccias. The cave is small, approx. 30 m long, with a large entrance and a thick layer of sediment on the floor, rich in flowstone and speleothems. The climatic conditions in Plitka peć as measured on 29 September 2010 are as follows: air temperature=12.7° C, sediment temperature=11.4° C, relative humidity=100%. The specimens were collected in both photic and aphotic zones, under stones and in the sediment. The cave is inhabited by spiders of the family Linyphiidae; Pseudoscorpiones: *Neobisium elegans* Beier, 1939, *Chthonius* (*Globbochthonius*) sp.; Isopoda: *Alpioniscus* sp., *Androniscus* sp., *Cyphopleon* sp., Collembola: Neelidae, Tullbergiidae, *Lepidocyrtus* sp. (Bregović et al. 2013).

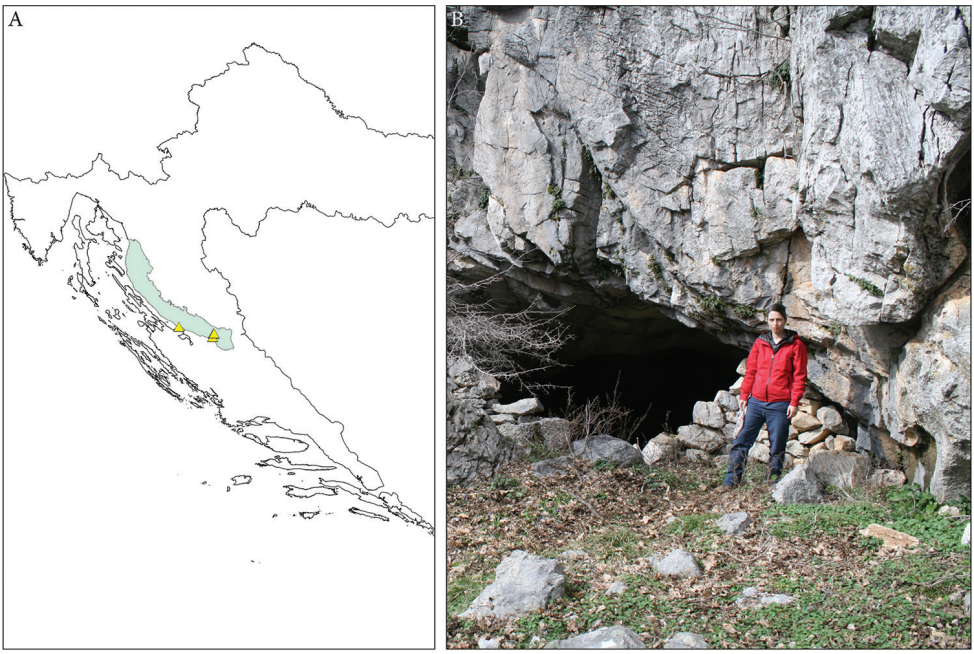

Figure 7. Occurrence of *E. liburnicus* sp. n. in Croatia. **A** Collecting sites (yellow triangle) **B** Entrance of the cave Plitka peć, type locality of *E. liburnicus* sp. n. (photo by K. Miculinić).

Other species

***Eupolybothrus spiniger* (Latzel, 1888)**
Figs 8, 11E

Lithobus spiniger Latzel, 1888: 93.

Material. Lectotype. adult ♂, Bosnia and Herzegovina, 1887, J. Karlinski leg., NHMW 1463, new designation. **Paralectotype**. 1 subadult ♂, Bosnia and Herzegovina, 1887, J. Karlinski leg., NHMW 8330.

Original description (translated from Latin). '*Robust, slightly punctate to smooth, posteriorly granulate, chestnut to reddish-brown; glossy. Two antennae slightly elongate, with 50-56 articles. Ocelli on each side: 16-19 (1 + 4, 4, 4, 3 - 1 + 4, 5, 5, 3, 1), in 4-5 longitudinal rows. Forcipular coxosternum: with 14-22 short teeth (7 + 7 - 11 + 11). Tergites 9, 11, 13 with posterior pointed projections, 14 with irregular margin, gradually narrowing posteriad in two pointed projections; coxal pores numerous, round, placed in irregular rows. Ultimate legs: elongate and robust with simple claw; spines: 1, 1, 4, 2, 0-1, coxa with 3 spines on lateral margins. In male ultimate legs, third article (femur) with a large protuberance anteriorly, and indented internal margins. Female: 28-35 mm long, 3.5-4 mm broad.*'

Descriptive notes based on the lectotype. Specimen with broken antenna; 15th legs detached, missing terminal articles, left legs 1, 3, 5 and part of the left forcipule missing.

Body length: (from anterior margin of cephalic plate to posterior margin of telson) *ca.* 33 mm.

Colour: reddish brown, head and first tergite darker.

Head: cephalic plate slightly broader than long (3.5 × 3.8 mm, respectively) and wider than T1 (Fig. 8B); surface smooth, with marks of scattered setae. Cephalic median sulcus contributing to biconvex anterior margin, marginal ridge with a median thickening; posterior margin straight to slightly concave; transverse suture situated at about 1/3rd of anterior edge; posterior limbs of transverse suture visible, connecting basal antennal article with anterior part of the ocellar area.

Ocelli: 18, blackish, in 4 irregular rows; outermost first seriate ocellus largest; ocelli of the middle two rows medium-sized, those of inferior row smallest.

Tömösváry's organ: moderately large (as large as a medium ocellus), oval and situated on a sub-triangular sclerotisation below the inferiormost row of seriate ocelli.

Clypeus: showing a cluster of 30 setae situated on the apex and near the lateral margins (Fig. 8C).

Antennae: Broken, with more than 54 articles.

Forcipular segment: Coxosternum with 9+9 teeth and a porodont situated lateral of the distalmost tooth on both sides (Fig. 8D, E).

Tergites: T1 wider than long, subtrapeziform, wider anteriorly (Fig. 8B), posterior margin straight or slightly emarginated, marginal ridge with a small median thickening; TT3 and 5 more elongated than T1, posterior margin slightly emarginated medially, posterior angles rounded; posterior angles of T4 rounded; posterior margin of T8 slightly emarginated medially, angles rounded (Fig. 8F); TT6, 7 without posterior projections (Fig. 8G), TT9, 11, 13 with posterior triangular projections (Fig. 8A, H), T14 with posterior margin gradually narrowing into two sub-triangular projections densely covered with setae indicated by marks on tergites (Fig. 8H); intermediate tergite hexagonal, posteriorly emarginated; median part with evident setal marks, laterally with two sub-triangular setae-free spots.

Legs: leg 15 18.4 mm long, *ca*. 56% of body length; pectinal (seriate) setae missing on tarsus1 and 2 of leg 15, present in one short row on tarsus 2 of leg 14, in one row on tarsus 1 and two rows on tarsus 2 of legs 1-13 (Fig. 8I, ***ss***). Prefemur of leg 15 with a large proximal knob (Fig. 8J, ***pk***) protruding mediad and possibly bearing a cluster of setae on tip (all setae broken but indicated by marks on prefemur), in dorsal view the knob is less broad than the prefemur and not as round as in *E. caesar* and *E. leostygis*. Mesial ridge thin, reaching 2/3rd the length of the prefemur, gently narrowing distad. Posterior edge of prefemur with a circular protuberance between *p* and *m* dorso-laterally (Fig. 8K, ***cp***); rest of prefemur with obvious marks of setae.

Coxal pores: generally round, arranged in 6-7 irregular rows, pores of inner rows largest, size decreasing outwards; pores separated from each other by a distance more than, or equal to their diameter (Fig. 8L).

Sternites: smooth, subtrapeziform, with few sparse setae, mainly at lateral margins; posterior margins straight.

Figure 8. *Eupolybothrus spiniger* Latzel 1889, lectotype NHMW 1463. **A** habitus **B** Cephalic plate, dorsal view **C** Clypeus, ventral view **D** Cephalic plate, ventral view **E** Close-up of the coxosternum, ventral view **F** Tergites 6-8, dorsal view **G** Tergites 9-12, dorsal view **H** Tergites 14-15, dorsal view **I** Tarsi 1, 2 and pretarsus of midbody leg **J** Prefemur of leg 15, ventral view **K** Close-up of the circular protuberance **L** Sternite 14 and intermediate sternite, ventral view. Abbreviations: ***cp***: circular protuberance, ***ss***: seriate setae, ***pk***: prefemoral knob.

Genitalia: posterior margin of male first genital sternite concave, broadly V-shaped, posterior margin densely covered with long setae, the rest of sternite sparsely covered with shorter setae (Fig. 8L). Gonopod small, not depicted.

Remarks. *E. spiniger* has not been collected since Latzel's original description. The type material consists of two syntypes – an adult male and a juvenile - collected in Foča (a town within Republika Srpska, coordinates: 43°30'N, 18°47'E) at approximately 1000 m altitude (Latzel 1888). Stoev et al. (2010) regarded *E.* (*Schizopolybothrus*) *spiniger* as a species of uncertain taxonomic status, presuming it to be a possible senior synonym of *E. caesar* (Verhoeff, 1899), and emphasizing the importance of the examination of the type material. Having now the opportunity to examine the types of *E. spiniger*, we were able to compare it directly with *E. caesar* and conclude that the species is valid, differing from *E. caesar* in several morphological traits, notably the distinctive sub-triangular projections on tergite 14 (see Table 2, Fig. 8H).

Eupolybothrus wardaranus (Verhoeff, 1937), stat. nov.

Figs 9, 11F

Eupolybothrus acherontis wardaranus Verhoeff, 1937: 100.

Material. Syntypes. 1 ♂ Reg. Nr. A 200500641; 1 ♀ juv., slide preparation, Reg. Nr. A20030873, "Mazedonien: Skoplje" (ZSM).

Descriptive notes based on the syntype ♂. Body length: (from anterior margin of cephalic plate to posterior margin of telson) approx. 29.2 mm.

Colour: uniform, yellowish brown.

Head: cephalic plate slightly broader than long (2 × 2.5 mm, respectively) and wider than T1; surface smooth, with scattered setae. Cephalic median sulcus contributing to biconvex anterior margin, marginal ridge with a median thickening; posterior margin straight to slightly concave; transverse suture situated at about 1/3rd of anterior edge; posterior limbs of transverse suture visible, connecting basal antennal article with anterior part of the ocellar area.

Ocelli: 18–20, pale, in 4 irregular rows; outermost first seriate ocellus largest; ocelli of the middle two rows medium-sized, those of inferior row smallest.

Tömösváry's organ: moderately large (as large as a medium ocellus), oval and situated on a sub-triangular sclerotisation below the inferiormost row of seriate ocelli.

Clypeus: showing a cluster of *ca*. 25 setae situated on the apex and near the lateral margins.

Antennae: 10.4 mm, with 80 (left) and 79 (right) articles.

Forcipular segment: Coxosternum with 11+10 teeth and a porodont situated lateral of the distalmost tooth.

Tergites: T1 wider than long, subtrapeziform, wider anteriorly, posterior margin slightly emarginated, marginal ridge with a small median thickening; TT3 and 5

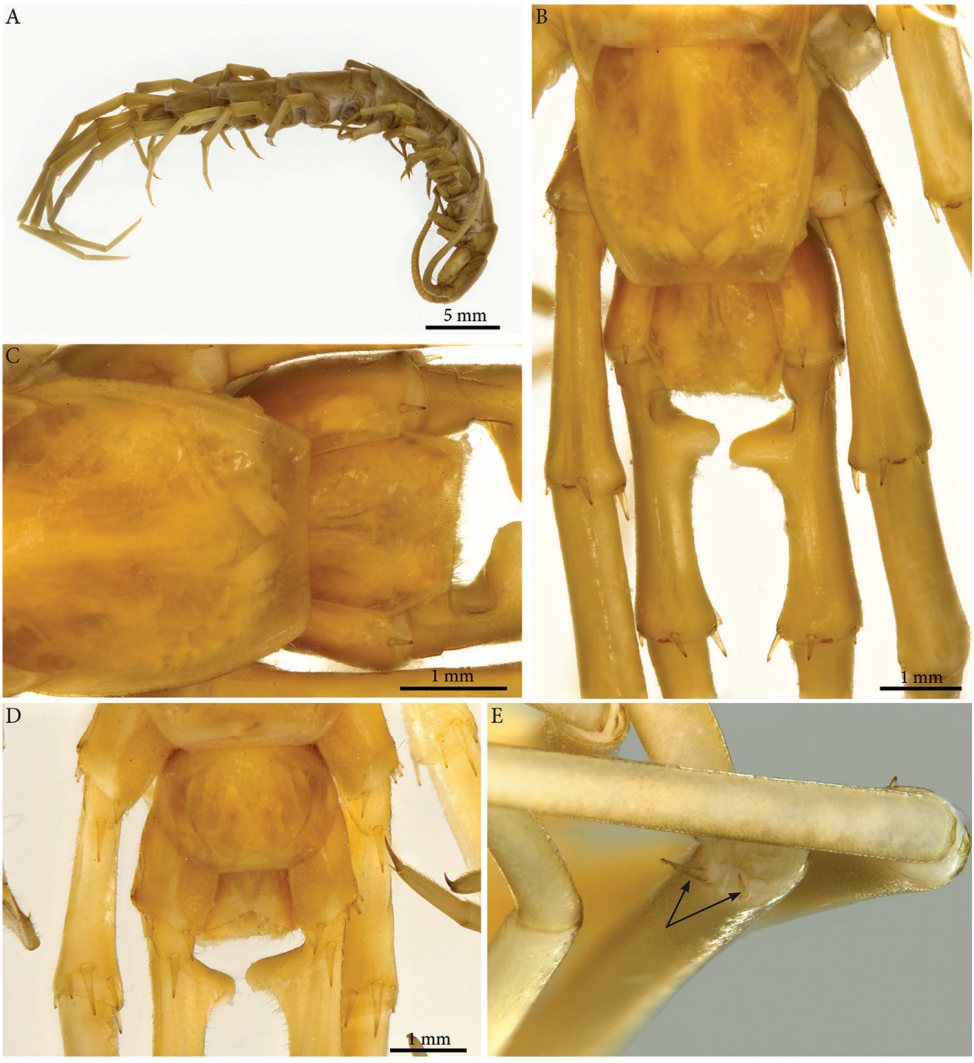

Figure 9. *E. wardaranus*, male syntype. **A** Habitus **B** Terminal part, dorsal view **C** TT14-15, dorsal view **D** Sternites 14-15, ventral view **E** Tibia of leg 15. Arrows pointing to the ventral spines.

more elongated than T1, posterior margin slightly emarginated medially, posterior angles rounded; posterior angles of T4 rounded; posterior margin of T8 slightly emarginated medially, angles rounded; TT6 and 7 with posterior angles abruptly rounded; TT9, 11, 13 with well-developed posterior triangular projections; posterior margin of TT10 and 12 slightly emarginated and 14 almost straight (Fig. 9C); intermediate tergite hexagonal, with a broad median groove narrowing distad and posterior margin almost straight, lateral edges thickened and covered with setae; middle part of posterior third of tergite densely covered with setae; laterally, on both sides of the central

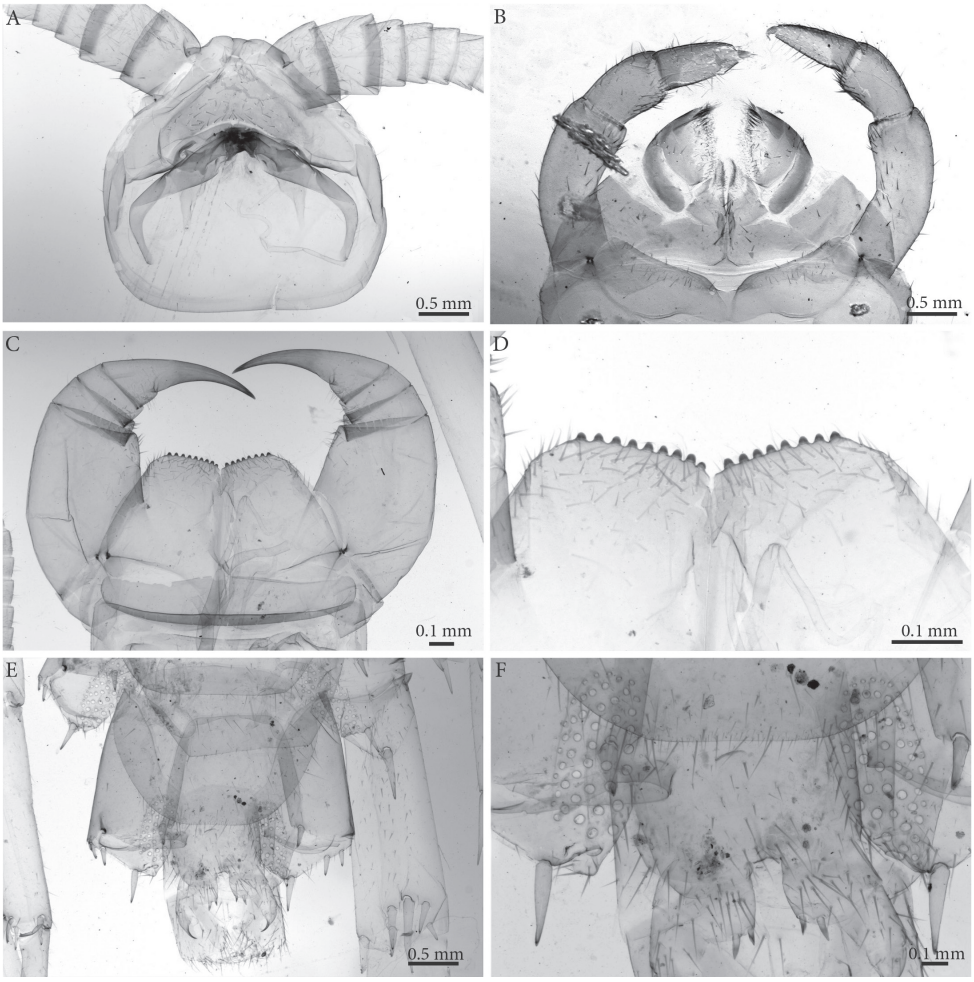

Figure 10. *E. wardaranus*, female syntype. **A** Cephalic plate ventral showing clypeus and mandibles **B** Maxillae **C** Forcipular coxosternum **D** Close-up of the tooth plate **E**, **F** Terminal segments and genitalia, ventral view.

setose area there are two specific bare subtrapezoid spots. All tergites smooth, setae present only along their lateral margins.

Legs: leg 15 10.9 mm long, *ca*. 37% of body length; pectinal (seriate) setae missing on tarsus 1 and 2 of leg 15, present in one short row on tarsus 2 of leg 14, in one row on tarsus 1 and two rows on tarsus 2 of legs 1-13. Tibia with two ventral spines (Fig. 9E). Prefemur of leg 15 with a large proximal knob (***pk***) protruding mediad and bearing long scattered setae on tip (Fig. 9B). Mesial ridge thin, extending 2/3 of prefemur length, gently narrowing distad. Posterior margin of prefemur without circular protuberance between *p* and *m* dorso-medially; rest of prefemur with obvious marks of setae.

Coxal pores: generally round, arranged in 5 irregular rows, pores of inner rows largest, size decreasing outwards; pores separated from each other by a distance more than, or equal to their diameter.

Sternites: smooth, subtrapeziform, with few sparse setae, mainly at lateral margins; posterior margins straight.

Genitalia: posterior margin of male first genital sternite concave, broadly V-shaped, posterior margin densely covered with long setae, the rest of sternite sparsely covered with shorter setae. Gonopod not depicted.

Description of the syntype ♀, based on the slide A20030873 (ZSM) (Fig. 10). The slide preparation contains the cephalic plate with mandibles *in situ*, maxillae (Fig. 10B), forcipular segment and terminal segments of a female syntype.

Clypeus: with a cluster of *ca*. 30 setae situated on the apex, near the lateral margins and smaller one scatted over the surface (Fig. 10A).

Forcipular segment: Coxosternum with 8+9 teeth and a porodont situated lateral of the distalmost tooth (Fig. 10C, D).

Female gonopods: densely setose, with 2+2 long and pointed spurs slightly bent and a single claw; outer spur 1.5 times longer than the inner one (Fig. 10E, F).

Remarks. Although originally described as a subspecies of *E. acherontis*, both the nominate subspecies as well as *E. acherontis wardaranus* have subsequently been suspected to be junior synonyms of *E. caesar* (Stoev 2001a, b). Re-examination of its types now shows that *E. wardaranus* can be distinguished from *E. caesar* by the presence of a distomedial projection on the leg 14 prefemur in the latter species (Fig. 11A), versus its absence in *E. wardaranus* (Fig. 9B), and especially by the paired ventral spines on the tibia in *E. wardaranus* (Fig. 9E). *E. caesar* also has a swelling on the dorsal proximalmost part of the leg 15 prefemur (proximal to the knob; Fig. 11A) that is less developed in all other species, including *E. wardaranus* (Fig. 11F). Since *E. acherontis* is known only from a female, the subspecific classification of Verhoeff is difficult to uphold. Accordingly, *E. wardaranus* is treated as a valid species herein.

Notes on the taxonomy of the subgenus *Schizopolybothrus*

The taxonomy of the subgenus *Schizopolybothrus* remains unsolved though it has been recently discussed on two occasions (Stoev et al. 2010, 2013). Among the taxa placed in this subgenus, *E. acherontis* and *E. stygis* remain of uncertain taxonomic status. Except for *E. tabularum* (Fig. 11D), all known members of the subgenus *Schizopolybothrus* exhibit modifications on the prefemur of ultimate legs in adult males (Fig. 11). The shape and arrangement of setae on the distinct proximal knob of the prefemur, the shape of the ridge on the prefemur, and presence of a circular protuberance with short setae on the distal dorsal part of the prefemur in males are the main distinctive characters for the members of this subgenus. This raises the question whether *E. tabularum* is indeed a member of the same group of species.

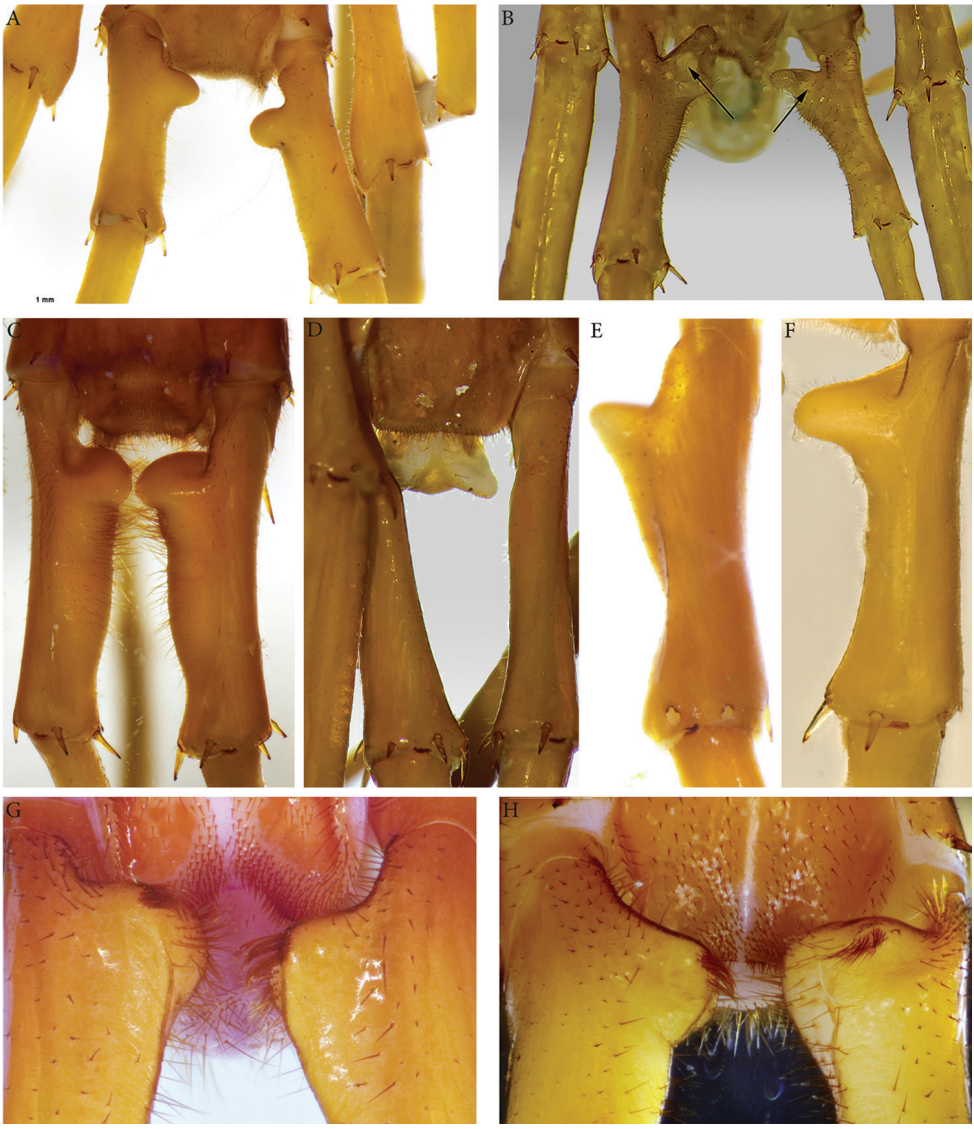

Figure 11. Prefemur of male leg 15 and intermediate tergite, dorsal view. **A** *Eupolybothrus caesar*, syntype **B** *E. excellens* **C** *E. leostygis* **D** *E. tabularum* **E** *E. spiniger*, lectotype **F** *E. wardaranus* **G** *E. cavernicolus*, male holotype **H** *E. liburnicus* sp. n., male holotype. (Figs B and D after Stoev et al. 2010 ZooKeys, https://doi.org/10.3897/zookeys.50.504)

Morphology

Morphological descriptions of species of the genus *Eupolybothrus* have traditionally relied on a number of standard external characters broadly used in lithobiomorph taxonomy (Tobias 1974, Andersson 1981) such as body length, length and width of cephalic plate, number of antennal articles, ocelli, coxosternal teeth, setae on clypeus,

Table 2. Comparison of standard taxonomic characters in six species of *Eupolybothrus* subgenus *Schizopolybothrus*.

			***E. liburnicus* sp. n. Holotype (CHP545)**	***E. leostygis***	***E. caesar***	***L. spiniger* Lectotype (NHMW1463)**	***E. cavernicolus***	***E. wardaranus* Syntype male (Nr. A 200500641)**
Body length (mm)			30	33–40	24.1 – 31,6	33	22.6–30	29.2
Head	**Cephalic plate**	L/W (mm)	3.1/3.6	3.3–4.6/3.0–3.8	2.4–3.7/2.4–3.8	3.5/3.8	3.6/4.0	2/2.5
	Antennae	Articles L-R	61–57	73–78	51–58	>54	>61–71	80
		Length	19.8	19.8–28.3 (min)	16,5	broken	20,0–24,0	10.4
	Ocelli	number	15	6–7	18–22	R 18	1+14	18–20
		rows	3	1–2	4	4	4	4
	Coxosternum	teeth	7+8	9+10 - 11+10	7+8 - 9+9	9+9	8+8	10+11
		setae/side	36	32–48	26–30	broken	22–35	*Ca*. 27
	Clypeus	setae	25	20–35	20–21	cca 30	25–30	25
Coxal pores number/rows	**12th coxa**	pores/rows	51/6	41–48/5–6	31–34/4–6	44/7	33–36/4–5	62/6–7 (right)
	13th coxa	pores/rows	61/6	51/6–7	43–56/5–6	53/7–8	41–44/4–5	55/75–6 (right)
	14th coxa	pores/rows	67/7	59–72/6–7	52–70/5–6	60/7–8	49–52/4–5	74/6–7 (right)
	15th coxa	pores/rows	44/6	49–71/5–6	40–48/5–6	37/6	34–39/4–5	55/5–6 (right)
Ultimate legs	**Coxa**	L/W (mm)	1/0.5	1.0–1.3/0.4–0.5	0.7–1.0/0.3–0.5	1/0.5	1.0–1.5/0.3–0.5	1.07/0.5
	Prefemur	L/W (mm)	2.7/0.8	3.3–4.3/0.7–0.9	2.3–3.0/0.6–0.8	3.6/0.7	2.4–3.7/0.8	1.87/0.5
	Femur	L/W (mm)	3/0.6	5.0–6.4/0.7	2.6–3.7/0.5–0.7	3.4/0.7	3.4–4.0	2.1/0.4
	Tibia	L/W (mm)	5.3/0.6	6.0–7.8/0.5–0.7	3.0–4.4/0.5–0.7	4.3/0.7	4.3–5.2	2.37/0.3
	Tarsus 1	L/W (mm)	4.8/0.5	5.3–7.9/0.3–0.5	2.8–4.3/0.5	3.9/0.4	3.8–5.0	2.69/0.3
	Tarsus 2	L/W (mm)	2.3/0.4	3.2–4.8/0.2–0.4	2.4–2.8–0.4	1.9/0.3	2.4–3.0	1.57/0.2
	Pretarsus	L/W (mm)	0.2	0.4–0.6	0.3–0.4	0.3	0.25–0.4	0.3
Antenna/body (%)			*Ca*. 66	>70	*Ca*. 52	–	*Ca*. 75–80	*Ca*. 3
Ultimate leg length			19.3	23.2 – 33.1	13.6 – 19.6	18.4	22.5	11.9
Ultimate legs/body length			*Ca*. 64%	*Ca*. 75%	*Ca*. 58%	*Ca*. 56%	*Ca*. 74%	*Ca*. 37%
Setae on intermediate tergite			Concentrated on posterior margin and on sides of median membranous area, two distinct subtriangular bare fields laterally.	Posterior margin completely covered with dense setae extending anteriad	Concentrated on posterior margin, rare setation, without visible bare fields	Present, concentrated on posterior margin	Wide area of posterior margin completely covered with dense setae, two distinct roundish bare fields laterally.	Concentrated on posterior margin, more setose medially

coxal pores on legs 12–15, shape of T1 and presence of setae on T14. Providing a valuable overview on the external anatomy of the species, these characters might also be subject to intraspecific variation related to postembryonic development and animal life stage, which renders species identification sometimes impossible or even erroneous when solely relying on them. To address these shortcomings, standard measurements of ratios, also hitherto used in the taxonomy of Lithobiomorpha (Andersson 1981) e.g. antenna and ultimate leg length to body length, as well as length and width of the cephalic plate can be informative for discerning the different taxa (see Table 2).

Focusing on the species attributed to the subgenus *Schizopolybothrus*, we additionally examined the arrangement of setae on the 14th and intermediate tergite and the shape of its posterior margin in males as well as the presence of lateral setae-free areas (e.g. Figs 11G, H). Males of *E. spiniger* are distinguished by two very noticeable sharp projections on T14 – usually straight in most species – and which were well documented by Latzel (1888) and illustrated here on the type specimen (Fig. 8H).

The sexual modification on leg 15 in males in *Schizopolybothrus* was very likely first recorded by Attems (1935) when he described *E. leostygis patens* – a subspecies which is now considered a junior synonym of *E. caesar* (see Zapparoli 1984) – as a setose round protuberance between spines *p* and *m* on the dorsal side of prefemur ("….behaarte Kegel zwischen Dornen p und m."). In other species of the subgenus *Schizopolybothrus*, the distal setose circular prefemoral protuberance was detected in *E. caesar*, *E. leostygis*, *E. spiniger*, *E. cavernicolus* and *E. liburnicus* sp. n., situated between the DPm and DPp spines (e.g., Figs 12A, B). It shows subtle variation in size and shape. Further examination of additional species will determine the taxonomic value of this character, as it is also present in congeners that have been classified as other subgenera. For example, Eason (1983: 120, fig. 12) described and figured this structure in *E. herzegowinesis* (confirmed in NHMW1456, Monte Gargano, Apuglia, Italy) and Attems (1902) mentioned it when he described the species *E. werneri* (Attems, 1902) (confirmed in NHMW1430, Parnes, Greece). Verhoeff (1937) described a similar morphology ("… in der Mitte innen angeschwollen und mit Haarbüschel") in *E. electrinus*, a synonym of *E. imperialis* (Meinert, 1872).

The presence of 'a knob' or a swelling on the proximal prefemur of the ultimate legs was first mentioned by Latzel (1888) when he described *E. spiniger* and it was subsequently noted for *E. leostygis, E. caesar, E. excellens, E. cavernicolus* and some other taxa which are now considered their synonyms. The knob extends meso-laterally on the proximal part of the prefemur and exhibits a typical shape for each species. It may be surmounted by a tuft of setae, surrounded by a subapical swirl of setae or covered with scattered ones. An additional feature of the prefemur is also noted, *viz*. 'a prefemoral ridge' situated dorso-medially and typically extending distad along two-thirds the length of the prefemur. A comparison of this trait within species of the subgenus *Schizopolybothrus* is given in Table 3.

The new species, *Eupolybothrus liburnicus* sp. n., is morphologically and genetically closest to *E. cavernicolus* (Tables 2 and 3). The two species were collected less than 100 km apart in caves with similar but not identical habitat conditions. Morphologically,

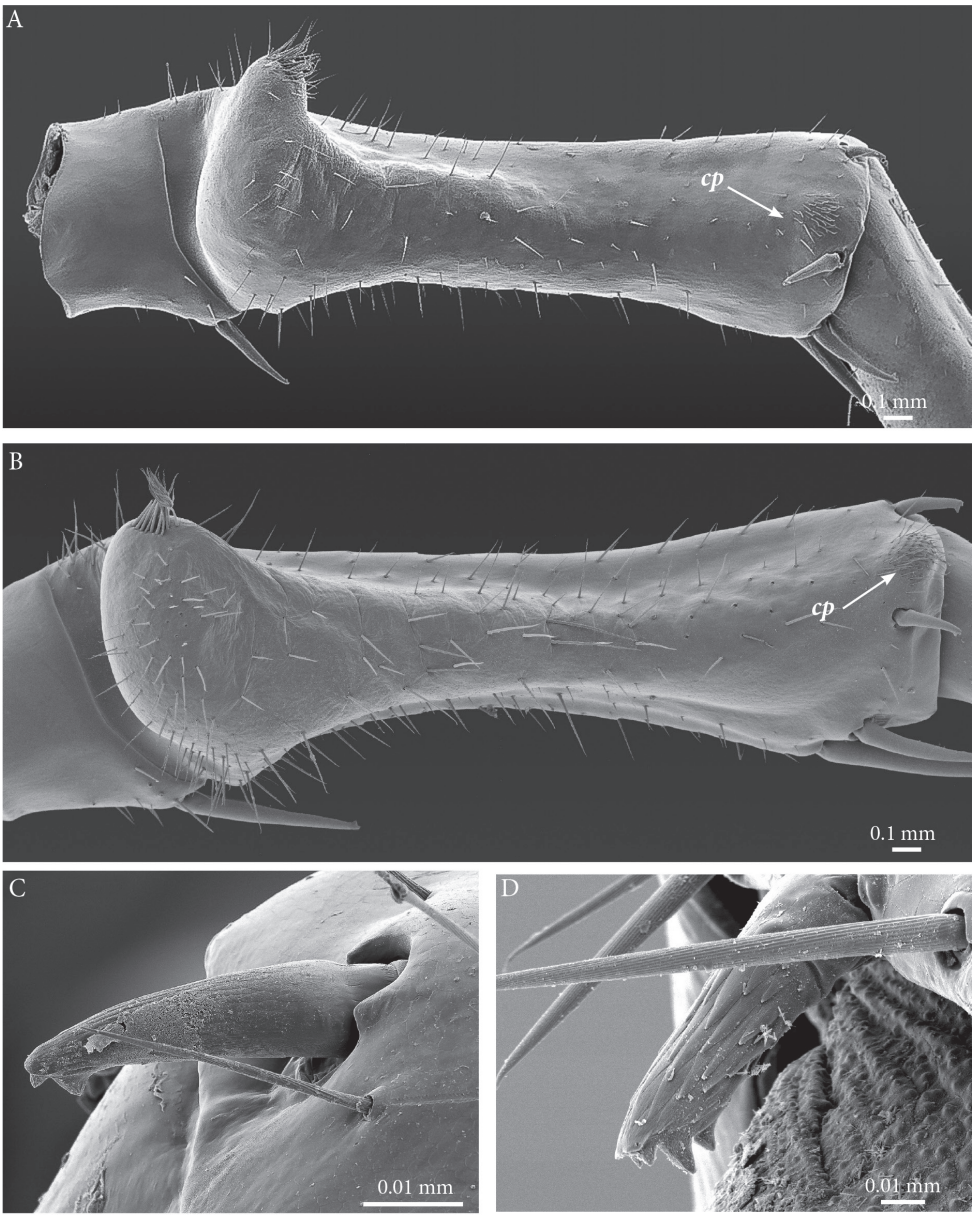

Figure 12. Prefemur of male leg 15 in mediolateral view (**A, B**) and close up of prefemoral spine (**C, D**). **A** *E. liburnicus* sp. n., male paratype **B** *E. cavernicolus*, male paratype **C** *E. liburnicus* sp. n., male paratype ZMUC 00040237 **D** *Eupolybothrus litoralis*. Abbreviation: cp. circular protuberance.

distinction between these cavernicolous species is subtle but, as discussed below, they are delineated as distinct species by both molecular species delimitation approaches. Morphological distinction is most reliably made using the shape of the posterior margin of T14, plectrotaxy of leg 15, and the length of the ultimate legs relative to the body.

Table 3. Modifications on male ultimate prefemur in *Eupolybothrus* species of the subgenus *Schizopolybothrus*.

	E. wardaranus	***E. caesar***	***E. cavernicolus***	***E. excellens***	***E. leostygis***	***E. liburnicus* sp. n.**	***E. spiniger***	***E. tabularum***
Proximal knob	Subangular, densely setose with thin scattered setae	Round, densely setose (median setae longest) accompanied by a more proximal dorsomedial swelling	Round, protruding mediad, bearing a dorsal tuft of dense setae.	With two protruding densely setose processes	Round, with a subapical whirl of setae (median setae longest)	Round, protruding mediad, bearing a dorsal tuft of dense setae.	Subangular, with probable apical tuft of setae indicated by sockets.	Absent
Ridge	Thin, gently narrowing towards the distal third of the prefemur	Even in width, parallel to the prefemur mesal margin	Broad, gently narrowing towards the distal third of the prefemur	Short (less than half length of prefemur), largest proximally, abruptly narrowing	Uniformly broad, narrowing only at the distal third of the prefemur	Broad, gradually narrowing at the distal half of the prefemur	Thin, gently narrowing towards the distal third of the prefemur	Absent
Circular protuberance	Absent	Present (small), flat	Present (large), bulged	?	Absent	Present (large), bulged	Present	?

In addition, *E. liburnicus* also shows a less setose posterior margin of the intermediate tergite, and usually has a narrower median membranous setae free area on that tergite.

An unusual character depicted and described by Stoev et al. (2013) for *E. cavernicolus* is a bifurcate tip of dorsal spine *p* on the prefemur. This character was further investigated here with SEM and it is also present in *E. liburnicus* (Fig. 12C), *E. leostygis* and *E. litoralis* (Fig. 12D). Whether this character is genus specific or is widely distributed in Lithobiidae remains doubtful and needs to be further examined in other taxa.

Molecular analyses

The four sequenced specimens of *Eupolybothrus liburnicus* sp. n. provided a full length DNA barcode (BOLD IDs: EUCR048-11, EUCR052-11, EUCR067-11 and EUCR068-11). The final dataset for species delimitation (our four new sequences + sequences of Stoev et al. 2013 and Spelda et al. 2011) consists of 43 specimens representing 12 *Eupolybothrus* morphospecies and two *Lithobius* outgroups: *L. austriacus* (Verhoeff, 1937) (MYFAB442-11) and *L. crassipes* L. Koch, 1962 (MYFAB443-11). Final alignment length was 658 bp with no internal gaps present. Molecular species delimitation via ABGD proposed 15 clusters congruent to the morphospecies assignments (Fig. 13). Only for *E. tridentinus* is a split into two clades proposed. The SP analysis resulted in a total number of 18 clusters, thereby splitting *E. nudicornis* and *E. leostygis* into three and two clusters, respectively. We follow a more conserved approach here and consider the ABGD results for the calculation of inter- and intraspecific genetic K2P-distance values. Nevertheless, specimens of *Eupolybothrus liburnicus* sp. n. always clustered as a single, exclusive group having a mean intraspecific distance of 0.7% (range 0.2–1.2%) and a minimal interspecific distance of 11.0 % to *E. cavernicolus* (Table 4).

Although only three species of *E.* (*Schizopolybothrus*) were available for sequencing, they are observed to unite as a monophyletic group (moderate bootstrap support of 65), with *E. leostygis* being sister group to *E. cavernicolus* and *E. liburnicus*. This reconstructed topology would be consistent with a single origin of the prefemoral knob, its associated mesial ridge and the posterior circular setose protuberance in the males of these species.

Habitat preferences and troglomorphism tendency

Elongation of antennae and legs and reduction of pigment and ocelli are considered morphological adaptations of centipedes to the cave environment (Negrea and Minelli 1994, Voigtländer 2011). In his redescription of *E. leostygis*, Eason (1983) considered long slender forcipules and a slender trunk as further characters of troglobitic species of *Eupolybothrus*. Among the *Schizopolybothrus* species, four were collected solely from caves *viz*. *E. cavernicolus*, *E. liburnicus* sp. n., *E. stygis* and *E. leostygis*, the last being the only true troglobite. Verhoeff (1900) speculated that *E. leostygis* was actually the cave form of *E. caesar*, and described *E. acherontis* as a transitional form between the

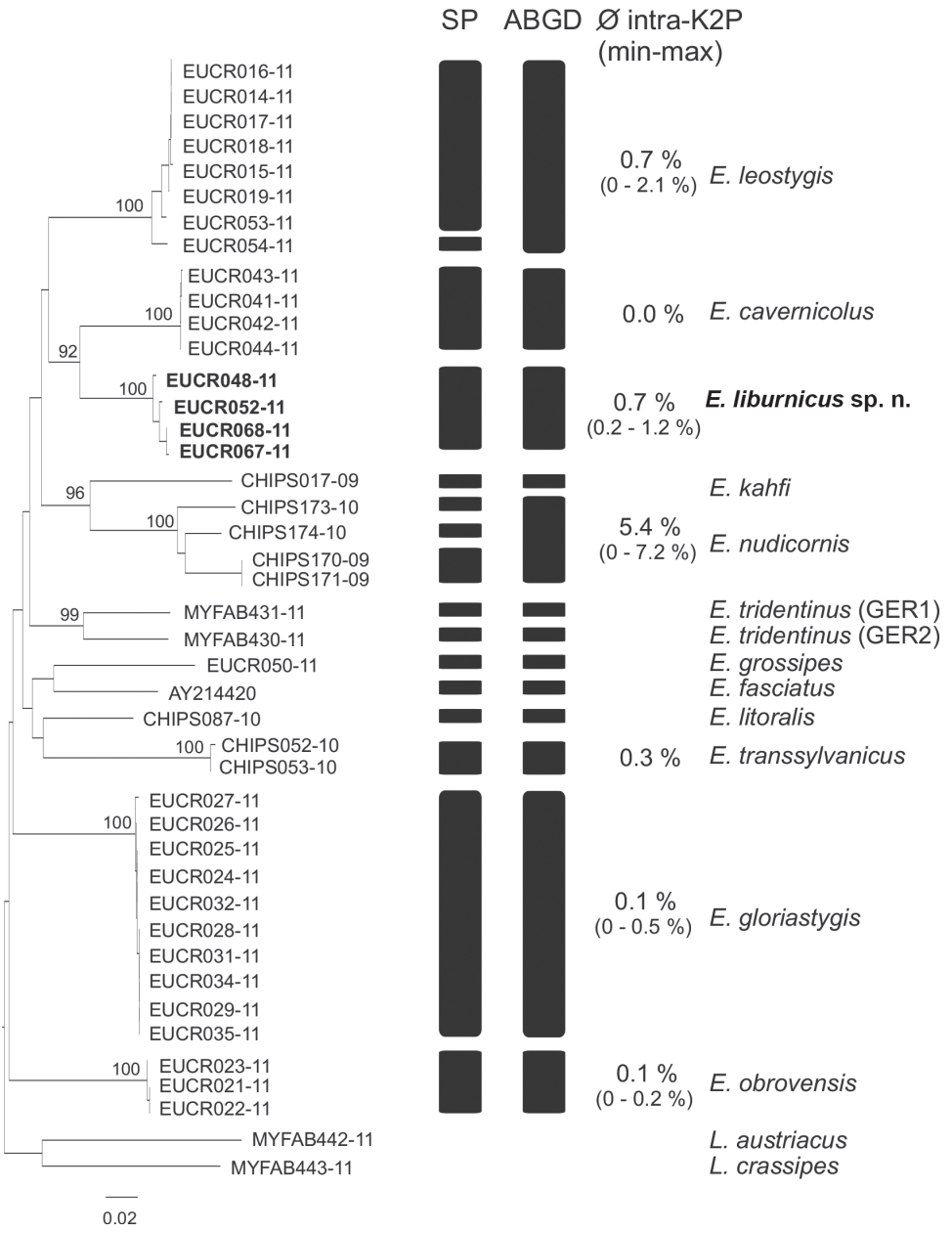

Figure 13. Molecular species delimitation. ABGD proposed 15 clusters congruent to the morphospecies assignments.

two species. Jeekel (1967) argued that the preference to cave habitats by some taxa of *Schizopolybothrus* may result in significant variability in a number of morphological characters and he suggested that the cave dwelling taxa of the subgenus are all cave forms of one troglophilic species.

Table 4. Overview of interspecific K2P-genetic distances of *Eupolybothrus* species.

	E. gloriastygis	*E. leostygis*	*E. obrovensis*	*E. cavernicolus*	*E. litoralis*	*E. fasciatus*	*E. tridentinus* GER1	*E. tridentinus* GER2	*E. transsylvanicus*	*E. kahfi*	*E. nudicornis*	*E. grossipes*	*E. liburnicus* sp. n.
E. gloriastygis **BOLD:AAY5019**													
E. leostygis **BOLD:AAY5071**	16.7–17.8												
E. obrovensis **BOLD:AAY5641**	16.2–17.0	18.5–19.4											
E. cavernicolus **BOLD:AAY4900**	17.6–18.0	14.5–15.4	20.8–21.2										
E. litoralis	14.7–15.1	17.1–17.5	17.1–17.3	18.0–18.1									
E. fasciatus	16.3–16.8	18.7–19.2	17.5–17.7	21.9–22.1	13.7								
E. tridentinus **GER1** **BOLD:AAV7132**	17.7–18.0	16.7–17.3	18.3–18.5	17.4–17.7	18.0	18.3							
E. tridentinus **GER2** **BOLD:AAV7131**	17.4–17.8	18.6–19.1	19.4–19.7	18.1–18.4	15.7	17.5	10.7						
E. transsylvanicus **BOLD:AAJ0488**	20.4–21.3	20.7–21.6	21.4–22.1	20.6–20.7	16.0–16.4	20.4–20.8	18.1	19.7–20.1					
E. kahfi **BOLD:AAY2955**	21.9–22.5	18.9–20.1	21.6–21.8	20.0–20.2	21.0	21.7	22.3	21.5	23.2–23.6				
E. nudicornis **BOLD:AAN2808** **BOLD:AAN2810** **BOLD:AAN2811**	20.1–23.2	19.4–21.8	21.1–24.1	21.2–22.7	20.1–21.7	21.7–22.6	20.7–22.4	19.4–21.0	21.4–22.3	17.2–18.8			
E. grossipes **BOLD:AAY7960**	19.2–19.6	21.0–21.9	20.9–21.1	24.2–24.5	16.6	15.3	20.9	18.9	20.3	22.1	20.7–22.1		
E. liburnicus **sp. n.**	16.4–17.7	15.0–16.4	19.8–20.6	11.0–11.7	16.6–17.1	18.7–19.3	16.1–16.4	16.6–17.2	20.0–20.5	17.4–17.7	19.5–20.2	20.3–21.0	

A number of characters indicative of troglomorphism were noted for the cave dwelling species among those studied herein in contrast to the surface dwelling ones. For instance, *E. caesar* shows the highest number of ocelli (22), the lowest number of antennal articles (51) and setae on coxosternum (26-30), the shortest ultimate leg podomeres (femur, tibia, tarsus 1 respectively 2.6; 3.0; 2.8) and the lowest ratio of ultimate leg to body length (52%). In contrast, *E. leostygis* is characterized by only (6-7) feebly pigmented ocelli (lowest in the subgenus), the longest antenna and ultimate leg podomeres, with the highest ratio of ultimate leg to body length (75%). *E. cavernicolus* and *E. liburnicus* sp. n., display some troglomorphic traits although they are probably not troglobitic, and should be considered as troglophiles. Both species have not been found outside caves although the surrounding areas were thoroughly investigated.

In 2010 and 2012, biospeleological investigations of the caves around Trebinje were conducted by one of us (AK) with the help of cavers from the Caving Club 'Zelena brda', which has led to the location of the following: 1) cave Iljina pećina, type locality of *E. stygis* and 2) cave Provalija or 'Acheron-schlund' (Verhoeff 1900: 163), type locality of *E. acherontis*. Unfortunately, cave Provalija has turned into an illegal waste disposal site, with its large vertical entrance shaft filled with waste. Iljina pećina has also been destroyed by the opening of an artificial entrance drilled in the 1920s. Both events drastically changed the conditions in these caves and all attempts to find specimens of *Eupolybothrus* there failed. However, recent active sampling was conducted in cave Vučja pećina or 'Wolfshöhle' (Verhoeff 1899), the type locality for *E. leostygis*. The cave is fortunately still intact and only *ca*. 300 m from Iljina pećina. In 2012, a single adult female specimen of *Eupolybothrus* was collected by AK, which was of practically no use for this paper. Meticulous sampling in the area would certainly be valuable for future studies on the subgenus, help unveil the identity of some dubious species, and shed some light on the general diversity of the genus *Eupolybothrus*.

Key to species of *Eupolybothrus* (*Schizopolybothrus*) based mainly on male secondary sexual characters

Note. *E. stygis* is based on the description provided by Folkmanova (1940). *E. acherontis* is excluded from the key.

1	Leg 15 prefemoral knob absent	***E. tabularum***
–	Leg 15 prefemoral knob present	**2**
2	Prefemoral knob apically incised, forming two rounded, densely setose processes	***E. excellens***
–	Prefemoral knob not incised	**3**
3	Posterior edge of T14 deeply emarginated, with sub-triangular posterior processes	***E. spiniger***
–	Posterior edge of T14 slightly emarginated to straight	**4**

4 Prefemoral knob with scattered setae.....**5**
– Prefemoral knob with specific setation (rim or tuft).....**6**
5 Prefemoral knob subangular, projections on leg 14 absent ....***E. wardaranus***
– Prefemoral knob round, projections on leg 14 present .....***E. caesar***
6 Prefemoral knob with rim of setae, six poorly defined and feebly pigmented ocelli.....***E. leostygis***
– Prefemoral knob with apical tuft of setae, more than ten pronounced ocelli....**7**
7 10+11 coxosternal teeth, *ca.* 84 antennal articles.....***E. stygis***
– 7+7-8+8(9+8) coxosternal teeth, 73 or fewer antennal articles **8**
8 T14 emarginated, 15CxVp and 15PDp absent.....***E. cavernicolus***
– T14 slightly convex to straight, 15CxVp and 15PDp present ....***E. liburnicus***

Acknowledgements

The authors are grateful to the Biology Students Association BIUS of University of Zagreb for collecting valuable specimens for this study, as well as members of Caving Club Samobor and Croatian Biospeleological Society for help with field research and collecting. We are grateful to Ivan Tuf (Palacky University), Jason Dunlop (ZMB), Jörg Spelda (ZSM), and Petr Dolejs (National Museum, Prague) who provided valuable information and helped us locate some of Verhoeff's obscure types. Special thanks to Stefan Fredrich (ZSM) for promptly and kindly arranging the loan of the *E. acherontis wardaranus* type. Our gratitude is extended to Henrik Enghoff (ZMUC) for his support and hosting AK and NA during their respective stays in Copenhagen. This project received support from the European Commission's (FP 6) Integrated Infrastructure Program SYNTHESYS (DK-TAF, AT-TAF) to support AK's stays in NHMW and ZMUC, respectively.

References

Andersson G (1981) Taxonomical studies on the post-embryonic development in Swedish Lithobiomorpha (Chilopoda). Entomologica Scandinavica 16: 105–124.

Attems C (1902) Myriopoden von Kreta nebst Beiträgen zur allgemeinen Kenntnis einiger Gattungen - Sitzungsberichte der Kaiserlichen Akademie der Wissenschaften. Mathematisch-Naturwissenschaftliche Classe, Wien 111: 527–561.

Attems C (1935) Myriapoden von Epirus. Zoologischer Anzeiger 110(5–6): 141–153.

Bonato L, Edgecombe GD, Lewis JGE, Minelli A, Pereira LA, Shelley RM, Zapparoli M (2010) A common terminology for the external anatomy of centipedes (Chilopoda). ZooKeys 69: 17–51. https://doi.org/10.10.3897/zookeys.69.737

Bregović P, Antonović I, Čuković T, Ćukušić A, Dražina T, Đud L, Hmura D, Komerički A, Kutleša P, Malenica M, Patarčić I, Pavlek M, Raguž N, Šimičev A, Škuljević P, Jalžić B (2013) Biospeleološka istraživanja šireg područja rijeke Zrmanje i dijela jugoistočnog Velebita. In:

Basrek L, Đud L (Ed.) Zbornik radova projekta „Istraživanje bioraznolikosti područja rijeke Zrmanje 2010". Udruga studenata biologije – „BIUS" i JU Park prirode Velebit, 15–42.

Clement MD, Posada D, Crandall KA (2000) TCS: a computer program to estimate gene genealogies. Molecular Ecology 9(10): 1657–1659. https://doi.org/10.1046/j.1365-294x.2000.01020.x

Eason EH (1983) The identity of the European and Mediterrranean species of Lithobiidae (Chilopoda) described by K. W. Verhoeff and now represented by material preserved in the British Museum (Natural History). Zoological Journal of the Linnean Society of London 77: 111–144. https://doi.org/10.1111/j.1096-3642.1983.tb00526.x

Folkmanova (1940) O nový̌c balkánských jeskynních Chilopodech ve sberech DR. K. Absolona. Species novae Chilopodorum cavernicolorum Balcanicorum in coll. Dr. K. Absolon. Vestnik Ceskoslovenské Zoologické Spolecnosti v Praze 8: 47–58.

Hart M, Sunday J (2007) Things fall apart: biological species form unconnected parsimony networks. Biology Letters 3(5): 509–512. https://doi.org/10.1098/rsbl.2007.0307

Jeekel CAW (1967) On two Italian *Lithobius* species described by Silvestri with taxonomic notes on the genus *Eupolybothrus* Verhoeff (Chilopoda Lithobiidae). Beaufortia 14: 165–175.

Kearse M, Moir R, Wilson A, Stones-Havas S, Cheung M, Sturrock S, Buxton S, Cooper A, Markowitz S, Duran C, Thierer T, Ashton B, Meintjes P, Drummond A (2012) Geneious Basic: an integrated and extendable desktop software platform for the organization and analysis of sequence data. Bioinformatics 28(12): 1647–1649. https://doi.org/10.1093/bioinformatics/bts199

Komerički A, Weigand A, Stoev P (2012) DNA barcoding of genus *Eupolybothrus* (Chilopoda, Lithobiidae) from Dinaric Karst reveals unexpected cryptic diversity. XXI International Conference on Subterranean Biology, Košice, Slovakia, 2–7 September 2012, 1. https://doi.org/10.1111/j.1365-294X.2011.05239.x

Lambert A, Brouillet S, Achaz G (2012) ABGD, Automatic Barcode Gap Discovery for primary species delimitation. Molecular Ecology 21(8): 1864–1877.

Latzel R (1888) Die vom k. k. Oberartze Herrn Dr. Justyn Karlinski im Jahre 1887 in Bosnien, der Herzegowina und in Novibazar gesammelten Myriopoden. Verhandlungen der Zoologisch-Botanischen Gesellschaft in Wien 1886: 91–94.

Negrea S, Minelli A (1994) Chilopoda. In: Christian J, Vasile D (Eds) Encyclopaedia biospeologica. Tome 1. Société de Biospéléologie. Moulis & Bucarest, 1994, 249–254.

Porco D, Stoev P, Zapparoli M, Simaiakis S, Akkari N, Edgecombe G (2011) DNA barcoding of Chilopoda: preliminary report on cryptic diversity cases in the genus *Eupolybothrus* Verhoeff, 1907 (Chilopoda: Lithobiomorpha: Lithobiidae). 15th International Congress of Myriapodology, Brisbane, Australia, 1.

Puillandre N, Lambert A, Brouillet S, Achaz G (2012) ABGD, Automatic Barcode Gap Discovery for primary species delimitation. Molecular Ecology 21(8): 1864–1877. https://doi.org/10.1111/j.1365-294X.2011.05239.x

Ratnasingham S, Hebert PD (2007) BOLD: The Barcode of Life Data System (http://www.barcodinglife.org). Molecular Ecology Notes 7(3): 355–364. https://doi.org/10.1111/j.1471-8286.2007.01678.x

Spelda J, Reip H, Oliveira-Biener U, Melzer R (2011) Barcoding Fauna Bavarica: Myriapoda – a contribution to DNA sequence-based identifications of centipedes and millipedes (Chilopoda, Diplopoda). ZooKeys 156: 123–139. https://doi.org/10.3897/zookeys.156.2176

Stoev P (2001a) On centipedes (Chilopoda) of Albania, 2. Arthropoda Selecta 9(3): 199–206. [for 2000]

Stoev P (2001b) On the centipedes (Chilopoda) of the Republic of Macedonia. Historia naturalis bulgarica 13: 93–107.

Stoev P, Akkari N, Zapparoli M, Porco D, Enghoff H, Edgecombe GD, Georgiev T, Penev L (2010) The centipede genus *Eupolybothrus* Verhoeff, 1907 (Chilopoda: Lithobiomorpha: Lithobiidae) in North Africa, a cybertaxonomic revision, with a key to all species in the genus and the first use of DNA barcoding for the group. ZooKeys 50: 29–77. https://doi.org/10.3897/zookeys.50.504

Stoev P, Komerički A, Akkari N, Liu S, Zhou X, Weigand A, Hostens J, Hunter C, Edmunds S, Porco D, Zapparoli M, Georgiev T, Mietchen D, Roberts D, Faulwetter S, Smith V, Penev L (2013) *Eupolybothrus cavernicolus* Komerički & Stoev sp. n. (Chilopoda: Lithobiomorpha: Lithobiidae): the first eukaryotic species description combining transcriptomic, DNA barcoding and micro-CT imaging data. Biodiversity Data Journal 1: e1013. https://doi.org/10.3897/BDJ.1.e1013

Tamura K, Stecher G, Peterson D, Filipski A, Kumar S (2013) MEGA6: molecular evolutionary genetics analysis version 6.0. Molecular Biology and Evolution 30(12): 2725–2729. https://doi.org/10.1093/molbev/mst197

Tobias D (1974) New criteria for the differentiation of species within the Lithobiidae. Symposia of the Zoological Society of London 32: 75–87.

Verhoeff KW (1899) Beitrage zur Kenntnis palaarktischer Myriopoden. XI. Aufsatz: Neue und wenig bekannte Lithobiiden. Verhandlungen der Zoologisch-botanischen Gesellschaft in Wien 49: 451–459. https://doi.org/10.5962/bhl.part.24105

Verhoeff KW (1900) Beitrage zur Kenntniss paläarctischer Myriopoden. XV. Aufsatz: Lithobiiden aus Bosnien, Herzogovina und Dalmatien. Berliner entomologische Zeitschritt 45: 153–179.

Verhoeff KW (1934) Beiträge zur Systematik und Geographie der Chilopoden. Zoologische Jahrbücher, Abteilung für Systematik 66: 1–112.

Verhoeff KW (1937) Chilopoden und Diplopoden aus jugoslawischen Höhlen, gesammelt von Dr. St. Karaman, Skoplje. Mitteil, über Höhlen- und Karstforschung 1937: 95–103.

Voigtländer K (2011) Chilopoda – Ecology. In: Minelli A (Ed.) Treatise of Zoology – Anatomy, Taxonomy, Biology. The Myriapoda. Volume 1, Brill, Leiden, Boston, 309–325. https://doi.org/10.1163/9789004188266_016

Zapparoli M (1984) Note su alcune specie del gen. *Eupolybothrus* della fauna di Grecia. Fragmenta Entomologica 17: 195–209.

Zapparoli M (2002) Catalogue of the centipedes from Greece (Chilopoda). Fragmenta Entomologica 34: 1–146.

ZooKeys 687: 45–51 (2017)
doi: 10.3897/zookeys.687.14872
http://zookeys.pensoft.net

RESEARCH ARTICLE

A peer-reviewed open-access journal
ZooKeys
Launched to accelerate biodiversity research

A new and unusual species of *Amastigogonus* Brölemann, 1913 from Tasmania, Australia (Diplopoda, Spirostreptida, Iulomorphidae)

Robert Mesibov[1]

1 *West Ulverstone, Tasmania 7315, Australia*

Corresponding author: *Robert Mesibov* (robert.mesibov@gmail.com)

Academic editor: *S. Golovatch* | Received 4 July 2017 | Accepted 13 July 2017 | Published 1 August 2017

http://zoobank.org/DA65A87E-E571-429A-BD9B-0F207EB7FC61

Citation: Mesibov R (2017) A new and unusual species of *Amastigogonus* Brölemann, 1913 from Tasmania, Australia (Diplopoda, Spirostreptida, Iulomorphidae). ZooKeys 687: 45–51. https://doi.org/10.3897/zookeys.687.14872

Abstract

Amastigogonus insularis **sp. n.** is described from Schouten and Tasman Islands off the east coast of Tasmania, and a key is presented for the identification of males of Tasmanian *Amastigogonus* species. The new species differs from the 10 previously described species of *Amastigogonus* in having a reduced coxite process on the anterior gonopod.

Keywords

Millipede, gonopod

Introduction

In a previous paper (Mesibov 2017) I reviewed the endemic Tasmanian genus *Amastigogonus* Brölemann, 1913 and added six new species. In all but one of the 10 known *Amastigogonus* species, the telopodite on the anterior gonopod is slightly longer than the coxite process (Fig. 1A). The latter is typically flattened with a slight lateral concavity, and faces the medial side of the telopodite so that the two structures form a "bird's beak" in which the pseudoflagellum is partly protected. The coxite process in *A. danpicola* Mesibov, 2017 deviates from this pattern in having shallow fossae at the apex and posterobasally.

In this paper I describe a new *Amastigogonus* species in which the coxite process is reduced (Fig. 1B) and does not protect the pseudoflagellum. The new species has so far only been recorded from two small islands off the Tasmanian east coast.

Materials and methods

Specimens are stored in 80% ethanol in the Queen Victoria Museum and Art Gallery, Launceston, Australia (QVM). Photomicrographs in Fig. 1 are focus-stacked composites made with Zerene Stacker 1.04. Photomicrographs were taken with a Canon EOS 1000D digital SLR camera mounted on a Nikon SMZ800 binocular dissecting microscope equipped with a beam splitter. Measurements were made to the nearest 0.1 mm with the same microscope using an eyepiece grid and a reference scale. The gonopod telopodite illustrated in Fig. 2 was temporarily mounted in 1:1 glycerine:water and imaged using an eyepiece video camera mounted on an Amscope binocular microscope. A preliminary drawing was traced from a printed copy of the image, with details confirmed by microscopic examination of the mounted object. Latitude/longitude figures are given in decimal degrees to four decimal places, together with an estimate of spatial uncertainty.

Results

Order Spirostreptida Brandt, 1833
Suborder Epinannolenidea Chamberlin, 1922
Family Iulomorphidae Verhoeff, 1924

***Amastigogonus insularis* sp. n.**
http://zoobank.org/1A6BD2B8-CB9D-46E8-AE63-5E653E7DA815
Figs 1B–D, 2

Holotype. Male, Tasman Island, Tasmania, 55G 581536 521818 (GDA94) [-43.2419 148.0042 ±100m], 210m a.s.l., 19 November 2005, S. Bryant + Hamish Saunders Memorial Island Survey Program personnel, pitfall, cliff mosaic, 5A, QVM 23: 46411.

Paratypes. Tasmania: 1 male, 4 females, 1 juvenile, Schouten Island [-42.3131 148.2850 ±2km], 23–26 September 1993, R. Taylor, QVM 2017:23:0047; 4 females, Tasman Island [-43.2384 148.0031 ±500m], 3 June 2016, L. Gadd, 2017:23:0093; 5 females, Tasman Island, -43.2357 147.9996 ±25m, 190m a.s.l., 21 April 2017, R. and L. O'Grady, under she-oak log, QVM 2017:23:0094.

Diagnosis. Male leg 7 coxa not noticeably elongated or distally swollen; coxite process on anterior gonopod much shorter than telopodite, not protecting pseudoflagellum; pseudoflagellum as in *A. peninsulensis* Mesibov, 2017 but longer, extending just past telopodite tip.

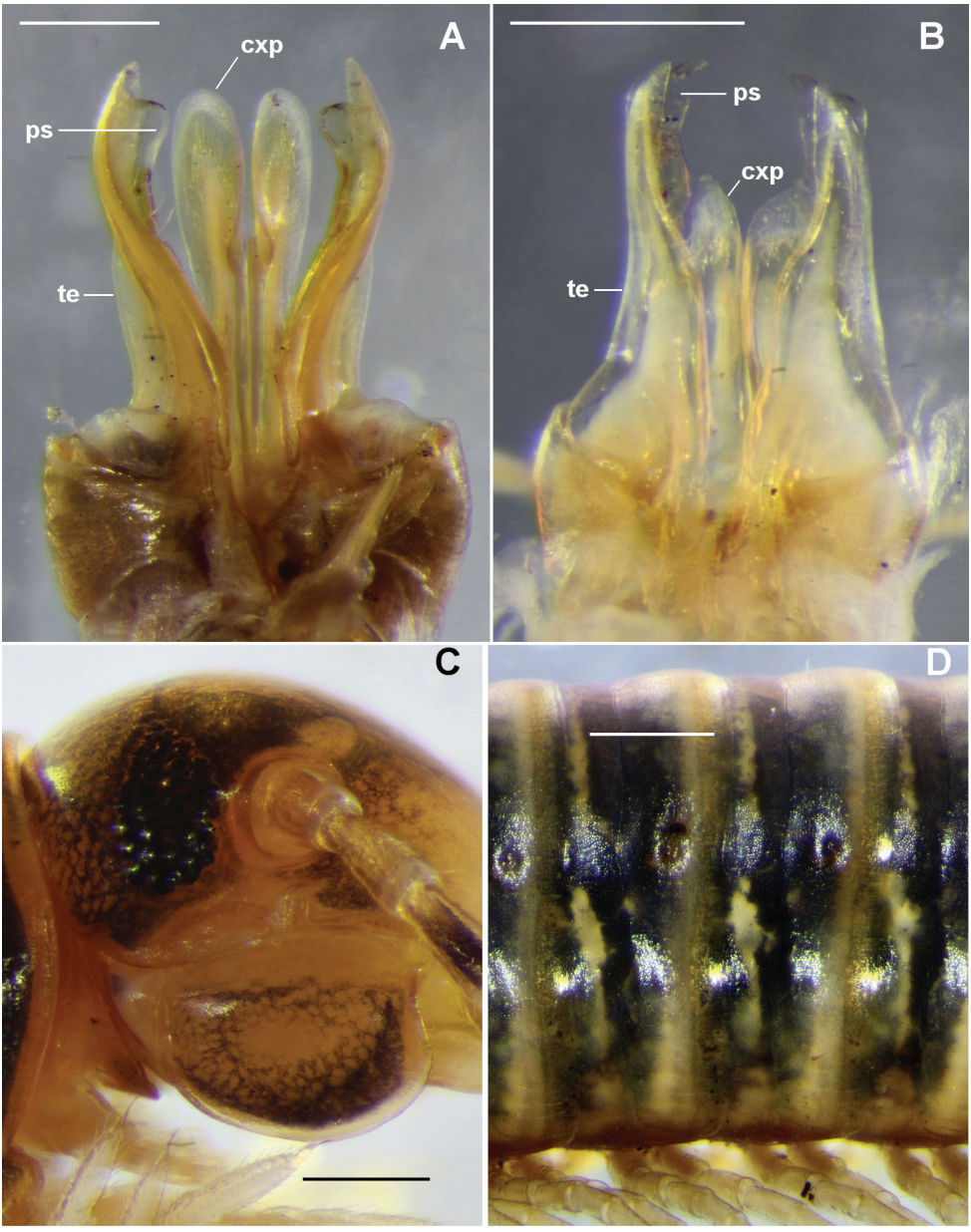

Figure 1. **A** *Amastigogonus tasmanianus* Brölemann, 1913 (type species of *Amastigogonus*), QVM 23:54404 **B–D** *A. insularis* sp. n., holotype, QVM 23: 46411 **A, B** Posterior views of gonopod complex; **C** right lateral view of head **D** left lateral view of midbody rings **cxp** coxite process **ps** pseudoflagellum **te** telopodite. Scale bars = 0.5 mm.

Description. As for the genus description (Mesibov 2017, p. 5) with the following details: holotype male with (59+1) rings, 2.0 mm midbody diameter; paratype male with (51+2) rings, 1.6 mm; longest female (in QVM 23:0093) with (63+1) rings, 2.5 mm. Trunk

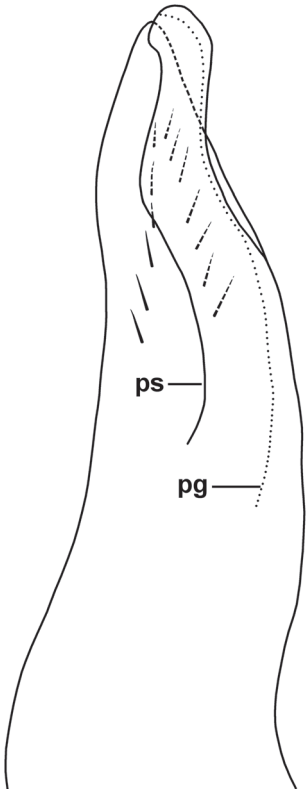

Figure 2. *Amastigogonus insularis* sp. n., paratype from QVM 2017:23:0047. Right anterior gonopod, medial and slightly posterior view of distal portion of telopodite. **pg** prostatic groove **ps** pseudoflagellum. Drawing not to scale.

rings dark grey with light annulus posteriorly and irregular, partly annular light markings on prozonite (Fig. 1D); striae on posterior metazonites reaching ca 1/2 ozopore height.

Male with cardo not deeper posteriorly (Fig. 1C). Leg 7 coxa not noticeably elongated or distally swollen. Prefemoral pad ca 1/2 femur length.

Coxite process on anterior gonopod (Fig. 1B) reaching ca 2/3-3/4 telopodite height, not protecting pseudoflagellum. Telopodite (Fig. 2) with slight medial thickening bordered by two rows of short setae behind pseudoflagellum, meeting near telopodite apex. Pseudoflagellum arising at ca 1/2 telopodite height, ca 1/2 telopodite width at base and only slightly narrowing distally; slightly sinuous, curving first posteriorly, then anteriorly, then posteriorly to terminate just distal to telopodite apex, the pseudoflagellum tip bent medially (Fig. 1B); prostatic groove running on anterior edge of pseudoflagellum to posterodistal portion of tip.

Distribution. Schouten and Tasman Islands off the east coast of Tasmania (Fig. 3).

Name. Latin *insularis*, insular; adjective.

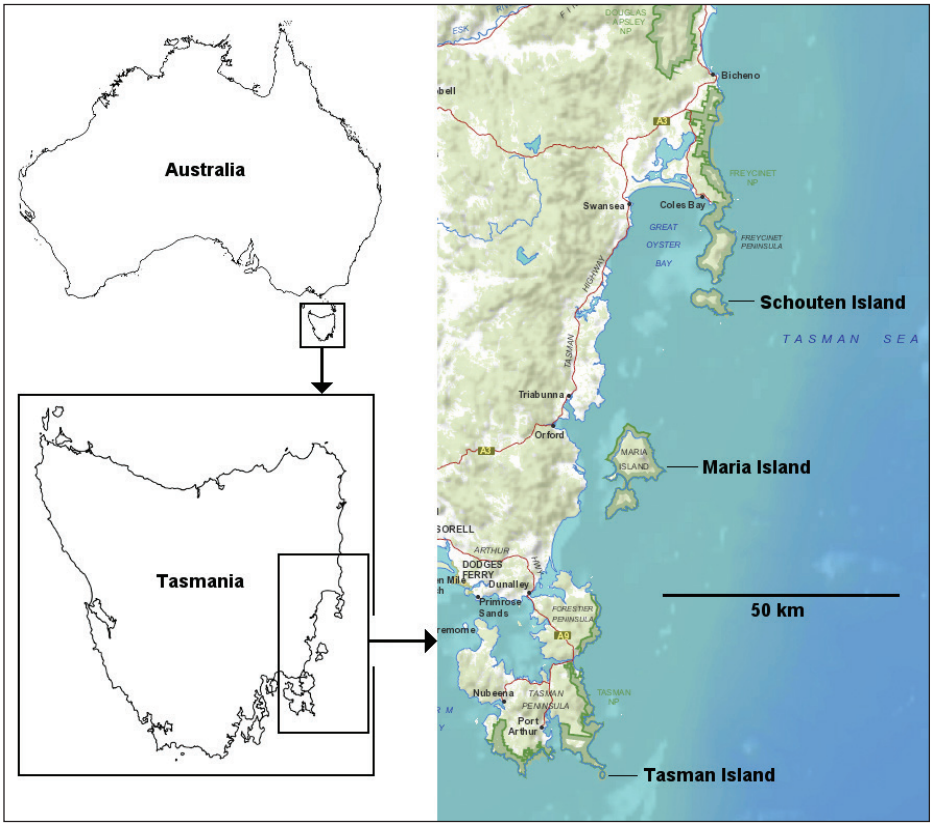

Figure 3. Outline maps of Australia and Tasmania, and topographic map of part of the east coast of Tasmania showing Schouten and Tasman Islands. Mercator projections; topographic basemap from the Land Information Service Tasmania (LIST), copyright State of Tasmania, used with permission.

Remarks. As with the two known males, the Schouten Island females are smaller than their Tasman Island counterparts: (51+2)–(59+1) rings, 1.5–2.3 mm midbody diameter from Schouten Island, (47+2)–(63+1) rings, 2.3–2.7 mm from Tasman Island. Further, the pseudoflagellum tip in the holotype male from Tasman Island is slightly longer, broader and more medially directed than the tip in the Schouten Island paratype. These are minor differences and I regard the two forms as conspecific.

I doubt that *A. insularis* sp. n. is restricted to its two widely disjunct localities, ca 105 km apart. However, the only iulomorphid so far collected on Forestier and Tasman Peninsulas, just north of Tasman Island (Fig. 3), is *A. peninsulensis* Mesibov, 2017. Similarly, the only iulomorphid recorded from the Freycinet Peninsula (Fig. 3), just north of Schouten Island, is *A. michaelsae* Mesibov, 2017. The latter species is also the only iulomorphid known from Maria Island, halfway between Schouten and Tasman Islands (Fig. 3). I suspect that *A. insularis* sp. n. will be found in future in coastal habitats along the east coast of the Tasmanian mainland, and possibly also on Maria Island.

Key to males of *Amastigogonus* (see figs 6 and 8 in Mesibov (2017), and Fig. 2 above)

1 Coxite process of anterior gonopod truncate with apical fossa; cardo deeper in posterior half ..... ***A. danpicola*** **Mesibov, 2017**

– Coxite process laminate with broadly rounded apex; cardo deeper in anterior half **2**

2 Coxite process much shorter than telopodite; no legs with elongated coxae ... . ***A. insularis*** **sp. n.**

– Coxite process almost as long as telopodite; elongated coxae on leg 7 only, or on legs 7, 10 and 11 ..... **3**

3 Pseudoflagellum tapering to sharp point **4**

– Pseudoflagellum bluntly rounded, expanded or apparently bifid at tip 7

4 Pseudoflagellum with distinct anterior shoulder, prostatic groove making sharp S-bend to reach tip; dense field of short, fine setae on telopodite behind pseudoflagellum ..... ***A. fossuliger*** **Verhoeff, 1944**

– Pseudoflagellum without anterior shoulder, prostatic groove without S-bend; only sparse, stout setae behind pseudoflagellum **5**

5 Pseudoflagellum broad at base, abruptly truncate apically, continued as sharp, pointed tip bent over laterally or medially ..... ***A. hellyeri*** **Mesibov, 2017**

– Pseudoflagellum not truncate apically **6**

6 Pseudoflagellum broad at base, gradually tapering to sharp point, not as long as telopodite ..... ***A. hardyi*** **(Chamberlin, 1920)**

– Pseudoflagellum narrow at base, very gradually tapering to sharp point, much longer than telopodite ..... ***A. tasmanianus*** **Brölemann, 1913**

7 Pseudoflagellum with tip strongly curving posterobasally and with small tooth on apicodistal margin, thus appearing bifid ..... ***A. elephas*** **Mesibov, 2017**

– Pseudoflagellum with bluntly rounded or expanded tip **8**

8 Pseudoflagellum with tip strongly curving posterobasally .... ***A. verreauxii*** **(Gervais, 1847)**

– Pseudoflagellum with tip directed distally or slightly posteriorly **9**

9 Pseudoflagellum with tip slightly expanded apically and truncate, with small tooth medially on distal margin ..... ***A. orientalis*** **Mesibov, 2017**

– Pseudoflagellum gradually narrowing to bluntly rounded tip **10**

10 Pseudoflagellum with tip directed slightly posteriorly and with posterobasal margin extended as bulge ..... ***A. peninsulensis*** **Mesibov, 2017**

– Pseudoflagellum with tip directed distally and with prominent sharp tooth on posterobasal margin ..... ***A. michaelsae*** **Mesibov, 2017**

Acknowledgements

I am grateful to Ben Clark, Luke Gadd and Sue Robinson (Department of Primary Industries, Parks, Water and Environment, Tasmania) and to Lyndon O'Grady, Rohan O'Grady and Ian Ross (Friends of Tasman Island) for their efforts in searching for millipedes on Tasman Island in 2016 and 2017. I also thank reviewer Nesrine Akkari for helpful suggestions.

References

Mesibov R (2017) Iulomorphid millipedes (Diplopoda, Spirostreptida, Iulomorphidae) of Tasmania, Australia. ZooKeys 652: 1–36. https://doi.org/10.3897/zookeys.652.12035

ZooKeys 687: 53–61 (2017)
doi: 10.3897/zookeys.687.13164
http://zookeys.pensoft.net

RESEARCH ARTICLE

A peer-reviewed open-access journal
ZooKeys
Launched to accelerate biodiversity research

Two new species of *Centrodora* (Hymenoptera, Aphelinidae) from China, with a key to Chinese species

Ye Chen[1], Cheng-De Li[1]

1 *School of Forestry, Northeast Forestry University, Harbin, 150040, China*

Corresponding author: *Cheng-De Li* (lichengde0608@sina.com)

Academic editor: *N. Johnson* | Received 9 April 2017 | Accepted 29 June 2017 | Published 1 August 2017

http://zoobank.org/829C912D-73FC-494D-B061-15AA21AA42B6

Citation: Chen Y, Li C-D (2017) Two new species of *Centrodora* (Hymenoptera, Aphelinidae) from China, with a key to Chinese species. ZooKeys 687: 53–61. https://doi.org/10.3897/zookeys.687.13164

Abstract

Two new species of *Centrodora* Förster, *C. crassiscapa* **sp. n.** and *C. pellucida* **sp. n.**, are described from China. A key to species from China based on females is given.

Keywords

Aphelininae, Aphytini, Chalcidoidea, taxonomy

Introduction

Centrodora Förster, 1878 currently comprises 61 species (Noyes 2017). A majority of the species in this genus are oophagous, developing in the eggs of economically important Hemiptera and Orthoptera, whereas other species are known to attack nymphs of Hemiptera, and pupae of Diptera, Hymenoptera, and Coleoptera (Hayat 1974, 2010; Polaszek 1991). Several regional revisionary studies of the genus include Mercet (1918, 1930) and Nikol'skaya and Yasnosh (1966) on the European region, Hayat (1998, 2010) on the Indian region.

The Chinese fauna of *Centrodora* is poorly known with only *C. lineascapa* Hayat known from the Fujian Province (Huang 1994), and *C. idioceri* Ferrière (Chou and Chou 1990) and *C. locustarum* (Giraud) (Chiu and Chou 1974) known from Taiwan. In the present paper, two new species are added to the Chinese fauna. A key to all five species from China based on females is given.

Materials and methods

All specimens in the present study were collected using yellow pan traps or Malaise traps, then dissected and mounted in Canada Balsam on slides following the method described by Noyes (1982). Photographs were taken with a digital CCD camera attached to an Olympus BX51 compound microscope and final modifications to the images were made using Adobe Photoshop. Most measurements were made from slide-mounted specimens using a reticle micrometre except the total body length (excluding the ovipositor), which was measured from alcohol-preserved specimens before being dissected. All measurements are given in micrometres (μm) except body length, which is measured in millimetres (mm). Scale bars are 100 μm. All the specimens listed below are deposited in Northeast Forestry University, Harbin, China. Terminology follows Hymenoptera Anatomy Consortium (2017).

The following abbreviations are used in the text

F1–3 funicle segments 1–3;
TI, TII etc. tergites 1, 2, etc. of gaster;
MT Malaise trap.

The following acronyms are used for the depositories

NEFU Northeast Forestry University, Harbin, China.

Results

Key to Chinese species (female) of *Centrodora* Förster

1 Clava with apex rounded, not curved ventrally; antenna with F3 distinctly longer than wide ..... ***C. idioceri*** **Ferrière**
– Clava with apex pointed and curved ventrally (Figs 2, 13) **2**
2 Ovipositor strongly exerted and with the exerted part more than 0.3× as long as ovipositor (Figs 8, 19) **3**
– Ovipositor very slightly exerted **4**
3 Scape 3.26× as long as wide, remarkably wider than any other antennal segments (Fig. 2); median area of the mesoscutum and mesoscutellum dark brown; fore wing (Fig. 5) with basal one fourth hyaline, area beneath marginal vein brown, remaining part faintly infuscate ..... ***C. crassiscapa*** **sp. n.**
– Scape (Fig. 13) 3.58–4.13× as long as wide; median area of the mesoscutum and scutellum yellowish-brown; fore wing mostly infuscate, with a transparent cross band on the median area of disc as in Fig. 16 ..... ***C. pellucida*** **sp. n.**

4 Gaster completely blackish, hind leg with coxa and femur black..... ..... ***C. locustarum*** **(Giraud)**

– Gaster with yellow and brown tergites, hind leg completely pale..... ..... ***C. lineascapa*** **Hayat**

Centrodora crassiscapa **Li & Chen, sp. n.**

http://zoobank.org/7A12C8EE-F827-444F-915F-D9FDA725D5F6

Figs 1–11

Type material. Holotype: female [on slide, NEFU], CHINA, Heilongjiang Province, Shangzhi City, Laoyeling (45°24.71'N, 127°40.41'E), 8–18.VII.2013, Cheng-de Li, Ye Chen, Chao Zhang, MT. **Paratypes:** 1 male [on slide, NEFU], same data as holotype. 1 male [on slide, NEFU], CHINA, Heilongjiang Province, Shangzhi City, Laoyeling, 7–16.VIII.2013, Cheng-de Li, MT.

Diagnosis. *Centrodora crassiscapa* sp. n. is easily distinguished by following combination of characters: enormously thick scape, largely dark brown mesosoma, completely dark brown metasoma, long and strongly exserted ovipositor.

Description. ***Female***. Holotype. Length about 1.2 mm. Head dark brown. Eyes and ocelli dark brown. Antenna mostly brown, except pedicel and F1 paler. Mandible dark brown. Mesosoma largely dark brown, except metanotum and propodeum yellow. Median area of the mesoscutum and mesoscutellum with a distinctly pale midlongitudinal groove. Fore wing with basal one fourth hyaline, area posterior to marginal vein brown, remaining wing disc faintly infuscate; hind wing hyaline. Legs largely yellow, except fore leg with distal half of femur and tibia brownish-yellow; mesofemur and hind leg with coxa and femur brown. Metasoma dark brown to black.

Head (Fig. 1), in frontal view, 0.95× as high as wide, and finely reticulate, with the sculpture on malar space lineolate reticulated. Frontovertex 0.43× head width and with numerous brown setae. Ocellar triangle with apical angle obtuse. Mandible with two acute teeth and a blunt dorsal tooth. Antennae (Fig. 2) with scape 3.26× as long as wide, remarkably wider than any other antennal segments and slightly longer than clava; pedicel 2.14× as long as wide, and 0.83× as long as F3; F1 subtriangular, with ventral margin 1.40× as long as wide; F2 2.0× as long as wide; F3 with dorsal margin 3.21× as long as wide, and 0.6× as long as clava; clava 3.95× as long as wide, pointed and distinctly curved ventrally at apex. Measurements, length (width): scape, 163 (50); pedicel, 75 (35); F1, 28 (20); F2, 40 (20); F3, 90 (28); clava 150 (38).

Mesosoma. Pronotum imbricate, mesoscutum and mesoscutellum mainly polygonal reticulate. Mesoscutum with median area (Fig. 3) 0.83× as long as wide, 1.4× as long as mesoscutellum, and with 10 setae; each lateral area of the mesoscutum and axilla with 2 and 1 setae respectively; mesoscutellum (Fig. 4) 0.58× as long as wide, with 2 pairs of setae. Distance between anterior pair of scutellar setae 0.9× that between posterior pair. Placoid sensilla much closer to anterior pair of setae than to posterior pair. Fore wing 3.57× as long as wide, with marginal setae 0.08× wing width. Costal cell slightly longer than marginal vein, with 2 distal setae on dorsal surface; submarginal vein with 4 setae,

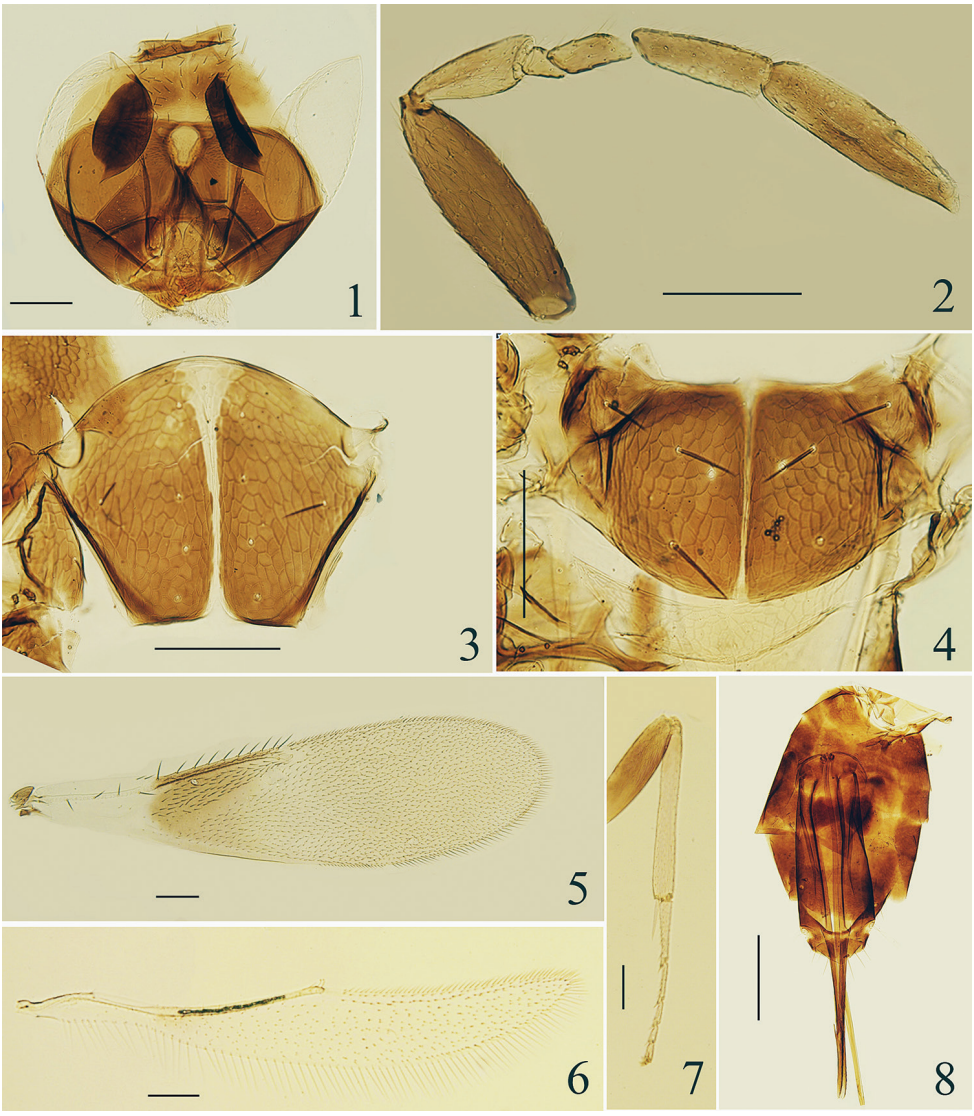

Figures 1–8. *Centrodora crassiscapa* sp. n., holotype female: **1** head, frontal view **2** antenna **3** mesoscutum **4** mesoscutellum and metanotum **5** fore wing **6** hind wing **7** mesotibia and tarsus **8** metasoma.

marginal vein with 8 long setae along anterior margin, postmarginal vein short and about one third of length of stigmal vein; basal cell with 2 setae. Linea calva closed by a line of setae posteriorly. Hind wing (Fig. 6) 7.17× as long as wide, marginal setae about 0.53× as long as wing width. Mesotibial spur (Fig. 7) distinctly shorter than (0.64×) corresponding basitarsus, and about as long as the second tarsomere. Measurements, length (width): fore wing 1250 (350); costal cell, 270; marginal vein, 260; postmarginal vein, 13; stigmal vein, 39; marginal setae, 28; hind wing, 1075 (150); marginal setae, 80; mesotibia, 390, mesotibial spur, 90, mesobasitarsus, 140.

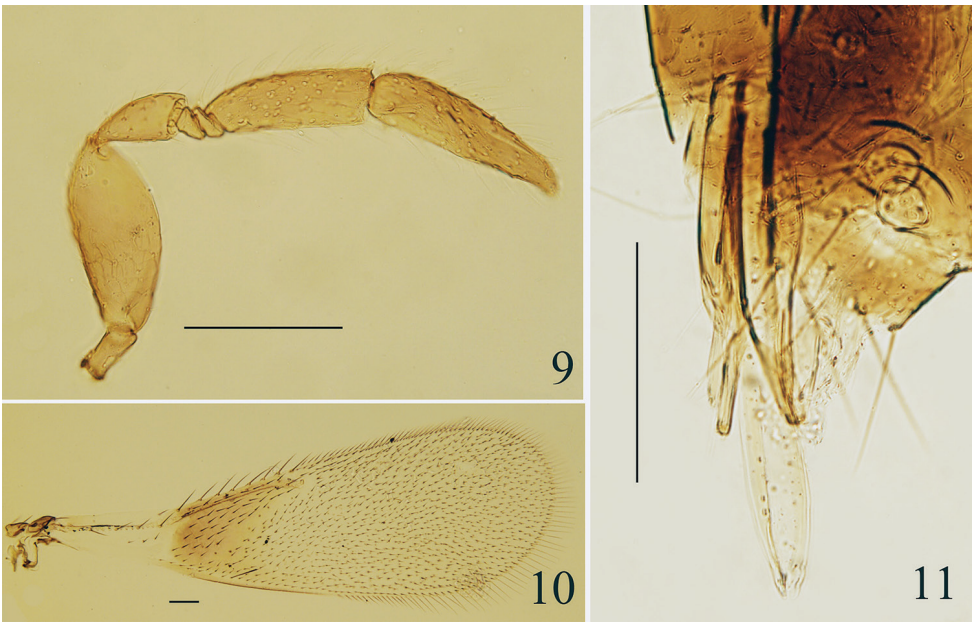

Figures 9–11. *Centrodora crassiscapa* sp. n., paratype male: **9** antenna **10** fore wing **11** genitalia.

Metasoma (Fig. 8) about 1.75× as long as mesosoma. Ovipositor 3.25× as long as mesotibia and strongly exerted, with the exerted part 0.46× as long as ovipositor. Third valvula 4.18× as long as mesobasitarsus. Length measurements: ovipositor, 1268; third valvula, 585.

Male. Length 0.73–0.78 mm. Colour similar to the female, except median area of mesoscutum a little paler.

Head, in frontal view, 0.9× as high as wide and frontovertex about 0.4× head width. Scape (Fig. 9) flattened and expanded medially, 2.37× as long as wide; pedicel 1.64–1.70× as long as wide; F1 triangular, 1.20× as long as wide, F2 anelliform, F3 long, 2.69–2.85× as long as wide, and 0.71–0.77× as long as clava; clava 3.69–4.08× as long as wide, slightly longer than scape. *Fore wing* (Fig. 10) 3.04× as long as wide, marginal setae 0.17× wing width; hind wing 7.11–7.25× as long as wide, marginal setae 0.63× wing width. *Genitalia* (Fig. 11) 5.30× as long as wide, and about as long as mesotibia.

Remarks. The new species is close to *C. amoena* Förster 1878, with similar colour on the head and metasoma and strongly exserted ovipositor. However, it can be separated from the latter by the thickened scape of the female antennae (normal in *C. amoena*), completely dark brown mesoscutum (*vs* largely yellow), clava 3.95× as long as wide (*vs* 3.5×), male antenna with F3 2.69–2.85× as long as wide (*vs* about 4×, *cf.* Nikol'skaya and Yasnosh 1966, fig. 162).

Host. Unknown.

Etymology. Latin: *crassus* = thick, fat; and the specific name refers to the enormously thick scape of the female antennae.

Distribution. China (Heilongjiang).

Centrodora pellucida **Li & Chen, sp. n.**
http://zoobank.org/8FBBCA89-706B-4FA2-8486-55E645648057
Figs 12–19

Type material. Holotype: female [on slide, NEFU], CHINA, Heilongjiang Province, Shangzhi City, laoyeling (45°24.71'N, 127°40.41'E), 8–18.VII.2013, Cheng-de Li, Ye Chen, Chao Zhang, MT. **Paratype:** 1 female [on slide, NEFU], CHINA, Shandong Province, Qingdao City, xiaozhu Mountain (35°58.38'N, 120°05.76'E), 18–20.V.2014, Xiang-xiang Jin, Guo-hao Zu, Si-zhu Liu, yellow pan trapping.

Diagnosis. *Centrodora pellucida* sp. n. can be easily distinguished from other species in this genus by the following combination of characters: upper half of head yellowish-brown; gaster dark brown; fore wing mostly infuscate and paler distally, with a wide transparent cross band on the median area of disc as in Fig. 16; F2 subquadrate, and ovipositor strongly exserted.

Description. ***Female***. Holotype [The colour of body faded during slide mounting, and the following descriptions of colour is based on alcohol-preserved specimens]. Length 0.95 mm. Head with frontovertex, upper face, and occiput above foramen yellowish brown; remainder of head brown. Eyes and ocelli yellowish-brown. Antenna brown. Mandible yellowish-brown, with apex dark brown. Mesosoma largely yellowish-brown, but with mesopleuron brown and with a pale yellow mid-longitudinal groove on median area of mesoscutum, mesoscutellum, metanotum, and propodeum. Fore wing mostly infuscate and paler distally, with a wide transparent cross band on the median area of disc as in Fig. 16. Hind wing faintly infuscate. Leg mostly brownish; mesocoxa paler; meso- and metafemur, both basal one third of meso- and metatibia dark brown. Metasoma mostly dark brown, with petiole and third valvula yellowish.

Head (Fig. 12), in frontal view, 0.77× as high as wide; face and malar space finely reticulate. Frontovertex about 0.37× head width, with numerous coarse and brown setae. Ocellar triangle with apical angle about 90°. Mandible with two teeth and a truncation. Antennae (Fig. 13) with scape 4.13× as long as wide, about as long as clava; pedicel 2.0× as long as wide, about as long as F3; F1 triangular, 1.64× as long as wide, with ventral margin very slightly shorter than F2; F2 subquadrate, slightly shorter than half of F3; F3 2.12× as long as wide, 0.44× as long as clava; clava 4.0× as long as wide, pointed and distinctly curved ventrally at apex. Measurements, length (width): scape, 124 (30); pedicel, 50 (25); F1, 23 (14); F2, 25 (23); F3, 53 (25); clava, 120 (30).

Mesosoma with fine, elongate reticulations on median area of mesoscutum and mesoscutellum (Figs 14, 15). Median area of mesoscutum 0.93× as long as wide, 1.53× as long as mesoscutellum, and with 10 setae; each lateral area of the mesoscutum and axilla with 2 and 1 setae respectively; mesoscutellum 0.73× as long as wide, with 2 pairs of setae. Distance between anterior scutellar setae subequal to that between posterior pair. Placoid sensilla much closer to anterior pair of setae than to posterior pair. Fore wing (Fig. 16) 4.21× as long as wide, marginal setae 0.22× wing width. Costal cell slightly shorter than marginal vein, with 1 distal seta on dorsal surface; submarginal vein with 4

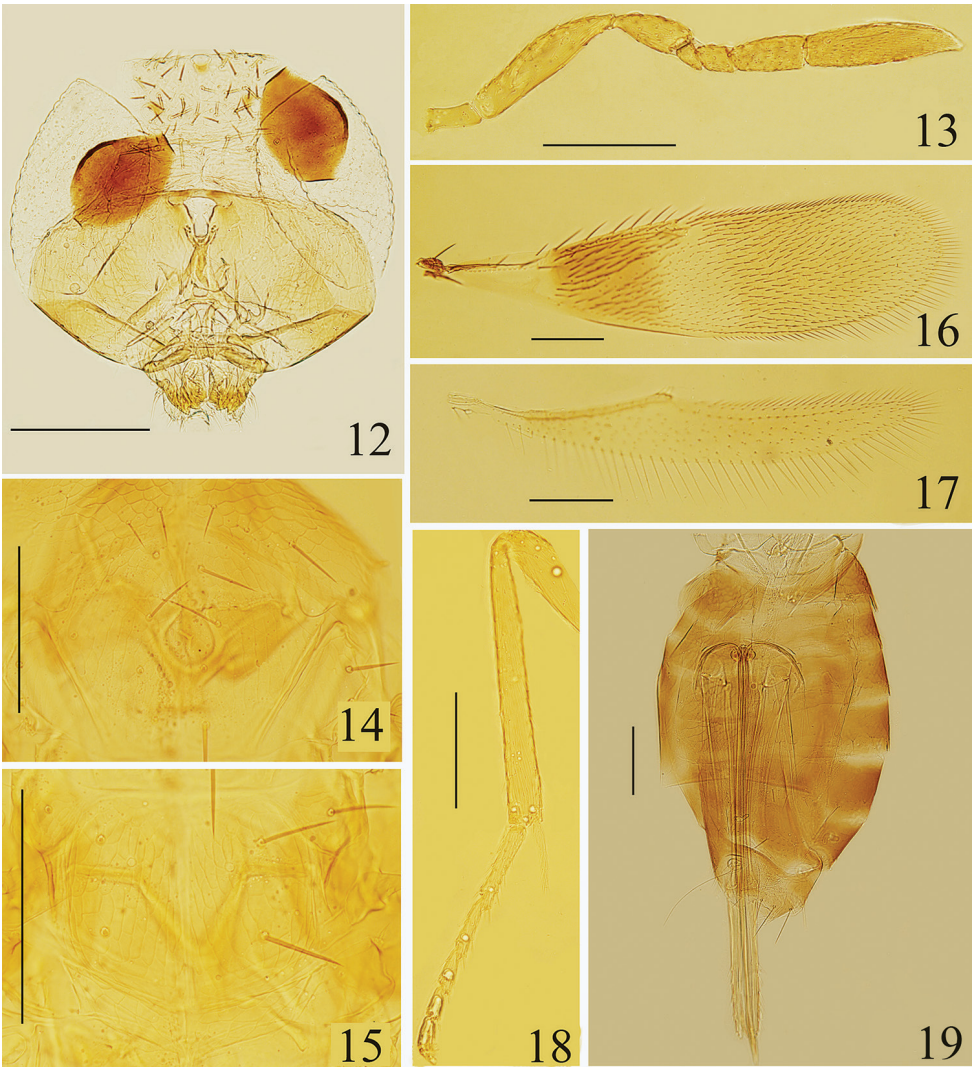

Figures 12–19. *Centrodora pellucida* sp. n., holotype female: **12** head, frontal view **13** antenna **14** mesoscutum **15** mesoscutellum and metanotum **16** fore wing **17** hind wing **18** mesotibia and tarsus **19** metasoma.

setae, marginal vein with 6 long setae along anterior margin, postmarginal vein 0.5× as long as stigmal vein; basal cell without seta. Linea calva closed by a line of setae posteriorly. Hind wing (Fig. 17) 6.86× as long as wide, marginal setae 0.67× wing width. Mesotibial spur 0.87× as long as corresponding basitarsus, and 0.83× as long as the second tarsomere. Measurements, length (width): fore wing, 738 (175); costal cell, 160; marginal vein, 170; postmarginal vein, 10; stigmal vein, 20; marginal setae, 38.5; hind wing, 600 (87.5); marginal setae, 59; mesotibia, 250; mesotibial spur, 65; mesobasitarsus, 75.

Metasoma (Fig. 19) about 1.4× as long as mesosoma. Ovipositor 2.45× as long as mesotibia and strongly exserted, with the exserted part 0.35× as long as ovipositor.

Third valvula 3.07× as long as mid basitarsus. Length measurements: ovipositor, 613; third valvula, 230.

Male. Unknown.

Remarks. The new species is very close to *C. amoena* Förster 1878 in having similar colour of the body and strongly exserted ovipositor. But it can be separated from the latter by F1 with ventral margin very slightly shorter than F2 (*vs* obviously shorter, *cf.* Nikol'skaya and Yasnosh 1966, fig. 150), F2 subquadrate (*vs* about 1.8× as long as wide), clava 4.0× as long as wide (*vs* 3.5×), fore wing mostly infuscate, with a transparent cross band on the median area of disc (*vs* mostly hyaline with the area beneath marginal vein and stigmal vein infuscate).

Host. Unknown.

Etymology. The specific name refers to the fore wing with a wide transparent cross band on the median area of disc.

Distribution. China (Heilongjiang, Shandong).

Acknowledgements

This project was supported by the National Natural Science Foundation of China (Grant No. 31470652). We are grateful to Dr Xiang-xiang Jin, Dr Guo-hao Zu, Mr Chao Zhang and Miss Si-zhu Liu for specimen collection. Special thanks to the staff at Laoyeling Ecological Observation Station for attentions to the experimental materials.

References.

Chiu SC, Chou KC (1974) Investigation on the egg parasites of *Oxya intricata* in Taiwan. Journal of Taiwan Agricultural Research 23(2): 116–125.

Chou KC, Chou LY (1990) Survey of the natural enemies of mango leaf-hopper in Taiwan. Journal of Agricultural Research 39(1): 70–75.

Hayat M (1974) Host-parasite catalogue of the egg-inhabiting aphelinid genera *Centrodora* Foerster, 1878, and *Tumidiscapus* Girault, 1911 (Hymenoptera, Chalcidoidea). Polskie Pismo Entomologiczne 44: 287–298.

Hayat M (1998) Aphelinidae of India (Hymenoptera: Chalcidoidea): A taxonomic revision. Memoirs on Entomology, International 13: 1–416.

Hayat M (2010) Additions to the Aphelinidae of India (Hymenoptera: Chalcidoidea) –2, Genus *Centrodora* Foerster. Oriental Insects 44: 49–68. https://doi.org/10.1080/00305316.2010.10417606

Huang J (1994) Systematic studies on Aphelinidae of China (Hymenoptera: Chalcidoidea). Chongqing Publishing House, Chongqing, 348 pp.

Hymenoptera Anatomy Consortium (2017) Hymenoptera Anatomy Ontology Portal. http://glossary.hymao.org [accessed June 2017]

Mercet RG (1918) El género *Centrodora* Foerster (Himénopteros Calcídidos). Boletin de la Real Sociedad Española de Historia Natural 18: 103–109.

Mercet RG (1930) Afelinidos paléarticos (Hym. Chalc.), 5a nota. Eos. Revista Española di Entomologia 6: 287–295.

Nikol'skaya MN, Yasnosh VA (1966) Aphelinids of the European part of the USSR and the Caucasus (Hymenoptera, Aphelinidae) Opredelitel' po Faune SSSR No. 91: 1–296.

Noyes JS (1982) Collecting and preserving chalcid wasps (Hymenoptera: Chalcidoidea). Journal of Natural History 16: 315–334. https://doi.org/10.1080/00222938200770261

Noyes JS (2017) Universal Chalcidoidea Database. http://www.nhm.ac.uk/chalcidoids [accessed March 2017]

Polaszek A (1991) Egg parasitism in Aphelinidae (Hymenoptera: Chalcidoidea) with special reference to *Centrodora* and *Encarsia* species. Bulletin of Entomological Research 81(1): 97–106. https://doi.org/10.1017/S0007485300053293

ZooKeys 687: 63–72 (2017)
doi: 10.3897/zookeys.687.13660
http://zookeys.pensoft.net

RESEARCH ARTICLE

A peer-reviewed open-access journal
ZooKeys
Launched to accelerate biodiversity research

A second locality for the Namib darkling beetle *Onymacris brainei* (Tenebrionidae, Coleoptera) and first report on its molecular phylogenetic placement

Trip Lamb[1], Eugene Marais[2], Jason E. Bond[3]

1 *Department of Biology, East Carolina University, Greenville, NC 27858, USA* **2** *National Museum of Namibia, Windhoek, Namibia* **3** *Department of Biological Sciences and Auburn University Museum of Natural History, Auburn University, Auburn, AL 36849, USA*

Corresponding author: *Trip Lamb* (lamba@ecu.edu)

Academic editor: *A. Smith* | Received 12 May 2017 | Accepted 19 July 2017 | Published 1 August 2017

http://zoobank.org/62C77060-6427-46AD-88B6-AD71BA3C9A1E

Citation: Lamb T, Marais E, Bond JE (2017) A second locality for the Namib darkling beetle *Onymacris brainei* (Tenebrionidae, Coleoptera) and first report on its molecular phylogenetic placement. ZooKeys 687: 63–72. https://doi.org/10.3897/zookeys.687.13660

Abstract

Onymacris brainei Penrith, 1984 – the most recent species of *Onymacris* to be described – is known only from its type locality in the Namib Desert, adjacent to the Cunene River in northern Namibia. No additional specimens are known to have been collected beyond the type series. Herein, we report on eight specimens discovered at a second site near the original locality. DNA from four beetles was used to determine the phylogenetic placement of *O. brainei* among congeners, based on sequence data from one nuclear (histone III) and two mitochondrial (*cox1*, *cox2*) genes. Maximum likelihood analysis identifies *O. brainei* as a member of the 'white' *Onymacris* clade, in which it forms a strongly supported subclade with *O. bicolor* and *O. marginipennis*. More broadly, its phylogenetic placement augments previous molecular results that revealed a sister taxon relationship between the 'white' *Onymacris* and a second genus, *Physadesmia*. The paraphyly of *Onymacris* with respect to *Physadesmia* highlights a need for nomenclatural change, but revision should await acquisition of genetic data for the few species outstanding in both genera.

Keywords

Adesmiini, Namib Desert, *Onymacris*, Tenebrionidae

Introduction

The darkling beetle genus *Onymacris* is a diverse assemblage of fast-running diurnal species endemic to Africa's Namib Desert and adjacent southwestern edges of the Kalahari. As substrate specialists, these beetles are restricted to loose sand that characterizes hummocks, dry riverbeds, and dune fields, where they occur in abundance and assume key ecological roles as detritivores (Louw 1983; Hanrahan and Seely 1990). The genus belongs to the flightless tribe Adesmiini, which includes 240+ species and is distributed largely within southwest Africa–a geographic center where adesmiines exhibit their greatest ecological breath and morphological diversity (Koch 1962; Penrith 1979). Regionally, *Onymacris* represents one of the tribe's more species-rich genera, with 26 currently recognized taxa (14 species and 12 subspecies) that include distinctive 'white' species, whose elytral color ranges from pure white to yellow or tan (Fig. 1). White elytral coloration, an unusual characteristic among beetles in general and darkling beetles in particular, is one of many remarkable evolutionary features observed among Namib tenebrionids that are unknown in beetles from other deserts (Hamilton and Seely 1976; Endrödy–Younga 1978; Roberts et al. 1991).

'White' *Onymacris* are restricted to the northern Namib, where they are patchily distributed, often with limited geographic ranges. *Onymacris brainei*–the most recent member of the genus to be described (Penrith 1984)–represents this case in the extreme: it is known only from the type locality in northern Namibia, just south of the Cunene River along the Angolan border (Fig. 2). Steven Braine collected the first specimens (3 males, 2 females) on 24 February 1983 and brought them to the attention of Mary-Louise Penrith, who at that time was actively revising the southern African Adesmiini (Penrith 1975, 1979, 1984, 1986). Early in the following year (12–15 February 1984), Penrith and Ruth Müller collected 16 additional specimens at the original locality, which provided sufficient material for describing the new species, named in Braine's honor (Penrith 1984). *Onymacris brainei* is distinguished from other 'white' species by the presence of three broad, pale yellow to tan stripes on otherwise white elytra (Fig. 3).

To our knowledge, no other specimens or localities for *O. brainei* have been documented since its description. In 2015, some 30 years after Penrith and Müller's expedition, we searched the general vicinity of the type locality in an attempt to update the status of *O. brainei*. Herein, we report on eight additional specimens taken from a second site. Importantly, these beetles provided a source of fresh tissue for DNA extraction, gene sequencing, and phylogenetic analysis. Hence we also offer the first report on the molecular phylogenetic placement of *O. brainei* among its congeners.

Methods

Field survey for *Onymacris brainei*

Penrith (1984) reported the type locality as "Kunene R. east of dunes at 17.12S, 12.10E," where beetles were collected "on dune hummocks." Working from this geographic ap-

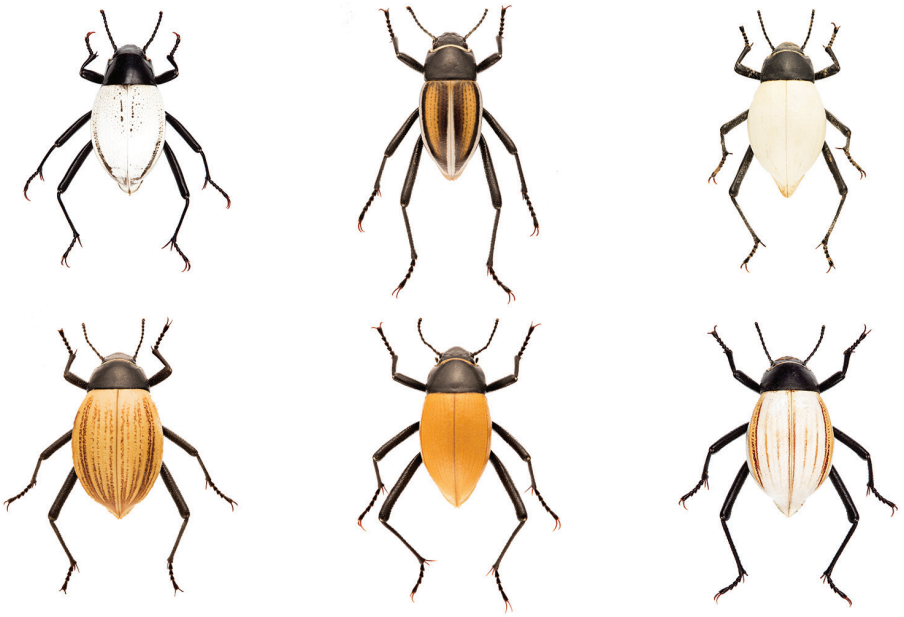

Figure 1. Color variation among members of the 'white' *Onymacris* clade, as represented by: (top row, left to right) *Onymacris bicolor*, *O. marginipennis*, *O. candidipennis*, and (bottom row, left to right) *O. langi visseri*, *O. langi cornelii*, and *O. langi meridionalis*.

proximation, we searched a series of appropriate sites (i.e., vegetated hummocks) across the region on 21–22 May 2015. Three of these sites yielded other white *Onymacris* (*O. bicolor*, *O. langi cornelii*), and at a fourth, final site (17°17.87'S; 12°06.20'E), we succeeded in locating *O. brainei* (Fig. 2). Several beetles were observed, of which eight specimens were captured, euthanized (ethanol injection), and carded.

Molecular phylogenetic analysis

Rear legs from four of the eight beetles were preserved in RNAlater for subsequent DNA isolation using Qiagen's DNeasy kit. The mitochondrial genes cytochrome oxidase I (*cox1*) and cytochrome oxidase II (*cox2*) and a nuclear gene (histone III, *H3*) were amplified using the primers and PCR conditions listed in Table 1. Amplicons were cleaned using exoSAP-IT (USB Corp.) and sequenced on an Applied Biosystems 3130 capillary sequencer. Sequences were edited and assembled in Sequencher 4.9 (GeneCodes, Ann Arbor, MI) and aligned using ClustalX ver. 2.0 (Larkin et al. 2007), after which sequences were translated to ensure a correct reading frame. Sequences are available through GenBank (Table 2).

DNA sequences for *O. brainei* were combined with sequence data previously generated for *Onymacris* (Table 2) to yield a concatenated dataset–*cox1* (1212 bp), *cox2* (688 bp), and *H3* (317 bp)–representing 18 of the 26 currently recognized species/

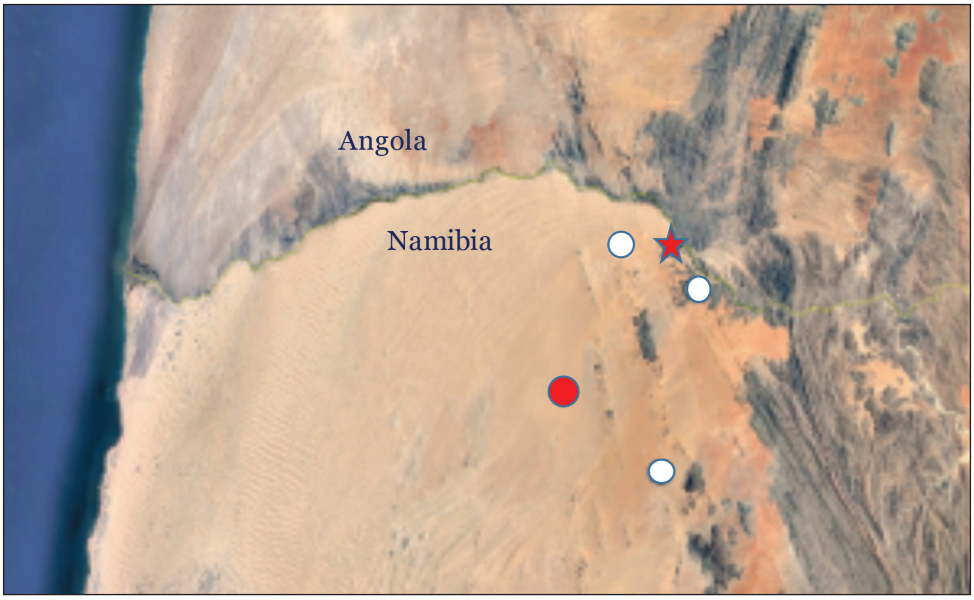

Figure 2. Map illustrating the type locality for *Onymacris brainei* (star), surveyed sites with appropriate habitat (white circles), and the second locality for *O. brainei* (red circle).

Table 1. PCR primers and amplification conditions.

Gene	Primer	Annealing	Cycles	Reference
cox1	TY-J-1460	50°C	35	Simon et al. (1994)
	TL2-N-3014			
	C1-J-2183	sequencing only		
cox2	TL2-J-3037	50°C	35	
	TK-N-3785			
H3	Hex AF	61.5°C	45	Odgen and Whiting (2003)
	Hex AR			

subspecies. Those taxa unavailable to us for sequencing included *O. candidipennis* and *O. langi langi*, both 'white' beetles from Angola, as well as the 'black' beetles *O. plana debilis* and *O. paiva conjuncta* (though our dataset contains their nominate subspecies). We also incorporated species sequences representing three additional adesmiine genera: *Physadesmia* (represented by *P. globosa*), shown to be the sister taxon to the white *Onymacris* clade (Lamb and Bond 2013) as well as *Eustolopus octoseriatus* and *Adesmia cribripes*, which served as outgroups.

We used maximum likelihood (ML) to analyze the concatenated gene dataset. The ML analysis, executed in RAxML ver. 7.2.8 (Stamatakis 2006), comprised 1,000 random sequence addition replicates (RAS) using the commands "-# 1000" and "–m GTRGAMMA." Bootstrap support values were calculated using the same search parameters with 1,000 replicates, and bootstrap results were applied to the best tree recovered in the RAS search.

Table 2. GenBank accession numbers for adesmiine sequences used in the ML analysis.

Species	GenBank *cox1*	GenBank *cox2*	GenBank *H3*
Onymacris brainei	MF459686	MF459688	MF459690
Onymacris brainei	MF459687	MF459689	—
O. bicolor	JX448896	JX448934	JX448972
O. marginipennis	JX448907	JX448945	JX448983
O. langi cornelii	JX448900	JX448938	JX448976
O. langi meridionalis	JX448909	JX448947	JX448985
O. langi visseri	JX448921	JX448959	JX448997
O. boschimana	JX448897	JX448935	JX448973
O. multistriata	JX448912	JX448950	JX448988
O. hottentota	JX448901	JX448939	JX448977
O. plana	JX448915	JX448953	JX448991
O. lobicollis	JX448906	JX448944	JX448982
O paiva	JX448913	JX448951	JX448989
O. rugatipennis	JX448917	JX448955	JX448993
O. laeviceps	JX448904	JX448942	JX448980
O. u. unguicularis	JX448919	JX448957	JX448995
O. u. schulzeae	JX448920	JX448958	JX448996
Physadesmia globosa	JX448887	JX448925	JX448963
Eustolopus octoseriatus	JX448886	JX448924	JX448962
Adesmia cribripes	JX448889	JX448927	JX448965

Results

New locality for *Onymacris brainei*

The second locality for *Onymacris brainei* was discovered on 22 May 2015. Based on the general geographic information provided in Penrith (1984), this new site is estimated to lie ~ 15–20 km SSW of the type locality (Fig. 2). The second site closely resembles the original locality's physical and ecological description, characterized by vegetated dune hummocks on which nara (*Acanthosicyos horridus*), an iconic Namib endemic, is the prevalent floristic component. Beetles were observed under and, in some cases, on hummock vegetation.

Elytral color variation

As noted, *Onymacris brainei* is diagnosed by the presence of three broad yellow to tan stripes on white elytra. Specifically, this patterning involves a prominent dorsal stripe that is bisected by the elytral suture and flanked by a slightly narrower lateral stripe on either side. All three stripes bear diffuse edges that coalesce anteriorly near the pronotum, taper posteriorly, and terminate at (or just before) the apical declivity.

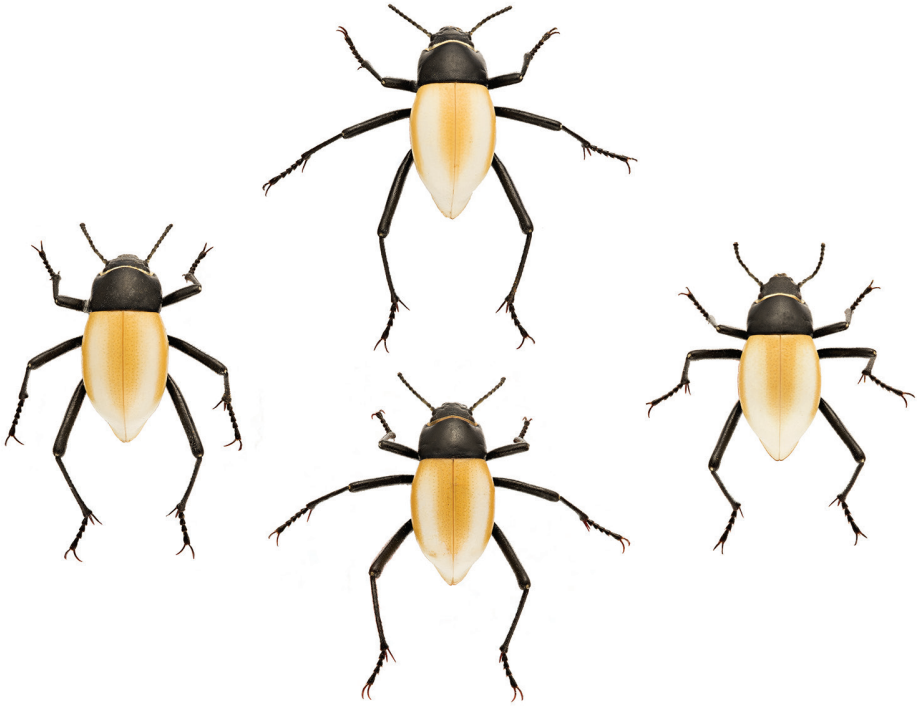

Figure 3. Specimens of *Onymacris brainei* from the second locality, illustrating variation in degree of elytral striping.

White elytral coloration is not due to any pigment product but rather a function of reflectivity involving microscopic "bubbles" within the cuticle (Kühnelt 1957). Thus, the stripes represent pigment expression within an otherwise colorless elytral matrix. Penrith (1984) noted that both stripe width and degree of pigment suffusion between stripes varied considerably across the type series. Our eight specimens of *O. brainei* exhibit comparable levels of dorsal color variation (Fig. 3).

Genetic variation

DNA sequences were invariant for the nuclear gene *H3* but did exhibit variation for both mitochondrial genes (two haplotypes for each gene); mean sequence divergence for the *cox1* and *cox2* was 1.49 % and 0.05%, respectively.

Molecular phylogenetic placement of *Onymacris brainei*

ML analysis of the concatenated dataset identified *O. brainei* as sister to *O. marginipennis* + *O. bicolor* in a highly supported clade (BS = 100%) that is sister to a second

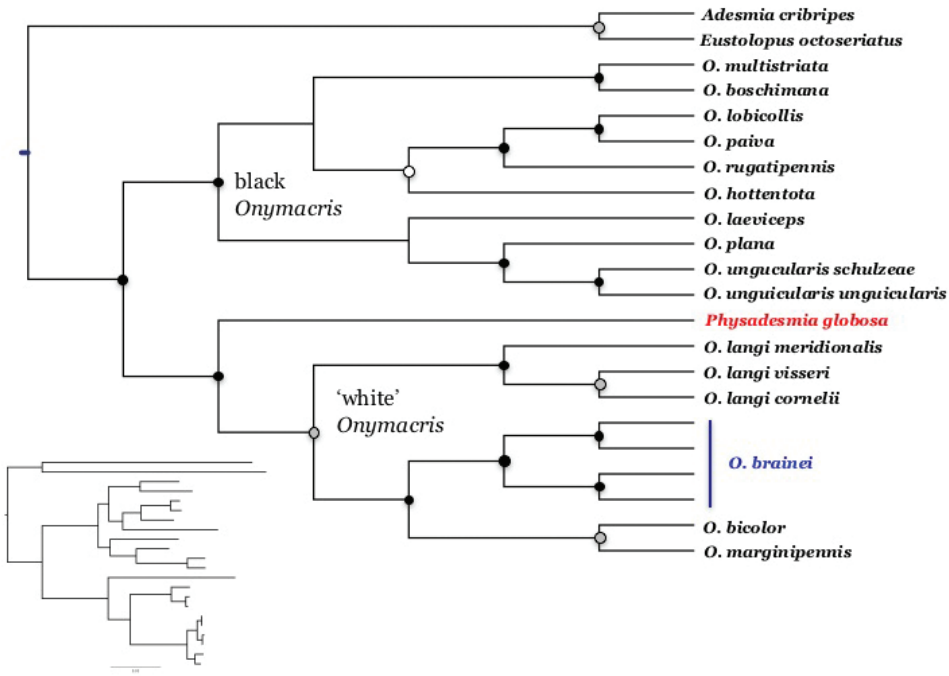

Figure 4. ML consensus topology of *Onymacris*, with bootstrap support indicated by black (> 95%), gray (> 90%), and white (> 70%) nodes. Inset at lower left is a ML tree showing branch lengths.

'white' clade comprising the three subspecies of *O. langi* represented in our dataset (Fig. 4). Overall, the ML topology is essentially identical to ML and Bayesian phylogenies previously derived from a larger multilocus dataset (Lamb and Bond 2013), which not only identified two distinct, well supported clades – one containing all 'white' species, the other, exclusively black species – but also revealed that *Onymacris* is paraphyletic. All three phylogenies [i.e., this report; Lamb and Bond (2013)] depict *Physadesmia globosa* as the sister taxon to the 'white" *Onymacris* lineage in a highly supported clade (herein, BS = 99%).

Discussion

In her paper originally describing *Onymacris brainei*, Penrith (1984) also reported the first cladistic analysis for the genus *Onymacris*, based on 23 morphological characters. To her credit, she examined several additional characters but rejected them "owing to suspected parallelism" or because "the direction of development could not be ascertained." Her analysis recovered two major clades: an all-black clade comprising six species (*O. boschimana*, *O. laeviceps*, *O. lobicollis*, *O. multistriata*, *O. paiva*, *O. rugatipen-*

nis), and a second clade composed of three additional black species (*O. hottentota*, *O. plana*, *O. unguicularis*) and the 'white' species group. Regarding relationships within Penrith's 'white' group, *O. brainei* was placed with *O. bicolor* and *O. marginipennis*, united by the loss of pseudopleural crests along the elytral margins. Furthermore, Penrith's cladogram depicts *O. brainei* and *O. marginipennis* as sister species on the basis of one synapomorphy–the epistome bearing a deep median emargination.

Our ML phylogeny corroborates *bicolor-brainei-marginipennis* monophyly but differs by depicting *O. bicolor* and *O. marginipennis* as sister species. To this end, we note a preliminary aspect of the molecular results–our somewhat limited geographic representation for *O. bicolor* and *O. marginipennis*. Relative to the other 'white' taxa, both these species have extended ranges and were recognized historically as being polytypic (Péringuey 1885; Koch 1952). Indeed, *O. bicolor* was for some time treated as two separate species (Koch 1952; Penrith 1975). Thus, while the precise sister status of *O. brainei* remains equivocal (pending further geographic sampling of *O. bicolor* and *O. marginipennis*, particularly Angolan populations), the strongly-supported monophyly of *O. bicolor* + *O. brainei* + *O. marginipennis* is unlikely to change.

The molecular phylogenetic placement of *O. brainei* with other 'white' *Onymacris* not only offers incremental support for the 'white' clade but, more broadly, augments a diphyletic *Onymacris* relative to *Physadesmia* (Lamb and Bond 2013). Penrith (1979) described the genus *Physadesmia* for three species [*Physadesmia globosa* (Haag), *P. bullata* (Péringuey), and *P. aculeata* (Péringuey)] formerly in *Physosterna.* (Of note, *Physosterna* was subsequently reduced to a subgenus of *Adesmia* (Penrith 1986)). She also observed that "*Physadesmia* and *Onymacris* are evidently very closely related, being separated only by the hypertrophy of the spurs and claws and the shortening of the tarsi in *Onymacris*." Support for her observation was provided in the first cladistic analysis of adesmiine genera, which recovered a clade comprising *Onymacris*, *Physadesmia*, and a third genus, *Eustolopus* (Penrith 1986). A refined phylogenetic view of *Onymacris-Physadesmia*, revealed herein and earlier (Lamb and Bond 2013), identifies a need for nomenclatural changes that will reflect the new found relationship between white *Onymacris* and *Physadesmia*. However, molecular genetic data are still missing for key taxa: two white *Onymacris* (*O. langi langi* and *O. candidipennis*, the latter being the type species of the genus) as well as the remaining two species of *Physadesmia* (*P. bullata* and *P. aculeata*). Though recognizing the necessity for taxonomic change (i.e., either subsuming *Physadesmia* or assigning the black species of *Onymacris* to a new genus), we consider this move to be premature at present and refrain from such effort until relationships for the remaining few species of *Onymacris* and *Physadesmia* have been thoroughly explored.

"Rediscovery" is a beguiling catchword, conveying equal parts accomplishment and optimism upon finding species thought to be rare or possibly extinct. We were indeed relieved to locate new specimens of *O. brainei*–a species gone unreported for 33 years. However, a claim of rediscovery might be overstated: the hiatus is attributable in large degree to the northern Namib's remote setting and limited accessibility. A more telling discovery may be the genetic divergence (1.49%, *cox1*) observed among individuals at the new locality, which could possibly indicate a historically

larger geographic distribution. It is worth noting that *O. candidipennis*, once thought to be restricted to the Namib's northern terminus in Angola, has been reported from Namibia at the Cunene River, near the type locality for *O. brainei* (Penrith 1984). Moreover, *O. bicolor* and *O. marginipennis*, the two species most closely related to *O. brainei*, occur on both sides of the Cunene. Thus, future assessment on the status of *O. brainei* (regarding genetic variation as well as range delimitation) should involve surveys of suitable habitat from the type locality west to the Cunene mouth, in Angola as well as Namibia. Close proximity of both type and new localities to the contiguous Skeleton Coast (Namibia) and Iona (Angola) national parks offers promise that additional populations of *O. brainei* might be discovered within park boundaries, where they would be afforded full protection.

Acknowledgements

We thank Patrice Bouchard, Edie Jeffreys, and Mike Wooten for their assistance in the field. Michael Brewer graciously provided access to his laboratory's composite imaging system. Specimens were processed under Research/Collecting Permit # 2015/2015 provided by Namibia's Ministry of Environment and Tourism. Funding for this project was provided by Research and Exploration grant # 9582-14 from the National Geographic Society.

References

Endrödy–Younga S (1978) Coleoptera. In: Werger MJA (Ed.) Biogeography and Ecology of Southern Africa. Junk, The Hague, 797–821. https://doi.org/10.1007/978-94-009-9951-0_26

Hamilton WJ, Seely MK (1976) Fog basking by the Namib Desert beetle *Onymacris unguicularis*. Nature 262: 284–285. https://doi.org/10.1038/262284a0

Hanrahan SA, Seely MK (1990) Food and habitat use by three tenebrionid beetles (Coleoptera) in a riparian desert environment. In: Seely MK (Ed.) Namib Ecology: 25 Years of Namib Research. Transvaal Museum Monograph No. 7. Transvaal Museum, Pretoria, 143–147.

Lamb T, Bond JE (2013) A multilocus perspective on phylogenetic relationships in the Namib darkling beetle genus *Onymacris* (Tenebrionidae). Molecular Phylogenetics and Evolution 66: 757–765. https://doi.org/10.1016/j.ympev.2012.10.026

Larkin MA, Blackshields G, Brown NP, Chenna R, McGettigan PA, McWilliam H, Valentin F, Wallace IM, Wilm A, Lopez R, Thompson JD, Gibson TJ, Higgins DG (2007) ClustalW and ClustalX version 2.0. Bioinformatics 23: 2947–2948. https://doi.org/10.1093/bioinformatics/btm404

Louw S (1983) The diversity and daily seasonal activity of ground-living Tenebrionidae (Coleoptera) in the southern Namib and Kalahari ecosystems. Cimbebasia A7: 35–56.

Koch C (1952) S. A. Tenebrionidae. XII. Supplementary notes to preliminary articles nos. I, III, V, and VIII. Annals of the Transvaal Museum 22: 79–196.

Koch C (1962) The Tenebrionidae of southern Africa. XXXI. Comprehensive notes on the tenebrionid fauna of the Namib Desert. Annals of the Transvaal Museum 24: 61–106.

Kühnelt W (1957) Weiss als Strukturfarbe bei Wüstentenebrioniden. Sitzungsberichte der Österreichischen Akademie der Wissenschaften 166: 103–112.

Ogden TH, Whiting MF (2003) The problem with the Paleoptera problem: sense and sensitivity. Cladistics, 19: 432–442. https://doi.org/10.1111/j.1096-0031.2003.tb00313.x

Penrith M-L (1975) The species of *Onymacris* Allard (Coleoptera: Tenebrionidae). Cimbebasia 4: 47–97.

Penrith M-L (1979) Revision of the western southern African Adesmiini (Coleoptera: Tenebrionidae). Cimbebasia 5: 1–94.

Penrith M-L (1984) New taxa of *Onymacris* Allard, and relationships within the genus (Coleoptera: Tenebrionidae). Annals of the Transvaal Museum 33: 511–533.

Penrith M-L (1986) Relationships in the tribe Adesmiini (Coleoptera: Tenebrionidae) and a revision of the genus *Stenodesia* Reitter. Annals of the Transvaal Museum 34: 275–302.

Péringuey L (1885) First contribution to the South African coleopterous fauna. Transactions of the South African Philosophical Society 3: 74–149. https://doi.org/10.1080/21560382.1881.9526176

Roberts CS, Seely MK, Ward D, Mitchell D, Campbell JD (1991) Body temperatures of Namib Desert tenebrionid beetles: their relationships in laboratory and field. Physiological Entomology 16: 463–475. https://doi.org/10.1111/j.1365-3032.1991.tb00586.x

Simon C, Frati F, Beckenbach A, Crespi B, Liu H, Paul F (1994) Evolution, weighting, and phylogenetic utility of mitochondrial gene-sequences and a compilation of conserved polymerase chain reaction primers. Annals of the Entomological Society of America 87: 651–701. https://doi.org/10.1093/aesa/87.6.651

Stamatakis A (2006) RAxML-VI-HPC: Maximum likelihood-based phylogenetic analyses with thousands of taxa and mixed models. Bioinformatics 22(21): 2688–2690. https://doi.org/10.1093/bioinformatics/btl446

ZooKeys 687: 73–88 (2017)
doi: 10.3897/zookeys.687.13156
http://zookeys.pensoft.net

RESEARCH ARTICLE

A peer-reviewed open-access journal
ZooKeys
Launched to accelerate biodiversity research

Three new species and one new record of the genus *Siphunculina* from China (Diptera, Chloropidae)

Xiao-Yan Liu[1], Emilia P. Nartshuk[2], Ding Yang[3]

1 *Hubei Insect Resources Utilization and Sustainable Pest Management Key Laboratory, College of Plant Science and Technology, Huazhong Agricultural University, Wuhan 430070, China* **2** *Zoological Institute, Russian Academy of Sciences, St. Petersburg 199034, Russia* **3** *Department of Entomology, China Agricultural University, Beijing 100193, China*

Corresponding author: *Xiao-Yan Liu* (yanziliu52@163.com)

Academic editor: *R. Meier* | Received 9 April 2017 | Accepted 21 June 2017 | Published 2 August 2017

http://zoobank.org/249E015E-F9DB-42CA-8C49-1BF26A60378E

Citation: Liu X-Y, Nartshuk EP, Yang D (2017) Three new species and one new record of the genus *Siphunculina* from China (Diptera, Chloropidae). ZooKeys 687: 73–88. https://doi.org/10.3897/zookeys.687.13156

Abstract

Three new species of the genus *Siphunculina* Rondani from China, *S. bulbifera* **sp. n.**, *S. scalpriformis* **sp. n.**, and *S. shangyongensis* **sp. n.**, are described and illustrated. One species, *S. funicola* (de Meijere), is reported from China for the first time. A key to the species of genus *Siphunculina* from China is given.

Keywords

China, Chloropidae, Diptera, new species, *Siphunculina*, Taxonomy

Introduction

The genus *Siphunculina* was erected by Rondani (1856). It belongs to the *Aphanotrigonum* genus group of the subfamily Oscinellinae (Andersson 1977). There are 34 species known from the world, of which 17 species are distributed in the Oriental Region, ten species in the Palaearctic Region, eleven species in the Afrotropical, three species in the Australian, only one species is known to occur in the Nearctic and Neotropical Regions (Cherian 1970, 1977; Sabrosky 1977, 1980, 1989; Kanmiya 1982, 1989, 1994; Nartshuk 1984, 2005, 2007; Ismay and Nartshuk 2000; Merz 2008; Iwasa et al. 2013). Adults of some species are attracted to decaying

meat, wounds, scratches, mucous membranes, eyes, lips, moist skin, in-between toes, sweat, and other secretions of the body and are suspected of mechanically transmitting pathogenic organisms to man and domestic animals (Graham-Smith 1930; Chansang et al. 2010). The larvae can be found in birds' nests, excrement, or dead animals, which are saprophilous or scatophagous (Kanmiya 1983; Ferrar 1987; Ismay and Nartshuk 2000).

To date, five species are known to occur in China, of which four are known from Taiwan and two species are distributed in mainland China. In this paper, three new species of the genus *Siphunculina* from China, *S. bulbifera* sp. n., *S. scalpriformis* sp. n. and *S. shangyongensis* sp. n., are described and illustrated. One species, *S. funicola* (de Meijere), is newly recorded from China. A key to the species of genus *Siphunculina* from China is given.

Materials and methods

Specimens were studied and illustrated with ZEISS Stemi 2000–c. Genitalic preparations were made by macerating the apical portion of abdomen in warm 10% NaOH for 17–20 min, after examination it was transferred to fresh glycerine and stored in a microvial pinned below the specimen. Specimens are deposited in the Entomological Museum of China Agricultural University (CAU), Beijing. The morphological nomenclature follows Cumming and Wood (2009). The following abbreviations are used:

bas	basiphallus;	**gon**	gonite;
cerc	cercus;	**hyp**	hypandrium;
dis	distiphallus;	**phal**	phallapodeme;
dm-cu	discal medial-cubital crossvein;	**r-m**	radio-medial crossvein;
ep	epandrium;	**sur**	surstylus.

Taxonomy

Family Chloropidae

Genus *Siphunculina* Rondani, 1856

Siphunculina Rondani, 1856: 128. Type species: *Siphunculina brevinervis* Rondani, 1856 (= *Siphonella aenea* Macquart, 1835), by original designation.

Microneurum Becker, 1903: 152. Type species: *Microneurum maculifrons* Becker, 1903 (= *Oscinis ornatifrons* Loew, 1858), by monotypy.

Liomicroneurum Enderlein, 1911: 230. Type species: *Siphonella funicola* de Meijere, 1905, by original designation.

Diagnosis. Head with vibrissal angle more or less distinctly produced beyond eye; face with deeply concave antennal foveae and a distinct median carina reaching epistoma; cephalic setae and setulae generally short; wing with veins R_1 and R_{2+3} extremely closed on basal portion, vein R_{2+3} very short, length of 2nd costal sector extremely shorter than the 3rd sector; femoral and tibial organs absent (Kanmiya 1983, 1994).

Distribution. Widespread world-wide distribution, see Nartshuk (2012). China: Beijing, Zhejiang, Hainan, Guizhou, Yunnan, Taiwan.

Key to species of *Siphunculina* from China

1 Cephalic setae and setulae black or brown.....**2**
– Cephalic setae and setulae light yellow or yellow.....**7**
2 Ocellar triangle shiny except for ocellar tubercle, without microtomentum; frons, ocellar triangle and scutum marked out by reticulate patterns with alternating microtomentose and bare maculae..... ***S. striolata*** **(Wiedemann)**
– Ocellar triangle not entirely shiny, partly or entirely microtomentose; frons, ocellar triangle and scutum not marked out by alternating microtomentose and bare maculae.....**3**
3 Notopleurals 1+2; apical scutellar seta as long as scutellum (Fig. 20)..... .....***S. funicola*** **(de Meijere)**
– Notopleurals 1+1; apical scutellar seta shorter than scutellum.....**4**
4 Two pairs of scutellar setae; 3rd costal sector 2 times as long as 2nd sector (Fig. 2).....***S. bulbifera*** **sp. n.**
– Three pairs of scutellar setae; 3rd costal sector 3-4 times as long as 2nd sector... **5**
5 Ocellar triangle nearly or completely reaching anterior margin of frons, with a median groove.....***S. nitidissima*** **Kanmiya**
– Ocellar triangle ending slightly but distinctly before anterior margin of frons, without median groove.....**6**
6 Hind tibia yellow with largely infuscate maculae medially; tarsi entirely yellow; surstylus as long as the epandrium in lateral view ..... ***S. bella*** **Kanmiya**
– Hind tibia yellow except for middle 1/3 brown; tarsi yellow except for hind tarsomeres 2-4 brown; surstylus 0.6 times as long as the epandrium in lateral view (Figs 13, 16) .....***S. shangyongensis*** **sp. n.**
7 Ocellar triangle extending to middle or slightly over middle of frons **8**
– Ocellar triangle extending near or completely to anterior margin of frons..... ..... ***S. minima*** **(de Meijere)**
8 Ocellar triangle microtomentose except for area in front of ocelli and on both sides of ocellar tubercle shiny (Fig. 8).....***S. scalpriformis*** **sp. n.**
– Ocellar triangle shiny with 2 microtomentose patches extending from nearly mediolateral of triangle to anterior ocellus ..... ***S. fasciata*** **Cherian**

***Siphunculina bulbifera* sp. n.**
http://zoobank.org/2A36E011-58B7-47A8-9B00-BEABB0027FFE
Figs 1–6

Diagnosis. Ocellar triangle smooth, shiny, reaching anterior margin of frons, with pointed apex. Scutellum with two pairs of scutellar setae on small tubercles. Cephalic and thoracic setae and setulae black. Notopleurals 1+1. Distal 2/3 of gonite long globose.

Description. ***Holotype. Male***. Body length 2.2 mm, wing length 1.6 mm.

Head black, 0.8 times as long as high in profile, as wide as thorax; face somewhat concave in lateral view, facial carina distinct, broad; frons as long as wide, projecting slightly in front of eye; gena broad, 0.5 times as wide as first flagellomere; parafacial linear; vibrissal angle distinctly produced beyond eye by subequal length to gena-width. Ocellar triangle smooth, shiny, reaching anterior margin of frons, with pointed apex; ocellar tubercle black. Cephalic setae and setulae black. Antenna yellow except for distodorsal 1/2 of first flagellomere brown, with thick grayish microtomentum; first flagellomere 0.6 times as long as wide; arista black except for basal segment yellow, with short pubescence. Proboscis brown to yellow with yellow setulae; palpus brown to yellow with yellow setulae.

Thorax black with gray microtomentum, evenly covered with short setulae. Scutum as long as wide. Thoracic pleuron shiny black. Scutellum 0.55 times as long as wide; two pairs of scutellar setae on small tubercles; apical scutellar seta short, 0.3 times as long as scutellum. Setae and setulae on thorax black; notopleurals 1+1, developed. Legs brown except for basal portion and distal 1/3 of fore tibia, both ends of mid and hind tibiae, fore and hind tarsomeres 1, mid tarsomeres 1-2 yellow. Setulae on legs brown. Wing 2.3 times as long as wide, hyaline; veins yellowish brown. Relative lengths of 2nd : 3rd : 4th costal sections = 5 : 10 : 3; cross-veins r-m and dm-cu not approximated, r-m at basal 0.65 of discal medial cell. Halter brown.

Abdomen shiny brown except for tergite 1 yellow with brown distally; venter yellow. Setulae on abdomen black.

Male genitalia (Figs. 3–6): Epandrium blackish brown with long brown setulae; surstylus distinctly shorter than epandrium in lateral view. Cercus short and broad, with moderately concave ventral margin in dorsal view. Pre- and postgonites fused, basal 1/3 narrow, distal 2/3 long globose; basiphallus longer than wide, cylindrical; distiphallus short, membranous; phallapodeme long, with basal stalk narrow in lateral view. Hypandrium broad, with two basal rounded projections, arms free and short, apex with internal projection long, external projection short.

***Female*.** Unknown.

Type material. Holotype, ♂, China: Beijing: Shidu, 1-2. VI. 2009, leg. Dan Zhou (photographed and genitalia prepared). Paratype, 2 ♂♂, same locality as holotype, 1-2. VII. 2009, leg. Jinjing Wang (in 75% alcohol, deposited in CAU).

Distribution. China (Beijing).

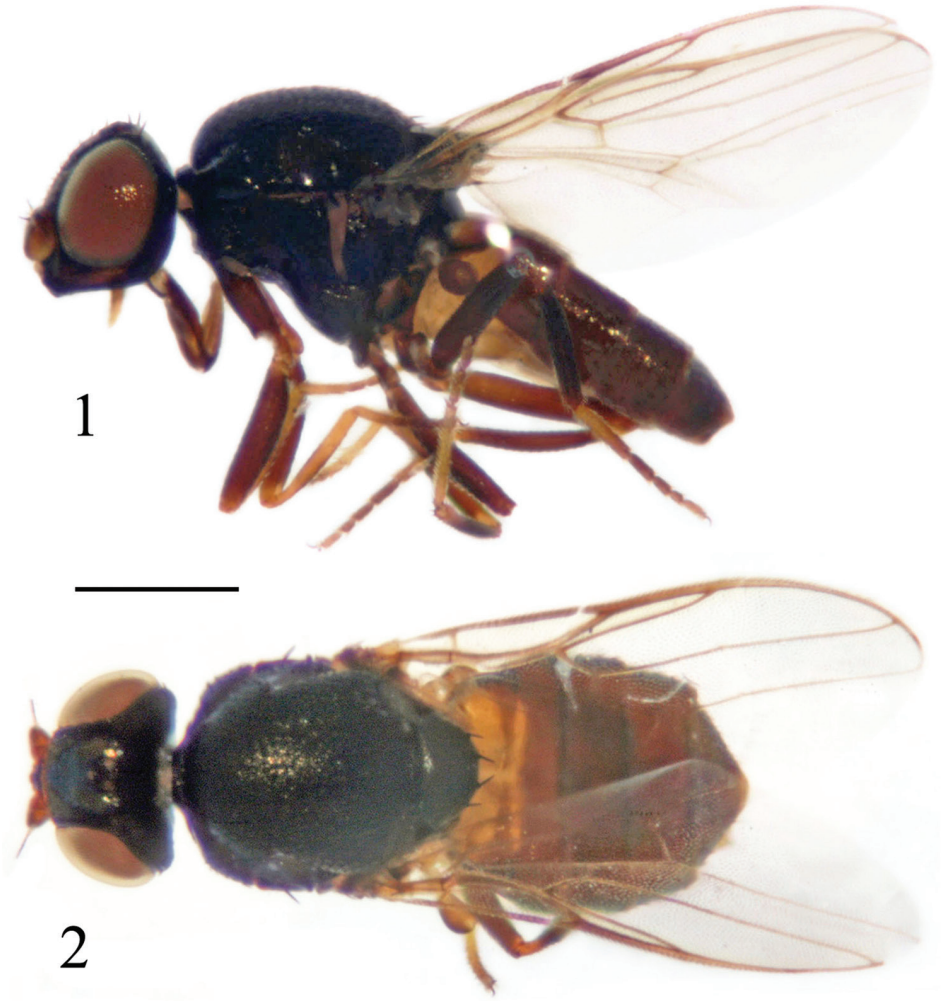

Figures 1–2. *Siphunculina bulbifera* sp. n., holotype. habitus, **1** lateral view **2** dorsal view. Scale bar 0.05 mm.

Remarks. The new species is somewhat similar to *S. nitidissima* Kanmiya, but can be separated from the latter by the following features: ocellar triangle smooth without median groove, two pairs of scutellar setae on small tubercles, and gonite has narrow base, its distal 2/3 long and globose; in *S. nitidissima*, the ocellar triangle has a median groove, the scutellum has three pairs of scutellar setae on small tubercles, and the gonite is finger-like (Kanmiya 1982).

Etymology. The specific name is from the Latin *bulbifera* ("bulbiform"), referring to the shape of gonite.

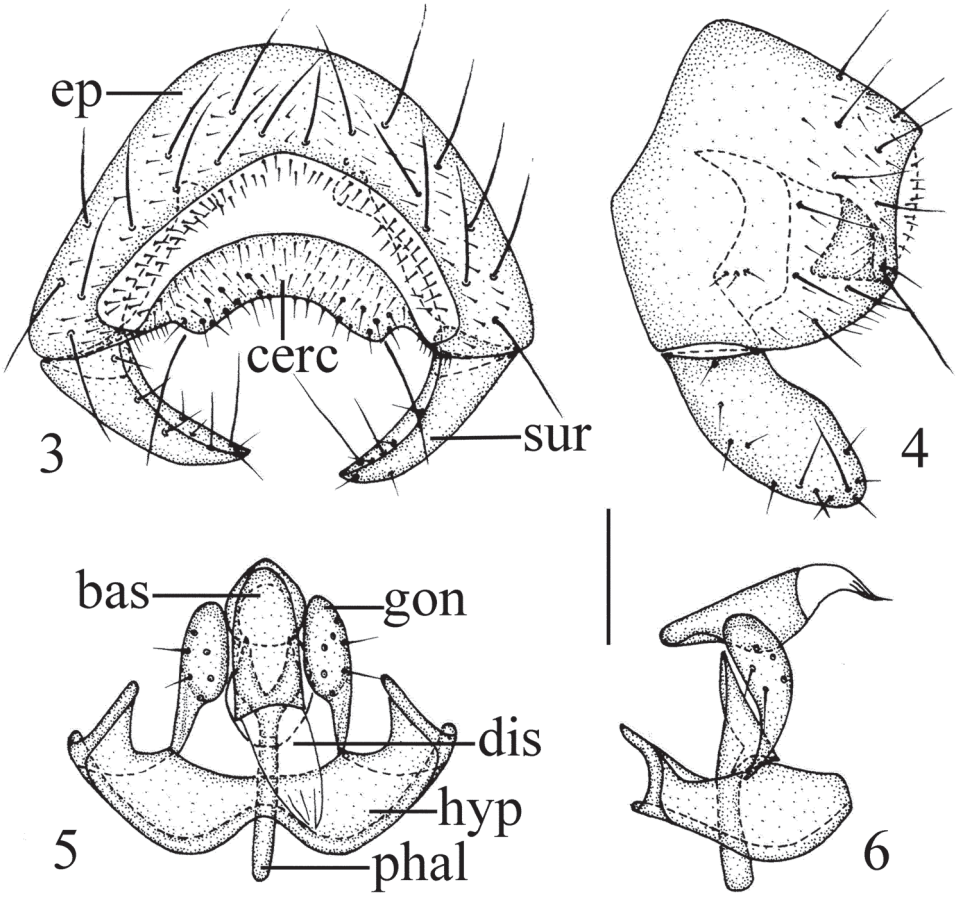

Figures 3–6. *Siphunculina bulbifera* sp. n., holotype. **3** epandrium, posterior view **4** epandrium, lateral view **5** hypandrium and phallic complex, ventral view **6** hypandrium and phallic complex, lateral view. Scale bar: 0.1 mm.

***Siphunculina scalpriformis* sp. n.**
http://zoobank.org/3DFBB88D-1403-4FD0-92D6-02AEC4090064
Figs 7–12

Diagnosis. Ocellar triangle black with gray microtomentum except for area in front of ocelli and on both sides of ocellar tubercle shiny, reaching anterior 0.6 of frons. Scutellum with three pairs of scutellar setae. Cephalic and thoracic setae and setulae yellow. Notopleurals 1+1. Gonite knife-like, incised on basal 1/3 of each inner margin.

Description. ***Holotype. Male***. Body length 1.9–2.0 mm, wing length 1.5–1.6 mm.

Head black with gray microtomentum, 0.7 times as long as high in profile, as wide as thorax; face somewhat concave in lateral view, facial carina narrow; frons 0.9 times

Figures 7–8. *Siphunculina scalpriformis* sp. n., holotype. habitus **7** lateral view **8** dorsal view. Scale bar 0.05 mm.

as long as wide, projecting slightly in front of eye; gena yellow except for ventral 1/3 black, broad, 0.5 times as wide as first flagellomere; parafacial linear; vibrissal angle weakly produced beyond eye. Ocellar triangle partly microtomentose, area in front of ocelli and on both sides of ocellar tubercle shiny, its apex reaching anterior 0.6 of frons, with slightly pointed apex; ocellar tubercle black. Cephalic setae and setulae yellow. Antenna yellow except for dorsal margin of first flagellomere brown, with thick grayish microtomentum; first flagellomere 0.75 times as long as wide; arista black except for

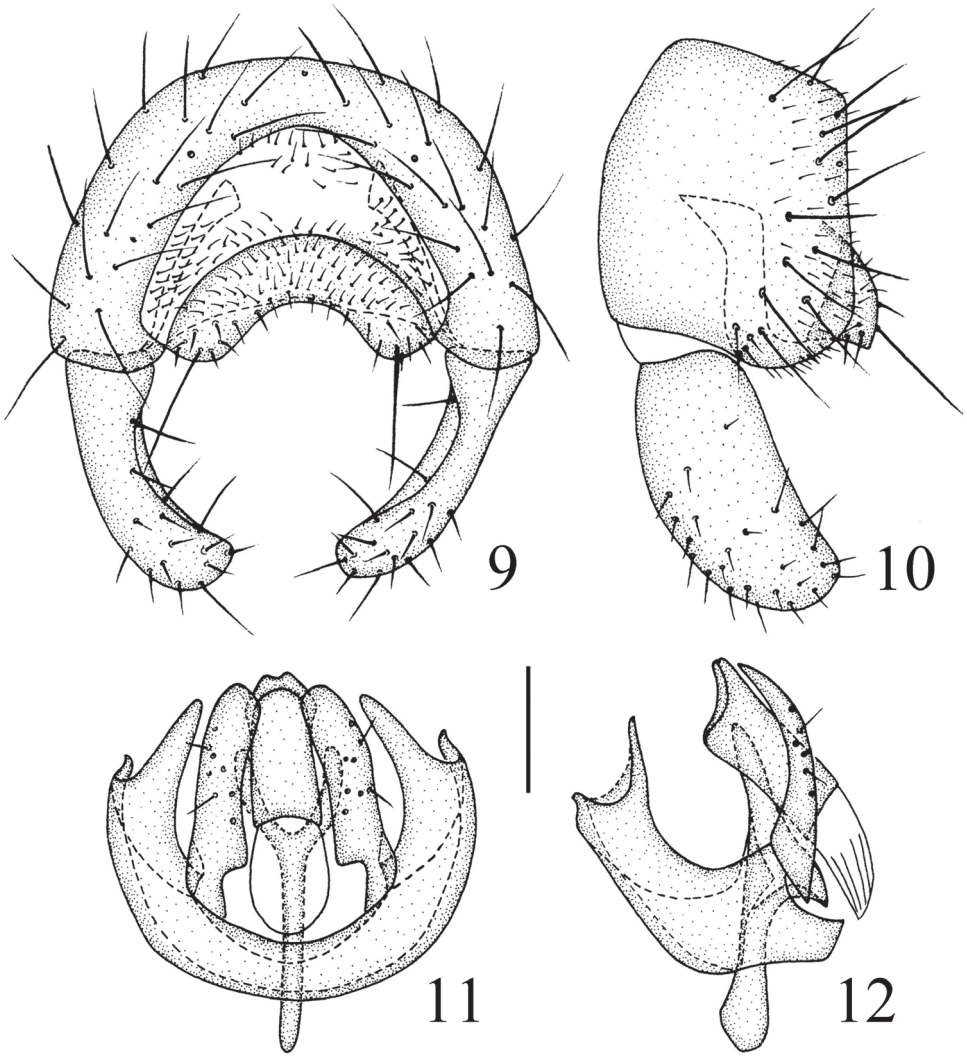

Figures 9–12. *Siphunculina scalpriformis* sp. n., holotype. **9** epandrium, posterior view **10** epandrium, lateral view **11** hypandrium and phallic complex, ventral view **12** hypandrium and phallic complex, lateral view. Scale bar: 0.1 mm.

basal segment brownish, with short pubescence. Proboscis black to yellowish brown with yellow setulae; palpus yellow with yellow setulae.

Thorax black with gray microtomentum, evenly covered with short setulae. Scutum as long as wide. Thoracic pleuron shiny black without microtomentum. Scutellum 0.6 times as long as wide; 3 pairs of scutellar setae on small tubercles; apical scutellar seta short, 0.5 times as long as scutellum. Setae and setulae on thorax yellow; notopleurals 1+1, developed. Legs with coxae black, femora black with distal tips yellow, fore tibia yellow with weakly infuscated medially, mid and hind tibiae black with both tips yel-

low, tarsi yellow. Setulae on legs yellow. Wing 2.2 times as long as wide, hyaline; veins brownish. Relative lengths of 2nd : 3rd : 4th costal sections = 6 : 17 : 4; cross-veins r-m and dm-cu not approximated, r-m at basal 0.65 of discal medial cell. Halter brown.

Abdomen shiny brown; venter yellow. Setulae on abdomen black.

Male genitalia (Figs. 9–12): Epandrium blackish brown with long brown setulae; surstylus as long as epandrium in lateral view. Cercus short and broad, with moderately concave ventral margin in dorsal view. Pre- and postgonites fused, knife-like, incised on basal 1/3 of each inner margin; basiphallus longer than wide, cylindrical; distiphallus short, membranous; phallapodeme long, with basal stalk narrow in lateral view. Hypandrium broad, without two basal rounded projections, arms free and long, apex with internal projection long, external projection short.

***Female*.** Unknown.

Type material. Holotype, ♂, China: Guizhou: Maolan, Yaoqu, 30. V. 2010, leg. Dan Zhou (photographed and genitalia prepared). Paratype, 2 ♂♂, same data as holotype (in 75% alcohol, deposited in CAU).

Distribution. China (Guizhou).

Remarks. The new species is somewhat similar to *S. minima* (de Meijere), but can be separated from the latter by the following features: ocellar triangle reaching anterior 0.6 of frons, gena 0.5 times as wide as first flagellomere; in *S. minima*, the ocellar triangle reaches anterior 0.9 of frons, the gena is as wide as the first flagellomere (Kanmiya 1982).

Etymology. The specific name is from the Latin scalpriformis ("knife-like"), referring to the shape of gonite.

***Siphunculina shangyongensis* sp. n.**
http://zoobank.org/67F6EFAD-6BE8-4820-B886-7A39745E3727
Figs 13–18

Diagnosis. Ocellar triangle black, smooth, shiny, reaching anterior 0.9 of frons, with slightly pointed apex. Scutellum with three pairs of scutellar setae on small tubercles. Cephalic and thoracic setae and setulae black. Notopleurals 1+1. Gonite nearly rectangular, slightly narrowed basally.

Description. ***Holotype. Male***. Body length 1.8 mm, wing length 1.6 mm.

Head black with gray microtomentum, 0.75 times as long as high in profile, as wide as thorax; face somewhat concave in lateral view, facial carina distinct; frons brown, 0.9 times as long as wide, projecting only slightly in front of eye; gena broad, 0.5 times as wide as first flagellomere, yellowish brown except for ventral margin black; parafacial indistinct; vibrissal angle distinctly produced beyond eye by subequal length to gena-width. Ocellar triangle black, smooth, shiny, reaching anterior 0.9 of frons, with slightly pointed apex; ocellar tubercle brown. Cephalic setae and setulae black. Antenna yellow with thick grayish microtomentum except for distodorsal margin of first flagellomere black; first flagellomere as long as wide; arista black except for basal

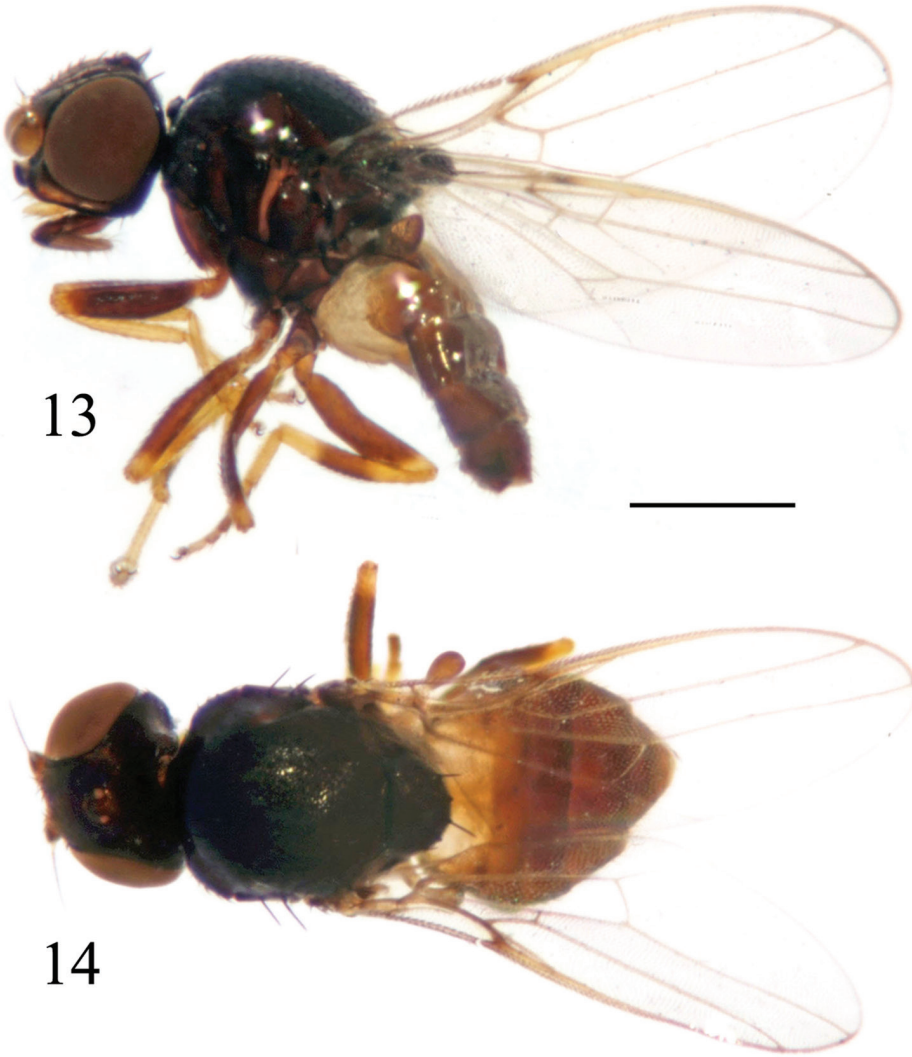

Figures 13–14. *Siphunculina shangyongensis* sp. n., holotype. habitus, **13** lateral view **14** dorsal view. Scale bar: 0.05 mm.

segment yellow, with short brown pubescence. Proboscis brown with brown setulae; palpus yellow with brown setulae.

Thorax black, evenly covered with short setulae. Scutum 1.1 times as long as wide. Thoracic pleuron shiny brown without microtomentum. Scutellum black, 0.6 times as long as wide; 3 pairs of scutellar setae on small tubercles; apical scutellar seta 0.5 times as long as scutellum. Setae and setulae on thorax black; notopleurals 1+1, developed. Legs with coxae brown, femora brown with distal tips yellow, tibiae yellow with middle 1/3 of mid tibia brownish, middle 1/3 of hind tibia brown, tarsi yellow with hind

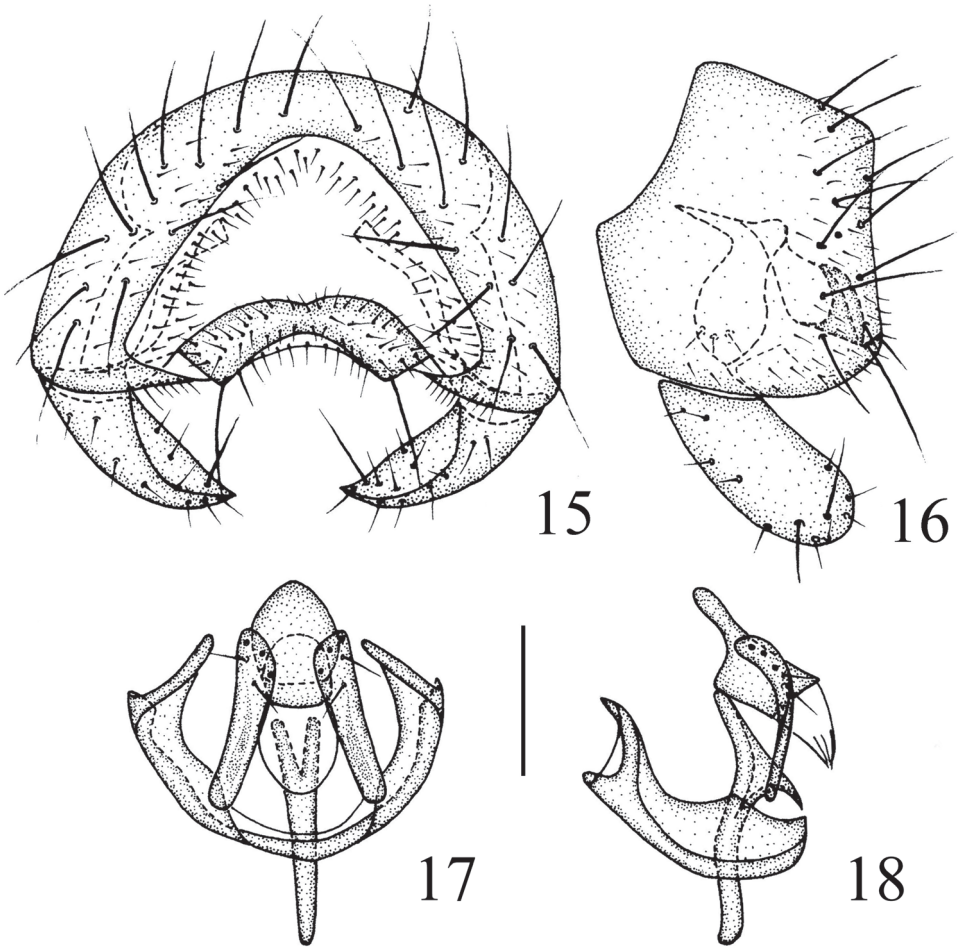

Figures 15–18. *Siphunculina shangyongensis* sp. n., holotype. **15** epandrium, posterior view **16** epandrium, lateral view **17** hypandrium and phallic complex, ventral view **18** hypandrium and phallic complex, lateral view. Scale bar: 0.1 mm.

tarsomeres 2-4 brown. Setulae on legs brown. Wing 2.2 times as long as wide, hyaline; veins yellowish brown. Relative lengths of 2nd : 3rd : 4th costal sections = 3 : 11 : 3; cross-veins r-m and dm-cu not approximated, r-m at basal 0.6 of discal medial cell. Halter brown.

Abdomen shiny brown except for tergite 1 yellow; venter yellow. Setulae on abdomen black.

Male genitalia (Figs. 15–18): Epandrium blackish brown with long brown setulae; surstylus 0.6 times as long as epandrium in lateral view. Cercus short and broad, with a concavity on ventral margin. Gonite nearly rectangular, slightly narrowed basally; basiphallus slightly longer than wide, cylindrical; distiphallus short, membranous; phallapodeme long, distinctly projecting beyond hypandrium, with basal stalk narrow in

lateral view. Hypandrium narrow, without two basal rounded projections, arms free and long, apex with internal projection long, external projection short.

***Female*.** Unknown.

Type material. Holotype, ♂, China: Yunnan: Xishuangbanna, Shangyong, 7. V. 2007, leg. Wenliang Li (photographed and genitalia prepared). Paratype, 3 ♂♂, same locality and date as holotype, leg. Hui Dong (in 75% alcohol, deposited in CAU).

Distribution. China (Yunnan).

Remarks. The new species is somewhat similar to *S. bella* Kanmiya, but can be separated from the latter by the following features: hind tibia yellow except for middle 1/3 brown, tarsi yellow except for hind tarsomeres 2-4 brown, surstylus 0.6 times as long as epandrium in lateral view; in *S. bella*, the hind tibia is yellow with largely infuscate maculae medially, the tarsi are entirely yellow, the surstylus is as long as epandrium in lateral view (Kanmiya 1989).

Etymology. The species is named after the type locality Shangyong.

Siphunculina funicola (de Meijere, 1905)

Figs 19–24

Siphonella funicola de Meijere, 1905: 160. Type locatity: Indonesia (Java).
Microneurum funicolum Becker, 1911: 141.
Liomicroneurum funicolum Duda, 1934: 112.
Siphunculina funicola (de Meijere): Becker et de Meijere, 1913: 303; de Meijere, 1918: 340; Sabrosky, 1977: 300; Cherian, 1977: 364; Kanmiya, 1989: 68.

Diagnosis. Frons black with gray microtomentum. Ocellar triangle entirely shiny black with a broad median groove, reaching anterior margin of frons, with slightly pointed apex. Gena broad, 0.5 times as wide as first flagellomere. Antenna yellow except for dorsal margin of first flagellomere brown; arista with short pubescence. Thorax black with gray microtomentum. Scutellum with 4 pairs of scutellar setae on small tubercles. Cephalic and thoracic setae and setulae black; notopleurals 1+2. Legs black except for fore tibia, both ends of mid and hind tibiae and all tarsi yellow. Male genitalia (Figs. 21–24): Surstylus shorter than epandrium in lateral view. Cercus 2 times as long as wide, deeply incised medially. Gonite long finger-like, basal 1/4 distinctly incised.

Specimens examined. 2 ♂♂, China: Hainan: Baisha, Hongmao, 19. V. 2007, leg. Ding Yang, 1 ♂, Hainan: Baisha, 22. V. 2007, leg. Kuiyan Zhang, 1 ♂, Hainan: Baisha, Yacha orchard, 19. IV. 2009, leg. Shan Huo (photographed and genitalia prepared).

Distribution. China (Hainan); Cambodia, India, Indonesia, Malaysia, Sri Lanka, Vietnam, Thailand, Nepal.

Remarks. This species has been called the Oriental eye-fly, predominantly inhabiting in the East and South Asian countries. The flies mass around men and cattle

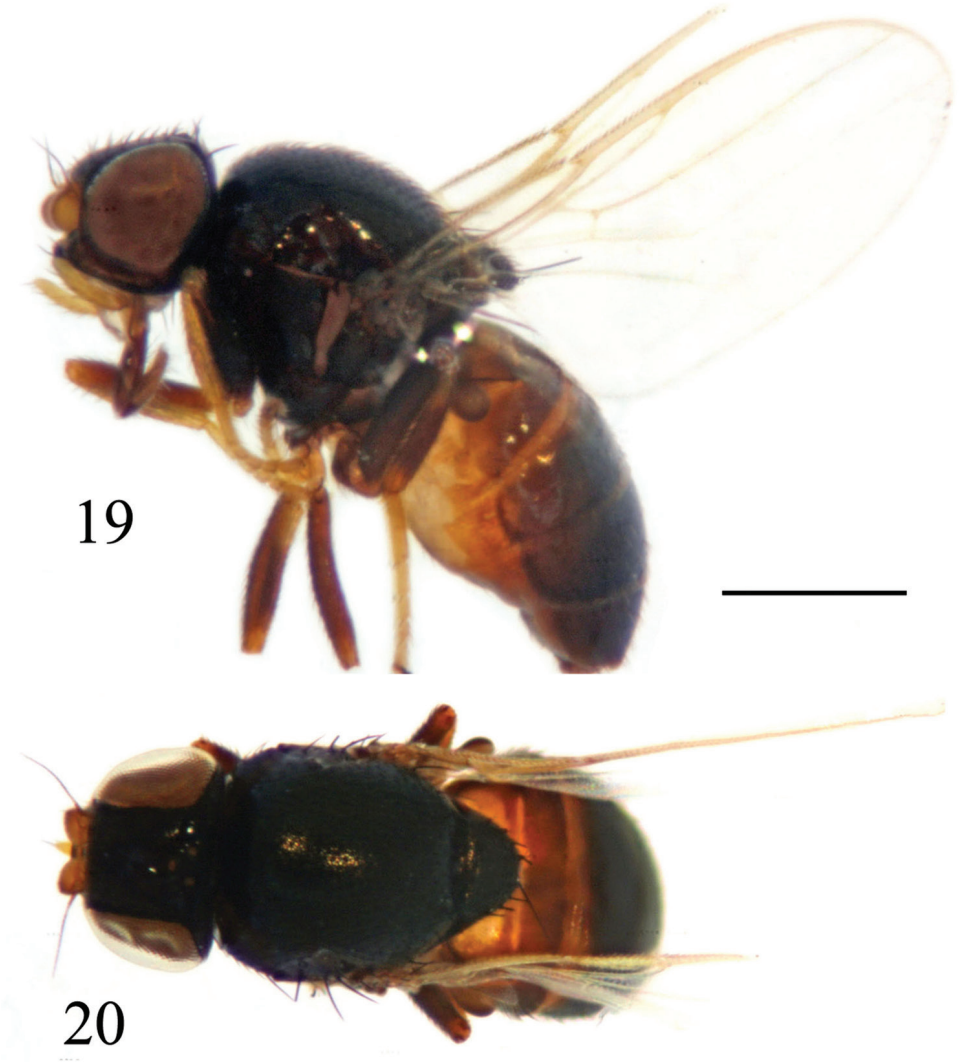

Figures 19–20. *Siphunculina funicola* (de Meijere), male. habitus **19** lateral view **20** dorsal view. Scale bar 0.05 mm.

and cause considerable annoyance, and are responsible for spreading eye diseases. It is somewhat similar to *S. ceylonica* Kanmiya, but can be separated from the latter by the following features: ocellar triangle reaching anterior margin of frons, notopleurals 1+2, apical scutellar seta as long as scutellum, cercus twice as long as wide, deeply incised medially; in *S. ceylonica*, ocellar triangle reaching anterior 4/5 of frons, notopleurals 1+1, apical scutellar seta much shorter than scutellum, cercus short, widely incised medially (Kanmiya 1989).

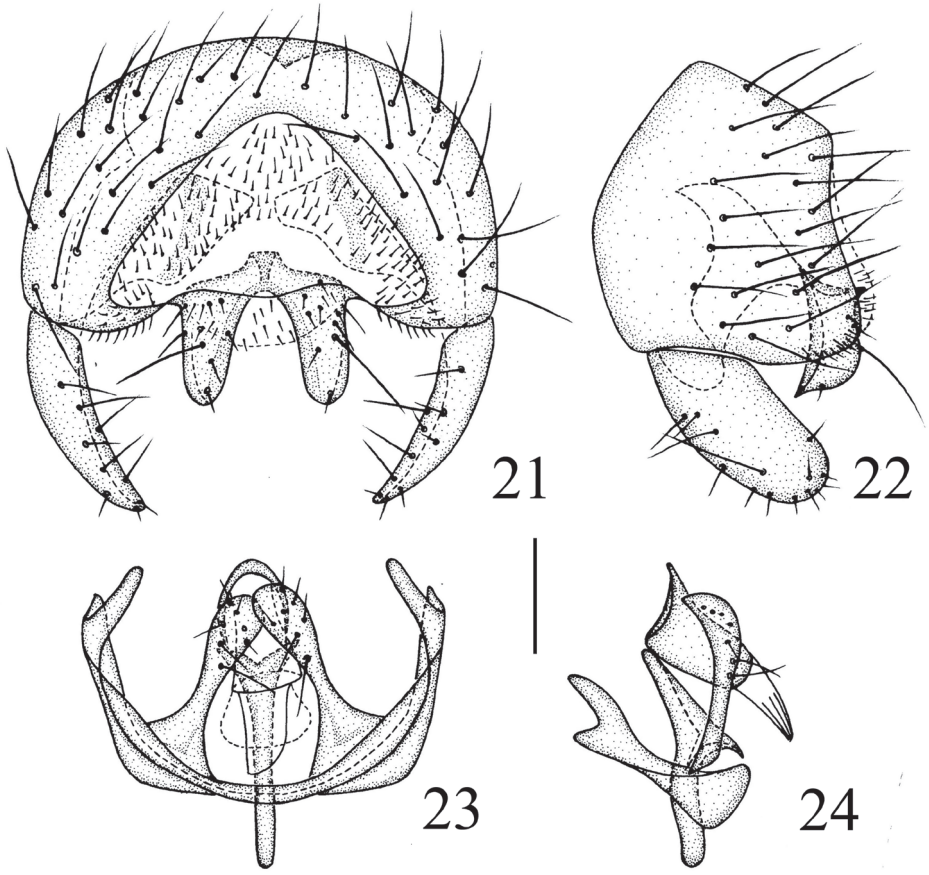

Figures 21–24. *Siphunculina funicola* (de Meijere), male. **21** epandrium, posterior view **22** epandrium, lateral view **23** hypandrium and phallic complex, ventral view **24** hypandrium and phallic complex, lateral view. Scale bar: 0.1 mm.

Acknowledgements

We are grateful to Dr. Kuiyan Zhang, Dr. Shan Huo and Dr. Jinjing Wang (Beijing), Dr. Hui Dong (Shenzhen), Dr. Wenliang Li (Luoyang) and Ms. Dan Zhou (Chenzhou) for collecting the specimens. Two anonymous reviewers are thanked for providing useful comments on an earlier draft of this paper. The research was funded by the National Natural Science Foundation of China (31301906) and the Russian State Project (01201351189) and RFFI (grant 15-54-53038).

References

Andersson H (1977) Taxonomic and phylogenetic studies on Chloropidae (Diptera) with special reference to Old World genera. Entomologica Scandinavica Supplementum 8: 1–200.

Becker Th (1903) Aegyptische Dipteren. (Fortsetzung und Schluss). Mitteilungen aus dem Zoologischen Museum in Berlin 2(3): 67–195.

Becker Th (1911) Chloropidae. Eine Monographische Studie. III. Teil. Die indo-australische Region. Annales Historico-Naturales Musei Nationalis Hungarici 9: 35–170.

Becker Th, de Meijere JCH (1913) Chloropiden aus Java. Tijdschrift voor Entomologie 56: 283–307.

Cherian PT (1970) Descriptions of some new Chloropidae (Diptera) from India. Oriental Insects 4(4): 363–371. https://doi.org/10.1080/00305316.1970.10433972

Cherian PT (1977) The genus *Siphunculina* (Diptera: Chloropidae) from India. Oriental Insects 11(3): 363–368. https://doi.org/10.1080/00305316.1977.10433816

Chansang U, Mulla MS, Chantaroj S, Sawanpanyalert P (2010) The eye fly *Siphunculina funicola* (Diptera: Chloropidae) as a carrier of pathogenic bacteria in Thailand. The Southeast Asian Journal of Tropical Medicine and Public Health 41(1): 61–70.

Cumming JM, Wood DM (2009) Adult morphology and terminology. In: Brown BV, Borkent A, Cumming JM, Wood DM, Woodley NE, Zumbado MA (Eds) Manual of Central American Diptera. Vol. 1. NRC Research Press, Ottawa, 9–50.

Duda O (1934) Fauna sumatrensis. Bijdrage No. 74, Chloropidae (Dipt.). Tijdschrift voor Entomologie 77: 55–161.

Enderlein G (1911) Klassifikation der Oscinosominen. Sitzungsberiche der Gesellschaft naturforschender Freunde zu Berlin 1911(4): 185–244.

Ferrar P (1987) A Guide to the Breeding Habits and Immature Stages of Diptera Cyclorrhapha. Entomonograph 8, Part 1: text, 1–478.

Graham-Smith GS (1930) The Oscinidae (Diptera) as vectors of conjunctivitis, and the anatomy of their mouth parts. Parasitology 22: 457−467. https://doi.org/10.1017/S0031182000011306

Ismay JW, Nartshuk EP (2000) A. 11. Family Chloropidae. In: Papp L, Darvas B (Eds) Contributions to a Manual of Palaearctic Diptera. Appendix Volume. Science Herald, Budapest, 387−429.

Iwasa M, Oikawa S, Kanmiya K (2013) *Siphunculina quinquangula* (Loew) (Diptera, Chloropidae) new to Japan: Emergence from the remains stage of pig carcass, with the implications for forensic entomology. Medical Entomology and Zoology 64(2): 103−106. https://doi.org/10.7601/mez.64.103

Kanmiya K (1982) Two new species and three new records of the genus *Siphunculina* Rondani from Japan (Diptera: Chloropidae). Japanese Journal of Sanitary Zoology 33(2): 111–121. https://doi.org/10.7601/mez.33.111

Kanmiya K (1983) A systematic study of the Japanese Chloropidae (Diptera). Memoirs of the Entomological Society of Washington 11: 1–370.

Kanmiya K (1989) Study on the eye-flies, *Siphunculina* Rondani from the Oriental Region and Far East (Diptera, Chloropidae). Japanese Journal of Sanitary Zoology 40(suppl.): 65–86. https://doi.org/10.7601/mez.40.65_2

Kanmiya K (1994) Study on the eye-flies *Siphunculina* Rondani from Nepal (Diptera, Chloropidae). Japanese Journal of Sanitary Zoology 45(suppl.): 55–69. https://doi.org/10.7601/mez.45.55

de Meijere JCH (1905) *Siphonella funicola* n. sp., eine neue Javanische Dipteren-Art. Notes from the Leyden Museum 25: 160–162.

de Meijere JCH (1918) Studien über südostasiatische Dipteren. XIV. Verzeichnis der von mir behandelten Arten. Tijdschrift voor Entomologie 60: 275–369.

Merz B (2008) Two new species of Chloropidae (Diptera) from Switzerland. Revue Suisse de Zoologie 115(4): 661–676. https://doi.org/10.5962/bhl.part.80452

Nartshuk EP (1984) Family Chloropidae. In: Soós A, Papp L (Eds) Catalogue of Palaearctic Diptera. Vol. 10. Clusiidae-Chloropidae. Akadémiai Kiadó, Budapest, 222–298.

Nartshuk EP (2005) Grassflies (Diptera, Chloropidae) of South Korea, with a review of species of the Genus *Centorisoma* Becker. Entomological Review 85(5): 555–568.

Nartshuk EP (2007) Fauna Europaea: Chloropidae. In: Pape ET (Ed.) Fauna Europaea: Diptera, Brachycera. Version 1.0 (online). http://www.faunaeur.org

Nartshuk EP (2012) A check list of the world genera of the family Chloropidae (Diptera, Cyclorrhapha, Muscomorpha). Zootaxa 3267: 1–43.

Rondani C (1856) Dipterologiae Italicae prodromus. Vol. I. Genera Italica ordinis Dipterorum ordinatum disposita et distincta et in familias et stirpes aggregata. A. Stoschi, Parmae, 228 pp. https://doi.org/10.5962/bhl.title.8160

Sabrosky CW (1977) Familiy Chloropidae. In: Delfinado MD, Hardy DE (Eds) A Catalog of Diptera of the Oriental Region, Volume 3. The University Press of Hawaii, Honolulu, 277–319.

Sabrosky CW (1980) Family Chloropidae. In: Crosskey RW (Ed.) Catalogue of the Diptera of the Afrotropical Region. British Museum (Natural History), London, 695–712.

Sabrosky CW (1989) Family Chloropidae. In: Evenhuis NL (Ed.) Catalog of the Diptera of the Australasian and Oceanian Regions. Bishop Museum Press, Honolulu, 650–665.

ZooKeys 687: 89–99 (2017)
doi: 10.3897/zookeys.687.11233
http://zookeys.pensoft.net

DATA PAPER

A peer-reviewed open-access journal
ZooKeys
Launched to accelerate biodiversity research

Data from the ichthyological collection of the Museu Paraense Emílio Goeldi

Timóteo Monteiro da Silva[1], Juliana Corrêa dos Santos[1], Victor Amazonas Viegas Ferreira[1], Lorran Alves da Cruz Ramos[1], Wolmar Benjamin Wosiacki[1], Marcos Paulo Alves de Sousa[1]

1 *Museu Paraense Emílio Goeldi, Av. Perimetral, 1901 - Terra Firme, 66077-830, Belém, Brazil*

Corresponding author: *Timóteo Monteiro da Silva* (timoteomsilva@gmail.com)

Academic editor: *D. Bloom* | Received 17 November 2016 | Accepted 26 June 2017 | Published 2 August 2017

http://zoobank.org/C7BE988B-8EDB-497E-A9FF-991EBE95AECB

Citation: Silva TM, Santos JC, Ferreira VAV, Cruz Ramos LA, Wosiacki WB, Sousa PA (2017) Data from the ichthyological collection of the Museu Paraense Emílio Goeldi. ZooKeys 687: 89–99. https://doi.org/10.3897/zookeys.687.11233

Resource citation: Museu Paraense Emílio Goeldi (2016) Ichthyology Collection of Museu Paraense Emílio Goeldi. Online at http://ipt.museu-goeldi.br/ipt/resource?r=museu_paraense_emilio_goeldi_ictiology_collection&v=11.2 doi:10.15468/njmykk, Version 11.2 (updated on Dec 15, 2016) GBIF key: http://www.gbif.org/dataset/b0059a3a-5cab-4a08-8d14-d92c23378e43

Abstract

This dataset contains information on the occurrence of Neotropical fishes (Actinopterygii, Chondrichthyes, Sarcopterygii) collected in South America, mostly from the Brazilian Amazon. The ichthyology collections of the Museu Paraense Emílio Goeldi (MPEG: http://www.museu-goeldi.br/) include specimens collected between 1900 and 2014. The dataset is now available for public consultation on the Global Biodiversity Information Facility portal (http://www.gbif.org/dataset/b0059a3a-5cab-4a08-8d14-d92c23378e43), and through Sistema de Informação sobre a Biodiversidade Brasileira (http://gbif.sibbr.gov.br/explorador/pt/recurso/62).

Keywords

Amazon, dataset, ichthyology, occurrence

Introduction

The Museu Paraense Emílio Goeldi (MPEG), or Goeldi Museum, located in Belém, Pará, Brazil, is a federal research institution within the Brazilian Ministry of Science, Technology and Communication (MCTIC). The Goeldi Museum is the site of the first Amazonian fish collection in Brazil with specimens dating as far back as the end of the nineteenth century.

The ichthyology collections of the Goeldi Museum receive and preserve material evidence, including specimens and associated data and metadata collected in the field, for research and educational purposes. The collections are a source of information and material used by national and international researchers as well as students of two post-graduate programs at MPEG focused on systematics, taxonomy, and biogeography. Due to its wide geographic range and representation of Amazonian fish diversity, over 60 scientific papers have been published over the last ten years based on specimens and types deposited in the Goeldi collections. The MPEG collections are most representative of the Brazilian Amazon, but also contain records of fishes collected in four other neotropical countries (Chile, Colombia, Panama, and Peru). According to Reis (2013), this region has the richest and most diverse fish fauna of the world, with more than 5400 species described. One of the main sources for this aquatic biodiversity is the Amazon basin, with more than 2000 species of freshwater fish, a quarter of all known freshwater species. Of these, 1800 are endemics (Peixoto et al. 2016). One of the greatest conservation challenges in Brazil currently is to harmonize economic development with the sustainable use and preservation of this tremendous aquatic biodiversity (Santos and Santos 2005). Among the principal threats to aquatic environments are hydroelectric dams, which are being built and planned at a growing rate. Although Brazil, Peru, and Bolivia are currently the countries most directly affected by impacts of hydroelectric power plants, other Southern American countries may feel the effects (Fearnside 2015). Large dams reduce fish biodiversity directly and also block the migration pathways of many species, which can be devastating to Neotropical fishes. Dams also cause changes in the dynamic of river nutrients and other biochemical process in deltas, estuaries, and marine-shelf ecosystems (Winemiller et al. 2016). Without effective conservation policies, the ichthyofauna of South America will be increasingly affected over the next few decades (Reis et al. 2016)

Describing new species is the first step in documenting and conserving biodiversity. However even after a new species is first described, it can take years or decades before a more complete understanding of species-level diversity can be apprehended throughout this vast region (Vari and Malabarba 1998). Scientific collections are a crucial source of information for establishing baseline parameters to help measure the ongoing impacts of development on biodiversity (Zaher and Young 2003). When collections data is properly organized, integrated, and made available for the benefit of pertinent studies, it can become a valuable source of information for planning and monitoring public policies, conservation efforts, and natural resource management (Magalhães et al. 2001). Biodiversity information should be available for policy makers and scientists

alike. More often than not such information is not easily available for policy makers, thus hindering scientifically based management decisions (Shanmughavel 2007).

The aim of this paper is to describe and synthesize information about Amazon fish biodiversity represented in the Goeldi Museum collections, providing summaries about taxonomic coverage and geographical distribution in order to facilitate rapid and dynamic access to the records present at MPEG. Biodiversity data in open, digital format has the potential to improve the scientific understandings and contribute to conservation policies (Sousa-Baena 2014).

With these factors in mind, the digitization of the Goeldi fish collections began in 2003, and records were initially inserted into Excel software; in 2009, they were transferred to Specify (SPECIFY SOFTWARE 6). All records have now been computerized, and are available to the scientific community and general public in the Sistema de Informação sobre a Biodiversidade Brasileira (SiBBr 2017) and in Global Biodiversity Information Facility (GBIF 2017)

Data published through SiBBr and GBIF: http://www.gbif.org/dataset/3bc27e57-a84d-4e0c-ba0d-9dbba8299674; http://gbif.sibbr.gov.br/explorador/pt/recurso/62

Project detail

Project title: Computerization of the ichthyological collection of the MPEG.

Personnel: Timóteo Monteiro da Silva (student), Marcos Paulo Alves de Sousa (head of informatics), Wolmar Benjamin Wosiacki (curator), Juliana Corrêa dos Santos (student), Victor Amazonas Viegas Ferreira (student), Lorran Alves da Cruz Ramos (student).

Funding: Ministério da Ciência, Tecnologia, Inovação e Comunicação (MCTIC); Conselho Nacional de Pesquisa (CNPq).

Taxonomic coverage

General description of taxonomic coverage:

The taxonomic organization of the collection followed Nelson (1994) and Nelson (2006). Currently, higher taxonomic groups are being reorganized according Betancur-R et al. (2013) and Eschmeyer et al. (2016), however the database update is incomplete and ongoing. The ichthyology collection of MPEG includes 260,000 specimens, distributed in 25,874 lots, representing 28 orders, 102 families, 506 genera, and 1710 species. All species in the collection belong to the classes Actinopterygii, Chondrichthyes, and Sarcopterygii. The three most common orders are Characiformes with 600 species in 13,560 lots, Silurifomes with 389 species in 5,290 lots, and Cichlidae with 211 species in 3,437 lots.

Among these are found 263 type specimens of which 33 are holotypes and 227 are paratypes. 261 of the 263 type specimens were collected during the last 15 years.

All type species found in the collection are detailed below:

List of species with holotype and paratype in the collection:

Acestridium triplax, *Archolaemus orientalis*, *Aspidoras gabrieli*, *Aspidoras marianae*, *Characidium nana*, *Characidium papachibe*, *Corydoras urucu*, *Cyphocharax aninha*, *Eigenmannia antonioi*, *Eigenmannia desantanai*, *Eigenmannia guairaca*, *Eigenmannia muirapinima*, *Eigenmannia pavulagem*, *Hemigrammus arua*, *Hemigrammus diagonicus*, *Hyphessobrycon montagi*, *Hypomasticus lineomaculatus*, *Hypopygus benoneae*, *Ituglanis ina*, *Stenolicmus ix*, *Tatia caxiuanensis*, *Tetranematichthys barthemi*, *Tometes ancylorhynchus*, *Tometes camunani*, *Tometes kranponhah*, *Trichomycterus guaraquessaba*, *Trichomycterus igobi*, *Trichomycterus mboycy*, *Trichomycterus naipi*, *Trichomycterus papilliferus*, *Trichomycterus plumbeus*, *Trichomycterus taroba*, *Xenurobrycon varii*.

List of species with only paratype in the collection:

Adontosternarchus duartei, *Anchoviella juruasanga*, *Ancistrus krenakarore*, *Ancistrus ranunculus*, *Apteronotus lindalvae*, *Apteronotus soneiro*, *Archolaemus ferreirai*, *Archolaemus janeae*, *Archolaemus luciae*, *Archolaemus santosi*, *Aspidoras gabrieli*, *Aspidoras marianae*, *Astroblepus nettoferreirai*, *Baryancistrus chrysolomus*, *Baryancistrus xanthellus*, *Bryconamericus pinnavittatus*, *Centromochlus orca*, *Chaetostoma jegui*, *Crenicichla anamiri*, *Cyphocharax jagunco*, *Cyphocharax lundi*, *Eigenmannia matintaperera*, *Eigenmannia meeki*, *Eigenmannia sayona*, *Eigenmannia waiwai*, *Furcodontichthys novaesi*, *Hassar gabiru*, *Hassar shewellkeimi*, *Hypostomus delimai*, *Hypostomus hoplonites*, *Ituglanis goya*, *Jupiaba citrina*, *Leporinus multimaculatus*, *Moenkhausia celibela*, *Moenkhausia chlorophthalma*, *Moenkhausia eurystaenia*, *Moenkhausia mikia*, *Moenkhausia petymbuaba*, *Moenkhausia plumbea*, *Nemuroglanis furcatus*, *Parotocinclus halbothi*, *Peckoltia compta, Peckoltia feldbergae*, *Phallobrycon synarmacanthus*, *Physopyxis ananas*, *Polycentrus jundia*, *Scoloplax baskini*, *Synbranchus lampreia*, *Trichomycterus anhanga*, *Trichomycterus balios*, *Trichomycterus cachiraensis*, *Trichomycterus crassicaudatus*, *Trichomycterus poikilos*, *Trichomycterus trefauti*, *Trichomycterus tupinamba*, *Tyttobrycon marajoara*.

Taxonomic ranks

Kingdom: Animalia
Phylum: Chordata
Classes: Actinopterygii, Chondrichthyes, Sarcopterygii
Orders: Atheriniformes, Batrachoidiformes, Beloniformes, Carcharhiniformes, Characiformes, Chimaeriformes, Clupeiformes, Cyprinodontiformes, Elopiformes, Gasterosteiformes, Gobiesociformes, Gymnotiformes, Lepidosireniformes, Lophiiformes, Mugiliformes, Myliobatiformes, Osmeriformes, Osteoglossiformes, Cichliformes, Pleuronectiformes, Pristiformes, Rajiformes, Scorpaeniformes, Siluriformes, Squaliformes, Synbranchiformes, Syngnathiformes, Tetraodontiformes (Figure 1).

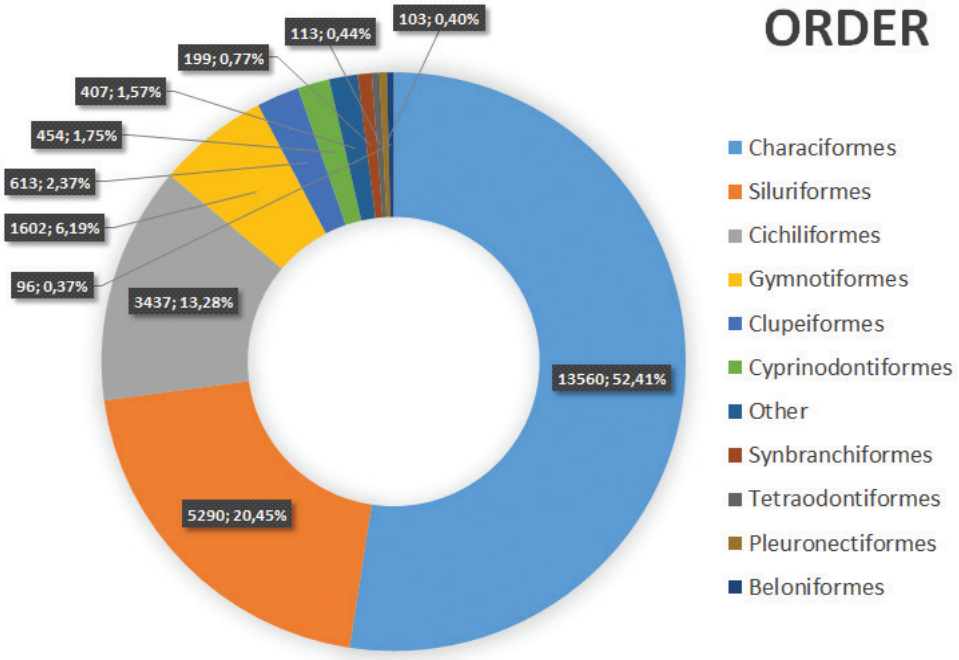

Figure 1. Distribution of species in the MPEG. Number of species and frequencies are represented for each order.

Families Acestrorhynchidae, Achiridae, Anablepidae, Anostomidae, Apteronotidae, Argentinidae, Ariidae, Aspredinidae, Atherinidae, Atherinopsidae, Auchenipteridae, Batrachoididae, Belonidae, Blenniidae, Bothidae, Callichthyidae, Carangidae, Carcharhinidae, Centrarchidae, Centropomidae, Cetopsidae, Chacidae, Characidae, Chilodontidae, Chimaeridae, Cichlidae, Clupeidae, Crenuchidae, Ctenoluciidae, Curimatidae, Cynodontidae, Cynoglossidae, Cyprinodontidae, Dasyatidae, Diodontidae, Doradidae, Echeneidae, Electrophoridae, Eleotridae, Elopidae, Engraulidae, Ephippidae, Erythrinidae, Gasteropelecidae, Gerreidae, Gobiesocidae, Gobiidae, Gymnotidade, Gymnotidae, Gymnuridae, Haemulidae, Helogeneidae, Hemiodontidae, Hemiramphidae, Heptapteridae, Hypopomidae, Lebiasinidae, Lepidosirenidae, Lobotidae, Loricariidae, Lutjanidae, Megalopidae, Mugilidae, Mullidae, Muraenidae, Myliobatidae, Nematogenyidae, Ogcocephalidae, Ophichthidae, Osteoglossidae, Paralichthyidae, Parodontidae, Pimelodidae, Poeciliidae, Polycentridae, Potamotrygonidae, Pristidae, Pristigasteridae, Prochilodontidae, Prystigasteridae, Pseudopimelodidae, Rajidae, Rhamphichthyidae, Rivulidae, Sciaenidae, Scoloplacidae, Scombridae, Serranidae, Serrasalmidae, Sphyraenidae, Sphyrnidae, Squalidae, Sternopygidae, Stromateidae, Synbranchidae, Syngnathidae, Tetraodontidae, Torpedinidae, Triakidae, Trichiuridae, Trichomycteridae, Triglidae.

Spatial coverage

General spatial coverage: The collections include specimens from Brazil, Chile, Colombia, Panama, and Peru. Most samples come from the Brazilian Amazon (Figure 2) from the following river basins: Araguari, Arapiuns, Juruti, Caxiuanã, Madeira, Rio Negro, Teles Pires, Xingu, Amazonas,Guamá, Trombetas, Jamanxim. Other river basins from Brazil represented in the collections include: Parana (Iguaçu, Paranapanema), Tocantins (Anapu, Itacaiunas), and Paraguai (Miranda). The south Atlantic basins is represented by the Laranjeiras river. River basins were attributed used maps from Agência Nacional de Águas (ANA 2017) and the Environmental Ministry (Ministério do Meio Ambiente) of the Brazilian Government.

Temporal coverage: Specimens in the collection date from 1900–2014 (Figure 2) with three significant increments during the early 1980s, in 1995, and after 2000, with more than 600 samples per year. The most recent peak period in collection is observed in 2002-2013, with more than 900 samples per year (Figure 3).

Natural collections description

Parent collection identifier: Museu Paraense Emílio Goeldi
Collection name: Ichthyology
Collection identifier: MPEG.ICT
Specimen preservation method: Alcohol

Methods

General method of publishing: Samples were obtained from collecting licenses, exchange, donation, or purchase. Samples are stored and preserved in the collection and data is stored in the Biodiversity Data Management System. The main data from specimens that are incorporated in the collection are published in "Sistema de Informação sobre a Biodiversidade Brasileira (SiBBr)" and "Global Biodiversity Information Facility" (GBIF) using an export tool from Specify Software and "Integrated Publishing Toolkit" (IPT) from GBIF which uses the Darwin core Standard version 1.4. The data was imported and published as per the schematic illustration below (Figure 4).

Sampling description: During its 150 years of history, the ichthyology collection of MPEG has received collections from dozens of scientists who have used various methods including gillnets, drag and throw (cast) nets, *matapis*, dip nets, sieves, harpoons, snorkeling, diving, etc.

Quality control description: The most recent taxonomic organization of the collection followed Nelson (1994), and currently Nelson (2006). Currently, the system is being updated according Betancur-R (2013) and Eschmeyer et al. (2016). Therefore, for purposes of this paper, the definition of large groups still follows Nelson (2006),

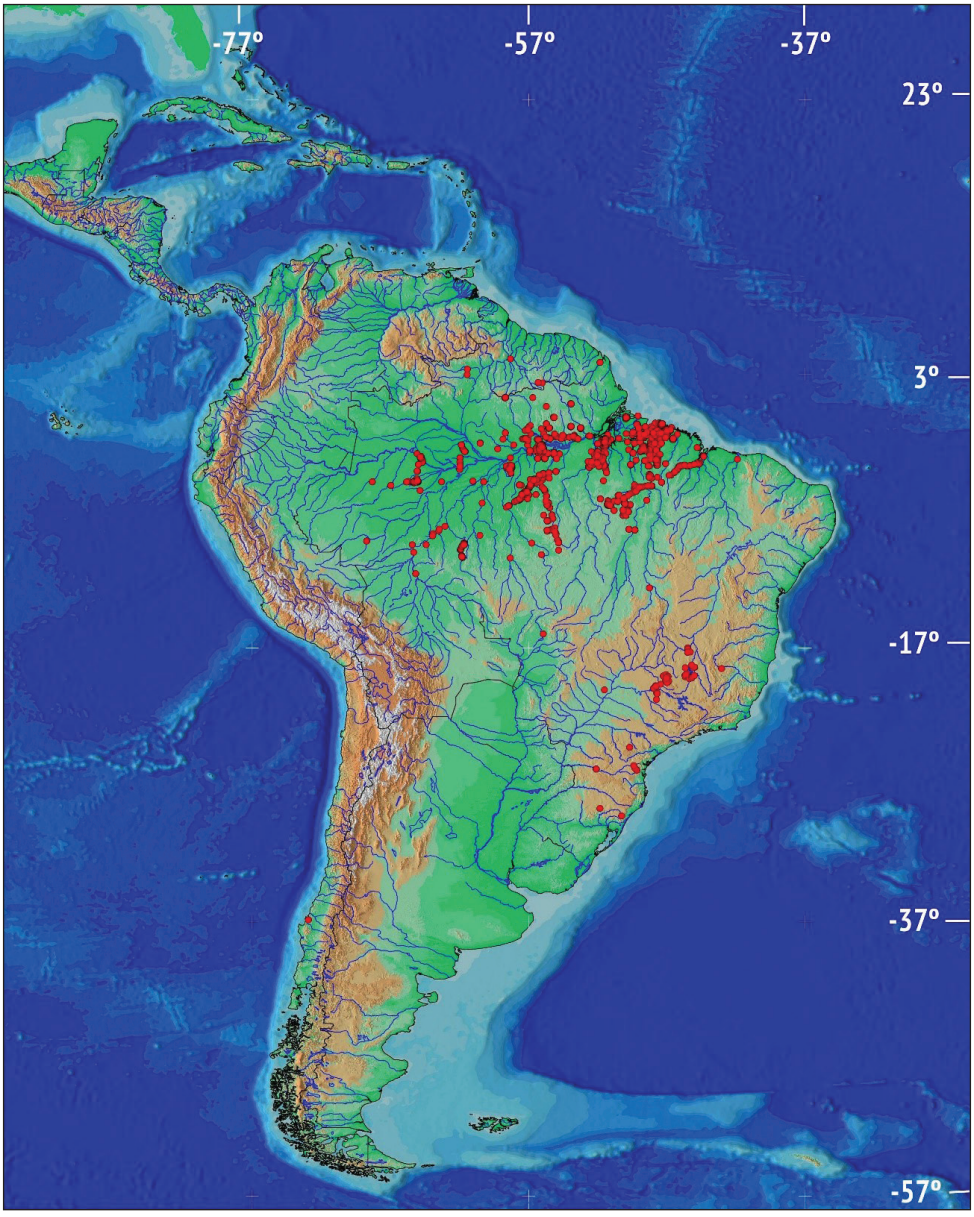

Figure 2. Map of South America showing the localities of all fish specimens with coordinates (dataset available at http://www.gbif.org/dataset/b0059a3a-5cab-4a08-8d14-d92c23378e43). Some dots represent more than one locality.

such that representative groups of the collection, for example, Cichlidae do not belong to Cichliformes. The identification of genus and species still follows the bibliography in Eschmeyeret et al. (2016), but all the data will be updated to Betancur-R et al. (2013).

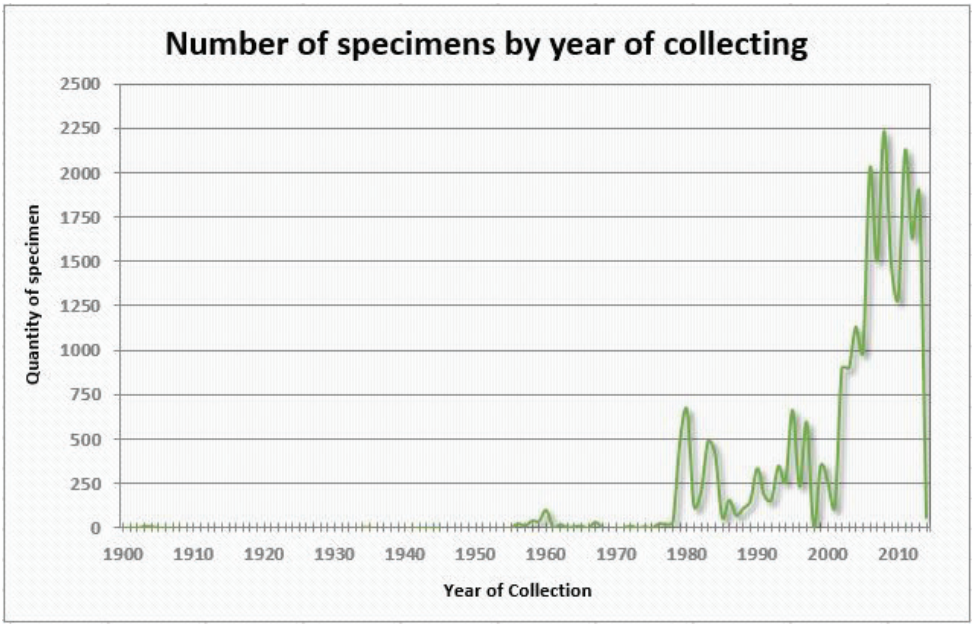

Figure 3. Distribution of the number of specimens collected by year.

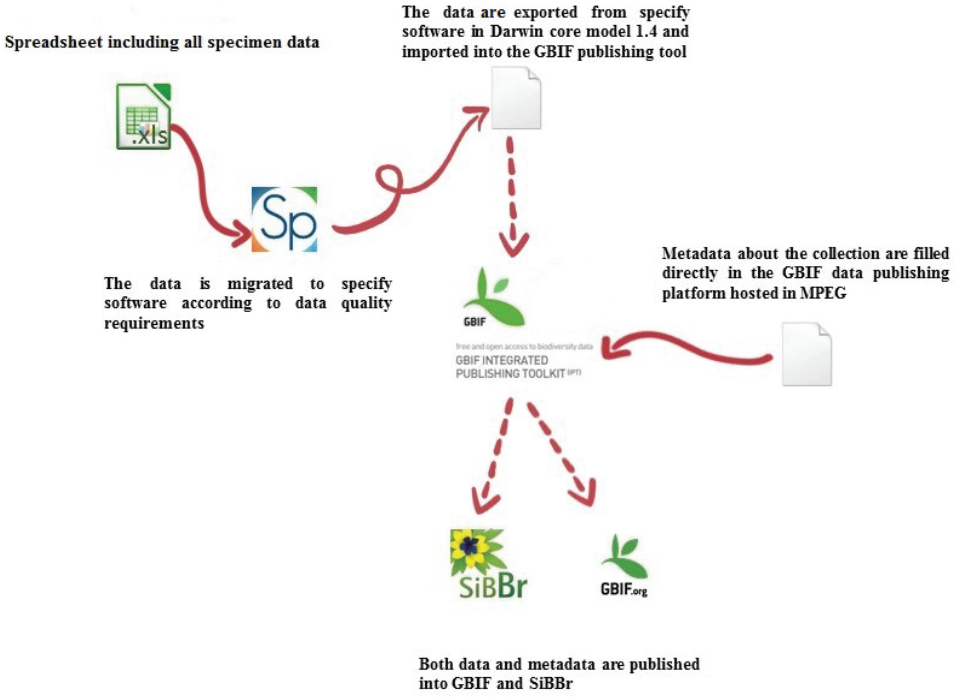

Figure 4. Flow chart of data publication process. Produced by the author.

Datasets

Curatorship and storage

The curatorial protocol involves receiving material that is identified and labelled, while data and metadata are digitized and deposited in a two story collection room measuring 192 m^2, air-conditioned to 22°C. The specimens are fixed in formalin for 50 hours and transferred into a 70% ethanol solution for permanent storage.

The process for the preservation of bone and cartilage samples is based on Taylor and Van Dyke (1985). The samples are stored in glass jars or other kinds of containers (e.g., high-density polyethylene drums) and the collection is organized taxonomically by order and family. Within the families, the genera and species are arranged in alphabetical order. The type material (holotypes and paratypes) is stored in metal cabinets. Protocol for loan, exchange, donation, and collection visits begins with e-mail contact with the curator, who evaluates the proposal and, if needed, requests the curatorial staff to prepare the requested specimens for viewing or shipping to any country.

Dataset description

Object name: Darwin Core Archive Museu Paraense Emílio Goeldi - ichthyology collection
Character encoding: UTF-8
Format name: Darwin Core Archive format
Format version: 11.2
Distribution: http://ipt.museu-goeldi.br/ipt/resource?r=museu_paraense_emilio_goeldi_ictiology_collectionand;
http://www.gbif.org/dataset/3bc27e57-a84d-4e0c-ba0d-9dbba8299674
Publication date of data: 2015-01-21
Language: Portuguese
Licenses of use: This dataset is licensed under a Creative Commons Attribution Non Commercial (CC-BY-NC) 4.0 License (https://creativecommons.org/licenses/by-nc/4.0/legalcode).
Metadata language: English
Date of metadata creation: 2014-08-01
Hierarchy level: Dataset

Acknowledgements

The authors would like to thank Izaura Maschio (collection manager), Alberto Bezerra (technical curator), Alberto Akama (researcher), and MPEG Biogeo-Informatics Department who helped process the data. WBW thanks Conselho Nacional de Desenvolvimento Científico e Tecnológico, CNPq (grants 300940/2015-7 and 405144/2013-0).

References

ANA (2017) Agência Nacional de Águas http://www2.ana.gov.br/Paginas/default.aspx

Betancur-R R, Broughton RE, Wiley EO, Carpenter K, López JA, Li C, Holcroft NI, Arcila D, Sanciangco M, Cureton Ii JC, Zhang F, Buser T, Campbell MA, Ballesteros JA, Roa-Varon A, Willis S, Borden WC, Rowley T, Reneau PC, Hough DJ, Lu G, Grande T, Arratia G, Ortí G (2013) The tree of life and a new classification of bony fishes. PLoS currents tree of life 1: 13–30. https://doi.org/10.1371/currents.tol.53ba2 6640df0ccaee75bb165c8c26288

Eschmeyer WN, Fricke R, van der Laan R (2016) Catalog of Fishes: Genera, Species, References. http://researcharchive.calacademy.org/research/ichthyology/catalog/fishcatmain.asp [Electronic version accessed 12/September/2016]

Fearnside PM (2015) Hidroelétricas na Amazônia: impactos ambientais e sociais na tomada de decisões sobre grandes obras. Editora do INPA, Manaus, 10 pp.

GBIF (2017) Global Biodiversity Facility http://www.gbif.org/

Magalhães C, Santos JLC, Salem JI (2001) Automação de coleções biológicas e informações sobre a biodiversidade da Amazônia. Parcerias Estratégicas 6(12): 294–312.

Magnusson WE, Holanda ASS, Freitas MA, Ramalho EE, Akama A, Ferreira L, Menin M, Nunez CV, Rodrigues DJ, Manzatto AG, Paggoto RC, Ishikawa NK (2016) Amazônia – Biodiversidade incontável. In: Peixoto AL, Luz JRP, Brito MA (Eds) Conhecendo a biodiversidade. Editora Vozes, Brasília, 112–123.

Nelson JS (1994) Fishes of the World (3rd edn). John Wiley & Sons, New York, 600 pp.

Nelson JS (2006) Fishes of the World (4th edn). John Wiley & Sons, Hoboken, NJ, 601 pp.

Reis RE (2013) Conserving the freshwater fishes of South America. In: Gordon MR (Ed.) International Zoo Yearbook. John Wiley & Sons, London, 65–70.

Reis RE, Albert JS, Dario DF, Mincarone MM, Petry P, Rocha LA (2016) Fish biodiversity and conservation in South America. Journal of fish biology 89(1): 12–47. https://doi.org/10.1111/jfb.13238

Robertson T, Döring M, Guralnick R, Bloom D, Wieczorek J, Braak K (2014) The GBIF Integrated Publishing Toolkit: Facilitating the Efficient Publishing of Biodiversity Data on the Internet. PLoS ONE 9(8) e102623: 1–7. https://doi.org/10.1371/journal.pone.0102623. 2014

Santos GM, Santos ACM (2005) Sustentabilidade da pesca na Amazônia. Estudos Avançados, 19(54): 165–82. https://doi.org/10.1590/S0103-40142005000200010

SiBBr (2017) Sistema de informação sobre a biodiversidade brasileira http://www.sibbr.gov.br/

Shanmughavel P (2007) An overview on biodiversity information in databases. Bioinformation 1(9): 367. https://doi.org/10.6026/97320630001367

Sousa-Baena MS, Garcia LC, Peterson AT (2014) Completeness of digital accessible knowledge of the plants of Brazil and priorities for survey and inventory. Diversity and Distributions 20(4): 369–381. https://doi.org/10.1111/ddi.12136

Specify Software Project (2016) Specify Software Project, versão 6.6.4. U.S. National Science Foundation Grants, 2016. http://specifyx.specifysoftware.org/

Taylor WR, Van Dyke GC (1985) Revised procedures for staining and clearing small fishes and other vertebrates for bone and cartilage study. Cybium 9(2): 107–119.

Vari RP, Malabarba LR (1998) Neotropical ichthyology: an overview. Phylogeny and classification of Neotropical fishes 1: 1–12.

Wieczorek J, Döring M, De Giovanni R, Robertson T, Vieglais D (2012) Darwin Core: An Evolving Community-Developed Biodiversity Data Standard. PLoS ONE 7(1): e29715. https://doi.org/10.1371/journal.pone.0029715

Winemiller KO, McIntyre PB, Castello L, Fluet-Chouinard E, Giarrizzo T, Nam S, Baird IG, Darwall W, Lujan NK, Harrison I, Stiassny MLJ, Silvano RAM, Fitzgerald DB, Pelicice FM, Agostinho AA, Gomes LC, Albert JS, Baran E, Petrere MJr, Zarfl C, Mulligan M, Sullivan JP, Arantes CC, Sousa LM, Koning AA, Hoeinghaus DJ, Sabaj M, Lundberg JG, Armbruster J, Thieme ML, Petry P, Zuanon J, Vilara GT, Snoeks J, Ou C, Rainboth W, Pavanelli CS, Akama A, Soesbergen AV, Sáenz L (2016) Balancing hydropower and biodiversity in the Amazon, Congo, and Mekong. Science 351(6269): 128–129. https://doi.org/10.1126/science.aac7082

Zaher H, Young PS (2003) As coleções zoológicas brasileiras: panorama e desafios. Ciência e Cultura 55(3): 24–26.

ZooKeys 687: 101–129 (2017)
doi: 10.3897/zookeys.687.13221
http://zookeys.pensoft.net

RESEARCH ARTICLE

A peer-reviewed open-access journal
ZooKeys
Launched to accelerate biodiversity research

A new species of *Pristimantis* from eastern Brazilian Amazonia (Anura, Craugastoridae)

Elciomar Araújo De Oliveira[1], Luis Reginaldo Rodrigues[2], Igor Luis Kaefer[3], Karll Cavalcante Pinto[4], Emil José Hernández-Ruz[5]

1 *Programa de Pós-Graduação em Biodiversidade e Biotecnologia da Rede BIONORTE, Universidade Federal do Amazonas, Av. Gen. Rodrigo Octávio Jordão Ramos, 3000, CEP 69077-000, Manaus, Amazonas, Brazil* **2** *Programa de Pós-Graduação em Biociências, Universidade Federal do Oeste do Pará, Rua Vera Paz, s/n (Unidade Tapajós), CEP 68035-110, Santarém, Pará, Brazil* **3** *Universidade Federal do Amazonas. Av. Gen. Rodrigo Octávio Jordão Ramos, 3000, CEP 69077-000, Manaus, Amazonas, Brazil* **4** *Biota Projetos e Consultoria Ambiental LTDA, Rua 86-C, 64, CEP 74083-360, Setor Sul, Goiânia, Goiás, Brazil* **5** *Programa de Pós-Graduação em Biodiversidade e Conservação, Faculdade de Ciências Biológicas, Campus Universitário de Altamira, Universidade Federal do Pará, Rua Coronel José Porfírio, 2515, CEP 68372-040, Altamira, Pará, Brazil*

Corresponding author: *Elciomar Araújo De Oliveira* (elciomar.atractus@gmail.com)

Academic editor: *A. Crottini* | Received 12 April 2017 | Accepted 1 June 2017 | Published 2 August 2017

http://zoobank.org/5E8C5007-7CEB-496F-A062-7C7E5B914344

Citation: Oliveira EA de, Rodrigues LR, Kaefer IL, Pinto KC, Hernández-Ruz EJ (2017) A new species of *Pristimantis* from eastern Brazilian Amazonia (Anura, Craugastoridae) ZooKeys 687: 101–129. https://doi.org/10.3897/zookeys.687.13221

Abstract

In this study a new species of *Pristimantis* (Anura: Craugastoridae) of the *P. conspicillatus* species group is described. *Pristimantis latro* **sp. n.** is known only from the municipalities of Altamira, Anapu, Brasil Novo, Medicilândia, Uruará and Aveiro (Flona Tapajós, right bank of Tapajós river), in Pará state, Brazil. Morphologically, the new species distinguishes from known congeners in the group mainly by the presence of dorsal tubercles and absence of discoidal folds, smooth belly skin, as well as the presence of supernumerary tubercles on hands. The call of the new species consists of seven ascending notes, the first of which has a dominant frequency of 2635 Hz and the last 3272 Hz. Molecular analysis of the 16S mtDNA indicates a genetic distance of 8% to *P. chiastonotus*, its closet relative, and between 9% and 11% to populations of *P. fenestratus*.

Keywords

mitochondrial DNA, *Pristimantis latro* sp. n., systematics, Terrarana

Introduction

The genus *Pristimantis* Jiménez de la Espada, 1870, currently contains 506 described species (Frost 2017). *Pristimantis* is the largest genus among all vertebrates (Fouquet et al. 2013) and its remarkable diversity could probably be explained by the evolution of direct development, allowing individuals not to rely on water bodies for reproduction and thus making them fit for niches unoccupied by other amphibians (Terán-Valdez and Guayasamin 2010). Another important feature of the genus is its highly variable body size, varying from 14.5 mm (*P. andinognomus* Lehr & Coloma, 2008) up to 73.0 mm (*P. lymani* Barbour & Noble, 1920) (Hedges et al. 2008), a factor also likely to have increased the exploitation of various niches. The *P. conspicillatus* group (Lynch and Duellman 1997) contains 33 species (Padial et al. 2014) distributed in east Honduras through Central America, Colombia and Ecuador to Peru, Bolivia, northern Argentina, Atlantic and Amazonian Forests in Brazil and the Guianas, Trinidad and Tobago, and Grenada, Lesser Antilles (Frost 2017).

The species *P. fenestratus* (Steindachner, 1864) belongs to the *P. conspicillatus* group and has a wide distribution in the Amazon region (Lima et al. 2006; Bernarde and Macedo 2008; França and Venâncio 2010; Ávila-Pires et al. 2010). The taxonomy of *P. fenestratus* is problematic because many morphologically different populations have been wrongly included under that name (Duellman and Lehr 2009; Siqueira et al. 2009). This can be, at least partly, attributed to inconsistencies regarding the type locality, which was suggested to be the upper Madeira River region by De la Riva et al. (2000) and the lower Madeira River by Siqueira et al. (2009). According to Häupl and Tiedemann (1978) and Häupl et al. (1994), *P. fenestratus* has two syntypes: NHMW 19940.1 (Río Mamoré) and 19940.2 (Borba). Reichle (1999), visiting the Naturhistorisches Museum Wien (NMW), designated the syntype NMW 19940:1 (Figure 1a, b, c) from the Mamoré River, Rondônia State, Brazil, as lectotype of *Pristimantis fenestratus* and the syntype NMW 19940:2 (Figure 1d, e, f) from the municipality of Borba, Amazonas State, Brazil, as a paralectotype. De la Riva et al. (2000) and Padial and De la Riva (2009) considered populations of *P. fenestratus* collected in the 'Rio Mamoré' (Bolivian Amazon) and adjacent Andes slopes as conspecific with *P. fenestratus* from the locality of the lectotype.

Here, using morphological, molecular, and bioacoustics data, we describe a new species of *Pristimantis* of the *P. conspicillatus* group that is morphologically similar to *P. fenestratus* and *P. koehleri*.

Materials and methods

Morphological analysis

Thirteen individuals of the Coleção Zoológica de Anfíbios e Répteis from the Instituto Nacional de Pesquisas da Amazônia (INPA-H), six of the Coleção Herpetológica of the Museu Paraense Emílio Goeldi (MPEG) and 69 (twenty-two belonging to type series)

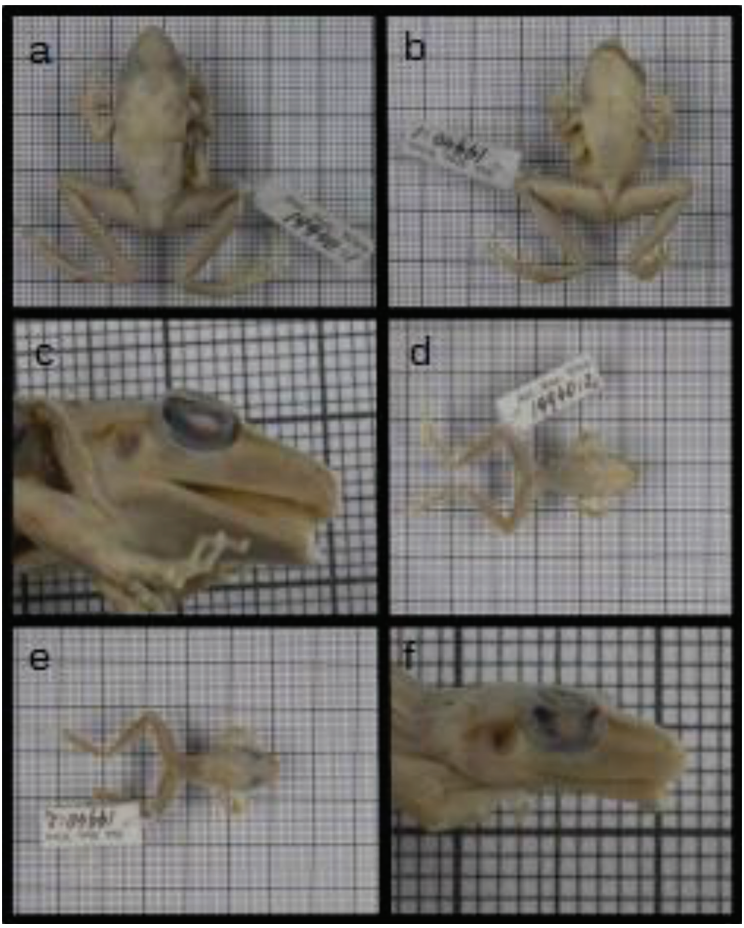

Figure 1. Lectotype of *Pristimantis fenestratus* from Rio Mamoré, Rondônia, Brazil. **A** dorsal view **B** ventral view **C** lateral view of the head. Paralectotype from the municipality of Borba, Amazonas, Brazil **D** dorsal view **E** ventral view **F** lateral view of the head.

of the Coleção de Répteis e Anfíbios of the Universidade Federal do Pará/Campus de Altamira (Appendix 1) were examined, totaling 88 individuals identified as *Pristimantis* aff. *fenestratus*. Direct comparisons of character states were performed with nine specimens of *P. fenestratus* from the municipality of Borba, Amazonas state, Brazil, deposited in the Coleção Zoológica de Anfíbios e Répteis from the Instituto Nacional de Pesquisas da Amazônia (INPA-H). The gathered information was then compared with descriptions from the literature (Duellman and Lehr 2009; Padial and De La Riva 2009).

The morphological characters were described according to the suggested nomenclature summarized in Kok and Kalamandeen (2008), Padial and De la Riva (2009) and Duellman and Lehr (2009): 1) belly skin texture (smooth or granular); 2) dorsal tubercles (present or absent); 3) fringes on fingers (present or absent); 4) dorsolateral folds (present or absent); 5) fringes on foot (prominent, weak or absent); 6) basal toe

webbing (present or absent); 7) tarsal fold (prominent, weak or absent); 8) color pattern of throat, chest and belly (heavily spotted, weakly spotted, immaculate); 9) supernumerary palmar tubercles (present or absent); 10) external palmar tubercle (entire, bifid, or semi-bifid).

Measurements were taken with a digital caliper to the nearest 0.01 mm and rounded to the nearest 0.1 mm as in Kok and Kalamandeen (2008), Padial and De la Riva (2009) and Duellman and Lehr (2009). The measurements obtained are as follows:

SVL Snout-Vent Length (from tip of snout to posterior margin of vent)
HL Head Length (from posterior margin of lower jaw to tip of snout)
HW Head Width (measured at level of rictus)
SL Snout Length (from anterior corner of eye to tip of snout)
DEN Distance from Eye to Nostril (from anterior corner of eye to posterior margin of naris)
ID Internarial Distance (taken between the median margins of the nares)
EL Eye Length (measured horizontally)
IoD Interorbital Distance (taken between the inner margins of the orbits)
EW Eyelid Width (the largest transverse width of the upper eyelid)
TL Tympanum Length (the largest length of the tympanum from the anterior margin to the posterior margin of the tympanum)
AL Arm Length (from the tip of the elbow to the proximal edge of the palmar tubercle)
HaL Hand Length (from the proximal edge of the palmar tubercle to the tip of Finger III),
ThL Thigh Length (from vent to knee)
TiL Tibia Length (from outer edge of flexed knee to heel)
TaL Tarsus Length (from the heel to the proximal edge of the inner metatarsal tubercle)
FL Foot Length (from proximal border of inner metatarsal tubercle to tip of fourth toe)
LL Leg Length (from the knee joint to the tip of Toe IV).

Sex and maturity were determined by direct examination of gonads through a lateral incision in the abdomen. In addition, we checked for secondary sexual characters in adult individuals, such as the presence or absence of vocal slits, vocal sac, and nuptial pads in males.

Bioacoustic analysis

Recordings of advertisement calls were obtained from six males of the new species: one male was recorded on February 10, 2016 between 17:30 h and 18:00 h, from a distance of 2 m in Brazil Novo, Pará, at a temperature of 28 ºC. Five additional males were recorded on February 17, 2017 between 18:30 h and 20:00 h from a distance of 2 m in Altamira, Pará, at a temperature of 28 ºC. The vocalizations of *Pristimantis koehleri*, *P.*

fenestratus and *P. samaipatae* (Köhler & Jungfer, 1995) available in the literature were used for comparisons with the new species. These are commonly used in descriptive bioacoustic studies (Padial and De La Riva 2009; Maciel et al. 2012). Data on the advertisement call of *P. chiastonotus* was obtained from the study of Lynch and Hoogmoed (1977).

The calls were analysed at a sampling rate of 44100 Hz using Audacity 2.0.3 software for Windows (Free Software Foudation Inc. 1991). Frequency information was obtained through Fast Fourier Transformations (FFT; width of 1024 points). Spectrograms and oscillograms were generated using Praat 5.3.43 for Windows (Boersma and Weenink 2006), following Yu and Zheng (2009), Zhou et al. (2014), and Preininger et al. (2016). The following variables were measured according to Padial and De la Riva (2009): call length (ms), number of notes per call, length of the note (ms), presence of pulses, fundamental frequency (frequency band to which the first sound is visualized through a spectral slice output, in Hz) and dominant frequency (measured from a spectral slice taken from the highest amplitude portion of the note, in Hz), in Praat 5.3.43 software.

Molecular analysis

Total genomic DNA was extracted from 46 specimens (Table 1) using the CTAB 2% protocol (Doyle and Doyle 1987). A fragment of 490 base pairs (bp) of the 16S mtDNA was amplified by PCR using primers 16Saf and 16Sbr (Palumbi 1991). Amplification was performed under the following conditions: 60s at 92 °C followed by 35 cycles of 92 °C (60 sec), 50 °C (50 sec) and 72 °C (90 sec). The final volume of the PCR reaction was 12 µL and contained 4.7 µL of ddH_2O, 1.5 µL of 25 mM $MgCl_2$, 1.25 µL of 10 mM dNTPs (2.5 mM each dNTP), 1.25 µL of tampon 10x (75 mM Tris HCl, 50 mM KCl, 20 mM $(NH_4)_2SO_4$), 1 µL of each primer (2 µM), 0.3 µL of 1 U Taq DNA Polymerase and 1 µL of DNA (30–50 ng/µL).

The sequencing reaction was performed according to the manufacturer's recommendations for sequencing mix ABI *BigDye Terminator*, using the primer 16Saf at an annealing temperature of 50 °C. The sequencing reactions were precipitated using the standardized protocol EDTA/Ethanol, resuspended with 10 µL deionized formamide (ABI) and sequenced in the automatic sequencer ABI 3130xl (*Applied Biosystems*).

Sequences were aligned using the ClustalW algorithm (Thompson et al. 1996) implemented in the software BioEdit 7.2 (Hall 1999). We used the software jModeltest 2.1.10 under the corrected Akaike information criterion to find the best evolutionary model. A maximum likelihood analysis was performed with the Treefinder software (Jobb 2008) using default settings and with 10000 bootstrap replicates. The Bayesian phylogenetic analysis using the evolutionary substitution model (GTR+G) was implemented in MrBayes v.3.2.6 software (Altekar et al. 2004), with the default heating values for two out of four chains, running 10^6 generations, with tree sampling every 2000 generations. The "burn in" value was selected by visualizing the log likelihoods associated with the posterior distribution of trees in the software Tracer v 1.5 (Rambaut et al. 2014). We assessed convergence by examining the average standard deviation of split frequencies

Table 1. List of specimens used for molecular analysis.

Species	Localities	GenBank	Nº in collection	Status of specimens	Source
Pristimantis latro sp. n.	Anapu, PA - Brazil	KX242519	LZATM 467	Holotype	this study
Pristimantis sp. n.	Anapu, PA - Brazil	KX925980	LZATM 743	Paratype	this study
Pristimantis sp. n.	Anapu, PA - Brazil	KX925981	LZATM 739	Paratype	this study
Pristimantis sp. n.	Anapu, PA - Brazil	KX925983	LZATM 744	Paratype	this study
Pristimantis sp. n.	Sen. José Porfírio, PA - Brazil	KX925984	LZATM 742	Paratype	this study
Pristimantis sp. n.	Sen. José Porfírio, PA - Brazil	KX925985	LZATM 748	Paratype	this study
Pristimantis sp. n.	Sen. José Porfírio, PA - Brazil	KX925986	LZATM 751	Paratype	this study
Pristimantis sp. n.	Altamira, PA - Brazil	KX925987	LZATM 386	Paratype	this study
Pristimantis sp. n.	Altamira, PA - Brazil	KX925988	BIOTA 1218	Paratype	this study
Pristimantis sp. n.	Altamira, PA - Brazil	KX925989	BIOTA 1111	Paratype	this study
Pristimantis sp. n.	Altamira, PA - Brazil	KX242523	BIOTA1214	Paratype	this study
Pristimantis sp. n.	Altamira, PA - Brazil	KX242523	LZATM 213	Paratype	this study
Pristimantis sp. n.	Altamira, PA - Brazil	KX242522	LZATM 277	Paratype	this study
Pristimantis sp. n.	Altamira, PA - Brazil	KX925990	LZATM 279	Paratype	this study
Pristimantis sp. n.	Altamira, PA - Brazil	KX925991	LZATM 281	Paratype	this study
Pristimantis sp. n.	Medicilândia, PA - Brazil	KX925992	LZATM 230	Paratype	this study
Pristimantis sp. n.	Medicilândia, PA - Brazil	KX925993	LZATM 243	Paratype	this study
Pristimantis sp. n.	Medicilândia, PA - Brazil	KX925994	LZATM 255	Paratype	this study
Pristimantis sp. n.	Flona Tapajós, PA - Brazil	KX242525	SISTAP 1145	Paratype	this study
Pristimantis sp. n.	Flona Tapajós, PA - Brazil	KX925995	SISTAP 1168	Paratype	this study
Pristimantis sp. n.	Flona Tapajós, PA - Brazil	KX925996	SISTAP 1235	Paratype	this study
Pristimantis sp. n.	Flona Tapajós, PA - Brazil	KX242524	SISTAP 1239	Paratype	this study
Pristimantis sp. n.	Flona Tapajós, PA - Brazil	KX925997	SISTAP 1240	Paratype	this study
Pristimantis sp. n.	Flona Tapajós, PA - Brazil	KX925998	SISTAP 1244	Paratype	this study
Pristimantis sp. n.	Flona Tapajós, PA - Brazil	KX925999	SISTAP 1246	Paratype	this study
Pristimantis sp. n.	Flona Tapajós, PA - Brazil	KX926000	SISTAP 1253	Paratype	this study
Pristimantis sp. n.	Flona Tapajós, PA - Brazil	KX926001	SISTAP 1256	Paratype	this study
Pristimantis sp. n.	Flona Tapajós, PA - Brazil	KX926002	SISTAP 1257	Paratype	this study
Pristimantis sp. n.	Flona Tapajós, PA - Brazil	KX926003	SISTAP 1259	Paratype	this study
Pristimantis sp. n.	Flona Tapajós, PA - Brazil	KX926004	SISTAP 1260	Paratype	this study
Pristimantis sp. n.	Flona Tapajós, PA - Brazil	KX926005	SISTAP 1261	Paratype	this study
Pristimantis sp. n.	Flona Tapajós, PA - Brazil	KX926006	SISTAP 1275	Paratype	this study
Pristimantis sp. n.	Flona Tapajós, PA - Brazil	KX926007	MPEG 095	Paratype	this study
Pristimantis sp. n.	Flona Tapajós, PA - Brazil	KX926008	MPEG 109	Paratype	this study
Pristimantis sp. n.	Flona Tapajós, PA – Brazil	KX926009	MPEG 160	Paratype	this study
Pristimantis sp. n.	Flona Tapajós, PA - Brazil	KX926010	MPEG 165	Paratype	this study
Pristimantis sp. n.	Flona Tapajós, PA - Brazil	KX926011	MPEG 177	Paratype	this study
P. fenestratus	Borba 2, AM – Brazil	KX242528	INPA-H 34565	Voucher	this study
P. fenestratus	Borba 2, AM – Brazil	KX926012	INPA-H 34580	Voucher	this study
P. fenestratus	Borba 2, AM – Brazil	KX926013	INPA-H 34579	Voucher	this study
P. fenestratus	Borba 1, AM – Brazil	KX242530	INPA-H 34571	Voucher	this study
P. fenestratus	Borba 1, AM – Brazil	KX926014	INPA-H 34577	Voucher	this study
P. fenestratus	Borba 1, AM – Brazil	KX926015	INPA-H 34562	Voucher	this study
P. fenestratus	Borba 1, AM – Brazil	KX242529	INPA-H 34573	Voucher	this study

Species	Localities	GenBank	Nº in collection	Status of specimens	Source
P. fenestratus	Borba 1, AM – Brazil	KX926016	INPA-H 34578	Voucher	this study
P. fenestratus	Borba 1, AM – Brazil	KX926017	INPA-H 34575	Voucher	this study
P. koehleri	Bolívia, Santa Cruz	EU192278	MNCN 42990	Paratopotype	Padial and De La Riva 2009
P. koehleri	Bolivia, Santa Cruz	EU192279	MNCN 6627	Paratopotype	Padial and De La Riva 2009
P. koehleri	Bolivia, Santa Cruz	EU192280	MNCN 42983	Paratype	Padial and De La Riva 2009
P. koehleri	Bolivia, Santa Cruz	EU192281	MNCN 43013	Paratype	Padial and De La Riva 2009
P. koehleri	Bolivia, Santa Cruz	EU192282	MNCN 42986	Paratype	Padial and De La Riva 2009
P. fenestratus	Bolivia, La Paz: Chalalan	EU192273	MNKA 6629	Voucher	Padial and De La Riva 2009
P. fenestratus	Bolivia, La Paz	EU192274	MNKA 6630	Voucher	Padial and De La Riva 2009
P. fenestratus	Bolivia, Cochabamba	EU192275	MNKA 6631	Voucher	Padial and De La Riva 2009
P. gutturalis	French Guiane	JN690705	577PG	Voucher	Fouquet et al. 2012
P. zeuctotylus	Suriname	JN691256	1069BPN	Voucher	Fouquet et al. 2011
P. achatinus	Colombia	JN104676	UVC15867	Voucher	Garcia et al. 2012
P. conspicillatus	Ecuador	EF493529	QCAZ28448	Voucher	Heinicke et al. 2007
P. skydmainos	Peru	EF493393			Heinicke et al. 2007
P. vilarsi	Colombia	KP149438	AJC 3945	Voucher	Guarnizo et al. 2015
P. samaipatae	Bolivia, Santa Cruz	EU192292	MNCN 42987	Voucher	Padial and De La Riva 2009
Oreobates cruralis	Bolivia	JF809994		Voucher	Padial et al. 2012

Abbreviations: MNCN, Museo Nacional de Ciencias Naturales (Spain); MNH-A, Museum of Natural History Noel Kempff Mercado (Bolivia); MNH, Museum of Natural History, Universidad Nacional de San Antonio Abad del Cusco, Peru; INPA – H, Instituto Nacional de Pesquisas da Amazônia – Herpetologia; MPEG, Museu Paraense Emílio Goeldi; SISTAP, Sisbiota Tapajós; LZATM, Laboratório de Zoologia de Altamira.

among runs (< 0.01). All trees generated before the flattening of the log likelihood curve were discarded. In all analyses, 10% of the samples were discarded as burn-in. The number of independent samples was considered sufficient when stationarity was reached and the effective sample sizes (ESS) were greater than 200. Uncorrected pairwise distances (*p*-distances) among *Pristimantis latro* sp. n. and other species of the *P. conspicillatus* group were calculated using MEGA 6.0 (Tamura et al. 2007). This analysis used se-

quences of several species belonging to the *Pristimantis conspicillatus* group (Padial et al. 2014) that are morphologically similar to *Pristimantis fenestratus* (Padial and De La Riva (2009). Hedges et al. (2008) indicates *Oreobates* as basal group of *Pristimantis*, therefore this genus was used as outgroup in our analyses. All sequences generated and/or analyzed in this study are available in GenBank (accession numbers are listed in Table 1).

Results

Phylogenetic analysis and genetic distances

The phylogenetic analysis of the nominal species *Pristimantis fenestratus* revealed the existence of four lineages (Figure 2): two present in the municipality of Borba, Amazonas, Brazil; a third one for specimens from Bolivia available on GenBank, and a fourth lineage – the new species – that groups together individuals of the Xingu and Tapajos rivers in Pará, Brazil. Samples collected in the paralectotype locality of *P. fenestratus*, municipality of Borba, presented two lineages (Borba 1 and Borba 2) with a genetic distance of 13%. The individuals of Borba 2 (INPA-H 34571, 34577, 34562, 34573, 34578 and 34575) presented a genetic distance of 3% to *P. fenestratus* (Bolivia) and of 2% to *Pristimantis koehleri*. The individuals of Borba 1 (INPA-H 34565, 34579 and 34580) presented a genetic distance of 15% to *P. fenestratus* (Bolivia) and 13% to *P. koehleri*. The new species, *Pristimantis latro* sp. n. has a genetic distance of 8% to *P. chiastonotus*, 9% to Borba 2, 10% to *P. koehleri*, and 11% to both Borba 1 and *P. fenestratus* of Bolivia (Table 2).

Bioacoustic analysis (Figure 3)

The call is characterized as ascending: its first note has a dominant frequency of 2635 Hz and the last one of 3272 Hz. The number of recorded notes of all specimens was seven, with a length from 31.60 to 45.91 ms (average = 39.68 ± 5.12). Total duration of the call averaged 454.83 ms (± 68.99, 402.36–581.27), presenting multiple pulses per note (6–9, average = 7.5 ± 2.12). The fundamental frequency ranged from 1342 to 1448 Hz (average= 1381.41 ± 35.71) and the dominant frequency ranged from 2635 to 3272 Hz (average= 3069.21 ± 253.61). A comparison between the advertisement call parameters of *Pristimantis latro* sp. n. and other species of *Pristimantis conspicillatus* group is shown in Table 3.

Morphological analysis

Based on qualitative morphological characters, the new species can be distnguished from other species of the *conspicillatus* group from the state of Pará by having divided palmar tubercle and venter cream with black spots, while *P. zeuctotylus* has undivided palmar tubercle and black venter. When compared with *P. chiastonotus*, the new spe-

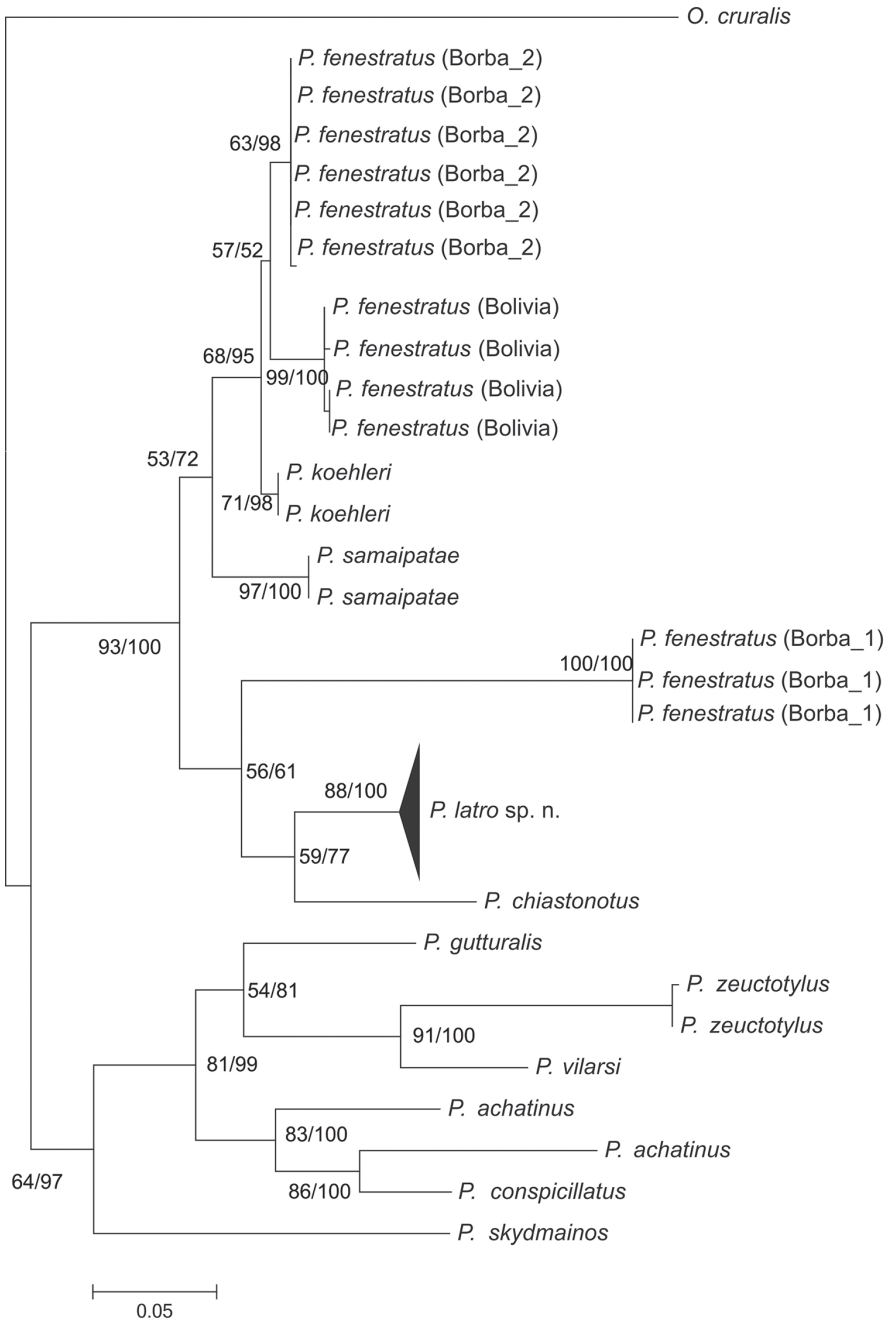

Figure 2. Maximum Likelihood (ML) tree using the evolutionary model GTR + G, inferring phylogenetic relationships of *Pristimantis* sp. n. and other species of the *P. conspicillatus* group based on mitochondrial 16S mtDNA (490 bp). ML support values are shown before the "/". Bayesian posterior probability support values (%) for major respective nodes are shown after the "/". The horizontal bar below the tree represents the genetic distance between branches. The branch of the new species was collapsed (black triangle) to improve tree visualization.

Table 2. Genetic uncorrected pairwise distances (%) among species of the Pristimantis conspicillatus group and the outgroup considered in this study. The numbers at the top of the table correspond to the locations in the first column.

	1	2	3	4	5	6	7	8	9	10	11	12	13	14	15	16	17	18
P. latro (Anapu) - 1																		
P. latro (Senador) - 2	0.01																	
P. latro (Altamira) - 3	0.01	0.00																
P. latro (Medicilândia) - 4	0.01	0.00	0.00															
P. latro (Flona Tapajós) - 5	0.01	0.01	0.02	0.02														
P. fenestratus (Borba 1) - 6	0.11	0.11	0.11	0.11	0.10													
P. fenestratus (Borba 2) - 7	0.09	0.10	0.10	0.09	0.10	0.12												
P. fenestratus (Bolivia) - 8	0.09	0.09	0.09	0.09	0.10	0.13	0.03											
P. chiastonotus (Brazil) - 9	0.08	0.07	0.08	0.08	0.09	0.13	0.10	0.09										
P. koehleri (Bolivia) - 10	0.10	0.09	0.10	0.10	0.09	0.11	0.02	0.03	0.10									
P. samaipatae (Bolivia) - 11	0.09	0.09	0.10	0.10	0.09	0.11	0.05	0.06	0.08	0.04								
P. gutturalis (French Guiana) - 12	0.14	0.14	0.15	0.15	0.14	0.17	0.14	0.14	0.17	0.13	0.13							
P. zeuctotylus (Suriname) - 13	0.14	0.15	0.15	0.15	0.14	0.16	0.16	0.15	0.16	0.15	0.13	0.11						
P. achatinus (Colombia) - 14	0.15	0.14	0.14	0.14	0.15	0.17	0.15	0.15	0.16	0.14	0.15	0.12	0.14					
P. conspicillatus (Ecuador) - 15	0.13	0.13	0.14	0.14	0.14	0.14	0.13	0.13	0.14	0.13	0.12	0.10	0.11	0.09				
P. skydmainos (Peru) - 16	0.18	0.18	0.18	0.18	0.19	0.19	0.15	0.15	0.16	0.14	0.15	0.15	0.14	0.15	0.13			
P. vilarsi (Colombia) - 17	0.12	0.12	0.13	0.13	0.12	0.16	0.15	0.15	0.14	0.15	0.13	0.10	0.09	0.13	0.11	0.14		
Oreobates cruralis (Bolivia) - 18	0.17	0.18	0.19	0.19	0.18	0.22	0.18	0.17	0.20	0.19	0.19	0.17	0.19	0.20	0.19	0.20	0.19	

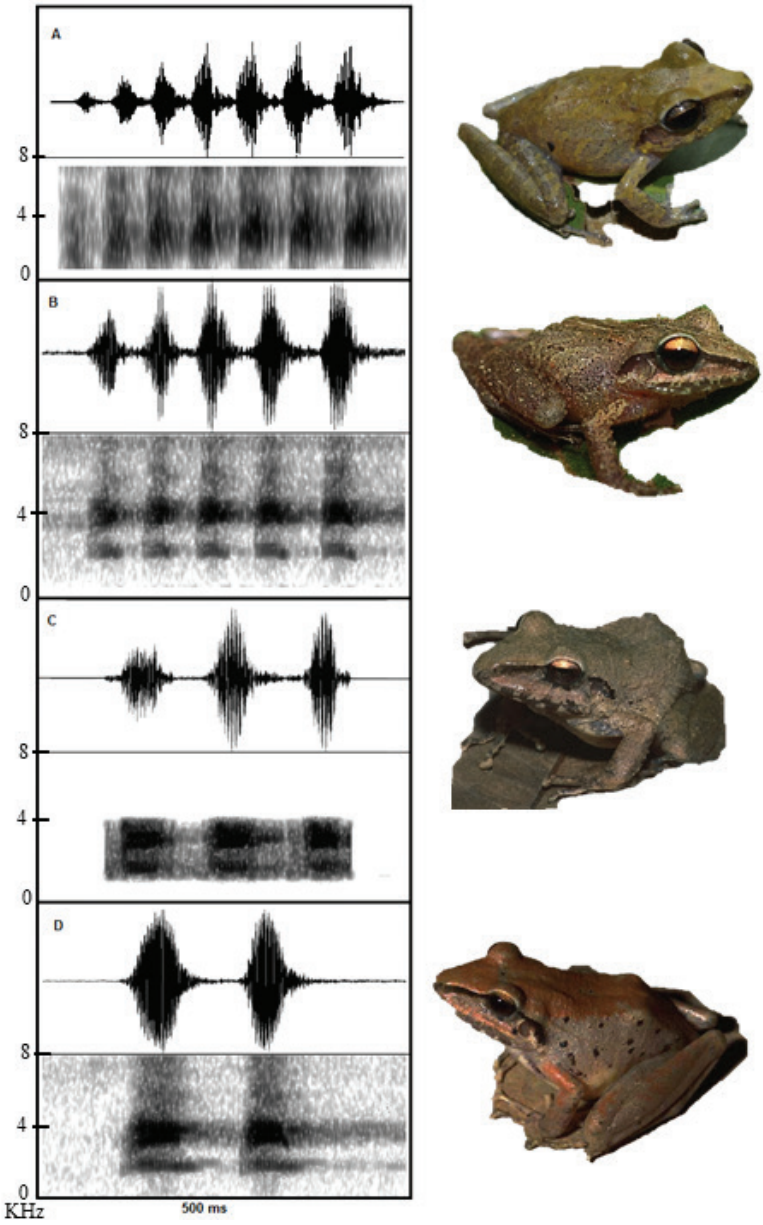

Figure 3. Comparison between advertisement calls among some species of the *Pristimantis conspicillatus* group: **A** *P. latro* sp. n. **B** *P. koehleri* **C** *P. fenestratus* and **D** *P. samaipatae*.

cies differs by the presence of a basal webbing among toes and the presence of a tarsal fold, absent in *P. chiastonotus*. When compared to *P. fenestratus*, lineage Bolivia, the new species lacks discoidal folds and presents a supernumerary tubercle in the hand. Additional details can be found in the section "Comparasion with other species".

Table 3. Diagnostic characters of advertisement calls from species of the *Pristimantis conspicillatus* group. Values are given as range (average ± standard deviation).

Species	Notes/Call	Call length (ms)	Note length (ms)	Pulses	Fundamental frequency (Hz)	Dominant frequency (Hz)	Notes	Calls	N specimens	N populations	Source
P. fenestratus	2–4 (2.6 ± 0.6)	157–458 (265.2 ± 81.6)	50–91 (63 ± 11.4)	9–17 (12.9 ± 42.2)	1542–2048 (1746 ± 158)	1710–3591 (3086.3 ± 580.7)	55	22	6	4	Padial and De La Riva (2009)
P. koehleri	3–8 (5.7 ± 1.0)	173–644 (421 ± 159.8)	20–54 (35.5 ± 6.6)	5–9 (7.5 ± 1)	1732–1971 (1853.5 ± 72.1)	3245–3971 (3662.4 ± 128.9)	119	21	6	2	Padial and De La Riva (2009)
P. samaipatae	1–3 (2 ± 0.2)	82.2–1062 (291.7 ± 168.1)	59–141 (89 ± 16.4)	11–23 (16.4 ± 2.6)	1535–1834 (1704.9 ± 64.3)	2922–3853 (3326.7 ± 175.9)	160	98	12	4	Padial and De La Riva (2009)
P. latro	7	**402.36–581.27** (454.83 ± 68.99)	**31–45.918 (39.686 ± 5.12)**	**6–9 (7.5 ± 2.12)**	**1342–1448,6 (1381.41 ± 35.71**	**2635.89–3272 (3069.21 ± 253.61)**	**49**	7	**6**	**2**	**This study**

With regard to quantitative morphological traits, males of the new species have a smaller SVL (N = 46, mean = 27.4 ± 7.2) compared to other lineages of *Pristimantis fenestratus* (Bolivia, N = 44, mean = 30.5 ± 2.1, from Padial and De La Riva 2009), lineage Borba 1 (N = 5, mean = 31.2 ± 1.9), lineage Borba 2 (N = 3, mean = 31.0 ± 0.2), and *P. chiastonotus* (N = 20, mean = 33.0). Only *P. zeuctotylus* has a smaller SVL than the new species (N = 20, mean = 25.2). Due to the low number of females form the localities Borba 1 and Borba 2, we restrict our comparisons with *P. fenestratus* from Bolivia (Padial and De La Riva (2009), *P. chiastonotus* and *P. zeuctotylus*. Females of the new species have a smaler SVL (N = 49, mean = 31.2 ± 7.9) than *P. fenestratus* from Bolivia (N = 44, mean = 43.7 ± 4.6), *P. chiastonotus* (N = 14, mean = 44.0) and *P. zeuctotylus* (N = 32, mean = 37.0). All measurements from the new species can be found on Appendix 2.

***Pristimantis latro* sp. n.**
http://zoobank.org/19BF72F8-BDA4-4C8C-965D-0D92B654B1DA
Figure 4

Holotype. LZATM – 467, adult female, collected on July 23, 2012 in the municipality of Anapu, Pará State, Brazil (3°9'28.15"S; 51°27'51.67"W) by Elciomar Araújo de Oliveira, Emil José Hernández Ruz and Joyce Celerino de Carvalho. Material stored in the collection of the Laboratório de Zoologia de Altamira (LZATM) of the Universidade Federal do Pará, Campus de Altamira, Brazil.

Paratopotypes. Two adult males: LZATM 739, LZATM 747 and nine adult females: LZATM 743, LZATM 749, LZATM 750, LZATM 740, LZATM 742, LZATM 754, LZATM 742, LZATM 748, LZATM 751, collected during field work by Claudia Liz Teles and Joyce Celerino de Carvalho. Material stored in the collection of the Laboratório de Zoologia de Altamira (LZATM) of the Universidade Federal do Pará, Campus de Altamira, Brazil.

Paratypes. Six males: LZATM 197, LZATM 0063, LZATM 1339, LZATM 818, LZATM 815, LZATM 816 and LZATM 1340. Eleven females: LZATM 386, LZATM 243, LZATM 360, LZATM 744, LZATM 281, LZATM 742, LZATM 748, LZATM 751, LZATM 230, LZATM 358 and LZATM 277 collected during field work by Claudia Liz Teles and Joyce Celerino de Carvalho. Material stored in the collection of the Laboratório de Zoologia de Altamira (LZATM) of the Universidade Federal do Pará, Campus de Altamira, Brazil. The collection locations of each specimen are listed in Appendix 1.

Allocation to genus and species group of the new species. No morphological synapomorphy has yet been identified to support the genus *Pristimantis* (Hedges et al. 2008). The new taxon is therefore assigned to the genus *Pristimantis* based on (1) molecular phylogenetic relationships (Figure 2); and (2) its morphological characteristics, which fall into the range of other known *Pristimantis* species. The new taxon is assigned to the genus *Pristimantis* based on its geographic distribution and overall

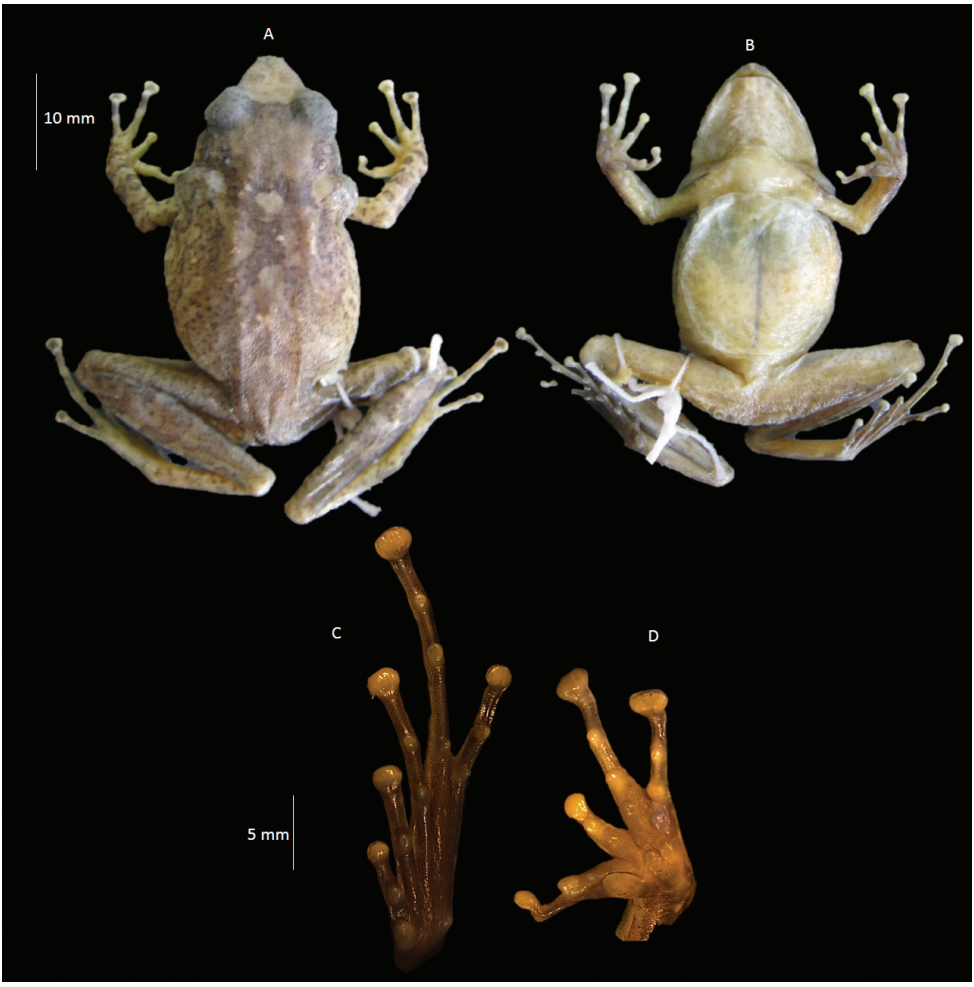

Figure 4. Holotype of *Pristimantis* sp. n. **A** ventral view **B** dorsal view **C** side view of the head **D** hand **E** and right foot (INPA-H 34576).

similarity to the majority of species of *Pristimantis* described. We assign the new species to the *P. conspicillatus* species group following Maciel et al. (2012) for having Finger I longer than Finger II, granular but nor aerolate belly, a tarsal fold, distinct tympanic membrane, and by its advertisement call composed of single pulsatile notes modulated in amplitude, as well as molecular phylogenetic relationships.

Diagnosis. *Pristimantis latro* sp. n. is distinguished from other species of the group by the following combination of characters (summarized in Table 4): (1) dorsal skin weakly shagreened or smooth, dorsal tubercles present, dorsolateral folds absent, smooth skin on belly; (2) whitish or yellowish ventral coloration with black spots; (3) one subarticular tubercle on fingers I and II and two on Fingers III and IV; (4) super-

Table 4. Comparison of diagnostic characters of some species of the *Pristimantis conspicillatus* group, including the new species: (1) belly texture (smooth or granular), (2) dorsal tubercles (present or absent); (3) fringe on finger (present or absent); (4) dorsolateral fold (present or absent); (5) fringe on toe (prominent, weak, absent); (6) basal membrane on toe (present or absent); (7) tarsal fold (prominent, weak or absent); (8) throat color pattern (stained, immaculate, variable or light); (9) supernumerary plant tubercle (present or absent); (10) External palmar tubercle (whole, split or semi-split).

Species	1	2	3	4	5	6	7	8	9	10
*P. fenestratus**	smooth	present	absent	–	weak	present	–	stained	absent	—
*P. fenestratus***	smooth	absent	present	absent	weak	present	present	variable	–	split
P. koehleri	granular laterally	absent	absent	absent	weak	absent	present	light	present	split
P. dundeei	granular	present	absent	absent	prominent	present	present	stained	–	split
P. samaipatae	smooth	absent	absent	absent	prominent	absent	present	stained	–	split
P. ventrigranulosus	granular	absent	weak or absent	absent	weak	present	promi-nent	weakly spotted	absent	single
P. zeuctotylus	smooth	absent	absent	present	absent	absent	absent	stained	present	inteiro
P. chiastonotus	smooth	absent	absent	present	absent	absent	absent	ligth	present	split
Pristimantis latro sp. n.	**smooth**	**present**	**present**	**present**	**weak**	**present**	**weak**	**stained**	**present**	**split**

numerary tubercles present at the base of fingers I, II, and III, and almost the same size of subarticular tubercles; (5) lateral fringes along fingers; (6) supernumerary tubercle present at the base of Toe IV; (7) basal webbing between toes and weak lateral fringes on toes; (8) twenty-one molecular autapomorphies for the gene fragment 16S mtDNA (Table 5); (9) call consisting of seven notes.

Comparison with other species. Due to difficulties in visiting museums to compare some of the species in the *Pristimantis conspicillatus* group with the species described in this work, data from the literature was used for this procedure. The consulted reference can be found, between brackets, at the end of each comparison. The character state of the compared species is between parentheses. *Pristimantis latro* sp. n. is distinguished from *P. fenestratus* by the absence of discoidal fold (present), the presence of supernumerary tubercles on hand (absent), length of notes in the male advertisement call ranging from 31 to 45.91 ms (50 to 91 ms) [Duellman and Lehr 2009; Padial and De La Riva 2009; Maciel et al. 2012]; from *P. koehleri* by smooth belly skin (finely granular), absence of discoidal fold (present), rostrum subacuminate in dorsal and protruding in lateral view (acuminate in dorsal view and subacuminate in lateral view), vocalization composed by seven notes (four, five, six, seven and eight notes) [Padial and De La Riva 2009]; from *P. samaipatae* by having whitish cream belly with black spots disposed randomly (immaculate), length of notes ranging from 31 to 45.91 ms (50 to 141 ms in *P. samaipatae*) [Köhler 2000; Padial and De La Riva 2009]; from *P. dundeei* by having smooth belly (areolate), presence of fringe in the fingers (absent), dorsolateral folds (absent), length of notes ranging from 31 to 45.91 ms (50 ms in *P. dundeei*)

Table 5. Diagnostic characters observed in the 16S mtDNA gene fragment from *Pristimantis* sp. n. and other species of the genus *Pristimantis*. The first column indicates the character position within the fragment. (-) indicates deletions.

Position (pb)	*P. latro* sp. n.	*P. fenestratus* (Borba 1)	*P. fenestratus* (Borba 2)	*P. fenestratus* (Bolivia)	*P. koehleri* (Bolivia)	*P. chiastonotus* (Brazil)
86	G	A	A	A	A	A
138	A	G	G	G	G	A
144	T	C	C	C	C	C
149	A	T	T	T	T	A
184	T	C	C	C	C	C
194	C	-	-	-	-	A
197	T	A	A	A	A	C
202	T	A	A	A	A	-
208	T	C	C	C	C	C
229	C	T	A	A	A	T
230	C	T	T	T	T	T
237	T	-	-	-	-	C
239	T	C	C	C	C	A
247	C	A	T	T	T	-
269	C	T	T	T	T	T
273	A	C	T	T	T	A
289	G	A	A	A	A	A
293	T	-	A	A	A	-
330	C	T	T	T	T	T
401	G	A	A	A	A	A
455	C	T	T	T	T	A

[Köhler 2000; Padial and De La Riva 2009]; from *P. ventrigranulosus* by having smooth belly skin (weakly areolate), dorsal tubercles (absent), presence of fringe in the fingers (weak or absent), dorsolateral fold present (absent), weak tarsal fold (prominent) [Maciel et al 2012]; from *P. zeuctotylus* by a divided palmar tubercle (entire), whitish cream-colored belly with black spots disposed randomly and dark brown dorsum (black belly and bronze dorsum) [Lynch and Hoogmoed 1977]; from *P. chiastonotus* for presenting basal webbing and fringe on the toes (absent), tarsal fold present (absent); snout subacuminate in dorsal view (acuminate), dorsal tubercles present (absent), vocalization composed by seven notes (one note) [Lynch and Hoogmoed 1977].

The comparisons were restricted to these species because they present the highest morphological and acoustic similarity with the new species. Another important factor is the geographical range of the new species, which becomes the only one in its group occurring in the eastern state of Pará, Brazil. The geographically-closest species are *P. zeuctotylus* and *P. chiastonotus*, north of Pará, whereas the most genetically-close are *P. chiastonotus* from the municipality of Monte Alegre in the state of Pará and the lineage of *P. fenestratus* from Borba 1 in the state of Amazonas.

Description of the holotype. Adult female 40 mm SVL. Dorsal skin shagreened, absence of dorsal tubercles; smooth ventral skin, granular posterior surface of thighs; head longer (39% of the SVL) than wide; long snout, subacuminate in dorsal view and protruding in lateral view; concave canthus rostralis, flat loreal region; ovoid tongue covering the whole floor of the mouth; dentigerous process of vomer oblique and posterior to choanae; eye 78.9% of Distance from Eye to Nostril; elliptical pupil; absent supraocular tubercles; absent cranial crests; prominent supra tympanic fold, not contacting the eye; tympanic membrane 40% of ED, rounded, tympanic annulus prominent; relatively small hands, 26.25% of the SVL; relative length of fingers: II < IV < I < III; discs of Fingers III and IV are wider than fingers I and II; prominent, semi divided, heart-shaped external metacarpal tubercle; large internal palmar tubercle; one subarticular tubercle prominent on Fingers I and II, two prominent subarticular tubercles on fingers III and IV; supernumerary tubercles present at the base of fingers I, II and III; long legs, tibia 57% of the SVL; relative length of toes: I <II <V <III <IV; well developed and oval inner metatarsal tubercle; external metatarsal tubercle much smaller than the internal one; one subarticular tubercle on toes I and II; two subarticular tubercles on toes III and V; and three subarticular tubercles on toe IV; basal webbing and lateral fringes present on toes (weak); tarsal fold present.

Measurements of holotype (in mm). SVL: 40.0; HL: 15.6; HW: 14.5; SL: 7.9; DEN: 5.7; ID: 3.1; EL: 4.5; IoD: 3.9; EW: 3.6; TL: 1.8; AL: 8.9; HaL: 10.5; ThL: 20.5; TiL: 22.8; TaL: 11.9; FL: 18.9; LL: 30.3.

Color in life. Light brown dorsum with some black tubercles. Posterior and anterior limbs heavily barred dark brown. Weak labial bars. Black band extending from eye to tip of snout. Belly clear with some randomly scattered dark spots. Iris presents a yellowish coloration in the upper and lower part, whereas in the anterior and posterior region the color red is predominant.

Coloration in preservative. In alcohol, the coloration is predominantly brown in the dorsal region, whether male or female. The belly can be immaculate white or present dark spots arranged randomly. The dorsal band, present in some individuals, is white.

Variation (Figures 5 and 6). The males LZATM 197, LZATM 063 and LZATM 1339 have dorsal color light brown, while the males LZATM 818, LZATM 815, LZATM 816 and LZATM 1340 have dark brown dorsal and dorsolateral regions with more apparent brown bars. The ventral face of males may be immaculate white (LZATM 197, LZATM 816) or have black spots scattered around the belly and throat (LZATM 1339, LZA 063, LZATM 818, LZATM 815 and LZATM 1340). LZATM 1340 presents a heavily pigmented black throat, legs and arms with clear bars. Females have predominantly light brown dorsum, with weakly barred legs and arms of darker brown (LZATM 386, LZATM 467, LZATM 243, LZATM 360, LZATM 744, LZATM 281, LZATM 742, LZATM 748 and LZATM 751), while LZATM 230 and LZATM 358 have a darker coloration and a dorsal band from the face to the cloaca of yellow color (in life) and white (in alcohol). The latter individual has strongly barred legs and arms. Its belly is usually either immaculate white or with a few dark spots, but LZATM 277 has a belly and throat heavily black pigmented. The dorsal skin is smooth in most of the examined individuals,

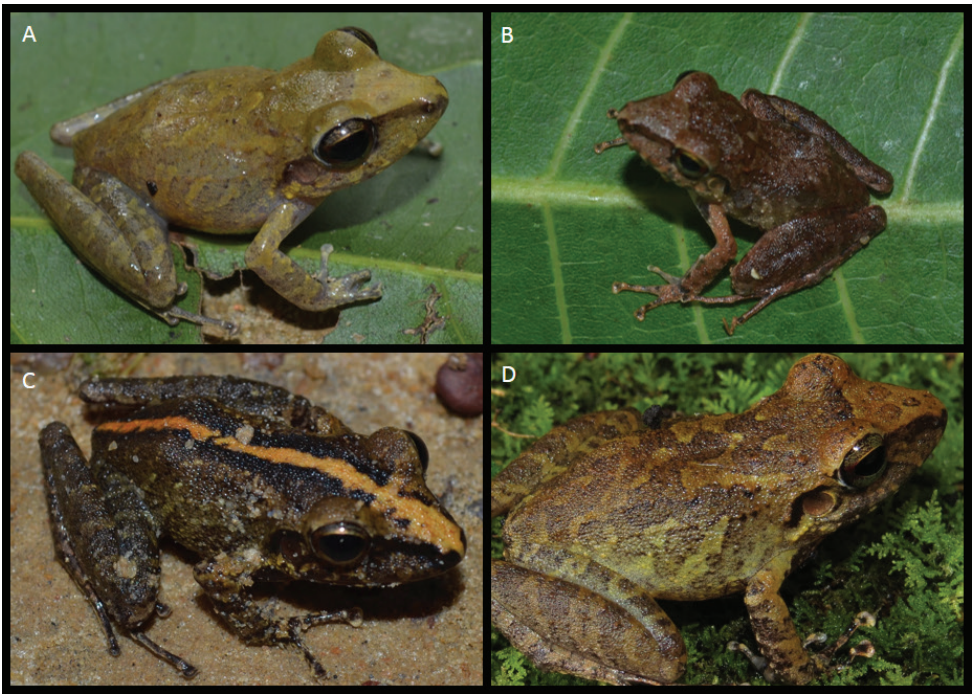

Figure 5. Color variation in life of some individuals of *Pristimantis latro* sp. n. **A** holotype **B, C** paratypes of Anapu and **D** Altamira.

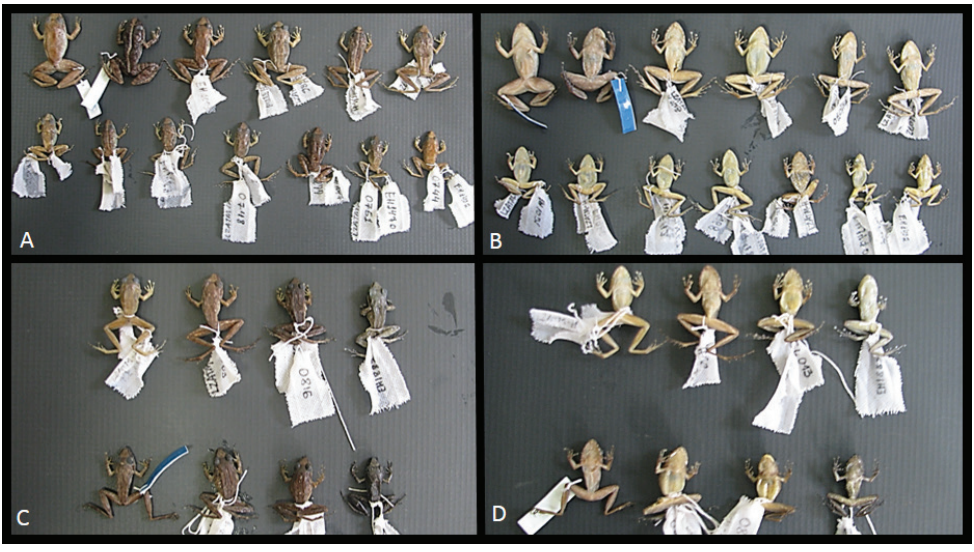

Figure 6. Dorsal and ventral morphological variation of the type series of *Pristimantis latro* sp. n. **A** Females in dorsal view **B** Females in ventral view **C** Males in dorsal view and **D** Male in ventral view.

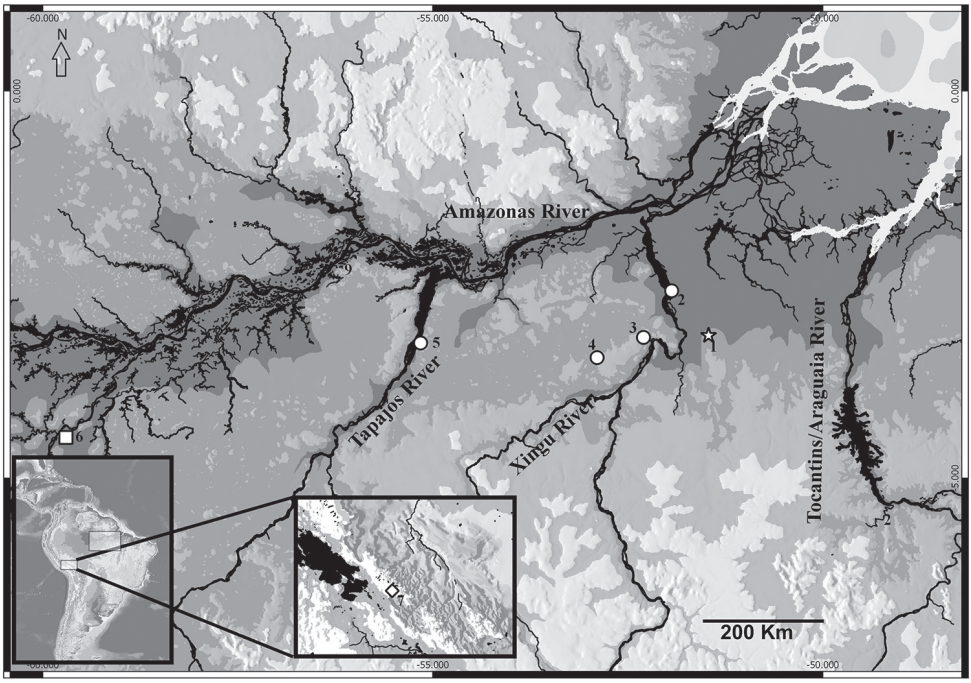

Figure 7. Type locality of *Pristimantis latro* sp. n., municipality of Anapu, Pará, Brazil (star). The circles represent the other localities where the new species was found. The square and the diamond represent the localities of *Pristimantis fenestratus* used for the morphological and genetic comparisons. **1** Anapu (3°4'57.26"S; 51°22'25.67"W) **2** Senador José Porfírio (2°34'51.63"S; 51°56'13.47"W) **3** Altamira (3°13'24.85"S; 52°14'22.74"W) **4** Medicilândia (3°26'37.93"S; 52°53'35.26"W) **5** Flona do Tapajós (3°38'49.06"S; 55°11'46.00"W) **6** Borba (4°28'29.88"S; 59°42'12.06"W) and **7** La Paz, Bolivia (16°24'12.89"S; 68°6'10.20"W).

although some specimens present a weakly shagreened texture: LZATM 358, LZATM 816, LZATM 63, LZATM 1339, LZATM 1340 and LZATM 467.

Etymology. The specific epithet "latro" (from the Latin *latro* = mercenary, robber) refers to the common name generally attributed to the species of *Pristimantis* – "Robber Frogs" – that exhibit a dark band on the snout, creating the illusion of a robber's mask.

Distribution, ecology, and habitat. *Pristimantis latro* sp. n. has been recorded in the municipalities of Anapu, Senador Jose Porfirio, Altamira, Medicilândia, Brasil Novo, Uruará and Flona Tapajós regions located in the interfluves Xingu / Tapajós and Xingu / Tocantins - Araguaia in Pará State, Brazil (Figure 7). It can be found in conserved areas of forests (Anapu, Flona do Tapajós) or with some environmental disturbance, e.g., forest fragments surrounded by pastures (Brasil Novo, Altamira and Vitória do Xingu). During the rainy/reproductive period, the males move up the vegetation to vocalize at a height of 1.5 m and in the dry period they can be found in the leaf litter.

Discussion

Pristimantis is a megadiverse genus with many species described mainly for the Andean region of Peru and Bolivia, Colombia, Ecuador and Venezuela, likely because a larger number of surveys have been carried out in these areas (Duellman and Hedges 2007, Elmer and Cannatella 2008, Padial and De la Riva 2009, Duellman and Lehr 2009, Barrios-Amorós et al. 2010, Arteaga-Navarro and Guayasamin 2011, Mueses-Cisneros et al. 2013, Navarrete et al. 2016, Shepack et al. 2016). In comparison, its diversity in the eastern Amazonian region appears to be lower, possibly due to a lack of taxonomic studies. As far as we know, *Pristimantis latro* sp. n. represents the first species described to the south of the Amazon River in Pará State, where it was erroneously identified as *P. fenestratus* due to their morphological similarities (Oliveira et al. 2013, Vaz-Silva et al. 2015).

Pristimantis fenestratus has been considered a widely distributed and recorded species in the Amazon, but we raise a problem already mentioned by other authors regarding its cryptic diversity (Padial and De la Riva 2009, Duellman and Lehr 2009, Smith et al. 2009). Our analyses show that *P. fenestratus* from the municipality of Borba and *P. fenestratus* from La Paz, Bolivia, represent three lineages separated by genetic distances larger than 3%, which studies suggest may indicate distinct species (Vences et al. 2005, Fouquet et al. 2007). Thus, a taxonomic revision of *P. fenestratus* is required since populations from the two locations mentioned in the original description show considerable genetic differences.

Pristimantis latro sp. n. is described for the Eastern Amazonia after a morphological, molecular and bioacoustics comparison with *P. fenestratus* and other species of the *P. conspicillatus* group. Recent studies have revealed that widely distributed frog species often include many cryptic taxa (Elmer et al. 2007, Padial and De la Riva 2009, Gehara et al. 2014). It is common to describe new species of *Pristimantis* based only on morphology (Barrios-Amorós et al. 2010, Mueses-Cisneros et al. 2013, Navarrete et al. 2016) or on a combination of morphological and genetic evidences (Arteaga-Navarro and Guayasamin 2011, Barrios-Amorós et al. 2012). Here, the combination of different lines of evidence revealed a new species of *Pristimantis* with morphological, genetic and bioacoustic diagnostic characters that allow not only differentiating it from other species of its group, but also illuminate the taxonomy of this speciose genus.

Acknowledgements

We thank two anonymous reviewers for valuable suggestions that greatly improved this paper; Evonildo Gonçalves from Universiade Federal do Pará (Campus de Belém) for assistance in molecular protocols at Instituto Evandro Chagas as well as to the entire staff of the Tecnologia Bio-molecular laboratory who helped in obtaining genetic data; to the Laboratory of Animal Evolution and Genetics from Universidade Federal do Amazonas (LEGAL) for the help in obtaining part of the sequences used in this study; to the project CNPq/SISBIOTA (grant no. 563348/2010 to Izeni Pires Farias),

which financed part of the field work; to Coleção de Anfíbios e Répteis of the Instituto Nacional de Pesquisas da Amazônia (INPA-H) and the Coleção Herpetológica of the Museu Paraense Emílio Goeldi (MPEG) for loaning material analyzed in this study; to the BIOTA Environmental Projects and Consulting LTDA for help in fieldwork logistics; to Leandro Wronski, Jailson Xavier, Marcos Penhacek and Renan Oliveira for their assistance in the field; to Program of Support for Qualified Production - PAPQ / UFPA (process 23073.026959/2016-92).

References

Altekar G, Dwarkadas S, Huelsenbeck JP, Ronquist F (2004) Parallel Metropolis-coupled Markov chain Monte Carlo for Bayesian phylogenetic inference. Bioinformatics 20: 407–415. https://doi.org/10.1093/bioinformatics/btg427

Arteaga-Navarro AF, Guayasamin JM (2011) A new frog of the genus *Pristimantis* (Amphibia: Strabomantidae) from the high Andes of Southeastern Ecuador, discovered using morphological and molecular data. Zootaxa 29: 17–29.

Ávila-Pires TCS, Hoogmoed MS, Rocha WA (2010) Notes on the Vertebrates of northern Pará, Brazil: a forgotten part of the Guianan Region, I. Herpetofauna. Boletim do Museu Paraense Emílio Goeldi, Ciências Naturais, Belém 5(1): 13–112

Barrio-Amorós CL, Rojas-Runjaic FJM, Barros TR (2010) Two new *Pristimantis* (Anura: Terrarana: Strabomantidae) from the Sierra de Perijá, Venezuela. Zootaxa 2329: 1–21.

Barrio-Amorós CL, Guayasamin JM, Hedges SB (2012) A new minute Andean *Pristimantis* (Anura: Strabomantidae) from Venezuela. Phyllomedusa 11(2): 83–93. https://doi.org/10.11606/issn.2316-9079.v11i2p83-93

Barbour T, Noble GK (1920) Some amphibians from northwestern Peru, with a revision of the genera *Phyllobates* and *Telmatobius*. Bulletin of the Museum of Comparative Zoology. Cambridge, Massachusetts 63: 395–427.

Bernarde PS, Macedo LC (2008) Impacto do desmatamento e formação de pastagens sobre a anurofauna de serapilheira em Rondônia. Iheringia 98(4): 454–459. https://doi.org/10.1590/S0073-47212008000400006

Boersma P, Weenick D (2006) Praat: doing phonetics by computer. Version 5.3.43.

De la Riva I, Köhler J, Lötters S, Reichle S (2000) Ten years of research on Bolivian amphibians: updated checklist, distribution, taxonomic problems, literature and iconography. Revista Española de Herpetología 14: 19–164.

Doyle JJ, Doyle JL (1987) Isolation of plant DNA from fresh tissue. Focus 12(1): 13–15

Duellman WE (1978) Three new species of *Eleutherodactylus* from Amazonian Perú (Amphibia: Anura: Leptodactylidae). Herpetologica 34: 264–270.

Duellman WE, Lehr E (2009) Terrestrial- Breeding frogs (Strabomantidae) in Peru. Ntv Natur Und Tier-Verlag, Germany, 386 pp.

Elmer KR, Dávila JA, Lougheed SC (2007) Cryptic diversity and deep divergence in an upper Amazonian leaflitter frog, *Eleutherodactylus ockendeni*. BMC Evolutionary Biology 7: 247. https://doi.org/10.1186/1471-2148-7-247

Elmer KR, Cannatella DC (2008) Three new species of leaflitter frogs from the upper Amazon forests: cryptic diversity within *Pristimantis* "*ockendeni*" (Anura: Strabomantidae) in Ecuador. Zootaxa 38: 11–38.

Fouquet A, Gilles A, Vences M, Marty C, Blanc M, Gemmell NJ (2007) Underestimation of species richness in neotropical frogs revealed by mtDNA analyses. PLoS ONE 10: 1–10. https://doi.org/10.1371/journal.pone.0001109

Fouquet A, Noonan BP, Rodrigues MT, Pech N, Gilles A, Gemmell NJ (2012) Multiple Quaternary Refugia in the Eastern Guiana Shield Revealed by Comparative Phylogeography of 12 Frog Species. Systematic Biology 61(3): 461–489. https://doi.org/10.1093/sysbio/syr130

Fouquet A, Martinez Q, Courtois EA, Dewynter M, Pineau K, Gaucher P, Blanc M, Marty C, Kok PJR (2013) A new species of the genus *Pristimantis* (Anura, Craugastoridae) associated with the moderately evelated massifs of French Guiana. Zootaxa 3750: 569–586. https://doi.org/10.11646/zootaxa.3750.5.8

França FGR, Venâncio NM (2010) Reptiles e amphibians of a poorly known region in southwest Amazonia. Biotemas 23(3): 71–84.

Frost DR (2017) Amphibian Species of the World: an Online Reference. Version 5.6, American Museum of Natural History, New York, USA. http://research.amnh.org/herpetology/amphibia/index.html [Accessed 9 January 2017]

Garcia RJC, Crawford AJ, Mendoza AM, Ospina O, Cardenas H, Castro F (2012) Comparative phylogeography of direct-developing frogs (Anura: Craugastoridae: *Pristimantis*) in the southern Andes of Colombia. PLoS ONE 7(9): E46077. https://doi.org/10.1371/journal.pone.0046077

Gehara M, Crawford AJ, Orrico VGDM, Rodríguez A, Lötters S, Fouquet A, Barrientos LS, Brusquetti F, De la Riva I, Ernst R, Urrutia GG, Glaw F, Guayasamin JM, Hölting M, Jansen M, Kok PJR, Kwe A, Lingnau R, Lyra M, Moravec J, Pombal JP, Rojas-Runjaic FJM, Schulze A, Señaris JC, Solé M, Rodrigues MT, Twomey E, Haddad CFB, Vences M, Köhler J (2014) High Levels of Diversity Uncovered in a Widespread Nominal Taxon: Continental Phylogeography of the Neotropical Tree Frog *Dendropsophus minutus*. PLoS ONE 9 (9): 1–12. https://doi.org/10.1371/journal.pone.0103958

Guarnizo CE, Paz A, Munoz-Ortiz A, Flechas SV, Mendez J, Crawford AJ (2015) DNA Barcoding Survey of Anurans across the Eastern Cordillera of Colombia and the Impact of the Andes on Cryptic Diversity. PLoS ONE 10(5): E0127312. https://doi.org/10.1371/journal.pone.0127312

Hall TA (1999) BioEdit: a user-friendly biological sequence alignment editor and analysis program for Windows 95/98/NT. Nucleic Acids Symposium Series 41: 95–98.

Häupl M, Tiedemann F (1978) Vertebrata 1. Typenkatalog der Herpetologischen Sammlung. Kataloge der Wissenschaftlichen Sammlungen des Naturhistorischen Museums in Wien 2: 7–34.

Häupl M, Tiedemann F, Grillitsch H (1994) 3—Vertebrata, I—Amphibia. Katalog der Typen der Herpetologischen Sammlung nach dem Stand vom 1. Jänner 1994. Kataloge der Wissenschaftlichen Sammlungen des Naturhistorischen Museums in Wien 9: 1–42.

Hedges SB, Duellman WE, Heinicke MP (2008) New World direct-developing frogs (Anura: Terrarana): Molecular phylogeny, classification, biogeography, and conservation. Zootaxa 1737: 182.

Heinicke MP, Duellman WE, Hedges SB (2007) Major Caribbean and Central American frog faunas originated by ancient oceanic dispersal. Proceedings of the National Academy of Sciences of the United States of America 104: 10092–10097. https://doi.org/10.1073/pnas.0611051104

Heyer WR, Muñoz AM (1999) Validation of *Eleutherodactylus crepitans* Bokermann, 1965, notes on the types and type locality of *Telatrema heterodactylum* Miranda-Ribeiro, 1937, and a description of a new species of *Eleutherodactylus* from Mato Grosso, Brazil (Amphibia: Anura: Leptodactylidae). Proceedings of the Biological Society of Washington 112: 1–18.

Jiménez de la Espada M (1870) Faunae neotropicalis species quaedam nondum cognitae. Jornal de Sciências, Mathemáticas, Physicas e Naturaes 65: 57–65.

Jobb G (2008) TREEFINDER version of March of 2011. Munich, Germany. Distributed by the author at www.treefinder.de [Accessed June 30, 2014]

Kieswetter CM, Schneider CJ (2013) Phylogeography in the northern Andes: Complex history and cryptic diversity in a cloud forest frog, *Pristimantis w-nigrum* (Craugastoridae). Molecular Phylogenetics and Evolution 69: 462–468. https://doi.org/10.1016/j.ympev.2013.08.007

Köhler J (2000) Amphibian diversity in Bolivia: a study with special reference to montane forest regions. Ph. D. Dissertation, Univ. Bonn, 281 pp.

Köhler J, Jungfer K-H (1995) Eine neue Art und ein Erstnachweis von Fröschen der Gattung *Eleutherodactylus* aus Bolivien. Salamandra 31: 149–156.

Kok PJR, Kalamandeen M (2008). Introduction to the Taxonomy of the Amphibians of Kaieteur National Park, Guyana. Abc Taxa 5: 279 pp.

Lehr E, Aguilar C, Siu-Ting K, Carlos-Jordán J (2007) Three New Species of *Pristimantis* (Anura: Leptodactylidae) from the Cordillera de Huancabamba In Northern Peru. Herpetologica 63: 519–536. https://doi.org/10.1655/0018-0831(2007)63[519:TNSOPA]2.0.CO;2

Lehr E, Coloma LA (2008) A minute new Ecuadorian Andean frog (Anura: Strabomantidae, *Pristimantis*). Herpetologica 64: 354–367. https://doi.org/10.1655/07-089.1

Lehr E, Catenazzi A, Rodríguez D (2009) A new species of *Pristimantis* (Anura: Strabomantidae) from the Brazilian Cerrado. Zootaxa 1990: 30–40. https://doi.org/10.1016/j.ympev.2007.05.020

Lehtinen RM, Nussbaum RA, Richards CM, Cannatella DC, Vences M (2007) Mitochondrial genes reveal cryptic diversity in plant-breeding frogs from Madagascar (Anura, Mantellidae, Guibemantis). Molecular Phylogenetics and Evolution 44: 1121–1129.

Lima AP, Mangnusson WE, Menin M, Erdtmann LK, Rodrigues DJ, Keller C, Hödl W (2006) Guia de sapos da Reserva Adolpho Ducke, Amazônia Central = Guide to the frogs of Reserva Adolpho Ducke, Central Amazonia. Manaus: Áttema Design Editorial, 168 pp.

Lynch JD (1980) A Taxonomic and Distributional Synopsis of the Amazonian Frogs of the Genus *Eleutherodactylus*. Americam Museum Novitates 2696: 1–24.

Lynch JD, Duellman WE (1997) Frogs of the genus *Eleutherodactylus* (Leptodactylidae) in western Ecuador: systematics, ecology, and biogeography. The University of Kansas Natural History Museum, 1–236.

Lynch JD, Hoogmoed MS (1977) Two species of *Eleutherodactylus* (Amphibia: Leptodactylidae) from northeastern South America. Proceedings of the Biological Society of Washington 90: 424–439.

Maciel NM, Vaz-Silva W, De Oliveira RM, Padial JM (2012) A new species of *Pristimantis* (Anura: Strabomantidae) from the Brazilian Cerrado. Zootaxa 56: 43–56.

Melin DE (1941) *Contributions to the knowledge of the Amphibia of South America*. Göteborgs Kungl. Vetenskaps-och Vitterhets-samhälles. Handlingar. Serien B, Matematiska och Naturvetenskapliga Skrifter 1: 1–71.

Mueses-Cisneros JJ, Perdomo-Castillo IV, Cepeda-Quilindo B (2013) A new species of the genus *Pristimantis* (Anura: Craugastoridae) from southwestern Colombia. Herpetotropicos 9: 37–45.

Navarrete MJ, Venegas PJ, Ron SR (2016) Two new species of frogs of the genus *Pristimantis* from Llanganates National Park in Ecuador with comments on the regional diversity of Ecuadorian *Pristimantis* (Anura, Craugastoridae). Zookeys 593:139–162. https://doi.org/10.3897/zookeys.593.8063

Oliveira EA, Hernandez-Ruz EJ, Barros FB (2013) Herpetodauna de las proximidades de la caverna Planaltina, Brazil Novo, Pará (Amazonia Brasileña). Herpetotropicos 9(1-2): 55–68.

Padial JM, Grant T, Frost DR (2014) Molecular systematics of terraranas (Anura: Brachycephaloidea) with an assessment of the effects of alignment and optimality criteria. Zootaxa 3825: 1–132. https://doi.org/10.11646/zootaxa.3825.1.1

Padial JM, De La Riva I (2009) Integrative taxonomy reveals cryptic Amazonian species of *Pristimantis* (Anura: Strabomantidae). Zoological Journal of the Linnean Society 155: 97–122. https://doi.org/10.1111/j.1096-3642.2008.00424.x

Padial JM, Chaparro JC, Castroviejo-Fisher S, Guayasamin JM, Lehr E, Delgado AJ, Vaira M, Teixeira M Jr., Aguayo R, De la Riva I (2012) A revision of species diversity in the Neotropical genus *Oreobates* (Anura: Strabomantidae), with the description of three new species from the Amazonian slopes of the Andes. American Museum Novitates 3752: 1–55. https://doi.org/10.1206/3752.2

Palumbi SR, Martin A, Romano S, McMillan WO, Stice L, Grabowski G (1991) "The Simple Fool's Guide to PCR, Version 2.0." Privately published document compiled by S. Palumbi, Dept. Zoology, Univ. Hawaii, 46 pp.

Peracca MG (1895) Viaggio del Dr. Borelli nella Rep. Argentina e nel Paraguay. Rettili e anfibi. Bollettino dei Musei di Zoologia e Anatomia Comparata della R. Universita di Torino 10(195): 1–32.

Preininger D, Handschuh S, Boeckle M, Sztatecsny M, Hödl W (2016) Comparison of female and male vocalisation and larynx morphology in the size dimorphic foot-flagging frog species *Staurois guttatus*. Herpetological Journal 26: 187–197.

Rambaut A, Suchard MA, Xie D, Drummond AJ (2014) Tracer v1.6, http://beast.bio.ed.ac.uk/Tracer

Reichle S (1999) Zur Kenntnis dreier Leptodactyliden aus Bolivien. *Ischnocnema sanctaecnicis* Harvey and Keck, 1995, *Eleutherodactylus fenestratus* (Steindachner, 1864) and *Eleutherodactylus samaipatae* Köhler and Jungfer, 1995. Herpetofauna 21(123): 5–9.

Reyes-Puig JP, Yánez-Munoz MH (2012) Una nueva especie de *Pristimantis* (Anura: Craugastoridae) del corredor ecológico Llangantes-Sangay, Andes de Ecuador. Bosque 52: 81–91.

Rodríguez L, Martinez JL, Azevedo-Ramos C, Reynolds R, Reichle S, Gascon C (2004) *Pristimantis fenestratus*. In: IUCN 2012. IUCN Red List of Threatened Species. Version 2012.2. www.iucnredlist.org [accessed 24 July 2013]

Shepack A, May RV, Ttito A, Catenazzi A (2016) A new species of *Pristimantis* (Amphibia, Anura, Craugastoridae) from the foothills of the Andes in Manu National Park, southeastern Peru. ZooKeys 594: 143–164. https://doi.org/10.3897/zookeys.594.8295

Siqueira S, Aguiar O, Souza MB, Lima AP, Recco-Pimentel SM (2009) Unusual intra-individual karyotypical variation and evidence of cryptic species in Amazonian populations of *Pristimantis* (Anura, Terrarana). Hereditas 146: 141–151. https://doi.org/10.1111/j.1601-5223.2009.02104.x

Steindachner F (1864) Batrachologische Mittheilungen. Verhandlungen des Zoologisch-Botanischen Vereins in Wien, 67 pp.

Tamura K, Dudley J, Nei M, Kumar S (2007) MEGA 6.0: Molecular Evolutionary Genetics Analysis (MEGA) software version 4.0. Molecular Biology and Evolution 24: 1596–1599. https://doi.org/10.1093/molbev/msm092

Terán-Valdez A, Guayasamin JM (2010) The smallest terrestrial vertebrate of Ecuador: A new frog of the genus *Pristimantis* (Amphibia: Strabomantidae) from the Cordillera del Cóndor. Zootaxa 68: 53–68.

Thompson JD, Higgins DG, Gibson TJ (1996) CLUSTAL W: improving the sensitivity of progressive multiple sequence alignment through sequence weighting, position specific gap penalties and weight matrix choice. Nucleic Acids Research 22: 4673–4680. https://doi.org/10.1093/nar/22.22.4673

Tsuji-Nishikido BM, Kaefer IL, Freitas FC, Menin M, Lima AP (2012) Significant but not diagnostic: differentiation through morphology and calls in the Amazonian frogs *Allobates nidicola* and *A. masniger*. Herpetological Journal 22: 105–114.

Vaz-Silva W, Oliveira RM, Gonzaga AFN, Pinto KC, Poli FC, Bilce TM, Penhacek M, Wronski L, Martins JXb, Junqueira TG, Cesca LCC, Guimarães VY, Pinheiro RD (2015) Contributions to the knowledge of amphibians and reptiles from Volta Grande do Xingu, northern Brazil. Brazilian Journal of Biology 75(3): 205–218. https://doi.org/10.1590/1519-6984.00814BM

Vences M, Thomas M, Meijden A van der, Chiari Y, Vieites DR (2005) Comparative performance of the 16S rRNA gene in DNA barcoding of amphibians. Frontiers in Zoology 2: 1–12. https://doi.org/10.1186/1742-9994-2-5

Yu B, Zheng R (2009) The advertisement call of the giant spiny frog *Paa spinosa*. Current Zoology 55(6): 411–415.

Zhou Y-L, Qiu X, Fang X-B, Yang L-Y, Zhao Y, Fang T, Zheng W-H, Liu J-S (2014) Acoustic characteristics of eight common Chinese anurans during the breeding season. Zoological Research 35(1): 42–50.

Appendix 1

Specimens examined. INPA-H (Instituto Nacional de Pesquisas da Amazônia – Herpetology); MPEG (Museu Paraense Emilio Goeldi); LZATM (Laboratório de Zoologia de Altamira); CTGANSISTA_D (Coleção de Tecidos de Genética Animal, Sisbiota Tapajós, margem direita).

Pristimantis fenestratus: INPA-H 34562, INPA-H 34565, INPA-H 34571, INPA-H 34573, INPA-H 34575, INPA-H 34577, INPA-H 34578, INPA-H 34579, INPA-H 34580, MPEG 7088, municipality of Borba, Amazonas, Brazil (type locality).

Pristimantis sp. n.: LZATM467, LZATM743, LZATM 739, LZATM749, LZATM747, LZATM750, LZATM740, LZATM742, LZATM754, LZATM742, LZATM748, LZATM751, MPEG 26050, MPEG 26059, MPEG 26052, MPEG 26063, MPEG 26065, municipality of Anapu, Pará, Brazil (type locality). LZATM 0063, LZATM139, LZATM155, LZATM213, LZATM265, LZATM270, LZATM277, LZATM280, LZATM281, LZATM386, LZATM 1344, LZATM 1112, MPEG 26055, MPEG 26053, MPEG 26054, MPEG 31415, MPEG 31416, MPEG 1113, municipality of Altamira, Pará, Brazil. LZATM137, LZATM138, LZATM197, LZATM 802, LZATM 876, LZATM 1340, municipality of Brazil Novo, Pará, Brazil. LZATM140, LZATM141, LZATM188, LZATM222, LZATM229, LZATM230, LZATM236, LZATM243, LZATM255, LZATM 818, LZATM 814, LZATM 816, LZATM 815, municipality of Medicilândia, Pará, Brazil. LZATM355, LZATM356, LZATM357, LZATM358, LZATM359, LZATM360, municipality of Uruará, Pará, Brazil. LZATM 753, LZATM 1125, LZATM 1140, municipality of Senador José Porfírio, Pará, Brazil. CTGANSISTA_D_1168, CTGANSISTA_D_1246, CTGANSISTA_D_1235, CTGANSISTA_D_1145, CTGANSISTA_D_1253, CTGANSISTA_D_1239, CTGANSISTA_D_1275, CTGANSISTA_D_1259, CTGANSISTA_D_1260, CTGANSISTA_D_1257, CTGANSISTA_D_1256, CTGANSISTA_D_1244, CTGANSISTA_D_1240 Flona Tapajós, Pará, Brazil.

Pristimantis zeuctotylus: LZATM1951, LZATM1054 and LZATM1057, municipality of Monte Alegre, Pará, Brazil.

Pristimantis chiastonotus: LZATM1050, LZATM1052, LZATM1055, and LZATM1056, municipality of Monte Alegre, Pará, Brazil.

Appendix 2

Morphological measurements of all Brazilian specimens of *Pristimantis latro* sp. n. examined in this study.

Locality	Exemplar	Sex	SVL	ThL	FL	HL	HW	IoD	WS	ID	DEN	EL	TL	LT	AL	SL	LL	TaL	HaL
Anapu – Brazil	LZATM 467	F	40	20.5	18.9	15.6	14.5	3.9	3.6	3.1	5.7	4.5	1.8	22.8	10.5	7.9	30.3	11.9	8.9
Anapu –	LZATM 743	F	19.1	10	8.3	7.5	6.5	2.1	2	1.9	2.9	2.5	1	11.6	5.2	3.9	14.3	6.2	4.3
Anapu –	LZATM 739	M	16.9	8.9	7.3	6.9	5.7	2	1.5	1.6	2.4	2.5	0.8	9.7	4.4	3.4	11.8	4.5	3.6
Anapu –	LZATM 749	F	40.2	20.4	19	16.2	15	3.3	3	3.7	5.8	4.7	2.1	22.8	10.1	8	29.4	10.6	8.8
Anapu –	LZATM 747	M	22.8	12.8	11	9.6	8.3	2.4	2.2	2	3.3	3.6	1.2	13.9	5.9	4.7	17.1	7	5.6
Anapu –	LZATM 750	F	21.7	11.5	10	8.7	7.6	2	2.1	1.9	3	3.1	1.1	12.7	5.5	4.7	16.4	6.8	4.7
Anapu –	LZATM 740	F	26.4	14.3	12.5	10.3	9.5	2.8	2.7	2.3	3.7	3.3	1.5	15.2	6.8	5.3	19.9	8.4	5.8
Anapu –	LZATM 744	F	26.4	14.5	11.7	10.7	9.4	2.2	2.4	2.1	3.8	3.2	1.2	15.7	6.9	5.6	20.4	8.4	6.2
Anapu –	LZATM 754	F	18.8	9.7	8.8	7.6	6.1	1.6	2.2	1.7	2.8	2.8	1	10.7	4.4	3.8	13.8	6.2	4.4
Anapu –	LZATM 742	F	26.8	14.5	13.9	10.6	9.8	2.5	2.9	2.4	3.9	3.2	1.4	16.6	7.3	5.3	21.9	8.9	5.9
Anapu –	LZATM 748	F	27.8	13.5	14.6	10.9	9.9	2.6	2.3	2.6	3.8	3.3	1.4	17.2	7.2	5.6	22.9	8.2	6.4
Anapu –	LZATM751	F	24.4	12.3	11.8	9.2	7.9	2.2	2.4	2.2	3.1	3.1	1.1	13.8	6.1	4.5	18	7.2	5.5
Anapu –	MPEG 26050	F	41.6	21.7	19.4	16.1	15.8	3.7	4.4	3.7	5.7	5.8	2.5	24.5	11.3	8.2	29.8	11.4	8.9
Anapu –	MPEG 26059	F	38	17.5	17.5	14.5	13.7	3.7	4.4	3.1	5.3	5.0	2.3	20.3	9.2	7.8	27	10	7.5
Anapu –	MPEG 26052	M	27	12.1	12.8	9.8	9.2	2.6	2.6	2.3	3.6	3.6	1.4	14.5	7	5.1	19.3	7.3	6
Anapu –	MPEG 26063	F	19.5	10.5	9.2	7.8	7	2.1	2.5	2.1	2.8	3.1	1	11.6	4.9	4	15.4	6	4.8
Altamira – Brazil	LZATM63	M	28.3	14.8	14.8	11.6	10.1	2.7	2.9	2.6	4.1	3.9	1.6	16.8	7.6	5.8	22.9	8.4	6.9
Altamira –	LZATM139	F	38.3	20.4	14.8	15	13.6	3.4	3.3	3	5.5	4.4	2	23.1	10	7.6	28.1	12	8.4
Altamira –	LZATM155	F	28.2	14.1	13.4	10.4	8.4	1.9	3.2	2.3	3.9	3.2	1.4	16.1	7.2	5.4	21.3	8.9	6.5
Altamira –	LZATM213	F	36.2	18.5	17	13.6	13.6	2.7	3.5	2.9	4.8	4	1.9	21.1	8.8	6.3	27.4	10.7	8.3
Altamira –	LZATM 265	F	26.2	13.9	13.9	10.5	9.4	2.7	2.2	2.2	3.9	3.8	1.4	16	7.2	5	21.4	7.8	6
Altamira –	LZATM270	F	32.4	18	18.4	13	11.8	3	3.1	2.8	4.8	4	2	21.2	9.7	6.2	28.5	10	8.5
Altamira –	LZATM277	F	29.7	15.4	13.9	11.7	10.6	2.7	2.9	2.5	4.3	3.5	1.7	16.3	6.8	6.1	21.8	8.5	6.4
Altamira –	LZATM279	F	28.9	15.5	13.2	14.9	10.2	2.3	3.6	2.6	3.9	3.4	1.6	15.7	7.1	5.2	29.6	8	6.4
Altamira – Brazil	LZATM280	F	24.8	13.2	12.5	10.4	10	2.3	2.8	2.3	3.5	3.4	1.2	15.1	6.8	5	19.7	8	5.8
Altamira –	LZATM281	F	26.2	14.3	12.8	10.3	9.4	2.8	2.6	2.3	3.6	3.3	1.3	15.7	6.6	5	20.4	8	6

Locality	Exemplar	Sex	SVL	ThL	FL	HL	HW	IoD	WS	ID	DEN	EL	TL	LT	AL	SL	LL	TaL	HaL
Altamira –	LZATM386	F	36.2	19.1	19.2	14.4	13.4	3.7	3.5	3.1	5.5	4.4	1.8	21.7	10.6	7.4	28.9	10.5	8.5
Altamira –	LZATM622	M	15.6	8	6.3	6	5.4	1.7	1.6	1.6	2	2.1	0.8	8.8	4	2.9	10.6	4.5	3.5
Altamira –	MPEG 31415	M	23.2	10.8	10.9	8.8	8.2	2.4	2.6	2.2	3	3	1.2	12.5	5.7	4.5	16.3	6.2	4.8
Altamira –	MPEG 31416	M	26.2	12.2	12.8	10.1	9.8	2.7	3.1	2.3	3.4	4	1.6	14.8	6.7	5.1	19.5	7.5	5.5
Brazil Novo – Brazil	LZATM802	F	36.2	18.8	19.3	13.1	11.9	3.6	3.2	2.9	4.8	4.4	1.7	21.6	10.2	7.5	29.8	11	8.4
Brazil Novo –	LZATM137	F	35.5	18.5	16.4	14	13.8	2.9	2.7	2.7	5.1	4	1.4	19.9	8.9	7	25.7	9.5	7.7
Brazil Novo –	LZATM138	F	38.2	20.3	18	15.3	14.4	3.3	3.3	3.3	5.4	4.6	2.2	21.8	9.6	7.7	28.7	10.9	8.8
Brazil Novo –	LZATM197	M	25	12.9	12.4	10	9.4	2.7	2.1	2.3	3.7	3.4	1.4	15.7	6.8	5.2	19.9	8.1	6.3
Medicilândia – Brazil	LZATM140	F	30.1	14.9	16.4	11.9	10.7	2.5	2.9	2.7	4.3	3.5	1.4	18.8	8.5	6.2	24.8	8.9	7
Medicilândia –	LZATM141	F	35.9	18.1	18.8	13.3	12.5	3.4	3.1	2.9	5	4.4	1.5	22.7	10.3	7.3	29.7	11.2	8.3
Medicilândia –	LZATM188	F	37.3	18.8	19.2	14	13	3	3.2	2.7	5.1	4.5	1.9	22.4	9.1	6.6	30	11.4	8.7
Medicilândia –	LZATM222	F	35.8	13.9	14	9.8	9.4	2.3	2.2	2.1	3.4	3.1	1.4	16	7	5	21.2	7.9	5.9
Medicilândia –	LZATM229	F	22.2	11.4	11.2	8.8	8.9	2	2	2	3.1	2.8	1.2	14	5.9	4.4	18.4	7.5	5
Medicilândia –	LZATM230	M	25.6	13.8	13	10.1	9.2	2.4	2.2	2.2	3.4	3.4	1.4	15.3	6.7	4.7	21.1	7.8	5.9
Medicilândia –	LZATM236	M	25	13.5	13	10.2	9.1	2.8	2.3	2.1	3.7	3.3	1.5	15.8	7	4.9	20.5	7.4	6.2
Medicilândia –	LZATM243	M	36	18.9	18.5	14.1	13.2	3.4	3.1	3.2	5.3	4	1.9	21.4	10.4	7.3	28.3	10.6	8.8
Medicilândia –	LZATM248	M	17.2	9	7.6	6.4	5.6	1.6	1.4	1.6	2	2.1	0.9	9.7	3.9	3	11.9	4.7	3.5
Medicilândia –	LZATM255	F	35	18.6	18.4	13.3	12.8	3.7	2.9	2.7	5	3.9	1.7	21.4	9.3	6.8	28.3	10.4	8.3
Uruará – Brazil	LZATM355	F	41	21.4	19.8	16.1	16.2	3.6	4	3	5.6	5	2.4	22.9	12	7.1	30.7	11.3	11.4
Uruará –	LZATM356	M	25.8	13.3	12.6	9.9	9.6	2.4	2.1	2	3.5	3.8	1.2	16.1	7.1	4.9	21	7.9	6.3
Uruará –	LZATM357	F	25.9	13.2	12.8	10.8	9.8	2.3	2.2	2.4	3.5	3.5	1.3	15.2	7	5.1	20.3	7.5	6.3
Uruará –	LZATM358	F	34	17.9	16.2	12.5	12.2	3	3.5	2.8	4.8	4	1.7	20	9	6.1	25.9	9.8	8.2
Uruará –	LZATM359	F	29.8	16.4	16	12.5	11.5	2.4	2.5	2.4	4.1	4	2.3	17.9	8.8	5.5	23.7	8.8	7.7
Uruará –	LZATM360	F	36.9	18.4	19.5	15	13.9	3.3	3.8	2.9	5.5	4.2	1.7	21.9	9.9	7	30.4	11	8.8
Senador José Porfírio	LZATM 753	F	23.2	11.5	10.7	8.9	7.8	2.1	2	2.1	3.2	2.9	1.2	14.2	5.6	4.6	17.5	7.1	5
Flona Tapajós – Brazil	CTGANSISTA_D_1168	F	41.5	21.7	20.1	14.1	14.7	3.4	3.3	3.3	5.0	4.2	2.0	23.4	10.2	7.5	31.0	10.7	9.3
Flona Tapajós – Brazil	CTGANSISTA_D_1246	F	38.9	21.0	20.7	14.6	13.9	3.0	4.1	3.4	5.3	4.8	2.1	23.9	10.7	7.9	31.6	10.4	9.3
Flona Tapajós –	CTGANSISTA_D_1235	M	39.5	19.3	20.0	14.6	13.6	4.0	4.0	3.6	5.5	5.0	2.3	22.9	10.4	7.4	30.1	11.7	8.2
Flona Tapajós –	CTGANSISTA_D_1145	F	36.6	20.9	19.3	13.8	13.8	2.7	3.7	3.3	5.2	4.3	2.0	22.3	10.5	7.3	29.5	10.8	9.4

Locality	Exemplar	Sex	SVL	ThL	FL	HL	HW	IoD	WS	ID	DEN	EL	TL	LT	AL	SL	LL	TaL	HaL
Flona Tapajós –	CTGANSISTA_D_1253	F	36.9	20.0	19.3	14.4	13.4	3.1	3.7	3.2	5.6	4.6	2.6	22.0	10.3	7.6	29.2	10.3	8.6
Flona Tapajós –	CTGANSISTA_D_1239	F	39.4	20.7	18.8	14.2	13.8	3.8	4.6	3.2	5.0	4.7	2.1	23.2	10.2	7.6	29.0	11.9	8.2
Flona Tapajós –	CTGANSISTA_D_1275	F	35.5	19.3	18.6	13.6	12.7	3.6	3.6	2.9	4.9	4.5	2.1	21.9	10.1	6.8	28.9	11.4	7.8
Flona Tapajós –	CTGANSISTA_D_1259	M	27.9	14.2	14.2	10.1	9.5	2.6	2.6	2.1	4.0	3.4	1.5	15.9	7.5	5.0	21.0	7.4	6.6
Flona Tapajós –	CTGANSISTA_D_1260	F	28.7	15.0	15.0	10.7	9.7	2.6	2.6	2.3	3.9	4.2	1.7	16.8	7.9	5.7	22.2	8.1	6.3
Flona Tapajós –	CTGANSISTA_D_1257	F	26.4	13.7	13.1	9.4	9.3	2.3	2.5	2.3	3.3	3.7	1.6	15.3	7.4	4.9	20.0	7.6	6.1
Flona Tapajós –	CTGANSISTA_D_1256	M	27.6	15.3	14.6	10.7	10.6	2.6	2.7	2.4	4.1	3.8	1.7	16.9	8.0	5.6	22.0	8.2	6.3
Flona Tapajós –	CTGANSISTA_D_1244	F	31.3	15.5	15.9	12.3	11.3	2.6	3.5	2.7	4.4	4.2	1.9	19.1	8.2	6.0	25.2	9.6	8.1
Flona Tapajós –	CTGANSISTA_D_1240	M	27.7	14.2	14.5	10.7	9.4	2.8	2.5	2.3	3.7	3.5	1.6	16.0	7.6	5.5	22.2	8.0	5.8
Borba – Brazil	INPA-H 34571	M	32.8	16.4	17	12.8	12.3	2.3	3.9	2.5	4.3	4.3	1.8	17.8	9.3	6.5	24.6	8.5	7.7
Borba –	INPA-H 34577	M	30.8	15.3	14.5	11.3	10.7	2.4	3.6	2.9	3.8	4.5	1.5	16.8	7.6	5.6	22.1	8.6	6.4
Borba –	INPA-H 34562	F	32.4	15.7	15.4	11.9	11.1	2.6	4.1	2.7	3.9	4.4	1.8	16.2	7.8	6.5	21.6	7.2	6.7
Borba –	INPA-H 34573	M	34.3	19.1	17.8	12.6	11.6	2.6	4	2.9	4.5	3.9	1.6	19	10.2	6.5	26.2	9	7.7
Borba –	INPA-H 34578	M	28.6	15.4	15.9	10.4	10	2.3	3.5	2.5	3.8	3.4	1.3	17	9.1	5.6	23.8	8.8	6.1
Borba –	INPA-H 34575	M	31.6	15.9	16.3	11.1	10.5	2.3	3.3	2.6	4.2	4	1.4	17.5	8.7	5.7	23.3	8.2	6.8
Borba –	MPEG 7088	F	36	18.7	17.6	14	13.4	3.9	3.5	3.1	5.2	4.2	2.2	20.2	10	7.3	28.3	11.1	9.2
Borba –	INPA-H 34580	M	31.1	14.4	14	11.6	10.2	2.6	3.8	2.8	4.2	4.3	1.6	16	7.4	6	21.1	8	5.7
Borba –	INPA-H 34579	M	30.7	15.3	14.6	11.7	10.8	2.6	3.9	2.9	4	3.8	1.7	16	7.8	5.8	21.9	8.8	6.5
Borba –	INPA-H 34565	M	31.4	15.1	14.1	11.9	10.3	2.8	3.6	3	4.4	4.4	1.7	16.7	8	6.1	21.6	8.5	6.2

ZooKeys 687: 131–148 (2017)
doi: 10.3897/zookeys.687.12742
http://zookeys.pensoft.net

RESEARCH ARTICLE

A peer-reviewed open-access journal
ZooKeys
Launched to accelerate biodiversity research

Taxonomic reassessment of two subspecies of Chinese skink in Taiwan based on morphological and molecular investigations (Squamata, Scincidae)

Kazuki Kurita[1], Yukiko Nakamura[1,2], Taku Okamoto[1], Si-Min Lin[3], Tsutomu Hikida[1]

1 *Department of Zoology, Graduate School of Science, Kyoto University, Kitashirakawa-oiwakecho, Sakyo-ku, Kyoto 606-8502, Japan* **2** *Department of Animal Development and Physiology, Graduate School of Biostudies, Kyoto University, Yoshida-Konoecho, Sakyo-ku, Kyoto 606-8501, Japan* **3** *Department of Life Science, National Taiwan Normal University, No. 88, Sec. 4, Tingzhou Road, Taipei 111, Taiwan*

Corresponding author: *Kazuki Kurita* (kurita@zoo.zool.kyoto-u.ac.jp); *Si-Min Lin* (lizard.dna@gmail.com)

Academic editor: *A. Herrel* | Received 16 March 2017 | Accepted 19 June 2017 | Published 2 August 2017

http://zoobank.org/9A9671D5-AD29-4EA3-9D85-AD2443487F00

Citation: Kurita K, Nakamura Y, Okamoto T, Lin S-M, Hikida T (2017) Taxonomic reassessment of two subspecies of Chinese skink in Taiwan based on morphological and molecular investigations (Squamata, Scincidae) ZooKeys 687: 131–148. https://doi.org/10.3897/zookeys.687.12742

Abstract

The Chinese skink, *Plestiodon chinensis* (Gray, 1838), is widely distributed across continental China, Taiwan, the Korean Peninsula, and offshore islets, and consists of several subspecies. Here morphological and molecular methods have been used to reassess the taxonomic status and distributions of *P. c. formosensis* (Van Denburgh, 1912) and *P. c. leucostictus* (Hikida, 1988), which are endemic to Taiwan and Green Island (an islet off the east coast of Taiwan), respectively. It can be confirmed that the eastern Taiwanese populations of *P. c. formosensis* exhibit similar juvenile color patterning and genetic composition to the islet subspecies *P. c. leucostictus*, and are distinct from consubspecific populations in western Taiwan. Therefore, the eastern Taiwanese populations are assigned to *P. c. leucostictus*, and this subspecies is recognized as a distinct species, *Plestiodon leucostictus* (Hikida, 1988), based on their unique juvenile coloration and highly divergent DNA sequences. Our results also revealed that *P. c. formosensis* in western Taiwan is close to nominotypical subspecies from the continent, suggesting the necessity of a comprehensive taxonomic analysis in the future.

Keywords

Green Island, *Plestiodon chinensis*, *Plestiodon leucostictus*, subspecies, Taiwan, taxonomy

Introduction

The scincid lizard genus *Plestiodon* Duméril & Bibron, 1839, comprises some 45 species, is distributed across East Asia and North America (Brandley et al. 2012, Feria-Ortiz and García-Vázquez 2012, Okamoto and Hikida 2012, Kurita and Hikida 2014a, b). Among these, *P. chinensis* (Gray, 1838) is a large-sized skink widely distributed in Asia including continental China, Taiwan, the Korean Peninsula, and islands offshore from these areas (Hikida 1993). Several available names have been given to the different geographic entities of *P. chinensis*, but their taxonomic status remain uncertain due to a paucity of studies on geographic variation in the complex. At least three subspecies have been commonly recognized by recent researchers: *P. c. chinensis* (Gray, 1838), *P. c. formosensis* (Van Denburgh, 1912), and *P. c. leucostictus* (Hikida, 1988) (Hikida 1993, Zhao and Adler 1993, Zhao et al. 1999), but the recognition of two additional subspecies, *P. c. pulcher* (Duméril & Bibron, 1839) and *P. c. daishanensis* (Mao, 1983), varies among different authors.

Two subspecies, *P. c. formosensis* and *P. c. leucostictus*, are known from Taiwan and its adjacent islets. Van Denburgh (1912a,b) first described the former subspecies as *Eumeces chinensis formosensis* from "San Shi Ka, Formosa" (see Discussion for current name and location), on the basis of differences in head scutellation and body coloration from the nominotypical subspecies. In a revision of *Eumeces sensu lato* (encompassing *Plestiodon* of the current classification), Taylor (1936) considered this subspecies a junior synonym of *P. c. chinensis*. However, subsequent researchers (e.g. Hikida 1993, Zhao and Adler 1993, Zhao et al. 1999) recognized its validity. It has been known to occur in lowland areas (less than 500 m) of Taiwan, with a large disjunction across the central mountain ranges which separates the island into the eastern and western geographic zones (Shang et al. 2009). The second subspecies was described by Hikida (1988) as *Eumeces chinensis leucostictus* from Green Island (also known as Ludao, Lyudao, or Lutao), located off the southeast of Taiwan. It is clearly distinct from the other subspecies of *P. chinensis* in having a white-spotted dorsal pattern in juveniles, in addition to some scutellation differences such as a higher number of scale rows around midbody, and the usual presence of postnasal (Hikida 1988). Currently it is known to occur only on this tiny islet (15.1 km^2), and is regarded as one of the most threatened taxon in *Plestiodon* because of the extremely restricted distribution.

However, *P. c. leucostictus*-like forms have been reported outside of Green Island. Pictures in a field report from Yu (1994) and a field guide by Shang et al. (2009), both taken in Hualien County of eastern Taiwan, indicated that *Plestiodon* individuals in this region have a white-spotted pattern on the dorsum. The geographic proximity of this area to Green Island, in conjunction with the similarity in juvenile color patterning, implies that eastern Taiwanese populations currently assigned to *P. c. formosensis* might be geographic variants of *P. c. leucostictus*. However, this debate remains because of the scarcity of specimens from eastern Taiwan. Here we reassess the taxonomic status and distributions of *P. c. formosensis* and *P. c. leucostictus* by comparing the morphological features and DNA sequences of *P. chinensis* from representative localities in Taiwan and Green Island.

Materials and methods

Study site and material examined

Specimens of *P. chinensis* from each of three regions (western Taiwan, eastern Taiwan, and Green Island) were assigned to a single operational taxonomic unit (OTU), and their taxonomic relationship was examined using morphological and molecular data. For the morphological examination, 69 specimens from Taiwan were used, including the type series of *P. c. formosensis*; and 54 specimens of *P. c. leucostictus*, including 27 newly investigated specimens and published data on the type series (Hikida 1988) (Suppl. material 1: Appendix I). In the molecular genetic analysis, representatives of each OTU were used, including specimens from the putative type locality of *P. c. formosensis* (Table 1; Fig. 1).

Morphological examination

Three morphological features reported to distinguish *P. c. leucostictus* from other subspecies of *P. chinensis* (Hikida 1988) were characterized. These features included juvenile color pattern on dorsal and lateral regions of body (JCP), the number of scale rows around midbody (MSR), and presence or absence of postnasal scale (PN). To investigate body coloration, preserved specimens were examined. Other scutellation characters were counted and observed using a stereomicroscope where necessary.

Molecular genetic analysis

DNA sequences of three independently evolving regions were determined for representative specimens of *P. chinensis* from Taiwan and Green Island. Two fragments of mitochondrial DNA (mtDNA) loci were sequenced for all materials. The first mtDNA fragment (termed mtDNA-1) included the 3' end of the transfer RNA^{Glu} gene ($tRNA^{Glu}$) and a portion of cytochrome *b* gene (cyt *b*). The second mtDNA fragment (termed mtDNA-2) included a portion of the 3' end of the 16S ribosomal RNA gene, $tRNA^{Leu}$, the first unit of the NADH dehydrogenase gene (ND1), $tRNA^{Ile}$, $tRNA^{Gln}$, and a portion of the 5' end of $tRNA^{Met}$. Two nuclear loci, the recombination activating gene-1 (RAG-1) and prolactin receptor (PRLR), were also sequenced for some specimens. These genes were chosen based on several relevant taxonomic and phylogenetic studies of *Plestiodon* (e.g. Brandley et al. 2012; Kurita and Toda 2017).

Total genomic DNA was extracted from liver or tail tissues stored at –80 °C or in 99% ethanol. Extractions were performed with the DNeasy Blood & Tissue kit (QIAGEN, Hilden, Germany) or by using a slightly modified version of Okamoto et al.'s (2006) method. Polymerase chain reactions (PCR) were conducted using the TaKaRa Ex Taq kit (Takara Bio, Otsu, Japan) with a GeneAmp PCR Systems 2700

Table 1. Information for samples of *Plestiodon chinensis* and its relatives examined in DNA analyses. Museum abbreviations follow Sabaj Perez (2014), with the exception of MCB (Matthew C. Brandley, private collection). Accession numbers with an asterisk show newly obtained sequences in this study.

Taxon	Locality	Voucher	GenBank accession number				Source
			Cyt *b*	ND1	RAG–1	PRLR	
P. c. formosensis	Jinshan, New Taipei City, Taiwan	KUZ R71772	LC147548	LC147646	-	-	Kurita and Toda (2017)
P. c. formosensis	Jinshan, New Taipei City, Taiwan	KUZ R71780	LC200983*	LC201001*	LC201019*	LC201031*	This study
P. c. formosensis	Jinshan, New Taipei City, Taiwan	KUZ R71794	LC200984*	LC201002*	LC201020*	LC201032*	This study
P. c. formosensis	Jinshan, New Taipei City, Taiwan	KUZ R71943	LC200985*	LC201003*	-	-	This study
P. c. formosensis	Bali, New Taipei City, Taiwan	KUZ R69425	LC200986*	LC201004*	LC201021*	LC201033*	This study
P. c. formosensis	Xiangshan, Hsinchu County, Taiwan	KUZ R69417	LC200987*	LC201005*	LC201022*	LC201034*	This study
P. c. formosensis	Xiangshan, Hsinchu County, Taiwan	KUZ R69418	LC200988*	LC201006*	-	-	This study
P. c. formosensis	Xiangshan, Hsinchu County, Taiwan	KUZ R69419	LC200989*	LC201007*	-	-	This study
P. c. formosensis	Qiding, Miaoli County, Taiwan†	MCB 675	-	HM160800	HM161178	HM160896	Brandley et al. (2012)
P. c. "*formosensis*"	Hualien City, Hualien County, Taiwan	KUZ R60584	LC200990*	LC201008*	-	-	This study
P. c. "*formosensis*"	Hualien City, Hualien County, Taiwan	KUZ R69420	LC200991*	LC201009*	LC201023*	LC201035*	This study
P. c. "*formosensis*"	Hualien City, Hualien County, Taiwan	KUZ R69421	LC200992*	LC201010*	LC201024*	LC201036*	This study
P. c. "*formosensis*"	Hualien City, Hualien County, Taiwan	KUZ R69422	LC200993*	LC201011*	-	-	This study
P. c. "*formosensis*"	Guangfu, Hualien County, Taiwan	KUZ R69423	LC200994*	LC201012*	LC201025*	LC201037*	This study
P. c. "*formosensis*"	Guangfu, Hualien County, Taiwan	KUZ R69424	LC200995*	LC201013*	LC201026*	LC201038*	This study
P. c. "*formosensis*"	Sansiantai, Taitung County, Taiwan	KUZ R71777	LC147549	LC147647	LC201027*	LC201039*	Kurita and Toda (2017) /This study
P. c. "*formosensis*"	Sansiantai, Taitung County, Taiwan	KUZ R71797	LC200996*	LC201014*	-	-	This study
P. c. "*formosensis*"	Sansiantai, Taitung County, Taiwan	KUZ R71819	LC200997*	LC201015*	-	-	This study
P. c. "*formosensis*"	Sansiantai, Taitung County, Taiwan	KUZ R71822	LC200998*	LC201016*	LC201028*	LC201040*	This study
P. c. leucostictus	Green Island, Taitung County, Taiwan	KUZ R60571	LC200999*	LC201017*	LC201029*	LC201041*	This study
P. c. leucostictus	Green Island, Taitung County, Taiwan	KUZ R60581	LC201000*	LC201018*	LC201030*	LC201042*	This study

Taxon	Locality	Voucher	GenBank accession number				Source
			Cyt *b*	ND1	RAG–1	PRLR	
P. c. chinensis	Lishui, Zhejiang Province, China	-	KT279358	KT279358	-	-	Zhang et al. (2016)
P. c. chinensis	Nan Ao Island, Guangdong Province, China	MCZ Z39481	-	HM160801	HM161179	HM160897	Brandley et al. (2012)
P. kishinouyei	Miyako Island, Okinawa Prefecture, Japan	Miy120318	LC147467	LC147565	-	-	Kurita and Toda (2017)
P. kishinouyei	Ishigaki Island, Okinawa Prefecture, Japan	MCB 658	-	-	HM161200	HM160918	Brandley et al. (2012)
P. tamdaoensis	Unknown locality (pet-traded)	KUZ R66879	LC147554	LC147652	-	-	Kurita and Toda (2017)
P. quadrilineatus	Cheung Chau Island, Hong Kong, China	KUZ R36541	LC147555	LC147653	-	-	Kurita and Toda (2017)

[†]The locality has been listed as "Hsingchu Province: road near Ji-Ding train station: 24.72158, 120.87086" in Brandley et al. (2012), but the GPS coordinate in that paper did not correspond with this locality.

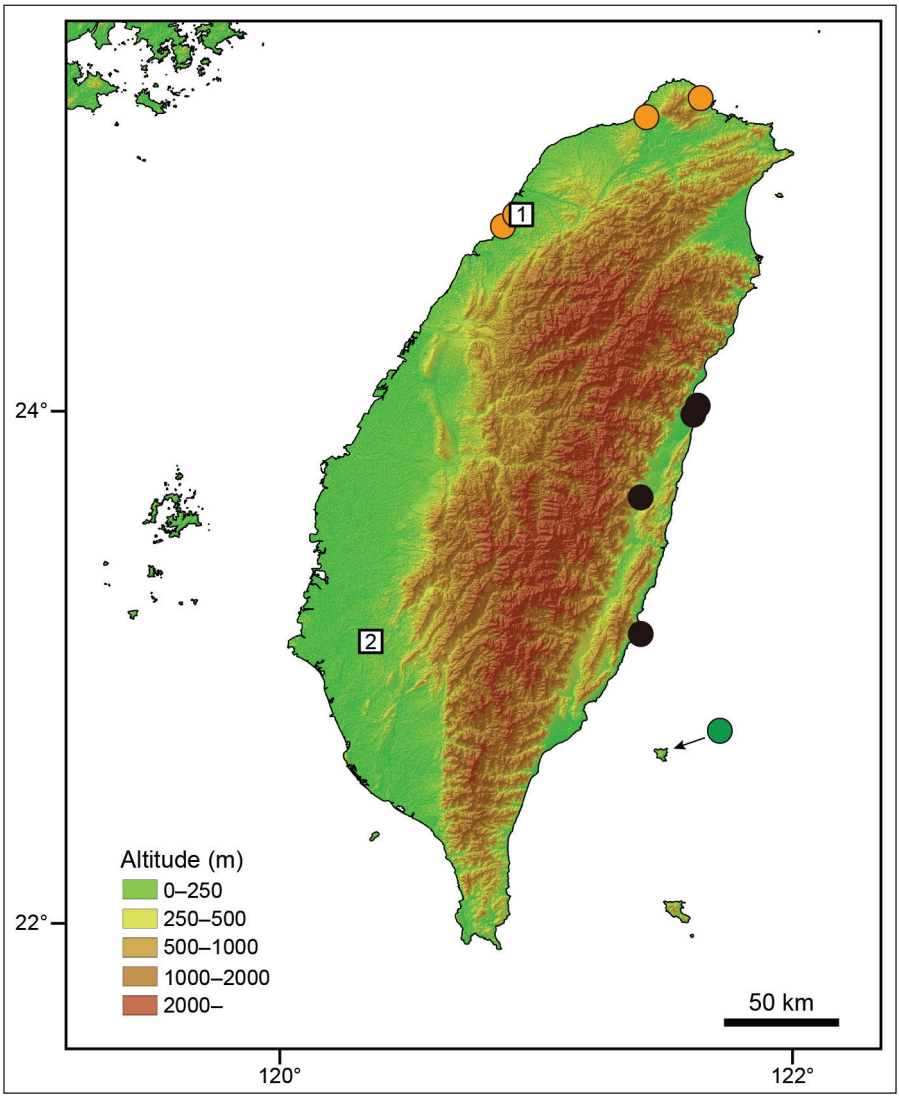

Figure 1. Locality map of *Plestiodon chinensis* samples used for molecular DNA genetic analysis. Orange circles: *P. c. formosensis* from western Taiwan. Black circles: *P. c.* "*formosensis*" from eastern Taiwan. Green circle: *P. c. leucostictus* from Green Island. These colors correspond to those of Figures 3 and 4. Open squares indicate the putative type locality for *P. c. formosensis* (**1** Xiangshan in Hsinchu County [Shang et al. 2009] **2** Shanshang in Tainan County [Zhao and Adler 1993]).

machine (Applied Biosystems, Foster City, CA, USA). The PCR cycle condition for the mtDNA-1 was as follows: initial denaturation at 95°C for 5 min, followed by 30 cycles of 94°C for 1 min, 45 or 50°C for 1 min, and 70°C for 2 min, with a final extension at 72°C for 7 min. The PCR cycle condition for the mtDNA-2 was as follows: initial denaturation at 94°C for 2 min, followed by 30 cycles of 94°C for 30 s, 55°C for 30 s,

and 72°C for 1 min 30 s, with a final extension at 72°C for 5 min. Amplification protocols for nuclear RAG-1 and PRLR were the same as those used by Kurita and Hikida (2014b) and Townsend et al. (2008), respectively. The amplified DNA fragments were purified by polyethylene glycol (PEG) precipitation using 0.6 volume of PEG solution (20% PEG 6000, 2.5 M NaCl). Sequencing reactions were performed using the BigDye Terminator v3.1 Cycle Sequencing Kit (Applied Biosystems). The products were cleaned by ethanol precipitation and sequenced on an Applied Biosystems 3130*xl* Genetic Analyzer (Applied Biosystems). The primers used for PCR and for sequencing are listed in Suppl. material 1: Appendix II. We used FinchTV 1.4.0 (Geospiza, http://www.geospiza.com/ Products/finchtv.shtml) and MEGA5.2.1 (Tamura et al. 2011) to view and align the sequences. Newly obtained sequence data were deposited in GenBank (accession nos. LC200983–LC201042; Table 1).

Sequences from previous studies of *P. chinensis* and its relatives were included in the analyses, including two other members of the *P. chinensis* species group (*P. kishinouyei* [Stejneger] and *P. tamdaoensis* [Bourret]), with a more distantly related species *P. quadrilineatus* Blyth used as outgroup for phylogenetic inferences (Brandley et al. 2012, Zhang et al. 2016, Kurita and Toda 2017) (Table 1). The nuclear DNA sequence dataset included *P. kishinouyei*, which was regarded as the most closely related clade of the ingroup taxa (see Results).

Mitochondrial DNA genealogy was inferred using maximum likelihood (ML) and Bayesian inference (BI) methods with TREEFINDER (March 2011 version; Jobb 2011) and MrBayes 3.2.2 (Ronquist et al. 2012), respectively. Each gene was aligned separately using MUSCLE (Edgar 2004) implemented in MEGA5 with default parameters. We then manually adjusted for rRNA and tRNA gene sequences based on their secondary structures, utilizing information from Gutell and Fox (1988) and Kumazawa and Nishida (1993), respectively. Neither stop codons nor insertions/deletions (indels) were found in the cyt *b* and ND1 gene sequences. Regions with gaps or ambiguous alignment were excluded from rRNA and tRNA sequence alignments. Dataset (total sequence of 2,351 bp) was partitioned according to genes (four tRNA regions were combined into a single partition) and codon positions (for cyt *b* and ND1). The appropriate substitution models for these datasets were selected with KAKUSAN4 (Tanabe 2011) under the corrected Akaike Information Criterion (AICc; Sugiura 1978) (Suppl. material 1: Appendix III). Statistic support for the inferred ML tree topology was assessed by using nonparametric bootstrap analysis (Felsenstein 1985) with 1,000 pseudoreplicates. In the BI analysis, we performed two independent runs of four Markov chains for 4×10^6 generations per run, sampling a tree every 100 generations. After checking the adequacy (the effective sample size ≥200) of the parameter estimates and convergence using Tracer 1.5 (Rambaut and Drummond 2007), we discarded the first 20,001 trees as burin-in and calculated a consensus topology and Bayesian posterior probabilities for the remaining 40,000 trees. Statistic supports with bootstrap values of ≥70%, or Bayesian posterior probabilities of ≥95%, were regarded as sufficiently resolved for ML analysis (Hillis and Bull 1993) and BI analysis (Leaché and Reeder 2002, Huelsenbeck and Rannala 2004), respectively.

Prior to the nuclear DNA analysis, gametic phases for the individuals that were heterozygous at more than one nucleotide position were inferred using PHASE 2.1.1 (Stephens et al. 2001, Stephens and Scheet 2005). We used SeqPHASE (Flot 2010) to interconvert PHASE input/output files and performed the PHASE analysis using default settings, with the exception of setting the probability threshold to 0.7 (Harrigan et al. 2008). Five independent runs were performed with different seeds to check the consistency of the haplotype frequency estimates and pseudo-likelihood scores across runs. The absence of indels or stop codons for inferred sequences was checked by translating them with the universal nuclear genetic code using MEGA5 (Tamura et al. 2011).

We inferred gene genealogy among the detected alleles of the two nuclear loci using median-joining analyses with NETWORK 5.0.0.0 (http://www.fluxus-engineering.com; Bandelt et al. 1999). In addition, we used the nuclear DNA dataset to perform an analysis of molecular variance (AMOVA; Excoffier et al. 1992) using Arlequin 3.5.1.2 (Excoffier and Lischer 2010) with 10,000 permutations to compare the current (western and eastern Taiwan vs. Green Island) and revised (western Taiwan vs. eastern Taiwan + Green Island; see Results) classifications.

Results

Morphological analyses

An examination of color variation demonstrated that specimens from the different focal areas had different color patterns. Almost all juvenile specimens (SVL = 47.9–60.4 mm; n = 9) from eastern Taiwan (Taitung County) showed a pattern of small white spots without light lines on the dorsum (Fig. 2). This is very similar to the color pattern of *P. c. leucostictus* described by Hikida (1988). Among these specimens, the white spotted pattern in larger juveniles was faded on the dorsal regions. One exceptional specimen (SVL = 57.6 mm) possessed white spots together with an obscure middorsal light line on the dorsum. In contrast, juveniles (SVL = 40.1–69.9 mm; n = 7) from northwestern Taiwan (New Taipei City and Miaoli County) clearly had three light lines on the dorsum and white spots on the flank (Fig. 2). This pattern was retained in the type specimens of *P. c. formosensis*, although they are adults.

Eastern Taiwanese specimens usually had 24 scale rows at midbody (range = 24–26, mean ± SD = 24.3 ± 0.7, n = 25) (Table 2). The range and mode of MSR were similar to those of western Taiwanese specimens (23–26, 24.3 ± 0.8, n = 38), while the mode was lower than that of Green Island specimens (24–27, 25.8 ± 0.7, n = 54).

Most of the eastern Taiwanese specimens examined possessed a postnasal on both sides (92%; Table 2). The frequency of the presence on both sides was higher than that of Green Island specimens (59%) and that of the western Taiwanese specimens (28%). The western Taiwanese specimens usually lack a postnasal on both sides (60%).

Figure 2. Color pattern alteration of *Plestiodon chinensis formosensis* (left, from western Taiwan) and *P. c. leucostictus* (right, from Green Island). Hatchlings (**A** vs. **E**), juveniles (**B** and **C** v.s. **F** and **G**), and adults (**D** v.s. **H**). Photographed by H.-Y. Tseng **A, C, G, H**; R.-J. Wang **B, F**; S.-M. Lin **D**; and C.-W. You **E**.

Table 2. Variation in scutellation characteristics (MSR, the number of scale rows around midbody; PN, the presence of a postnasal: A = absent or P = present) of *Plestiodon chinensis* in Taiwan and Green Island.

Locality	MSR						PN (left-right)				
	N	23	24	25	26	27	N	A-A	A-P	P-A	P-P
P. c. formosensis, western Taiwan											
Keelung County	3		2[P]		1		3	3[P]			
New Taipei City	17	1	15		1		17	9		4	4
Taipei City	6		4		2		6	6			
Hsinchu County	5		4[P]		1[H]		6	3[P]		1	2[HP]
Miaoli County	10		8		2		11	5			6
Total	41	1	33		7		43	26		5	12
P. c. formosensis, eastern Taiwan											
Hualien County	4		3		1		5		1		4
Taitung County	21		18	1	2		21			1	20
Total	25		21	1	3		26		1	1	24
P. c. leucostictus											
Green Island[†]	54		6	2	45	1	54	16	1	5	32

[H]Including holotype of *P. c. formosensis*; [P]Including paratype of *P. c. formosensis*

[†]Data including the type series from Hikida (1988)

Molecular phylogenetic analyses

The ML and BI trees were almost identical in topology. Therefore, we present only the ML tree in Fig. 3. The phylogeny did not support reciprocal monophyly between *P. c. formosensis* and *P. c. leucostictus*, but did demonstrate that *P. chinensis* from Taiwan is divided into two distinct clades (Clades A and B), although their sister relationship is not well supported in ML methods (69%/0.95 = ML bootstrap value/Bayesian posterior probability). Clade A contained *P. c. formosensis* from western Taiwan (noted as orange in Fig. 3), including the putative type locality (i.e. Xiangshan, Hsinchu County), together with *P. c. chinensis* from the southeastern region of continental China (red). Clade B contained *P. c. formosensis* from eastern Taiwan (black) and *P. c. leucostictus* from Green Island (green, topotypes). The mean uncorrected *p*-distance between Clades A and B was 5.1%/4.0% (= cyt *b*/ND1), which was comparable to the distances between these clades and their closest relative, *P. kishinouyei* (*i.e.* Clade A vs. *P. kishinouyei* = 5.7%/4.2%; Clade B vs. *P. kishinouyei* = 5.9%/4.6%).

In nuclear DNA sequences, one individual from Jinshan (KUZ R71794) in the RAG–1 dataset was not phased with significant support (phase probability = 0.66), and was omitted. The remaining heterozygous sequences were inferred with phase probabilities ≥0.98. In the RAG–1 dataset, nine inferred alleles were obtained from *P. chinensis* (Fig. 4a). Of these, four alleles were obtained from eastern Taiwanese specimens. One of these four alleles was shared by specimens from western Taiwan, and

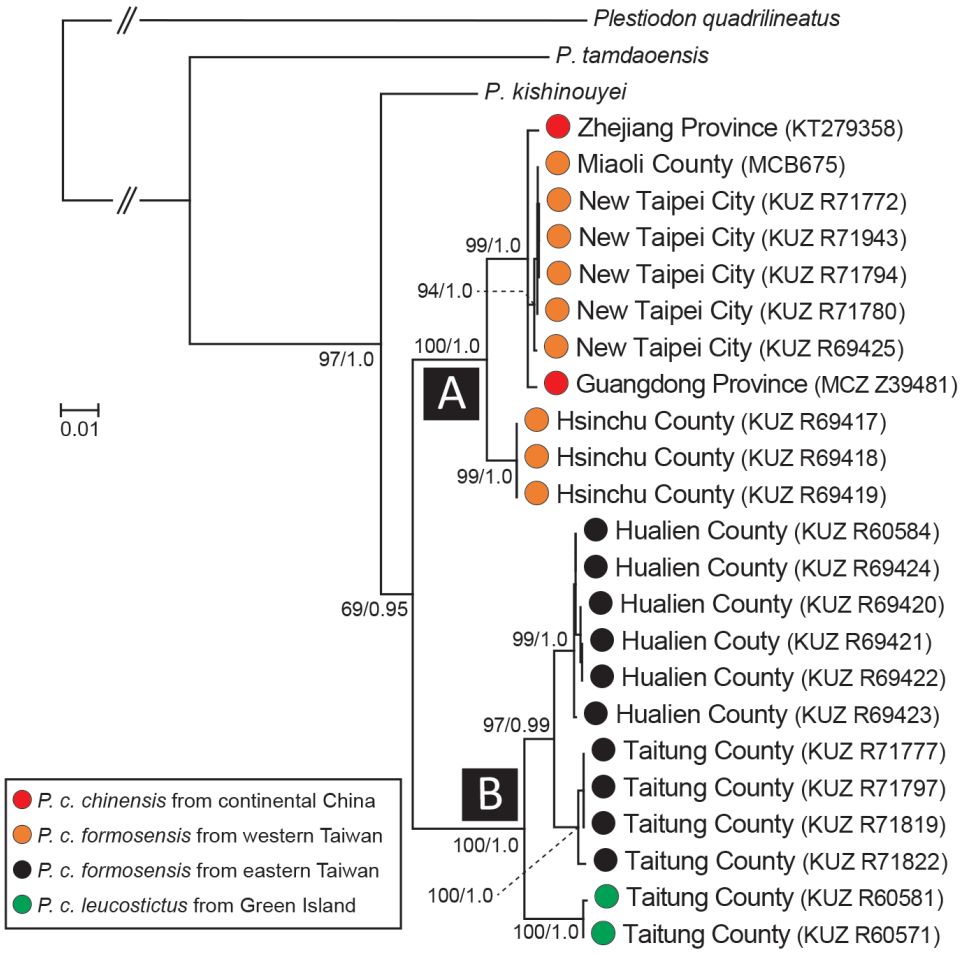

Figure 3. Maximum likelihood tree estimated using mitochondrial DNA sequences (2,351 bp). Numbers near interior branches show the bootstrap probabilities/Bayesian posterior probabilities. Sample names correspond to those given in Table 1.

two were shared by Green Island specimens. In the PRLR dataset, five inferred alleles were obtained from *P. chinensis* (Fig. 4b). Two alleles were found in specimens from eastern Taiwan, consisting of an allele endemic to this population and an allele shared with both specimens from western Taiwan and Green Island. The results of AMOVA for both nuclear datasets showed significant genetic differentiation between specimens from western Taiwan and eastern Taiwan plus Green Island (F_{ST} = 0.24, P = 0.0032 in the RAG–1 dataset; F_{ST} = 0.66, P < 0.0001 in the PRLR dataset). In contrast, there was no significant genetic differentiation between specimens from Taiwan (including western and eastern areas) and Green Island in either dataset (F_{ST} = –0.05, P = 0.5934 in the RAG–1 dataset; F_{ST} = 0.23, P = 0.0530 in the PRLR dataset).

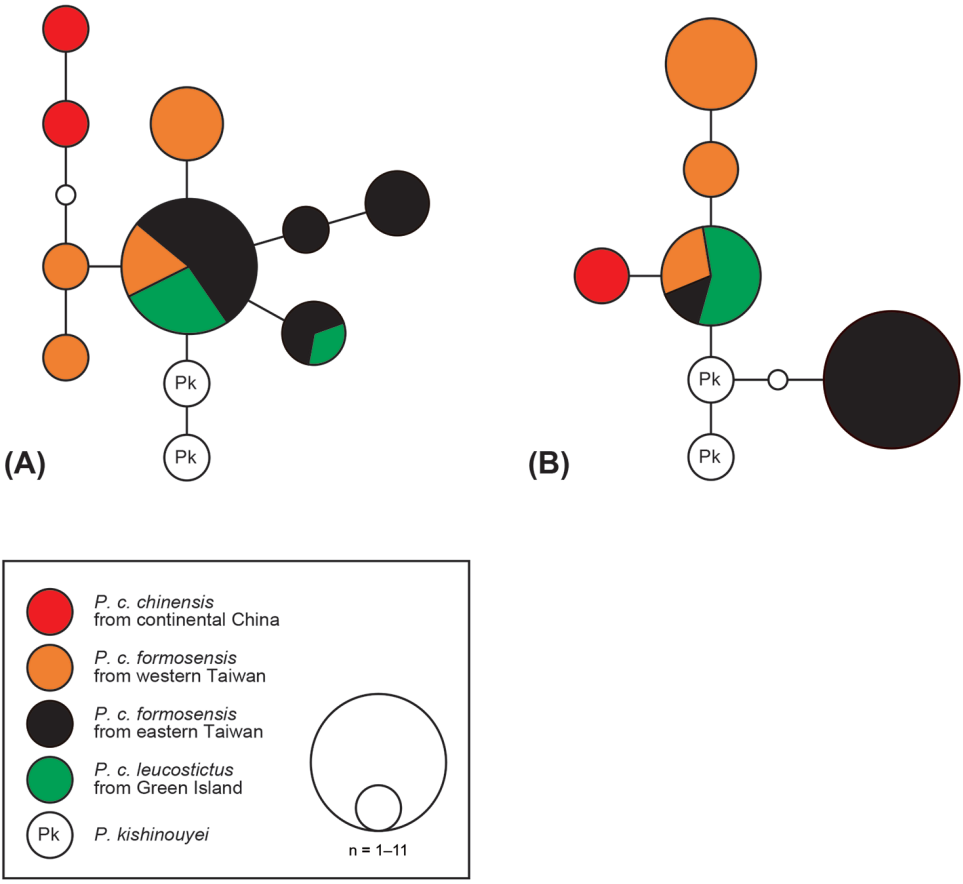

Figure 4. Median-joining networks of the RAG–1 **A** and PRLR **B** datasets. Open circles indicate missing alleles.

Discussion

The morphological investigation in this study confirmed that *P. chinensis* from eastern Taiwan are more similar in morphology to *P. c. leucostictus* than to *P. c. formosensis* from western Taiwan, especially in possessing a white spotted pattern without light lines on the dorsum (Fig. 2). Although the eastern Taiwanese specimens were similar to the western specimens in MSR, they showed a different frequency pattern from the western and Green Island specimens in PN (Table 2). Thus, the scale characters did not seem decisive as the basis of allocation of the eastern Taiwanese population. However, with the same coloration to *P. c. leucostictus* which is unique in this genus, the eastern Taiwanese populations should be assigned to this taxon. This morphologically based classification was also supported by molecular data: the genetic markers collectively suggested differentiation between western and eastern Taiwanese populations and close affinity between the eastern Taiwanese populations and *P. c. leucostictus* (Figs 3, 4). Therefore,

the eastern Taiwanese and Green Island populations should be placed in a single taxon that is distinct from western Taiwanese populations. Based on the morphological differentiation of this taxon (Fig. 2) and a level of genetic differentiation comparable to that with another species (i.e. *P. kishinouyei*), we conclude that *P. c. leucostictus* should be recognized as a distinct species, i.e., *Plestiodon leucostictus* (Hikida, 1988).

According to the original description by Van Denburgh (1912a), the holotype of *P. c. formosensis* was collected from "San Shi Ka, Formosa". The name probably derives from both Japanese and Taiwanese pronunciations. It signifies a "mountain foot" (Yi-Hung Chen, personal communication). Shang et al. (2009) proposed Xiangshan (Hsinchu County in western Taiwan) as the collection locality, while Zhao and Adler (1993) proposed Shanshang (Tainan County in western Taiwan) as the collection locality (sites 1 and 2 in Fig. 1, respectively). Based on our investigations on the island, this lizard is very abundant in northwestern, but very rare in southwestern Taiwan, indicating that the former place has a higher probability to be the real type locality. Unfortunately, we could not analyze specimens from both localities because population from the latter place was scarce. However, considering the continuous habitat and landscape pattern in western Taiwan, lizards from both localities should be assigned as the western taxon (Clade A). Furthermore, since the light lines was reported by Van Denburgh (1912b) from the holotype, it helps to confirm that *P. c. formosensis* should be applied only to the western lizard, while *P. leucostictus* stands for a valid specific name. Their disjunct distribution suggests that the Central Mountain Range in Taiwan may have played a major role as a natural barrier for these lowland lizards, congruent to the other phylogeographic cases which have shown huge diversification between eastern and western clades such as cobras (Lin et al. 2008), rhacophorid treefrogs (Lin et al. 2012), and lacertid lizards (Tseng et al. 2014, 2015).

Beyond the clear differentiation of *P. leucostictus* from other members of the *P. chinensis* complex, the intraspecific taxonomy of *P. chinensis* remains obscure. Subsequent to the description of *P. c. formosensis* by Van Denburgh (1912a), *P. chinensis* has been recognized as a polytypic species. Taylor (1936) placed *P. c. formosensis* in a junior synonym of the nominotypical subspecies without any comments, while he added a northern continental form, *P. c. pulcher*, to the subspecific rank of *P. chinensis*. He suggested that their geographic boundary might be located south of the Yangtze River. Hikida (1993) recognized the validity of *P. c. formosensis* and three other subspecies (*P. c. chinensis*, *P. c. leucostictus*, and *P. c. pulcher*), and regarded a Korean species, *P. coreensis* (Doi and Kamita 1937), as a synonym of *P. c. pulcher*. Zhao and Adler (1993) and Zhao et al. (1999) mostly agreed with Hikida's (1993) classification, but did not recognize *P. c. pulcher* at subspecies rank. Instead, they regarded *P. c. daishanensis*, which was described by Mao (1983) based on specimens from the Zhoushan Islands, as a valid subspecies, although the other senior synonym, *P. c. rufoguttatus*, which was described by Cantor (1842) from another island in the same archipelago, is available for this taxon (Schmidt 1927, Taylor 1936).

As our study did not include representative specimens assigned to *P. c. pulcher*, *P. c. daishanensis* (or *P. c. rufoguttatus*), and *P. coreensis*, we could not undertake comprehensive revision of infraspecific taxonomy of *P. chinensis*. However, the low level

of mtDNA genetic divergence we found between *P. c. formosensis* and *P. c. chinensis* (Fig. 3) supports their conspecific status, and *P. c. formosensis* should be assigned to *P. chinensis*. Additional detailed investigations of geographic variation in *P. chinensis*, including all of the putative nominal taxa, are needed to clarify the validity of the proposed subspecies in *P. chinensis*.

In this study, we solved the long and lasting debate to revise the taxonomic assignment of *Plestiodon* in eastern Taiwan from *P. c. formosensis* to *P. leucostictus*. The validity of *P. leucostictus* as a distinct species was confirmed, and we also revise its distribution from Green Island only to the eastern part of Taiwan. Nevertheless, this species in eastern Taiwan is far from common; Green Island is still the only locality for this species to show stable population size. In recent years, the dominant, large-sized skink *Eutropis multifasciata* was found to invade this island (Chen et al. 2009), which gave rise to a close tension from scientists. Although a project has been initiated to remove this invader, the problem requires sustained attention because of the notorious invasion history of this skink in Taiwan and other places (Ota et al. 1994, Witmer et al. 2007). On an islet like this size, invasive species, as well as other stochastic effects such as climate or demographic changes, may cause serious impacts to native species, and lead to negative consequence to this endangered taxon.

Acknowledgements

We are grateful to M. Toda, Y. Kadota, T, Sasai, K. Mochida, W.-B. Gong, J.-W. Lin, K.-H. Lee, S.-F. Yang, W.-Y. Tsai, C.-W. Lu, and Y.-W. Hsiao for their help in collecting and managing specimens; J. V. Vindum for allowing KK to examine type specimens in California Academy of Science; Y.-H. Chen for providing valuable information on a name of a place in Taiwan; T. Makino for preparing the locality map; and H.-Y. Tseng, R.-J. Wang, and C.-W. You for allowing us to use their pictures. This study was financially supported by Fujiwara Natural History Public Interest Incorporated Foundation, Japan to KK, and Ministry of Science and Technology, Taiwan to SML.

References

Bandelt HJ, Forster P, Röhl A (1999) Median-joining networks for inferring intraspecific phylogenies. Molecular Biology and Evolution 16: 37–48. https://doi.org/10.1093/oxfordjournals.molbev.a026036

Brandley MC, Wang Y, Guo X, Nieto Montes de Oca A, Fería-Ortíz M, Hikida T, Ota H (2011) Accommodating heterogenous rates of evolution in molecular divergence dating methods: an example using intercontinental dispersal of *Plestiodon* (*Eumeces*) lizards. Systematic Biology 60: 3–15. https://doi.org/10.1093/sysbio/syq045

Brandley MC, Ota H, Hikida T, Nieto Montes de Oca A, Fería-Ortíz M, Guo X, Wang Y (2012) The phylogenetic systematics of blue-tailed skinks (*Plestiodon*) and the family Scincidae.

Zoological Journal of the Linnean Society 165: 163–189. https://doi.org/10.1111/j.1096-3642.2011.00801.x

Cantor T (1842) General features of Chusan, with remarks on the flora and fauna of that iland. Annals and Magazine of Natural History 9: 481–493. https://doi.org/10.1080/03745484209445368

Chen SF, Chen SL, Li ZL, Lin HC, Chang MH (2009) A survey of terrestrial vertebrates on Green Island. National Park Quarterly 19: 1–22.

Duméril AMC, Bibron G (1839) Erpétologie générale ou Histoire Naturelle complète des Reptiles, V. Libairie Encyclopédique de Roret, Paris, viii + 854 pp.

Doi H, Kamita T (1937) A new species of *Eumeces* from West Corea. Zoological Magazine 49: 211–215.

Edgar RC (2004) MUSCLE: multiple sequence alignment with high accuracy and high throughput. Nucleic Acids Research 32: 1792–1797. https://doi.org/10.1093/nar/gkh340

Excoffier L, Lischer HEL (2010) Arlequin suite ver 3.5: a new series of programs to perform population genetics analyses under Linux and Windows. Molecular Ecology Resources 10: 564–567. https://doi.org/10.1111/j.1755-0998.2010.02847.x

Excoffier L, Smouse PE, Quattro JM (1992) Analysis of molecular variance inferred from metric distances among DNA haplotypes: application to human mitochondrial DNA restriction data. Genetics 131: 479–491.

Felsenstein J (1985) Confidence limits on phylogenies: an approach using the bootstrap. Evolution 39: 783–791. https://doi.org/10.1111/j.1558-5646.1985.tb00420.x

Feria-Ortiz M, García-Vázquez UO (2012) A new species of *Plestiodon* (Squamata: Scincidae) from Sierra Madre del Sur of Guerrero, México. Zootaxa 3339: 57–68.

Flot JF (2010) SEQPHASE: a web tool for interconverting PHASE input/output files and FASTA sequence alignments. Molecular Ecology Resources 10: 162–166. https://doi.org/10.1111/j.1755-0998.2009.02732.x

Gray JE (1838) Catalogue of the slender-tongued saurians, with descriptions of many new genera and species. Annals of Natural History 2: 287–293. https://doi.org/10.1080/00222933809496676

Gutell RR, Fox GE (1988) A compilation of large subunit RNA sequences presented in a structural format. Nucleic Acids Resserch 16: r175–r269. https://doi.org/10.1093/nar/16.suppl.r175

Harrigan RJ, Mazza ME, Sorenson MD (2008) Computation vs. cloning: evaluation of two methods for haplotype determination. Molecular Ecology Resources 8: 1239–1248. https://doi.org/10.1111/j.1755-0998.2008.02241.x

Hikida T (1988) A new white-spotted subspecies of *Eumeces chinensis* (Scincidae: Lacertilia) from Lutao Island, Taiwan. Japanese Journal of Herpetology 12: 119–123.

Hikida T (1993) Phylogenetic relationships of the skinks of the genus *Eumeces* (Scincidae: Reptilia) from East Asia. Japanese Journal of Herpetology 15: 1–21.

Hillis DM, Bull JJ (1993) An empirical test of bootstrapping as a method for assessing confidence in phylogenetic analysis. Systematic Biology 42: 182–192. https://doi.org/10.1093/sysbio/42.2.182

Huelsenbeck JP, Rannala B (2004) Frequentist properties of Bayesian posterior probabilities of phylogenetic trees under simple and complex substitution models. Systematic Biology 53: 904–913. https://doi.org/10.1080/10635150490522629

Jobb, G (2011) TREEFINDER version of March 2011. http://www.treefinder.de

Kearney M, Stuart BL (2004) Repeated evolution of limblessness and digging heads in worm lizards revealed by DNA from old bones. Proceedings of the Royal Society of London B 271: 1677–1683. https://doi.org/10.1098/rspb.2004.2771

Kumazawa Y, Nishida M (1993) Sequence evolution of mitochondrial tRNA genes and deep-branch animal phylogenetics. Journal of Molecular Evolution 37: 380–398. https://doi.org/10.1007/BF00178868

Kurita K, Hikida T (2014a) Divergence and long-distance overseas dispersals of island populations of the Ryukyu five-lined skink, *Plestiodon marginatus* (Scincidae: Squamata), in the Ryukyu Archipelago, Japan, as revealed by mitochondrial DNA phylogeography. Zoological Science 31: 187–194. http://dx.doi.org/10.2108/zs130179

Kurita K, Hikida T (2014b) A new species of *Plestiodon* (Squamata: Scincidae) from Kuchinoshima Island in the Tokara Group of the Northern Ryukyus, Japan. Zoological Science 31: 464–474. http://dx.doi.org/10.2108/zs130267

Kurita K, Toda M (2017) The role of ecological factors in determining phylogeographic and population genetic structure of two sympatric island skinks (*Plestiodon kishinouyei* and *P. stimpsonii*) Genetica 145: 223–234. http://doi.org/10.1007/s10709-017-9960-3

Leaché AD, Reeder TW (2002) Molecular systematics of the Eastern Fence lizard (*Sceloporus undulatus*): a comparison of parsimony, likelihood, and Bayesian approaches. Systematic Biology 51: 44–68. https://doi.org/10.1080/106351502753475871

Lin HC, Li SH, Fong J, Lin SM (2008) Ventral coloration differentiation and mitochondrial sequences of the Chinese Cobra (*Naja atra*) in Taiwan. Conservation Genetics 9: 1089–1097. https://doi.org/10.1007/s10592-007-9418-8

Lin HD, Chen YR, Lin SM (2012) Strict consistency between genetic and topographic landscapes of the brown tree frog (*Buergeria robusta*) in Taiwan. Molecular Phylogenetics and Evolution 62: 251–262. https://doi.org/10.1016/j.ympev.2011.09.022

Mao J (1983) A new subspecies of *Eumeces chinensis* (Gray) from Daishan County, Zhejiang. Acta Herpetologica Sinica 2: 57–60. [in Chinese with English summary]

Okamoto T, Motokawa J, Toda M, Hikida T (2006) Parapatric distribution of the lizards *Plestiodon* (formerly *Eumeces*) *latiscutatus* and *P. japonicus* (Reptilia: Scincidae) around the Izu Peninsula, Central Japan, and its biogeographic implications. Zoological Science 23: 419–425. http://dx.doi.org/10.2108/zsj.23.419

Okamoto T, Hikida T (2009) Three genetic lineages of the Japanese skink *Plestiodon japonicus* (Scincidae, Squamata) and the genetic composition of their contact zones. Journal of Zoological Systematics and Evolutionary Research 47: 181–188. https://doi.org/10.1111/j.1439-0469.2008.00513.x

Okamoto T, Hikida T (2012) A new cryptic species allied to *Plestiodon japonicus* (Peters, 1864) (Squamata: Scincidae) from eastern Japan, and diagnoses of the new species and two parapatric congeners based on morphology and DNA barcode. Zootaxa 3436: 1–23.

Ota H, Chang HW, Liu KC, Hikida T (1994) A new record of the viviparous skink, *Mabuya multifasciata* (Kuhl, 1820) (Squamata: Reptilia), from Taiwan. Zoological Studies 33: 86–89.

Rambaut A, Drummond AJ (2007) Tracer v1.5. http://tree.bio.ed.ac.uk/software/tracer/

Richman AD, Price T (1992) Evolution of ecological differences in the Old World leaf warblers. Nature 355: 817–821. https://doi.org/10.1038/355817a0

Ronquist F, Teslenko M, van der Mark P, Ayres DL, Darling A, Höhna S, Larget B, Liu L, Suchard MA, Huelsenbeck JP (2012) MrBayes 3.2: efficient Bayesian phylogenetic inference and model choice across a large model space. Systematic Biology 61: 539–542. https://doi.org/10.1093/sysbio/sys029

Sabaj Pérez MH (2014) Standard symbolic codes for institutional resource collections in herpetology and ichthyology: an Online Reference. Version 5.0. American Society of Ichthyologists and Herpetologists. http://www.asih.org/

Schmidt KP (1927) Notes on Chinese reptiles. Bulletin of the American Museum of Natural History 54: 467–551. [+ pls XXVIII–XXX]

Shang G, Li P, Yang Y (2009) Field Guide to Amphibians and Reptiles in Taiwan. Owl Publishing House, Taipei, 336 pp. [in Chinese]

Stephens M, Scheet P (2005) Accounting for decay of linkage disequilibrium in haplotype inference and missing-data imputation. The American Journal of Human Genetics 76: 449–462. http://dx.doi.org/10.1086/428594

Stephens M, Smith NJ, Donnelly P (2001) A new statistical method for haplotype reconstruction from population data. The American Journal of Human Genetics 68: 978–989. http://dx.doi.org/10.1086/319501

Sugiura N (1978) Further analysis of the data by Akaike's information criterion and the finite corrections. Communications in Statistics—Theory and Methods 7: 13–26. http://dx.doi.org/10.1080/03610927808827599

Tamura K, Peterson D, Peterson N, Stecher G, Nei M, Kumar S (2011) MEGA5: molecular evolutionary genetics analysis using maximum likelihood, evolutionary distance, and maximum parsimony methods. Molecluar Biology and Evolution 28: 2731–2739. https://doi.org/10.1093/molbev/msr121

Tanabe AS (2011) Kakusan4 and Aminosan: two programs for comparing nonpartitioned, proportional and separate models for combined molecular phylogenetic analyses of multilocus sequence data. Molecular Ecology Resources 11: 914–921. http://www.doi.org/10.1111/j.1755-0998.2011.03021.x

Taylor EH (1936) A taxonomic study of the cosmopolitan scincoid lizards of the genus *Eumeces* with an account of the destribution and relationships of its species. Kansas University Science Bulletin 23[1935]: 1–643.

Townsend TM, Alegre RE, Kelley ST, Wiens JJ, Reeder TW (2008) Rapid development of multiple nuclear loci for phylogenetic analysis using genomic resources: an example from squamate reptiles. Molecular Phylogenetics and Evolution 47: 129–142. http://dx.doi.org/10.1016/j.ympev.2008.01.008

Tseng SP, Li SH, Hsieh CH, Wang HY, Lin SM (2014) Influence of gene flow on divergence dating – implications for the speciation history of *Takydromus* grass lizards. Molecular Ecology 23: 4770–4784. http://dx.doi.org/10.1111/mec.12889

Tseng SP, Wang CJ, Li SH, Lin SM (2015) Within-island speciation with an exceptional case of distinct separation between two sibling lizard species divided by a narrow stream.

Molecular Phylogenetics and Evolution 90: 164–175. http://dx.doi.org/10.1016/j.ympev.2015.04.022

Van Denburgh J (1912a) Advance Diagnoses of New Reptiles and Amphibians from the Loo Choo Islands and Formosa. Privately printed, July 29, 1912, San Francisco, 8 pp.

Van Denburgh J (1912b) Concerning certain species of reptiles and amphibians from China, Japan, the Loo Choo Islands, and Formosa. Proceedings of the California Academy of Sciences 3: 187–258.

Witmer GW, Burke PW, Pitt WC, Avery ML (2007) Management of invasive vertebrates in the United States: An overview. In: Witmer GW, Pitt WC, Fagerstone KA (Eds) Managing Vertebrate Invasive Species: proceedings of an International Symposium. USDA/APHIS Wildlife Services, National Wildlife Research Center, Fort Collins, Colorado, 127–137. http://digitalcommons.unl.edu/nwrcinvasive/56

Yu T-L (1994) Tsungtsuo Lakulaku Hsi (Going upstream the Lakulaku River). The Earth 79: 106–116. [in Chinese]

Zhang C, Sun X, Chen L, Xiao W, Zhu X, Xia Y, Chen J, Wang H, Zhang B (2016) The complete mitochondrial genome of *Eumeces chinensis* (Squamata: Scincidae) and implications for Scincidae taxonomy. Mitochondrial DNA A 27: 4691–4692. http://dx.doi.org/10.3109/19401736.2015.1106505

Zhao E-M, Adler K (1993) Herpetology of China. Society for the Study of Amphibians and Reptiles, Oxford, Ohio, 522 pp.

Zhao E, Zhao K, Zhou K (1999) Fauna Sinica Reptilia, Vol. 2, Squamata Lacertilia. Science Press, Beijing, 394 pp. + pls I–VIII. [In Chinese]

Supplementary material 1

Appendices

Authors: Kazuki Kurita, Yukiko Nakamura, Taku Okamoto, Si-Min Lin, Tsutomu Hikida

Data type: Adobe Acrobat (pdf)

Explanation note:

Appendix I: Specimens examined in the morphological analysis of this study

Appendix II: Primers used in the PCRs of this study.

Appendix III: MtDNA sequence partitions and the best-fit models for phylogenetic analysis.

Link: https://doi.org/10.3897/zookeys.687.12742.suppl1

ZooKeys 687: 149–159 (2017)
doi: 10.3897/zookeys.687.14903
http://zookeys.pensoft.net

RESEARCH ARTICLE

A peer-reviewed open-access journal
ZooKeys
Launched to accelerate biodiversity research

A new species of *Pnigalio* (Hymenoptera, Eulophidae) parasitizing *Eriocrania semipurpurella alpina* (Lepidoptera, Eriocraniidae) in China, with its biology and a key to Chinese known species

Tao Li[1], Zhong-Qi Yang[2], Shu-Ping Sun[1], Rong Wang[3]

1 *General Station of Forest Pest Management, State Forestry Administration, Shenyang 110034, P. R. China* **2** *The Key laboratory of Forest Protection of China State Forestry Administration, Research Institute of Forest Ecology, Environment and Protection, Chinese Academy of Forestry, Beijing 100091, P. R. China* **3** *Qinghai Forest Pest Control and Quarantine Station, Xining 810008, P. R. China*

Corresponding author: *Zhong-Qi Yang* (yangzhqi@126.com)

Academic editor: *Michael Ohl* | Received 6 July 2017 | Accepted 27 July 2017 | Published 2 August 2017

http://zoobank.org/7E4C574A-54AD-4D59-9588-68F178C0954C

Citation: Li T, Yang Z-Q, Sun S-P, Wang R (2017) A new species of *Pnigalio* (Hymenoptera, Eulophidae) parasitizing *Eriocrania semipurpurella alpina* (Lepidoptera, Eriocraniidae) in China, with its biology and a key to Chinese known species. ZooKeys 687: 149–159. https://doi.org/10.3897/zookeys.687.14903

Abstract

A new species of Eulophinae, *Pnigalio eriocraniae* Li & Yang, **sp. n.**, is described and illustrated. This new species is a larval ectoparasitoid of *Eriocrania semipurpurella alpina* Xu (Lepidoptera, Eriocraniidae), a leaf miner in birch trees, *Betula* spp. (Betulaceae), in Qinghai Province, northwest China. The biology of the new species and a key to the known species from China are provided.

Keywords

Betula, ectoparasitoid, *Eriocrania semipurpurella alpina*, Eulophinae, new species, *Pnigalio*

Introduction

Pnigalio Schrank, 1802 (Hymenoptera: Eulophidae: Eulophinae), is comprised of 61 valid species (Noyes 2017). Eight species of *Pnigalio* were known from China (Sheng 1995; Zhu and Huang 2001, 2002; Zhang et al. 2007; Yang et al. 2015).

The species of *Pnigalio* includes numerous species which are potentially important for biological control of leaf miners belonging to Lepidoptera, Diptera, Coleoptera and Hymenoptera (Yoshimoto 1983; Askew 1984; Bernardo et al. 2006, 2007; Compton and Askew 2007; Grabenweger et al. 2009; Yefremova and Mistchenko 2009; Yegorenkova and Yefremova 2012; Strakhova et al. 2013; Yefremova et al. 2013, 2015; Noyes 2017). Four species have been reported parasitizing *Eriocrania* (Lepidoptera: Eriocraniidae) moths: *P. agraules* (Walker), *P. longulus* (Zetterstedt), *P. pectinicornis* (Linnaeus), *P. soemius* (Walker) (Askew and Shaw 1974; Hansson 1987; Koricheva 1994; Zvereva and Kozlov 2006).

Eriocrania semipurpurella alpina Xu has one generation a year in China. Heavy infestations in birch forests were observed in the Qilian Mountains, Qinghai Province, from 2004 to 2014. The life history and biological characteristics of *E. s. alpina* were observed (Li et al., 2016). Two ichneumonids were reported parasitizing overwintering cocoons of *E. s. alpina* (Cairangdanzhou et al., 2013; Zhang et al., 2016). A new parasitoid species of *Pnigalio* was reared from the larvae of the pest and it is described in the present paper. We also provide a key to the known Chinese species of the genus *Pnigalio*.

Material and methods

The life history and biological characteristics of *E. s. alpina* were observed at the Beishan Forest Farm (N37°01', E102°21', 2400–2500 m), Huzhu County, Qinghai Province from 2011 to 2016. Adults of *E. s. alpina* and its parasitoids were collected using intercept traps (IT, Li et al., 2012). As well, birch leaves mined by 3rd to 4th instars larva of the pest were collected from 10 May to 16 June 2011. The leaves were dissected and examined for parasitism. Parasitoid larvae and pupae were kept in glass culture dishes (60 × 10 mm) at room temperature for rearing until parasitoid emergence. The host species was identified by Dr Hou-Hun Li (Nankai University, Tianjin, China).

For the morphological terminology used in this paper, see Bouček (1988) and Gibson (1997). The figures were taken using a Leica M205A microscope with a Leica Microsystem DFC550 digital camera. Photographs were combined using Leica Application Suite (Version 4.5.0).

The holotype, most paratypes of the new species and hosts are deposited in the Insect Museum of the General Station of Forest Pest Management (GSFPM), State Forestry Administration, Shenyang, China. Some paratypes are deposited in the Insect Museum of the Chinese Academy of Forestry (CAF), Beijing, China. Some hosts are deposited in the Insect Museum of Nankai University (NKUM), Tianjin, China.

Taxonomy

Pnigalio Schrank, 1802

Pnigalio Schrank, 1802: 315. Type-species *Ichneumon pectinicornis* L.

Diagnosis. Body color usually metallic blue-green to blue-black (only few species black and with or without metallic reflections). Head rounded, subtriangular or subrectangular, wider than high; antenna with 2 annelli, 3–4 funicle segments and 2–3 club segments; mandible subquadrate, usually with a strongly developed acute upper tooth and 4 rounded lower teeth. Pronotum campanulate to subrectangular; scutellum with 2 or 3 pairs of bristles; propodeum with strongly developed median carina, anterior 1/3 with tongue-like projection or without projection, plicae and costulae present or absent, sometimes with additional costulae either complete or incomplete; propodeal spiracle rounded to subovate. Fore wing usually hyaline, veins developed. Metasoma elongate-ovate to narrow and long (Yoshimoto 1983).

Key to species of *Pnigalio* known in China

1 Costulae of propodeum absent (Fig. 6), or if present, then weak and not reaching median carina (Fig. 9, arrow) **2**

– Costulae of propodeum present and reaching median carina..... **4**

2 Axilla reticulate; fore wing length 2.3 × width, costal cell length 8.0 × width; hind leg (female) black except coxa with blue-green with purple metallic tinge ..... ***P. scabraxillae*** **Yang & Yao**

– Axilla weakly sculptured; fore wing (Fig. 11) length 2.7 × width, costal cell length 10.0 × width or fore wing length 2.1 × width, costal cell length 3.6 × width; hind femur, tibia, yellow to yellowish white (female) **3**

3 Scape white; posterior margin of mesoscutum with three pairs of stout bristles; propodeal disc laterally reticulate; fore wing length 2.1 × width, costal cell length 3.6 × width; hind leg white, coxa smooth dorsally..... ..... ***P. maijishanensis*** **Yang & Yao**

– Scape blue-green with purple metallic tinge; posterior margin of mesoscutum with one pair of stout bristles (Fig. 6, arrow); propodeal disc laterally smooth (Fig. 6); fore wing (Fig. 11) length 2.7 × width, costal cell length 10.0 × width; hind femur, tibia (apical portion brown), yellow to yellowish white, coxa with coarse reticulate sculpture dorsally ..... ***P. eriocraniae*** **Li & Yang, sp. n.**

4 Costula meeting anterior margin of propodeum or anterior part of median carina..... **5**

– Costula meeting median portion of median carina..... **6**

5 Costula reaching anterior margin of propodeum or anterior part of median carina; mesoscutum with micro-reticulate sculpture ..... ***P. longulus*** **(Zetterstedt)**
– Costula reaching anterior 2/5 of median carina; mesoscutum with reticulate ..... ***P. flavipes*** **(Ashmead)**
6 Gaster of female 1.4–1.8 times as long as broad, usually shorter than mesosoma **7**
– Gaster of female twice as long as broad, longer than mesosoma **8**
7 Hind tarsus of female with all segments from pale testaceous to fuscous, never white; inner face of mid-coxa with some setae..... ***P. soemius*** **(Walker)**
– Hind tarsus of female with one to three basal segments whitish; inner face of mid-coxa without setae ..... ***P. agraules*** **(Walker)**
8 Legs of female with femora and tibiae predominantly pale yellow, only slightly fuscous; in male the dark coloration is more extensive; mesosoma green; wings hyaline ..... ***P. phragmitis*** **(Erdös)**
– Legs of female reddish-testaceous, blackish, or often a combination of the two colors, never pale yellow; mesosoma bronze-green or blue-green to almost black; fore wing of female usually with yellowish or greyish tinge..... ..... ***P. pectinicornis*** **(L.)**

Pnigalio eriocraniae **Li & Yang, sp. n.**
http://zoobank.org/22A447DD-FD41-47E4-AAA1-245E6DB6C4A4
Figures 1–17

Etymology. The specific name is derived from the host's generic name *Eriocrania*.

Type material. Holotype, ♀, (GSFPM), Ganchonggou, Huzhu County, Qinghai Province, leg. Tao Li, 31 May 2011, collected using intercept traps. Paratypes (101♀♀ 60♂♂): (GSFPM, 36♀♀ 12♂♂ are deposited in CAF): 32♀♀ 2♂♂, same data as holotype; 1♀ 4♂♂, same but 10 May 2011; 13♀♀ 15♂♂, same, 30 May 2011; 9♀♀ 5♂♂, same, 1 June 2011; 5♀♀ 9♂♂, same, 2 June 2011; 5♀♀ 3♂♂ (reared from larva of *Eriocrania semipurpurella alpina* Xu), same, 27 June 2011; 11♀♀ 6♂♂ (reared), same, 28 June 2011; 7♀♀ 4♂♂(reared), same, 29 June 2011; 18♀♀ 12♂♂ (reared), same, 30 June 2011.

Diagnosis. Body (Fig. 1) green to blue-green with purple metallic tinge. Antenna (Fig. 5) dark brown. Scape same color as body. Posterior margin of mesoscutum with one pair of bristles (Fig. 6, arrows). Propodeal disc smooth; costulae absent (Fig. 6) or if present, then weak and not reaching median carina (Fig. 9, arrow). Fore wing (Fig. 11) length 2.7 × width; costal cell length 10.0 × width. Hind coxa (Fig. 7) coarse reticulate dorsally; hind femur, tibia (apical portion brown), yellow to yellowish white.

Description. *Female*, holotype (Fig. 1). Length of body of females 3.1–3.4 mm. and of fore wing 2.8–3.0 mm. Body green to blue-green with purple metallic tinge.

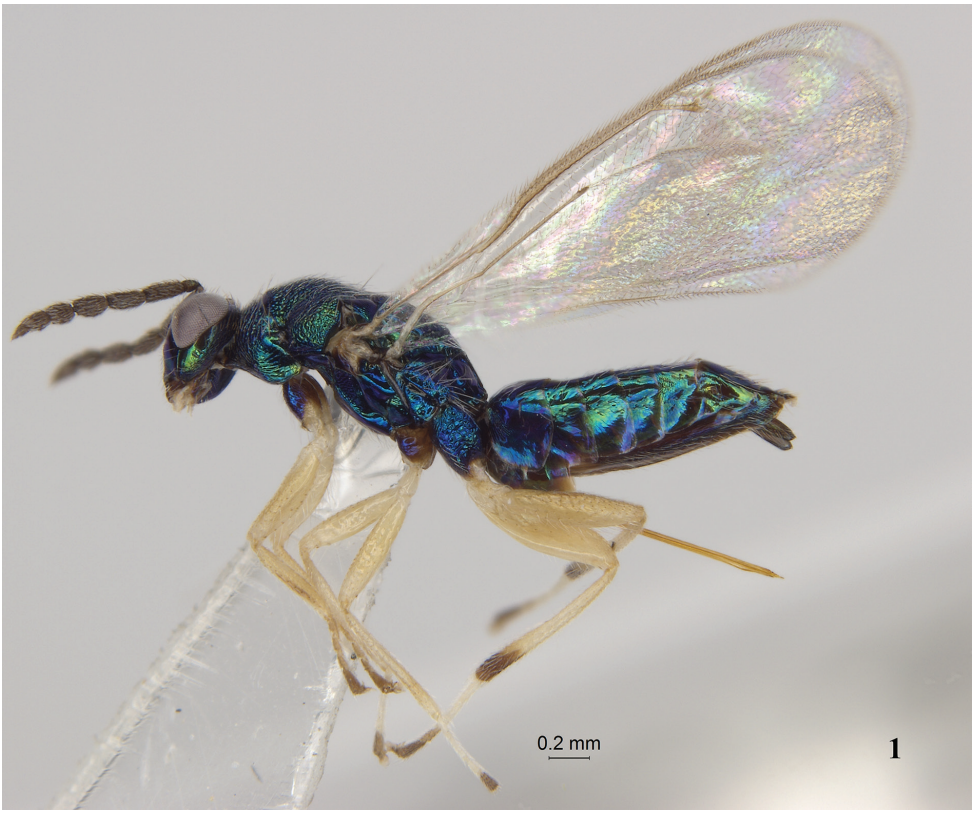

Figure 1. *Pnigalio eriocraniae* Li & Yang, sp. n., female, holotype, habitus lateral.

Vertex golden-green. Antenna (Fig. 5) dark brown. Mandible brown. Maxillary and labial palpi, tegula, fore leg (coxa same color as body, tarsi and claw pale brown), mid leg (coxa same color as body, tarsus 4 brown), hind leg (coxa same color as body, apical portion of tibia and tarsi 3–4 brown) yellow to yellowish white. Wing membrane hyaline, venation and pilosity brown.

Head. In dorsal view, width 2.8 × length. Ocellar triangle convex, micro-reticulate, smooth with long brown setae. Ocelli medium-sized, and lateral areas of ocellar triangle concave. POL 1.7 × OOL, OOL 1.6 × OD. Area between eyes and ocellar triangle smooth. Head (Fig. 3) in anterior view width 1.4 × height. Eye oval, with dense microtrichia; length 1.3 × width. Malar space 0.5 × length of eye, malar sulcus straight and obvious. Face (Fig. 3) smooth, micro-reticulate texture, with sparse long white setae; Median portion of lower face with fine transverse wrinkles. Lower margin of toruli located above ventral line of eyes (Fig. 3). Distance between toruli 0.9 × diameter of toruli, 0.7 × distance between socket and eye. Antenna (Fig. 5) with 4 funiculars and 2 clavomeres. Scape length 3.8 × its width, reaching median ocellus, 3.3 × as long as pedicel. Pedicel length 1.4 × its width. Funicle 1 length 2.8 × as long as pedicel. Ratio

Figure 2. *Pnigalio eriocraniae* Li & Yang, sp. n., male, paratype, habitus lateral.

of length of funicles 1.6:1.4:1.3:1.0, and ratio of width 1.0:1.1:1.1:1.1. Clavomere 1 length 1.3 × as long as segment 2.

Mesosoma (Figs 6–7). Width about 1.2 × as long as head. Mesosoma reticulate, length 1.4 × width. Pronotum length 0.3 × as long as mesoscutum, width 0.7 × mesoscutum. Mesoscutum (Fig. 6) slightly convex, length 0.7 × its width, with dense white setae; anterior half of notaulus obvious; median and apical portions of mesoscutum reticulate, setae relatively sparse; posterior margin with one pair of stout bristles (Fig. 6, arrows). Axilla elongate, micro-reticulate. Mesoscutellum (Fig. 6) nearly circular, sublaterally more coarsely reticulate than apical and median portions; laterally micro-reticulate; with two pairs of bristles. Dorsellum narrow, median length 0.6 × as long as propodeum length. Propodeal disc (Figs 6, 9) smooth; width of median area 1.6 × its length; costula incomplete (Fig. 9, arrow); spiracles nearly circular, posterior to hind margin of metanotum; callus densely setose. Fore wing (Fig. 11) length 2.7 × width; costal cell length 10.0 × width; area of speculum mostly bare posterior to parastigma; marginal vein length 1.3 × length of submarginal vein, 1.8 × length of postmarginal vein; postmarginal vein length 2.1 × length of stigma. Lateral and ventral panel of pronotum and prepectus with coarse reticulate sculpture; mesepisternum (Fig. 7) imbricate anteriorly; subalar area and upper mesepimeron smooth. Dorsal area of hind coxa (Fig. 7) reticulate; basitarsus (Fig. 8) length 0.8 × as long as tarsus 2.

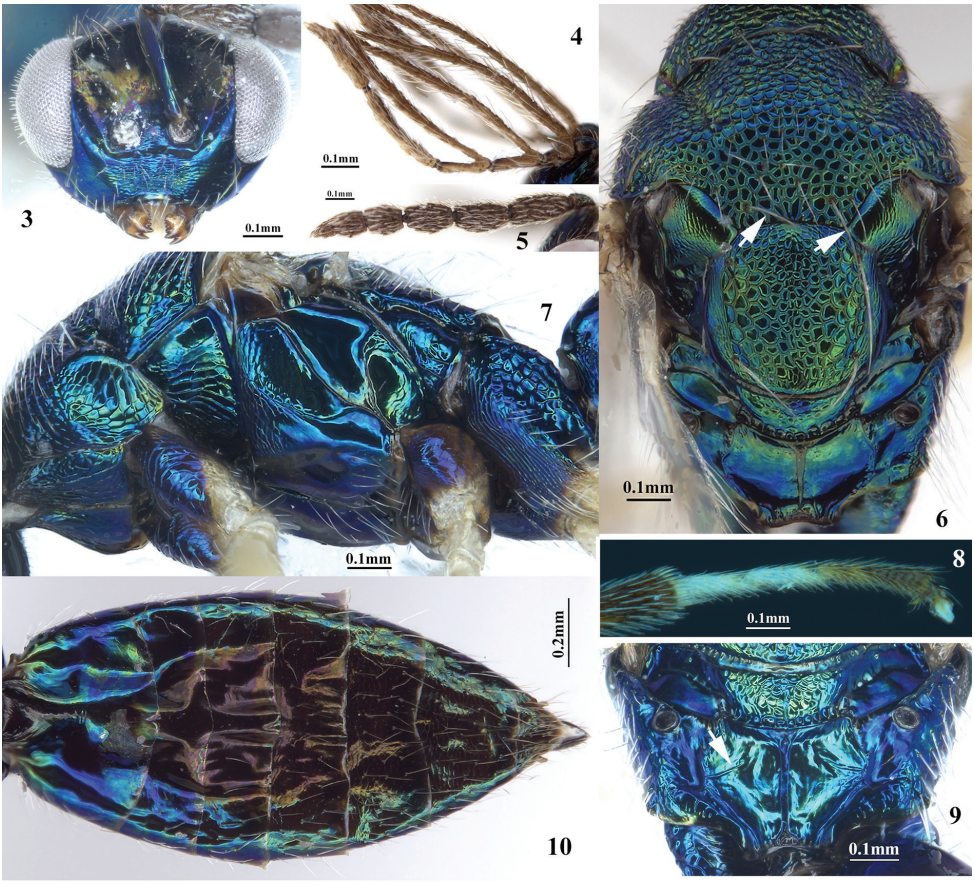

Figures 3–10. *Pnigalio eriocraniae* Li & Yang, sp. n., female (**3, 5–10**) male (**4**). **3** Head, anterior view **4** Antennal flagellum **5** Antenna **6** Mesosoma, dorsal view (bristle, arrow) **7** Mesosoma, lateral view **8** Hind tarsi **9** Propodeum (costula, arrow) **10** Metasoma, dorsal view.

Metasoma (Fig. 10). Elongate-ovate in dorsal view; length about equal to head plus mesosoma, 2.0 × width of metasoma. Tergite 1 smooth; lateral area of tergite 2 with sparse white setae; sub-lateral portion of tergite 3 with sparse white setae; tergites 4–7 with dense setae; ratio of length of tergites 7.0:2.5:3.0:3.5:4.0:2.0. Ovipositor sheath slightly longer than apex of metasoma.

Male (Figs 2, 17). Length of body 2.1–2.6 mm, and of fore wing 2.1–2.3 mm. Similar to female except as follows: Antennal (Fig. 4) flagellum dark brown; fore leg with coxa same color as body, basal half of femur brown with purple metallic tinge, apical tarsomere brown; mid leg with coxa same color as body, most of femur brown with purple metallic tinge, tarsus 4 brown); hind leg with coxa, most of femur same color as body, trochanters, apical half of tibia, tarsus 4 brown to fuscous, apex of femur and basal half of tibia yellowish brown; apex of tergite 1, tergite 2 and basal half of

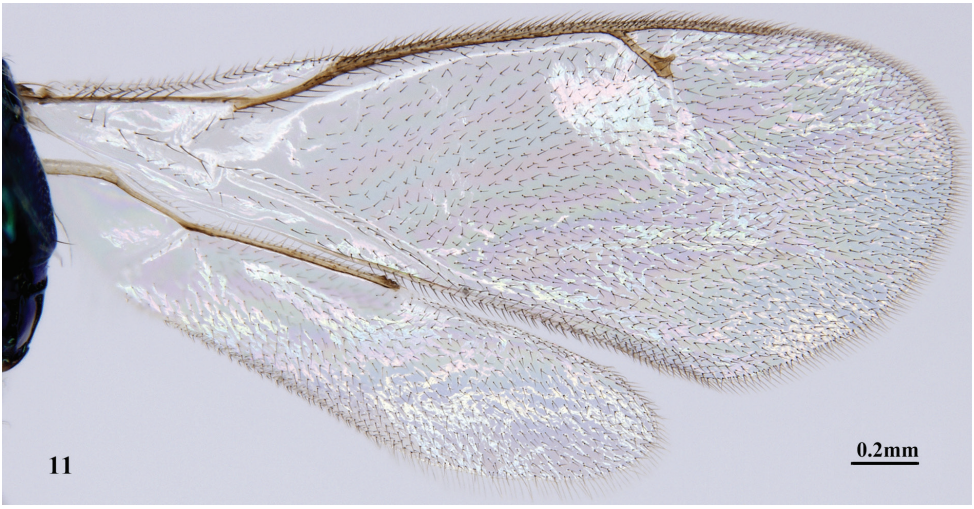

Figure 11. *Pnigalio eriocraniae* Li & Yang, sp. n., female, holotype, wings.

tergite 3 yellowish white to yellowish brown. Scape length 3.2 × width, 4.7 × length of pedicel; pedicle nearly circular; ratio of length of funiculars (Fig. 4) 1.0:1.6:1.6:3.1; funiculars 1–3 pectinate, projections with long setae. Dorsellum smooth, micro-reticulate. Costula absent.

Variation. The variation of specimens is mainly focus on the body color, size, and costulae absent or present. The body color green with metallic tinge (26♀♀ 13♂♂) to blue-green with purple metallic tinge (76♀♀ 47♂♂); tarsi 1–3 of fore leg yellowish (72♀♀, others pale brown); apical portion of mid tibia brown (68♀♀); costula weak (79♀♀, Fig. 9) or absent (23♀♀ 60♂♂, Fig. 6). Costulae of male absent.

Biology. Parasitoid eggs were deposited on the surface of the host's cuticle (Fig. 12). It is a larval ectoparasitoid (Fig. 13) of the third to fourth instar larvae of *E. s. alpina* Xu (Lepidoptera, Eriocraniidae) which forms leaf mines on birch trees, *Betula platyphylla* Suk., *B. albo-sinensis* Burkill and *B. utilis* D. Don (Betulaceae) in Qinghai Province.

The prepupa (Fig. 14) is motionless, fusiform and with distinct lateral protuberances along the abdominal segments, length of body about 0.6–0.7 mm. The pupa is initially white to white brown (Fig. 15) and then begins to darken to brown or black (Fig. 16), with length 0.4–0.5 mm.

Distribution. Northwestern China (Qinghai Province)

Remarks. The new species is similar to *Pnigalio maijishanensis* Yang & Yao but can be distinguished from the latter by the following combination of characters: scape blue-green with purple metallic tinge; propodeal disc laterally smooth; hind coxa with coarse reticulate sculpture dorsally; hind femur, tibia (apical portion brown), yellow to yellowish white. In addition, the shape of the costulae and the stout bristle are different as indicated in the key.

Figures 12–17. The preimaginal stages of *Pnigalio eriocraniae* Li & Yang, sp. n. **12** Egg on 4th instar larva of *E. semipurpurella alpina*, arrow **13** Larva of *P. eriocraniae* parasitizing 4th instar larva of *E. s. alpina* **14** Prepupa **15** Early pupa **16** Mature pupa **17** Emerged male.

Acknowledgements

The authors grateful acknowledge Dr. Hou-Hun Li (Nankai University, Tianjin, China) for identifying the parasitoid's host species, *i.e. Eriocrania semipurpurella alpina* Xu, Dr. Richard R. Askew (private address, St. Marcel du Périgord, 24510 Ste Alvère, France), Dr. Julia Koricheva (Department of Biological Sciences, University of London, United Kingdom) and Dr. Dicky S. K. Yu (Canadian National Collection, Ottawa, Canada) for providing valuable reference papers. We also thank Dr. Michael Ohl (Subject editor) (Museum für Naturkunde Berlin, Berlin, Germany) and Dr. John M. Heraty (Department of Entomology, University of California, Riverside, United States of

America) for valuable comments and suggestions. This research was supported by the "Twelfth Five-Year" National Science and Technology Support Program of China (No. 2012BAD19B0701) and the National Natural Science Foundation of China (NSFC, No. 31070585).

References

Askew RR (1984) Species of *Pnigalio* and *Chrysocharis* (Hymenoptera: Eulophidae) parasitic on Tischeriidae (Lepidoptera), with the description of a new species. Entomologist's Gazette 25: 103–109.

Askew RR, Shaw MR (1974) An account on the Chalcidoidea (Hymenoptera) parasiting leafmining insects of deciduous trees in Britain. Biological Journal of the Linnean Society 6: 289–335. https://doi.org/10.1111/j.1095-8312.1974.tb00727.x

Bernardo U, Pedata PA, Viggiani G (2006) Life history of *Pnigalio soemius* (Walker) (Hymenoptera: Eulophidae) and its impact on a leafminer host through parasitization, destructive host-feeding and host-stinging behavior. Biological Control 37: 98–107. https://doi.org/10.1016/j.biocontrol.2005.11.011

Bernardo U, Pedata PA, Viggiani G (2007) Phenotypic plasticity of pigmentation and morphometric traits in *Pnigalio soemius* (Hymenoptera: Eulophidae). Bulletin of Entomological Research 97: 101–109. https://doi.org/10.1017/S0007485307004816

Bouček Z (1988) Australasian Chalcidoidea (Hymenoptera). A biosystematic revision of genera of fourteen families, with a reclassification of species. CAB International, Wallingford, Oxon, 832 pp.

Cairangdanzhou, Li T, Sheng ML (2013) A new Chinese record species of *Grypocentrus* Ruthe (Hymenoptera, Ichneumonidae, Tryphoninae) parasitizing *Eriocrania semipurpurella alpina*. Acta Zootaxonomica Sinica 38(3): 672–674.

Compton SG, Askew RR (2007) *Pnigalio tricuspis* (Erdos, 1954) (Hym., Eulophidae), a parasitoid of sawflies new to Britain, with notes on allied species. Entomologist's Monthly Magzaine 143: 157–160.

Gibson GAP (1997) Morphology and terminology. In: Gibson GAP, Huber JT, Woolley JB (Eds) Annotated keys to the genera of Nearctic Chalcidoidea (Hymenoptera). NRC Research Press, Ottawa, Ontario, Canada, 16–44.

Grabenweger G, Hopp H, Schmolling S, Koch T, Balder H, Jäckel B (2009) Laboratory rearing and biological parameters of the eulophid *Pnigalio agraules*, a parasitoid of *Cameraria ohridella*. Journal of Applied Entomology 133(1): 1–9. https://doi.org/10.1111/j.1439-0418.2008.01310.x

Hansson C (1987) New records of Swedish Eulophidae and Pteromalidae (Hymenoptera: Chalcidoidea), with data on host species. Entomologisk Tidskrift 108(4): 167–173.

Koricheva J (1994) Can parasitoids explain density patterns of *Eriocrania* (Lepidoptera: Eriocraniidae) miner in a polluted area? Acta Oecologica 15(3): 365–378.

Li T, Sheng ML, Sun SP, Chen GF, Guo ZH (2012) Effect of the trap color on the capture of ichneumonid wasps (Hymenoptera). Revista Colombiana de Entomología 38(2): 338–342.

Li T, Zeng HQ, Sheng ML, Cairangdanzhou, Zhou WF, Sun SP (2016) Biological characteristics of *Eriocrania semipurpurella alpina* (Lepidoptera: Eriocraniidae) and its natural enemy parasitoids. Scientia Silvae Sinicae 52(10): 102–108.

Noyes JS (2017) Universal Chalcidoidea Database. http://www.nhm.ac.uk/chalcidoids [accessed April 2017]

Schrank FP (1802) Fauna Boica. Ingolstadt 2(2): 1–412.

Sheng JK (1995) Hymenoptera: Chalcidoidea. In: Wu H (Eds) Insects of Baishanzu Mountain, eastern China. China Forestry Publishing House, Beijing, 565–567.

Strakhova IS, Yefremova ZA, Tschirnhaus MV, Yegorenkova EN (2013) The parasitoid complex (Hymenoptera, Eulophidae) of leafminer flies (Diptera, Agromyzidae) in the Middle Volga Basin. Entomological Review 93(7): 865–873. https://doi.org/10.1134/S0013873813070087

Yang ZQ, Yao YX, Cao LM (2015) Chalcidoidea parasitizing forest defoliators (Hymenoptera). Science Press, Beijing, China, 283 pp.

Yefremova Z, Strakhova I, Kravchenko V, Tschirnhaus MV, Yegorenkova E (2015) Parasitoid complex (Hymenoptera: Eulophidae) of the leaf-mining fly *Chromatomyia horticola* (Goureau) (Diptera: Agromyzidae) in Russia. Phytoparasitica 43: 125–134. https://doi.org/10.1007/s12600-014-0426-1

Yefremova ZA, Mistchenko AV (2009) New data on trophic relations between eulophid parasitic wasps (Hymenoptera, Eulophidae) and lepidopterans in Ul'yanovsk Province. Entomological Review 89(3): 249–256. https://doi.org/10.1134/S0013873809030014

Yefremova ZA, Yegorenkova EN, Mishchenko AV (2013) Eulophid wasps (Hymenoptera, Eulophidae), parasitoids of leaf-mining moths (Lepidoptera: Gracillariidae, Nepticulidae, Tischeriidae) on the English oak in the middle Volga area. Entomological Review 93(3): 309–315. https://doi.org/10.1134/S0013873813030044

Yegorenkova E, Yefremova Z (2012) The preimaginal stages of *Pnigalio gyamiensis* Myartseva & Kurashev, 1990 (Hymenoptera, Eulophidae), a parasitoid associated with *Chrysoesthia sexguttella* (Thunberg) (Lepidoptera, Gelechiidae). ZooKeys 214: 75–89. https://doi.org/10.3897/zookeys.214.3266

Yoshimoto CM (1983) Review of North American *Pnigalio* Schrank (Hymenoptera: Eulophidae). The Canadian Entomologist 115(8): 971–1000. https://doi.org/10.4039/Ent115971-8

Zhang Y, Li T, Sheng ML, Yang QQ (2016) New Chinese record *Lathrolestes eriocraniae* Seyrig (Hymenoptera: Ichneumonidae) parasitizing *Eriocrania semipurpurella alpina* Xu. South China Forestry Science 44(3): 58–60.

Zhang YZ, Ding L, Huang HR, Zhu CD (2007) Eulophidae fauna (Hymenoptera, Chalcidoidea) from south Gansu and Qinling mountains areas, China. Acta Zootaxanomia Sinica 32(1): 6–16.

Zhu CD, Huang DW (2001) A taxonomic study on Eulophidae from Zhejiang, China (Hymenoptera: Chalcidoidea). Acta Zootaxanomia Sinica 26(4): 533–547.

Zhu CD, Huang DW (2002) A taxonomic study on Eulophidae from Guangxi, China (Hymenoptera: Chalcidoidea). Acta Zootaxanomia Sinica 27(3): 583–607.

Zvereva EL, Kozlov MV (2006) Top-down effects on population dynamics of *Eriocrania* miners (Lepidoptera) under pollution impact: does an enemy-free space exist? Oikos 115: 413–426. https://doi.org/10.1111/j.2006.0030-1299.14923.x